FABRICATION AND EXPERIMENTAL ANALYSIS OF ALUMINIUM COMPOSITES AND OPTIMIZATION OF PROCESS PARAMETERS

THESIS

Submitted in fulfillment of the requirement of the degree of

DOCTOR OF PHILOSOPHY

to

YMCA UNIVERSITY OF SCIENCE & TECHNOLOGY

by

GURPREET SINGH SAINI

Registration No: YMCAUST/Ph48/2012

Under the supervision of

DR. SANJEEV GOYAL

ASSISTANT PROFESSOR

Department of Mechanical Engineering

YMCA UST, Faridabad

Department of Mechanical Engineering

Faculty of Engineering & Technology

YMCA University of Science & Technology

Sector-6, Mathura Road, Faridabad, Haryana, India

May, 2017

Dedicated

to

My Father and Mother

DECLARATION

I hereby declare that this thesis entitled **"FABRICATION AND EXPERIMENTAL ANALYSIS OF ALUMINIUM COMPOSITES AND OPTIMIZATION OF PROCESS PARAMETERS"** by **GURPREET SINGH SAINI,** being submitted in fulfillment of the requirements for the Degree of Doctor of Philosophy in MECHANICAL ENGINEERING under Faculty of Engineering and Technology of YMCA University of Science & Technology Faridabad, during the academic years 2012-17, is a bonafide record of my original work carried out under guidance and supervision of **DR. SANJEEV GOYAL, ASSISTANT PROFESSOR, MECHANICAL ENGINEERING, YMCA UNIVERSITYOF SCIENCE AND TECHNOLOGY, FARIDABAD** and has not been presented elsewhere.

I further declare that this thesis does not contain any part of any work which has been submitted for the award of any degree either in this university or in any other university.

(Gurpreet Singh Saini)
Registration No.: MCAUST/PH48/2012

CERTIFICATE

I hereby declare that this thesis entitled **"FABRICATION AND EXPERIMENTAL ANALYSIS OF ALUMINIUM COMPOSITES AND OPTIMIZATION OF PROCESS PARAMETERS"** by **GURPREET SINGH SAINI,** being submitted in fulfillment of the requirements for the Degree of Doctor of Philosophy in MECHANICAL ENGINEERING under Faculty of Engineering and Technology of YMCA University of Science & Technology Faridabad, during the academic years 2012-17, is a bonafide record of work carried out under my guidance and supervision

I further declare that to the best of my knowledge, the thesis does not contain any part of any work which has been submitted for the award of any degree either in this university or in any other university.

Dr. Sanjeev Goyal
ASSISTANT PROFESSOR
Department of Mechanical Engineering
Faculty of Engineering & Technology
YMCA University of Science and Technology, Faridabad

Dated:

ACKNOWLEDGEMENT

It is a great pleasure for me to express my gratitude and heartfelt respect to my supervisor Dr. Sanjeev Goyal, Assistant Professor, Department of Mechanical Engineering, YMCA University of Science and Technology, Faridabad for his unconditional help, constructive suggestions, thought provoking discussions, encouragement, moral support and affection through the course of my work. It has been a blessing for me to spend many favourable moments under the guidance of the perfectionist at the zenith of professionalism. The present work is evidence to his promptness, encouragement and devoted personal interest, taken by him during the course of this research work.

I am very grateful to Dr. Tilak Raj (Professor and Chairman) and Dr. M.L. Aggarwal (Professor and former Chairman), Department of Mechanical Engineering, YMCA University of Science and Technology, Faridabad for providing facilities to carry out the work. Thanks are also due to Dr. Sandeep Grover, Dean (Engineering and Technology), Department of Mechanical Engineering, YMCA University of Science and Technology, Faridabad to motivate me for my research work. I am equally grateful to Dr. Rajeev Saha (Assistant Professor and PhD Coordinator), Department of Mechanical Engineering, YMCA University of Science and Technology, and Dr. Maneesha Garg, Assistant Professor, Department of Humanities and Sciences, YMCA University of Science and Technology for their cooperation and support throughout my research work.

The services of the staff of Department of Mechanical Engineering, YMCA University of Science and Technology, Faridabad are acknowledged with sincere thanks. I would also like to thank and acknowledge all the staff and faculty member of Thapar University, Patiala who helped me so sincerely in the course of my work.

I would like to thank Dr. Neeraj Sharma for his support, help and encouragement from time to time during my research work.

I cannot close these prefatory remarks without expressing my deep sense of gratitude and reverence to my father Dr. Hari Singh, who has been a constant source of inspiration and support for me through one way or the other from the very childhood and who stood by me always at all phases of my life. My gratitude goes to my mother, Smt. Inderjeet Kaur for her blessings and endeavours to keep my moral high throughout the period of my work. A special

thanks goes to my sister Harpreet for unflagging love and unconditional support throughout my life and my studies. I would also like to express my thanks to my wife Rishu and lovely son Akshveer for their understanding, care, support and encouragement. This thesis is the outcome of the sincere prayers and dedicated support of my family.

I wish to acknowledge the financial support given to me by Science and Engineering Research Board (SERB), Department of Science and Technology, Government of India for participating and presenting my research paper in the International conference held in San Diego, USA.

I want to express my sincere thanks to all those who directly or indirectly helped me at various stages of this work.

Above all, I express my gratitude to the "**ALMIGHTY GOD**" for all his blessing and giving me the will power and strength to make this work possible.

(Gurpreet Singh Saini)
Registration No. YMCAUST/Ph48/2012

ABSTRACT

Aluminium Matrix Composites (AMC's) over the years has become an excellent alternate for the aluminum alloys because of its excellent mechanical, physical and thermal properties. The present research work is undertaken to study the development, characterization and wear performance of particle reinforced aluminium composites.

A lot of work has been done on the fabrication of composites using different type of materials In the present work, an attempt has been made to produce aluminium composites in the presence of Magnesium (Mg) in a certain amount along with the argon gas. The use of Mg and Argon together along with other process parameters gives superior casting results. Compared to the reinforcements like (Gr, Al_2O_3, TiC) which are most commonly used in research, the work on B_4C and (B_4C+SiC) as reinforcement is very less. A very limited work has been reported on the physical and mechanical properties of (B_4C+SiC) reinforced hybrid composites. The present research work has been undertaken with an objective to carry out the comparative analysis of hybrid composites with Al-SiC and Al-B_4C reinforced composites using the same alloy.

Attempts have been made to fabricate aluminum matrix composites using base material AA6082-T6. SiC and B_4C particulates are used as reinforcement to obtain hybrid and non-hybrid composites through the conventional stir casting process under argon atmosphere. AA6082-T6/SiC composites with 5, 10, 15 and 20 wt % of SiC; AA6082-T6/B_4C composites with 5, 10, 15 and 20 wt % of B_4C and AA6082-T6/(SiC+B_4C) hybrid composites with 5, 10, 15 and 20 wt % of (SiC+B_4C) taking equal fraction of SiC and B_4C are made and the microstructure study was carried out. X-Ray diffraction (XRD) patterns revels the presence of reinforcement within the matrix along with some other compounds. The microstructure of the fabricated composites is examined with the help of Scanning electron microscope (SEM) and the micrographs revealed that the dispersion of reinforced particles is reasonably uniform at all weight percentages.

Mechanical and physical properties such as micro-hardness, impact strength, ultimate tensile strength, percentage elongation, density and porosity are investigated on the fabricated composites at room temperature. The wear behaviour of the composites is investigated using a pin-on-disc apparatus at room temperature and optimization of process parameters used for

wear behaviour analysis is done using Response Surface methodology. The weight percentage of reinforcement, sliding speed, load and sliding distance are selected as process parameters with five levels of each process parameter. Experiments were constructed using central composite design (CCD) as it is an effectual tool for building quadratic models consisting of a number of factors. The predictive models are validated by conducting confirmation tests and certified that the developed wear predictive models are accurate and can be used as predictive tools for wear apllications.

TABLE OF CONTENTS

LIST OF TABLES

LIST OF FIGURES

LIST OF ABBREVIATIONS

Symbol	Description
AA	Aluminium alloy
Al	Aluminium
Al_4C_3	Aluminium carbide
Al_2O_3	Aluminium oxide
AMC	Aluminium matrix composite
ANOVA	Analysis of Variance
ASTM	American Society for Testing and Materials
B	Boron
B_4C	Boron Carbide
Ca	Calcium
CaC_2	Calcium carbide
CCD	Central Composite Design
CF	Carbon fiber
CMC	Ceramic matrix composite
cm^3	Centimetre cube
Cr	Chromium
CTE	Coefficient of thermal expansion
Cu	Copper
°C	Degree Celsius
CV	Coefficient of variation
D	Sliding distance
DOF	Degree of freedom
Fi	Iron
g	Gram
Gr	Graphite
HCL	Hydrochloric acid
HF	Hydrofluoric acid
HNO_3	Nitric acid

H_2O	Water
HV	Vickers Hardness
K	Kelvin
KHz	Kilo hertz
Kg	Kilogram
KW	Kilowatt
L	Load
Li	Lithium
LPI	Low pressure infiltration
Mg	Magnesium
MMC	Metal matrix composite
Mn	Manganese
MPa	Mega Pascal
Ni	Nickel
p	Probabilty
PMC	Polymer matrix composite
R	Reinforcement
rpm	Revolutions per minute
RSM	Response surface methodology
S	Sliding speed
SEM	Scanning electron microscope
SiC	Silicon Carbide
SiO_2	Silicon dioxide
Std. Dev	Standard deviation
Sr	Strontium
T6	Solution heat treated
Ti	Titanium
TiB_2	Titanium diboride
TiC	Titanium Carbide
TiO_2	Titanium dioxide
UTS	Ultimate Tensile Strength
Vn	Vanadium
vol	Volume

wt	Weight
XRD	X-Ray diffraction
Zn	Zinc

CHAPTER 1

INTRODUCTION

1.1 ALUMINUM ALLOY

History is often marked by the materials and technology that reflect human capability and understanding. Many times scales begins with the stone age, which led to the Bronze, Iron, Steel, Aluminium (Al) and Alloy ages as improvements in refining, smelting took place and science made all these possible to move towards finding more advance materials possible. Alloy is a mixture of two or more elements where at least one of them is a metal. The resulting alloy can be a solution or a solid. Aluminium Alloy is the alloy in which aluminum is the predominant metal. The major contributors in Al alloy are copper, manganese, magnesium, Silicon, and Zinc **(Sahin and Misiril, 2012).** Aluminium does not exist as a pure metal in nature, it originates as an oxide called alumina. Today casting is the most commonly used method to prepare aluminium. Aluminium is usually not found in pure form **(Kaufman, 2005).** The most commonly used techniques for producing aluminium are die casting, permanent mould casting and sand casting **(James et al., 2014)**. Some of the common application of Al alloys includes building products, rigid and flexible packaging such as foils and cans and for transportation which mainly includes automobile, aircraft, rail cars etc **(Ramnath et al., 2014)**. These alloys are used in automobile and aircraft industry because of their high strength to weight ratio **(Schwartz, 2002).** The principal classification of Al alloy includes wrought and cast **(Davis, 1993).** Mainly they are differing on account of their fabrication method. Some of the alloys can also be heat treated to enhance their properties. Wrought alloys can be casted mechanically into desired shapes such as tubes or rods, production of sheets, production of complex shapes by forming **(Davis, 1993)**. Cast alloys usually adopt the methods of pressure die casting or sometimes castings by sand as well to give the final shapes. Silicon may also be added for the betterment in cast ability **(Rana et al., 2012)**. As of now, there are 8 series of Al alloys and these are designated by four digit numbers **(Reboul and Baroux, 2011).**

Purest metal (1xxx grade) is more corrosion resistant than the Al alloys whereas Al-Cu alloys (2xxx grade) exhibits lowest pitting corrosion as compared to other Al alloys **(Davis, 1993; Hollingsworth and Hunsicker, 1987)**. 1xxx series belongs to non-heat treatable alloys with minimum of 99% aluminium content **(Davis, 1993)**. The major alloying elements are Fe

and Si (Both less than 1%). These increase the strength of the alloys. Due to higher percentage of pure aluminium, 1xxx series alloys have low tensile strength.

2xxx Alloys are heat treatable. These are Al-Cu alloys mainly. The addition of copper (range from 0.7-6.8%) strengthens the alloys over a wide range of temperature. However these alloys are not very good for arc welding processes because of stress corrosion in these alloys **(Kissell, 2004)**. Copper also improves its brittle nature and fatigue properties. Other than copper as major alloying elements Vanadium, Titanium, Manganese, Iron, Nickel, Cadmium, and Tin are some other elements used in 2xxx series alloys **(Kissell, 2004)**. Vanadium and Titanium helps to improve crystallization temperature and manganese raises the tensile properties of Al-Cu-Mn alloys. Iron when added to Al-Cu-Ni alloys increases the strength at elevated temperature. Nickel even added in very low proportion lowers down the coefficient of expansion **(Kissell, 2004)**. Cadmium having low melting point increases corrosive resistance and strength. Tin increases the ageing response of Al-Cu alloys and its resistance to corrosion. Copper, Nickel, Silicon with Tin enhances the load carrying capacity of the alloys and addition of Lead increases Machinability of alloys **(Kissell, 2004)**.

The major alloying element in Aluminium 3xxx series is Manganese (Mn). Manganese makes the alloys ductile and enhances its formability. These alloys exhibit wide range of mechanical properties. The alloys are medium in strength. 3xxx series alloys are non-heat treatable and usually have less tensile strength then 2xxx alloys. The alloys are good in pressing, drawing, and roll forming due to excellent formability. These alloys contribute highly in power plants and vehicles as heat transfer material because of their low thermal conductivity **(Zuo et al., 2014).** Due to their good corrosive resistance, these are also used for various home appliances and packaging such as cans. Manganese also helps to stabilize the grain size of 3xxx series at elevated temperature. Manganese along with Iron improves the casting ability of alloys and lowers down the shrinkage when undergoing metal solidification **(Zuo et al., 2014)**. To increase the strengthening effect of these alloys, Magnesium can also be added to some proportion. 3xxx series alloys can also be welded with the filler alloys depending upon the nature of service requirement and application.

4xxx series alloys can be hardened through heat for improving the mechanical properties. The major alloying element for 4xxx alloys is silicon (Si) **(Beckers et al. 2002)**. Mostly these alloys are less ductile in nature. These alloys are used for casting products where good rigidity and low ductility is required. Addition of silicon mainly improves its

fluidity and reduces ductility. The other main elements added to these alloys are phosphorous, calcium, and Nickel. Phosphorous improves machinability and calcium forms $CaSi_2$ with Silicon which improves its conductivity. Nickel helps to enhance the hardness and strength of alloys **(Jaradeh and Carlberg, 2011)**. The alloys find application in forging such as aircraft piston and are used as filler alloys for welding in automotive application **(Jaradeh and Carlberg, 2011)**. **Ezuber et al., (2008)** found that Al-Si alloys (4xxx grade) and Al-Si-Mg alloys (6xxx grade) exhibits lower corrosion resistance in wet condition whereas Al-Mg alloys (5xxx grade) shows comparatively better resistance to corrosion.

In 5xxx series alloys, magnesium is the main alloying element. These alloys are easy to weld and find application in transportation, buildings and bridges **(Liu et al., 2011)**. The alloys having magnesium content of more than 3.0% are usually not employed for higher temperatures because of their susceptibility to stress corrosion cracking; otherwise these alloys have good corrosive resistance as compared to other alloy series **(Liu et al., 2011)**. The other alloying elements for 5xxx series alloys are chromium and manganese. **Toros et al. (2008)** reported that 5xxx alloys are excellent for automotive industry because of their excellent high-strength to weight ratio, corrosion resistance and weldability.

6xxx series alloys are heat treatable and uses magnesium and silicon as the major alloying elements **(Kaufman, 1997).** These alloys are generally low in strength as compared to 2xxx and 7xxx alloys, but have good formability and welding ability **(Kaufman, 1997).** The special property of these alloys is their extrudabilty which makes these alloys superior for the application of architectural and structural members. The combination of magnesium and silicon forms a compound Mg_2Si which enhances its ability as a solution to heat treatment and increases its strength **(Sahoo and Sivaramakrishnan, 2003)**. Depending upon the service and application, these alloys can be welded with both 4xxx and 5xxx alloys. Calcium, chromium and cadmium are the other major alloying elements for 6xxx alloys. Calcium forms $CaSi_2$ with silicon and improves conductivity of the alloys. Chromium helps to improve electrical resistivity and addition of cadmium enhances machinability.

Alloys of 7xxx series exhibit good tensile strength. The major alloying elements for 7xxx series is zinc (Zn) **(Engler et al., 2013)**. The alloys have high strength and toughness and have a wide range of application in automotive and aerospace sector. Magnesium, chromium, copper, zinc, silver, cadmium, are the notable contributors for 7xxx alloys **(Jurczak and Kyziol, 2012)**. Magnesium along with zinc forms $MgZn_2$ and improves the age

hardening property. Chromium increases electrical resistivity but addition of chromium has the disadvantage as well as it increases the quench sensitivity during the hardening phase. Addition of copper to Al-Zn-Mg alloys along with small proportions of chromium and manganese results in higher strength Al alloys **(Zhong et al. 2014).** Silver is beneficial for stress corrosion resistance and cadmium reduces ageing time of Al-Zn-Mg alloys.

The last series for aluminum alloys is the 8xxx series. This series comprises of alloys in which the major alloying elements are Iron, Nickel, and Lithium. In this series; along with Fe, Ni, Li the other alloying elements are Ca, Sn, Si, Mn and Zn. The 8xxx series are relatively new developed alloys and find great application in aerospace industry and service at high temperatures **(Ahmed et al., 2014).** These alloys have relatively high conductivity, strength and hardness.

It is very much apparent from this short discussion that Al alloys possesses attractive characteristics when put together with different elements and can be used in different industrial and sectors as per the demand of the application. However, certain limitations or in other words, the need of material with improved properties like light weight, higher stiffness to weight ratio, higher strength to weight ratio, good damping characteristics, and excellent wear resistance gave birth to a new material called as Aluminium Matrix Composites (AMC's) which over the years has become an excellent alternate for the aluminum alloys because of its excellent mechanical and thermal properties.

1.2 ALUMINUM MATRIX COMPOSITES

Before coming to Aluminium matrix composites, it is important to have a brief understanding of composites and its classification as this would facilitate to understand the concept of AMC's.

1.2.1 What Are Composites?

Composite materials are defined as the mixture or combination of two or more nano, micro or macro constituents with a boundary separating them in various physical and chemical compositions **(Boopathi et al., 2013)**. Composites are composed of at least two phases; a matrix phase (polymers, metals, or ceramics) and a reinforcement phase (fibers, particles, flakes, and/or fillers). Over the years, Composites have arrived as an excellent substitute for conventional aluminum alloys because of their superior mechanical and

tribological properties **(Boopathi et al., 2013)**. In practice, most composites consist of a bulk material (the 'matrix'), and a reinforcement of some kind, added primarily to increase the mechanical properties of the matrix.

The composites on the basis of matrix can be classified as:

- Polymer matrix composites (PMC's)
- Metal Matrix composites (MMC's)
- Ceramic Metal composites (CMC's)

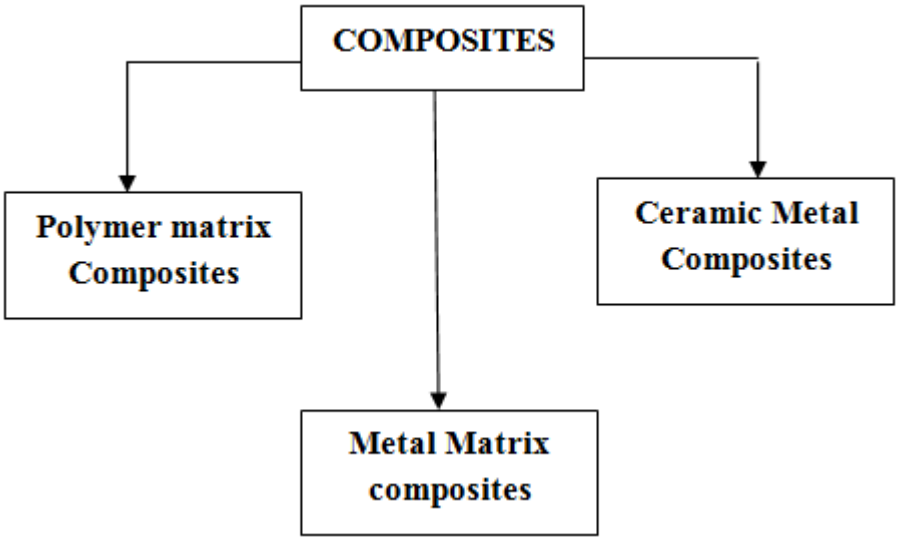

Figure 1.1: Classification of composites on the basis of matrix

1) **Polymer matrix composites (PMC's)**: The composites in which the polymer based material is used as matrix are considered as Polymer matrix composites

Table 1.1: Merits and Demerits of PMC's (Boopathi et al., 2013)

Merits	Demerits
Low densities	Low transverse strength
Good corrosion resistance	Low operational temperature limits
Low thermal conductivities	
Low electrical conductivities	
Translucence	
Aesthetic Colour effects	

The polymer can be thermosetting and/or thermoplastic. Generally speaking, the resinous binders (polymer matrices) are selected on the basis of adhesive strength, fatigue resistance, heat resistance, chemical and moisture resistance etc. The resin must have mechanical strength commensurate with that of the reinforcement. The PMC's has some merits and demerits as listed in Table 1.1.

1) **Metal Matrix composites (MMC's):** The metal matrix composites are the composites in which metal is one of the constituent and the other constituent may be a metal or some other substance such as a ceramic or any organic substance. Metals like aluminium, magnesium or titanium are mainly used as matrix which reinforced with fibers, particulates or whiskers to form MMC's.

   Metal matrix composites possess some attractive properties when compared with organic matrices. These include (i) strength retention at higher temperatures, (ii) higher transverse strength, (iii) better electrical conductivity, (iv) Superior thermal conductivity, (v) higher erosion resistance etc. However, the major disadvantage of metal matrix composites is their higher densities and porosity and consequently lower specific mechanical properties compared to polymer matrix composites [25].

2) **Ceramic Metal composites (CMC's):** Ceramic metal composites are highly beneficial in the applications where high temperature is desirable. These composites use a ceramic material such as alumina or some other type of fibers as the matrix and reinforced with ceramic fibers like silicon carbide (SiC) or boron carbide (B_4C) thereby forming CMC's.

The composites on the basis of a reinforcement phase can be broadly classified as:

- Fabric particle reinforcement
- Whisker or Short fibre Reinforcement
- Long Fibre or continuous Fibre reinforcement

1) **Fabric particle reinforcement:** Fabric Particle reinforcement has no specific orientation and also does not have a specific shape **(Li and Ramesh, 1998)**. This type of reinforcement is the most common and the cheapest as compared to the others **(Li and Ramesh, 1998)**. This produces the isotropic property of MMCs, which shows a

promising application in structural fields. Initially, low volume fraction of particle reinforced (<10%) were used for composite fabrication but presently higher volume fractions of reinforcements have been achieved for various kinds of ceramic particles (oxide, carbide, nitride) **(Aggarwal and Dixit, 1981; Krishnan et al., 1981; Kumar et al., 2011).**

2) **Whisker or Short fibre Reinforcement:** Single crystals grown having zero defects are termed as whiskers. The whiskers have preferred shape, but have smaller diameter and length as compared to long fibres **(Corrochano et al., 2008)**. Whiskers are short fibres made from material such as graphite, silicon carbide, copper, iron etc. Whiskers are differ from particles in the manner that whiskers have definite length to diameter ratio and have an extraordinary strength of up to 7000 MPa. Whisker reinforcement is generally employed using the methods of powder metallurgy and slip casting techniques **(Corrochano et al., 2008)**. Silicon carbide, silicon nitride, carbon and potassium titanate whiskers are available already. Among these, silicon carbide whiskers seem to offer the best opportunities for MMC reinforcement. Presently, silicon carbide whisker reinforcement is produced from rice husk, which is a low cost material. The physical characteristics of whiskers are responsible for different chemical reactivity with the matrix alloy **(Girot et al., 1987)** and also health hazard posed in their handling. Therefore the inherent interest shown by the researches in whiskers reinforcement has declined.

3) **Long Fibre or continuous Fibre reinforcement:** Continuous fibres are characterized as long axis fibre in one direction and often circular in cross-section. The particle size is usually less than 20 μm in diameter. The orientation, shape, length and composite of a fibre are the main factors which decide the performance of a fibre and the properties of the matrix **(Vinson et al., 1985).** The fibre is unique for unidirectional load when it is oriented in the same direction as that of loading, but it has low strength in the direction perpendicular to the fibre orientation. Continuous fibers are much higher in cost as compared to discontinuous fibers and therefore there usage in limited for special application only **(Vinson et al., 1985)**.

Reinforcement has a significant role in increasing the mechanical properties of a composite material. Typical reinforcements are asbestos, carbon, boron, graphite, metal glass, jute, ceramic fibre, alumina and synthetic fibre **(Thirumalai et al., 2014)**. The prime factor that distinguishes reinforcement with filler is the property of reinforcement to improve the tensile and flexural rigidity and also makes strong adhesive bond with the resigns **(Ceschini et al. 2006)**.

All the fibres used in composite exhibits different properties. Mostly fibres as discussed above are arranged in some form of sheets or layers so as to withstand the loading. Different orientation of the fibre is possible which leads to distinguish between fabric and their characteristics.

1.2.2 Composites with 'Aluminium' as Matrix

As we know, the composites having metal as the parent material considers as MMC's but the use of pure metals is very rare and generally the alloys are being used to produce MMC's. The most commonly used metallic alloys are the alloys of light metals like aluminium (Al), titanium (Ti) and magnesium (Mg) however, alloys of nickel (Ni) and copper (Cu) have also been used **(Alaneme and Olubambi, 2013; Alaneme and Bodunrin, 2013)**. It is very much evident that the composites obtained using aluminum or its alloys are called as 'Aluminium Matrix Composites' (AMC's).

Aluminum matrix composites (AMCs) have drawn much attention over the past few decades and are the most promising materials to meet the ever increasing demand of modern day technology, due to their excellent properties such as light weight, high strength, elastic modulus, good damping characteristics, thermal conductivity, low thermal expansion, better high temperature properties, low ductility and excellent wear resistance **(Alaneme and Aluko, 2013; Miracle, 2005).** Aluminium and its alloys have continued to maintain their mark as the matrix material for the development of Composites. This is because of the broad range of superior mechanical and thermal properties as mentioned above and in addition to these, one another advantage that AMC's offer is their low processing cost **(Patnaik et al., 2008)**.

A relatively new generation in the family of AMCs comes with aluminum hybrid composites that have the potential of achieving the growing demands of advanced engineering application. Researchers have used two or more reinforcements to form hybrid

metal matrix composites and the objective is to gain the admirable properties of both the reinforced material so as to give more stability and superior mechanical properties such as high strength, high thermal stability, low density, and high corrosive resistance to the fabricated product **(Patnaik et al., 2008)**. A number of researchers have fabricated different hybrid composites and reported their mechanical properties **(Poovazhagan et al., 2013; Arslan and Kalemtas, 2009)**.

1.2.3 Application of AMC's

The performance characteristics of AMC's for a particular application mainly depends upon the three factors namely composition of the base Al alloy, type of reinforcement used and the processing technique adopted for the composite fabrication **(Qu et al., 2007; Valdez et al., 2008; Chawla et al., 2009)**. Although the application area for AMC's is very vast but here we divide the application part in four principle sectors namely: Automotive, Defence, Electronics and Sporting goods.

1) **Automotive:** For many years, the use of AMC's has been found in the automotives mainly for the engine components. The purpose for this is to lower down the weight of the reciprocating parts and to reduce the noise levels and the vibrations. The most commonly aimed parts are piston crown, piston pins and connecting rods. The piston crowns are squeeze cast with Al matrix and with particle fibers in planes perpendicular to the piston axes **(Eliasson and Sandstrom, 1995).** This results in condensed radial expansion which helps to control fatigue damage. Other benefits claimed for AMC pistons are: a better match in thermal expansion to a steel cylinder block, some inherent self damping of vibration, and improved wear resistance. Honda has used steel wire reinforced aluminium connecting rods on cars. These have been sold commercially, but Honda admits that this is not an avenue to pursue for the future **(Eliasson and Sandstrom, 1995)**. Aluminum engine blocks, suspension components, body panels, and frame members are increasingly common in addition to the use of magnesium in components such as instrument panels, valve covers, transmission housings, and steering column components **(Prasad and Asthana, 2004).**

2) **Defence:** In military vehicles, weight reduction in structural components translates to greater operational flexibility - the ability to carry more payloads, drive more easily

over unimproved roads and/or support more protective armour. Over the years, metal matrix composites have been used in brake rotors and pads but these are typically costlier. In order to reduce the cost, metal matrix composites with aluminum as matrix has been used which results in relatively low weight.

Tank tracks are another potential application. There is an incentive to save weight to improve the speed and manoeuvrability of the vehicle. AMC's reinforced with particle fibers also find application in missile fins, missile body casings, compressor blades and launch tubes.

3) **Electronics:** Metal Matrix Composite (MMC) is rapidly becoming prime candidates as structural materials in engineering as well as in electronic application. Aluminium (Al) and Copper (Cu) reinforced by SiC is used in various industries due to its excellent thermo-physical properties such as low coefficient of thermal expansion (CTE), high thermal conductivity and improved mechanical properties such as higher specific strength, better wear resistance and specific modulus. Recently, these MMCs with high ceramic contents have become another focus for thermal management applications in electronic packaging **(Efzan et al., 2016)**. Normally, in packaging power devices, Aluminium (Al) or Copper (Cu) has been used as a heat sink or base plate for attaching ceramic substrates that carry the chips and the associated lead structures. The large difference in coefficient of thermal expansion (CTE) between the ceramic and Aluminium or Copper is a drawback, as it results in a less reliable packaging and also restricts the size of the ceramic substrate that can be attached to the base plate **(Efzan et al., 2016)**.

   Looking at this drawback, there is now an opportunity for new materials to be developed, study and characterize in order to meet the prescribed requirements of thermally enhanced materials. With an improve properties in thermal conductivity as well as in coefficient of thermal expansion (CTE), MMCs of Cu/SiC and Al/SiC/B_4C are now the possible solution for electronic packaging industry.

4) **Sporting Goods:** The use of fibre reinforced composites in sports equipments is relatively recent. Composite materials are nowadays used in sports equipment because they offer: ease of transport, resistance, reduced weight, durability and low maintenance. Light metals like aluminum and titanium; have become very popular in sports applications, due to their rigidity and lightness **(Zhang, 2015).** AMCs has

found applications in many different kinds of sport equipment for example golf clubs, horseshoes, tennis racquets, bicycle parts frames, wheel rims etc. Some of the applications of AMC's in the sports equipment are shown in Table 1.2.

Table 1.2: Some applications of AMC's in the sports equipment (Zhang, 2015)

FORM	APPLICATION
Plate-like structure	Skis, surfboards, windsurfing, table tennis boards, slats and gliding wing spar etc.
Tubular structures	Tennis, badminton, fishing rods, golf clubs, baseball bats, hockey sticks, pole shaft, etc
Sheet structure	All kinds of helmets, golf club heads, the hull structure of the various boat classes
Other structures	Match with a variety of vehicles, Sword, climbing ropes, various lines etc

1.2.4 Processing Routes for AMC's

Based on the state of matrix in which AMC's are fabricated, processing routes for AMC's are categorized into two types: *1) liquid state processing* and *2) solid state processing*. Liquid state processing is usually energy-efficient and cost-effective. Moreover, products of complex shape can be formed directly through the melt. However, particle agglomeration is a critical issue that hinders adoption of liquid state processing for AMC's. Solid state processing is typically a powder metallurgy based process, in which the matrix powder and reinforcement particles are mixed together and compacted to form a bulk shape. Figure 1.2 shows the different processing routes for AMC's.

Liquid State Processing: Liquid state fabrication involves molten matrix metal having reinforcement, followed by its Solidification in metal matrix composites. Good interfacial bonding (wetting) between the liquid matrix and reinforcement should be obtained to provide improved mechanical properties of metal matrix composites. The methods to fabricate liquid state of AMC's are:

- Stir Casting process
- Infiltration process

- Pressurized Gas Infiltration
- Squeeze Casting Infiltration
- Pressure Die Infiltration

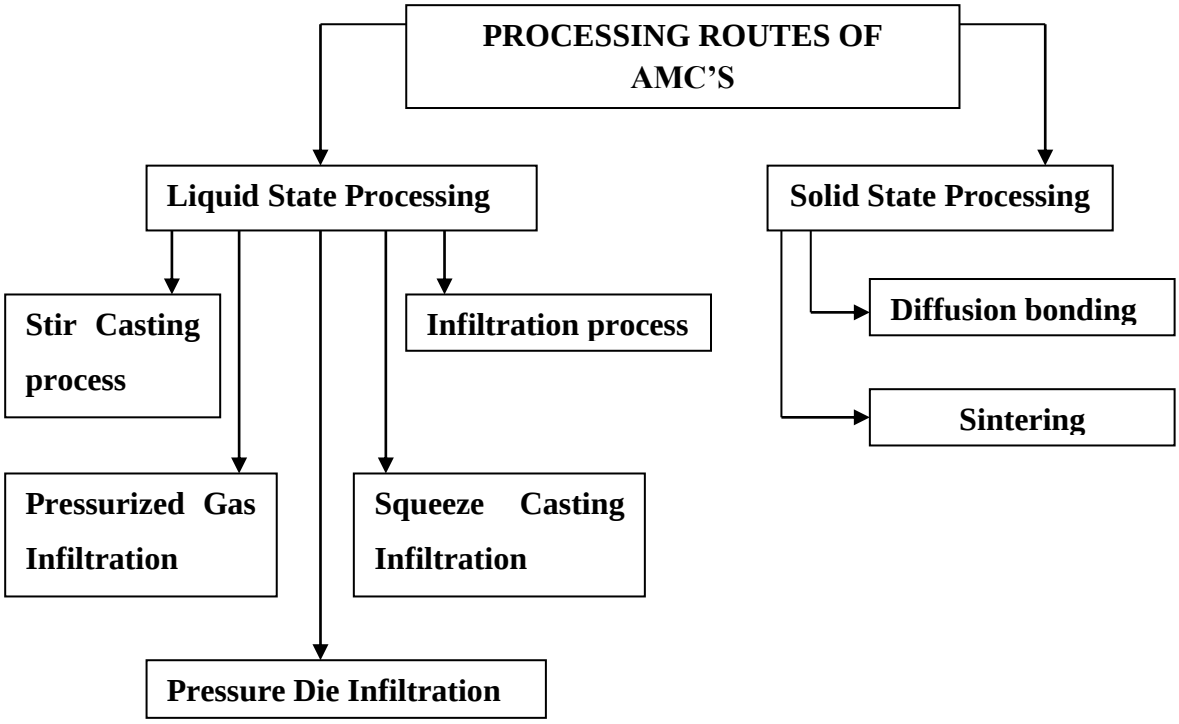

Figure 1.2: Processing Routes of AMC's

- **Stir Casting**

Stir Casting is a process to fabricate AMC's in liquid state. In stir casting process, reinforcement (ceramics, fibers, and particles) is mixed with matrix (molted material) by using mechanical stirrer. Then molten mixture is cast into mould.

The fabrication of liquid AMC's by stir casting process was initiated in 1968; R. Ray use alumina powder into molted aluminum alloy by mechanical stirring. The main step of stir casting process is mechanical stirring. The distribution of reinforcement in matrix mainly depends on conditions like: - strength of mixing, stirring parameters, melting temperature, geometry of stirrer, relative density etc. Distribution of reinforcement can be improved when matrix is in semi- solid phase. This process is most effective for cost and simplest method to fabricated liquid phase composites.

- **Infiltration**

Infiltration is a process to fabricate liquid state matrix composites, in which reinforcement (fiber, ceramic particles, woven) is drawn in a liquid metal matrix, which filled the dispersed phase inclusion. Capillary force of the reinforcement is known as spontaneous infiltration and an external pressure such as mechanical, electromagnetic, gaseous, centrifugal or ultrasonic are applied to the liquid matrix phase called as forced infiltration. So, infiltration process has these two motive force.

- **Gas Pressure Infiltration**

Gas pressure infiltration is a unique process to fabricate the liquid matrix composite. In this process pressurized inert gas is applied on liquid matrix phase to infiltrate in reinforcement. Gas pressure infiltration is also known as forces infiltration method to fabricate liquid metal matrix composites, in which molten metal is forced to penetrate into a preformed dispersed phase by applying pressure on it, using pressurized gas. For manufacturing the large composites part, Gas pressure infiltration method is mainly used for manufacturing the large composites part. The process is rapid with no such limitation. In this method non-coated fibers are used due to less contact time of the hot metal with fibers. Figure 1.3 shows the schematic of gas pressure infiltration.

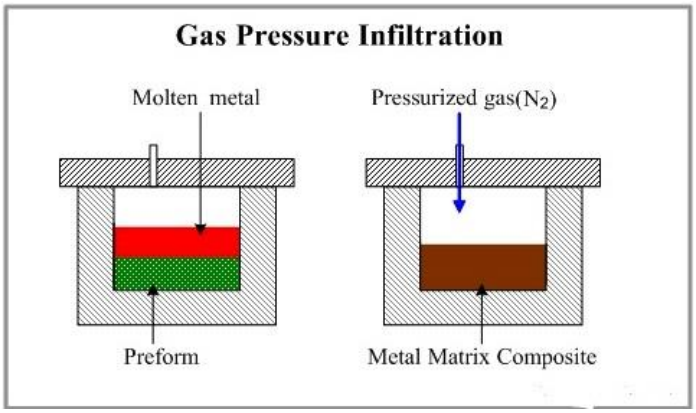

Figure 1.3: Gas Pressure Infiltration [www.substech.com]

- **Squeeze Casting Infiltration**

Squeeze casting infiltration is also a forced infiltration method. This is used to fabricate liquid phase metal matrix composites. The molten metal is filled into lower fixed mold half part with reinforcement. In this method ram is used for applying pressure on the

molten matrix and forcing it to infiltrate into reinforcement. The solidification process of infiltrated material is completed under the pressure. The ejector pin is used to remove the part from mould. It is used to produce net shape and small component. Figure 1.4 shows the schematic of squeeze casting infiltration.

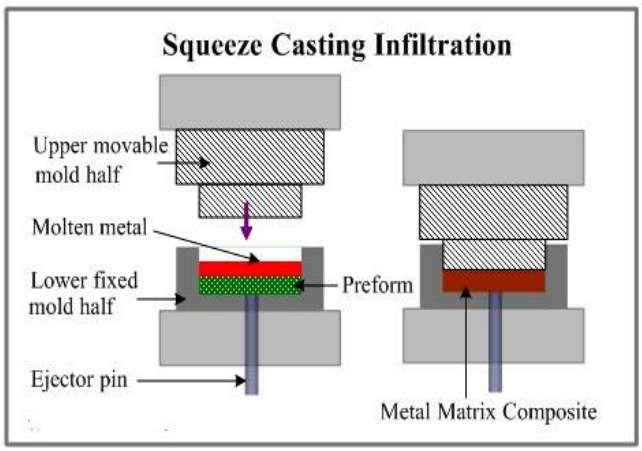

Figure 1.4: Squeeze casting Infiltration [www.substech.com]

- **Pressure Die Infiltration**

Pressure Die Infiltration is a forced infiltration method of liquid phase fabrication of Composites, using a Die casting technology. In this method, a movable piston (Plunger) is used to pressurize the molten metal as shown in Figure 1.5. A preformed dispersed phase (particles, fibers) is placed into a die (mold). The preform is allowed to fill with molten metal which enters the die through sprue and the pressure of a movable piston causes penetration within the dispersed phase. The ejector pins are used to remove the cast material from the ejector die.

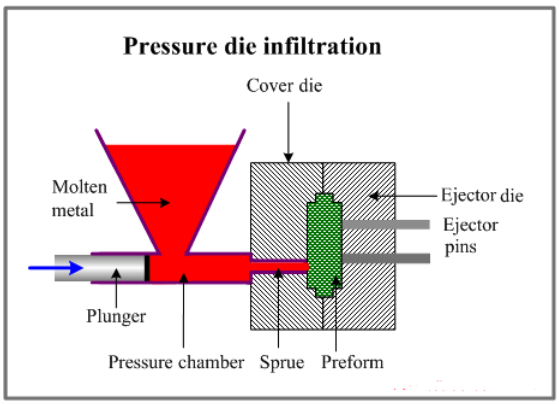

Figure 1.5: Pressure Die Infiltration [www.substech.com]

Solid State Processing: Solid state processing is typically a powder metallurgy based process, in which the matrix powder and reinforcement particles are mixed together and compacted to form a bulk shape. The methods to fabricate Solid State of AMC's are:

- Diffusion bonding
- Sintering

- **Diffusion Bonding**

Diffusion Bonding is a solid state fabrication method. In this method, foils form of matrix and long fibers form of dispersed phase are stacked in a specific order and are pressed together at high temperature. The finished laminated composite material obtained has a multilayer structure. Simple shape parts are fabricated by diffusion bonding process. Roll bonding and fiber/wire winding are the alternative of diffusion bonding.

- **Sintering**

Sintering fabrication of AMC's is a process, in which a powder of a matrix metal is mixed with a powder of dispersed phase in the form of particles or short fibers for subsequent compacting and sintering in solid state (sometimes with presence of some liquid). In sintering process the 'green' compact part is heated to the elevated temperature below melting point for consolidation of power grains, when the neighbouring powder particles are diffused by separate particle's material. In contrast to the liquid state fabrication of Metal Matrix Composites, sintering method allows obtaining materials containing up to 50% of dispersed phase.

1.2.5 Mechanical Properties of AMC's

Among the mechanical properties of the AMC's, Hardness, Tensile strength, percentage elongation, Impact Strength and wear behaviour are some important properties which are focused during the study of the present work.

- **Hardness**

Hardness is a measure of how resistant solid matter is to various kinds of permanent shape change when a force is applied. It is the property of material that resists it to undergo deformation usually by penetration. Hardness of material mainly depends upon strain, ductility, elastic stiffness, strength, plasticity, toughness and viscosity. It can also

be defined as the property of material that enables it to resist penetration, indentation, scratching and deformation.

Hardness is generally measured by tree techniques;

(a) Scratch: It measures fracture and plastic deformation due to friction from sharp object. Most common test is Mohs scale.
(b) Indentation: It measures the sample's resistance to deformation of material due to compressive load from a sharped object. Most common indentation tests are Rockwell, Vickers, and Brinell.
(c) Rebound: It is also called dynamic hardness. It measures height of the 'bounce' from a fixed height onto a material. It is measured by a device called Scleroscope. It is generally measured by Leeb rebound test and Benett hardness scale.

- **Tensile strength**

The tensile strength or the ultimate tensile strength (UTS) is the capacity of a material to withstand loads against the pulling (tensile) force or forces. The ability to resist breaking under tensile stress is one of the most important and widely measured properties of materials used in structural applications. Tensile strength is important in the use of brittle materials more than ductile materials. The results from the test are commonly used to select a material for an application, for quality control, and to predict how a material will react under other types of forces. It also enables to determine the transition of material from elastic to plastic deformation.

There are three types of tensile strength:

a) Yield strength - The stress a material can withstand without permanent deformation
b) Ultimate strength - The maximum stress a material can withstand
c) Breaking strength - The stress coordinate on the stress-strain curve at the point of rupture

In a simple tensile test, the test sample is securely held by top and bottom grips attached to the tensile or universal testing machine. During the tension test, the grips are moved apart at a constant rate to stretch the specimen. The force on the specimen and its displacement is continuously monitored and plotted on a stress-strain curve until failure.

- **Percentage elongation**

Percent elongation quantifies the ability of an element or compound to stretch up to its breaking point. It is measured by dividing the change in length (up to the breaking point) by the original length, then multiplying by 100. Materials with a higher percentage elongation can stretch more before breaking

Percent elongation = [(change in length) / (original length)] x 100

Elongation is a form of physical deformation, or a change in the physical shape or orientation of a material. Brittle materials, such as glass or most ceramics have low elongation while very ductile materials, such as rubber or some plastics have very high elongation. AMC's tend to have low to moderate elongation capabilities.

- **Impact Strength**

Impact strength or toughness is another important property of a material and to evaluate this, two types of tests are generally being carried out namely charpy and Izod tests. In the present work charpy tests have been employed to evaluate the impact strength of the AMC's. In this test, the notched specimen is broken by the impact of a heavy pendulum or hammer, falling at a predetermined velocity through a fixed distance. The test measures the energy absorbed by the fractured specimen.

- **Wear**

Wear is the phenomenon by which material removal takes from a surface due to interaction with mating surface. Plastic deformation at interface generally leads to wear which can be caused by the chemical reaction between the mating surfaces. Wear is a progressive loss of material surface due to mechanical cause such as contact and relative motion of surface. The presence of wear is shown by detached wear particles, material and shape changes of surface at tribological load or material removal from one surface of friction body to other. Figure 1.6 illustrates the different types of Wear.

Types of Wear

Wear can be classified into 5 types:-

a) Adhesive

b) Abrasive
c) Fatigue
d) Corrosive
e) Erosive

a) **Adhesive**

Adhesive wear occur when there is a localized bonding between two solid surfaces that leads the material transfer between surfaces or loss from either surface. In adhesive wear, it is necessary that both the surfaces should remains in contact. Adhesive wear can be reduced by contacting of surface with lubricating films and oxide.

b) **Abrasive**

Abrasive wear occurs when a hard rough surface slides across a softer surface. It occurs when two surfaces get interlocked and ploughing takes places in sliding. The two modes of abrasive wear are known as two-body and three-body abrasive wear. Two-body wear occurs when the grits or hard particles removes material from the opposite surface. The common analogy is that of material being removed or displaced by a cutting or plowing operation. Three-body wear occurs when the particles are not constrained and are free to roll and slide down a surface.

c) **Fatigue**

It occurs due to certain number of repeated contact between asperities due to high stresses and wear caused by a cycling loading during friction. The result of fatigue wear is severe plastic deformation.

d) **Corrosive**

Most of the metals are thermally unstable and makes reaction with the atmospheric oxygen to build up an oxide form, which developed a layer on the surface of metal and alloy. Corrosion wear is the gradual distortion of unprotected metal from surface by effect of acids, gas atmosphere etc.

e) **Erosive wear**

It is expected within a short time interval with extremely short sliding motion. It is caused by impacts of solid or liquid particles against the object surface. When a solid

particles impinge in a surface then the metal removal process take place. This type of wear is known as erosive wear. Wear produced is closely analogous to abrasion due to small impingement angle.

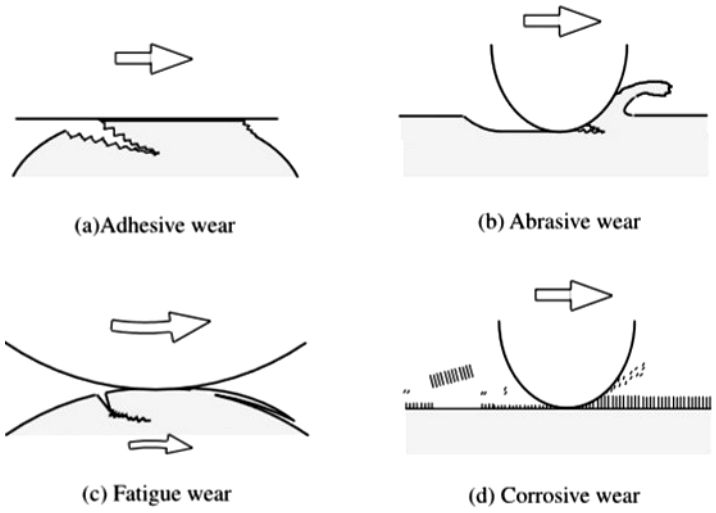

Figure 1.6: Types of wear (a) Adhesive wear (b) Abrasive wear (c) Fatigue (d) Corrosive wear (Kato and Adachi, 2001)

1.2.6 On Particulate filled AMC's

AMC's reinforced with particulates have now been used in various fields due to the low production cost and the ease with which they can be produced into the complex and desired shapes. AMC's filled with particulates are generally isotropic in nature and are less sensitive as compared to the long fiber composites where there can be a mismatch of thermal expansion between the matrix and the reinforcement **(Takei et al., 1991; Ranganath, 1997).** The use of particulates in aluminum composites is mainly due to the low cost of reinforced material, better thermal conductivity and density control, improved mechanical properties like hardness, strength and wear resistance and improved thermal expansion.

Hard particulate fillers consisting of ceramic or metal particles are being used these days to improve the performance of composites to a great extent. Particulate filled composites finds application in many engineering sectors which includes engine pistons, engine cylinders, connecting rods, engine push rods, braking systems, callipers assembles, gears, valves, belts, pulleys, turbines, compressors etc **(Florian et al., 2005).** The use of AMC's are also has been in use for research from the past few decades.Another important aspect associated with the particulate reinforced composites is the particle size, particle-matrix

interface, adhesion and particle loading. It is widely accepted that both the particle distribution and particle size have significant effects on the mechanical properties of the composites. The voids coexisted with the clustered particles and the large-sized particles can be treated as pre-existing cracks **(Tang et al., 2004).** The particles along with the voids cannot transfer any load from the soft matrix to the hard reinforcements, resulting in degraded mechanical properties. For a composite with a constant particle volume fraction, there is a close relationship between the particle size and the deformation behaviour of the composite. It has been observed that large sized particles usually decrease the density and mechanical properties of the composites. Decrease of the particle size contributes in improving the tensile strength and the yield strength because of the larger interfacial surface area and larger work hardening rate; but decreases the ductility of the composites **(Tang et al., 2004).** Usually the strength of a composite strongly depends on the stress transfer between the particles and the matrix. For well-bonded particles, the applied stress can be effectively transferred to the particles from the matrix resulting in an improvement in the strength. However, for poorly bonded micro particles, reduction in strength is found to have occurred **(Pukanszky and Voros, 1993)**.

1.3 OBJECTIVES

In the present work Aluminum matrix composites has been fabricated using SiC and B_4C particulate to carry out the experimental analysis and optimization of process parameters has been done using response surface methodology. More specifically the below mentioned work has been undertaken.

- Studying the alloying material and their effect on aluminum alloy.
- Preparation of aluminum alloy work-pieces.
- Evaluate the properties of work-piece prepared.
- Analysis and adoption of machining process.
- Modification in process according to requirement.
- Design the set of experiments for the given set of input and output parameters.
- Investigation of work-piece by experimentation according to the design of experiments.

1.4 ORGANISATION OF THESIS

The current thesis is divided into eight chapters followed by the references and is organized as follows:

- **Chapter 1:** This is the first chapter in the thesis which has been discussed above. It includes the brief study of aluminum alloys. This chapter further includes the introduction about aluminum matrix composites, the types of reinforcements, some important applications of aluminum composites, processing routes of the composites, mechanical properties, a brief study of particulate filled aluminum composites in particular and the thesis objectives.

- **Chapter 2:** Includes a literature review designed to provide a summary of the knowledge already available on fabrication processes of AMC's using the ceramic reinforcements; mainly SiC and B_4C and the research work on the mechanical behaviour of particulate reinforced aluminum composites by various investigators. The chapter also includes the literature survey on the wear behaviour of aluminium composites and the research gaps.

- **Chapter 3:** Includes the description of the starting materials, the experimental set-up details, fabrication process and the process parameters used for the production of composites. The chapter also includes the discussion about the sample preparation and test methods adopted for mechanical characterisation.

- **Chapter 4:** Includes with the details of the Response Surface Methodology (RSM) technique.

- **Chapter 5**: Includes the description of the microstructure study of the fabricated composites using X-Ray diffraction (XRD) patterns and Scanning electron microscope (SEM) study.

- **Chapter 6:** Presents the physical and mechanical characteristics of the composites and comparisons are drawn for hybrid and single particle reinforced aluminum composites.

- **Chapter 7:** Includes the study of dry sliding wear behaviour of aluminum hybrid and non-hybrid composites using RSM. This includes the various process parameters and their levels adopted for this study. A comparison has also been drawn between the theoretical and the experimental results by conducting confirmation tests.

- **Chapter 8:** Provides the conclusions/findings drawn from this research work and suggests some ideas and directions for future research on the related topic.

CHAPTER 2

LITERATURE REVIEW

The literature survey is studied in order to gather the knowledge provided by the previous researchers on the issues related with the work carried out in this thesis. The literature studies are mainly focused on the fabrication processes, mechanical properties and wear behaviour of aluminum matrix composites and the emphasis is been given on the particulate filled composites. The literature survey in this chapter is divided into three categories which are as follow:

- Based on the fabrication routes of AMC's
- Bases on the mechanical properties of AMC's
- Based on the wear behaviour of AMC's

2.1 BASED ON THE FABRICATION OF AMC'S

AMC's can be produced by different conventional methods available as also discussed in Chapter 1. Some of the methods that were most commonly adopted by the researchers are studied and discussed in this section. Each method of fabrication consists of its own merits and demerits and depending upon various factors such as material type, cost etc; fabrication process can be selected. Over the years a large number of researchers have produced the composite materials to carry out different type of investigations like mechanical studies, tribological and wear behaviour analysis along with many others.

2.1.1 Composite Fabrication through processes other then Stir casting

Yih and Chug, (1995) fabricated metal matrix composites through powder metallurgy route. The authors used three types of fillers namely TiB_2 with the particle size of 3 - 5 µm, Mo with particle size of 3.5 – 5.5 µm and SiC whiskers with 0.5 – 1.5 µm in diameter. All the three fillers were coated with copper metal using the coating process developed by the authors. The mixing of the copper powder and the filler was done in a ball mill for all the cases. The fillers were subjected to compacting and the sintering process by hot pressing. A graphite die was used for the compaction process with a pressure of 155 MPa to from green compact. Same die was used for hot pressing where 116 MPa of pressure was applied in the presence of nitrogen at 1000 °C for 25 minutes for Mo particles, 1000 °C for 20 minutes for TiB_2 particles and 950 °C for 20 minutes for SiC whiskers. For the comparison, the

composites were also fabricated by admixture method using the similar conditions. Figure 2.1 shows the fabrication process from the powder metallurgy method.

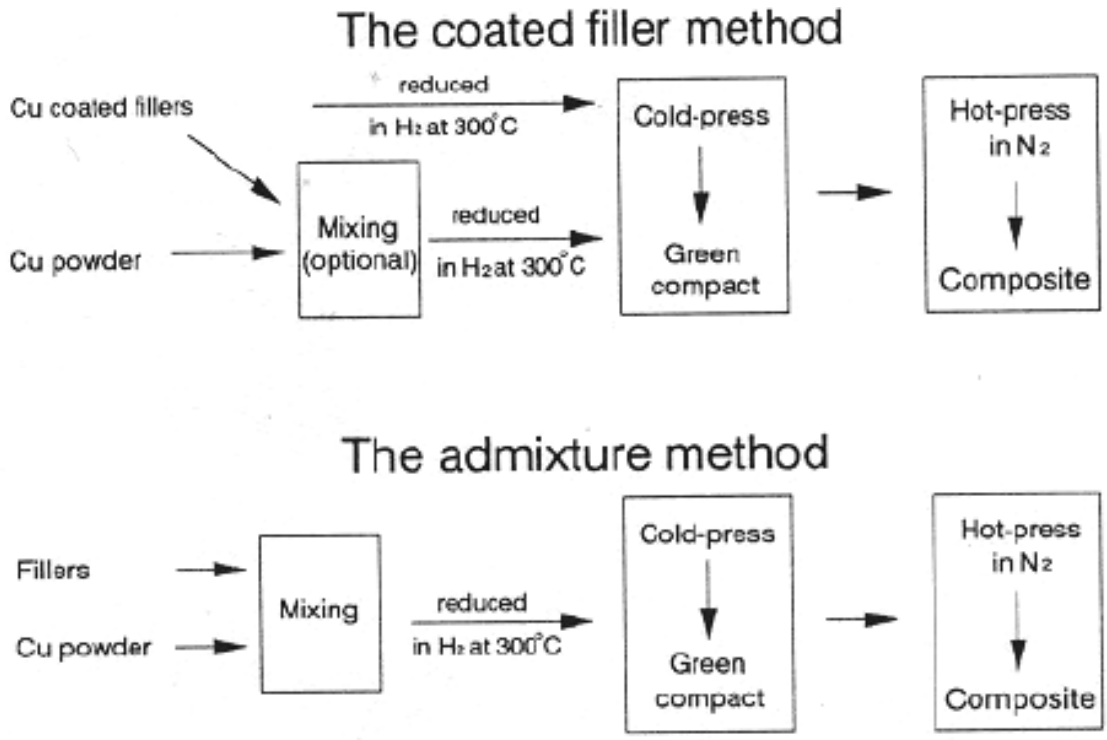

Figure 2.1 – Powder metallurgy illustrating the coated filler and the admixture method (Yih and Chug, 1995)

Kang and Chan, (2004) produced nanometric Al_2O_3 reinforced aluminium matrix composites through powder metallurgy route. The starting material was pure aluminium containing 3.8 % Cu, 2 % Mg, 3.8 % Si, and 12 % Fe. The average particle size of the starting material was 20 µm and the purity of Al_2O_3 powder was nearly 98.5 % with particle size of 50 nm. The steps followed here for composite fabrication involves wet mixing of the starting material and the nanometric Al_2O_3 powder followed by cold isotropic pressing and sintering. The slurry of starting material and the different volume fractions of Al_2O_3 was made in the presence of ethanol and then it was dried at 150 °C. The dried slurry was then compacted by cold isotropic pressing. The compacted specimens were sintered at 620 °C for 2 hours and the then removed at 450 °C for machining and further processing.

Besterci, (2006) fabricated strengthened aluminium compacts through powder metallurgy route. The compacted specimen were prepared with aluminium powder having particle size of 100 µm having carbon content of up to 3%. The reinforced particles of Al_4C_3 and the aluminium powder was compacted with 600 MPa and thermally treated at 450, 500, 550 and

600 °C. For the final compaction, the mixture was extruded under the temperature of 550 °C and the reduction rate of 94% was applied on the cross section.

Ahlatci et al., (2006) fabricated aluminium hybrid composites by pressure infiltration technique. The composites were fabricated using Al-Mg alloy and the particulates of SiC and Al_2O_3 with average diameters of 23 and 60 µm respectively. The schematic of the apparatus is shown in Figure 2.2.

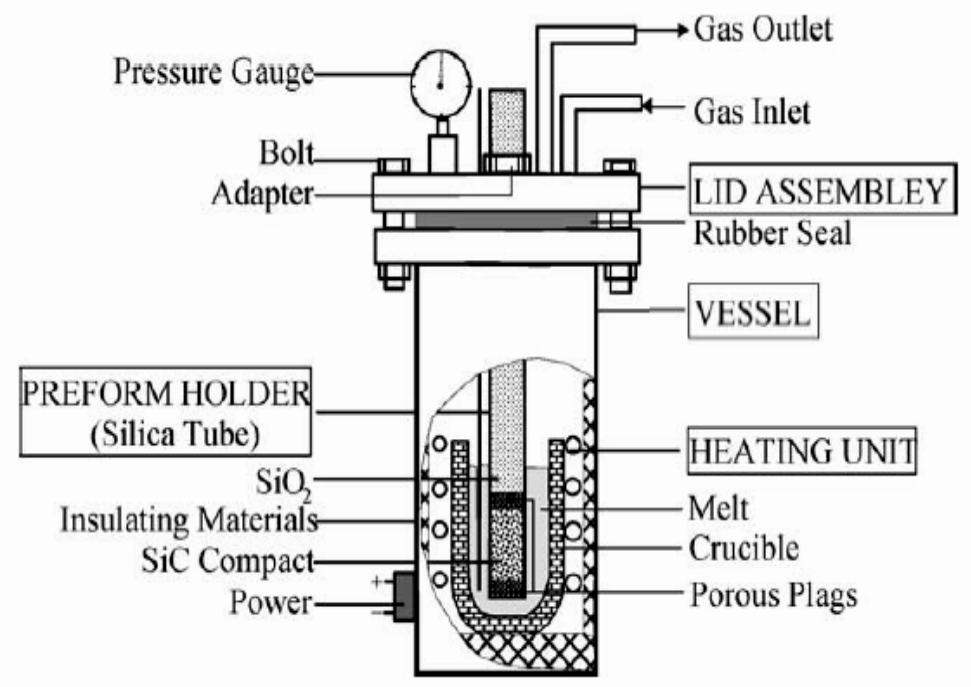

Figure 2.2 – Schematic of pressure infiltration apparatus (Ahlatci et al., 2006)

The apparatus has three major units namely heating unit, vessel and lid assembly. The particulate mixture of SiC and Al_2O_3 of 1.5 g was charged with the help of a preform holder which was made from silica tubes. The temperature of infiltration was maintained at 750 °C and the aluminium alloy was added to the particle mixture under the argon gas atmosphere. After the completion of infiltration process, the samples were removed and cooled down in the open atmosphere. Dry sliding metal-metal and metal-abrasive wear behaviour of composite were investigated. The result shows that as the matrix hardness and strength increased porosity and toughness decrease with increasing of Mg content. Metal-metal and metal-abrasive wear decrease with increasing Mg content. With increasing of test temperature, abrasive wear rate of hybrid composite increase.

Dobrzanski et al., (2007) used ceramic particles with AlSi12 eutectic aluminium alloy to manufacture aluminum matrix composites through pressurised infiltration process. Powders of Al_2O_3 and carbon fibers were mixed and sintered to from the ceramic preform. In order to improve the wettability of the Al_2O_3 with liquid aluminum, the internal surfaces of the ceramic preform were coated with nickel. Solutions containing metallic palladium were used for activation of the ceramics surface. A specially designed apparatus shown in Figure 2.3 was used to pump the reagents so as to cover the internal surfaces of the preforms.

Figure 2.3 - Device used for pumping operation of reagents through ceramic preforms (Dobrzanski et al., 2007)

After the completion of nickel coating, the preforms were heated at a temperature of 800 °C to avoid any chances to premature melt followed by infiltered with AlSi alloy. In this process of composite casting the preforms were preheated and placed in the die and then the melt was poured into the cavity. After this, the upper punch was placed and pressure of 100 MPa was applied with the help of a hydraulic press having plunger speed of 17mm/s. After the composite fabrication, the specimens were removed and allowed to cool down at normal room temperature.

Arslan and Kalemtas, (2008) worked on Al/SiC/B_4C composites produced through infiltration of 7075 Al alloys into the ceramic mixture of SiC and B_4C particles. The mixture of SiC and B_4C were preheated in a microwave oven to remove the moisture content from the particles. The particles of SiC and B_4C were ball milled in the presence of alcohol and the slurry has been made. After the milling process the slurry was dried out with the help of rotary evaporator. To prepare the preform, the SiC and B_4C mixture was pressed along one single axis under the load of 100 MPa. Infiltration of Al alloy has been carried out under the inert gas atmosphere at relatively low temperature. The production of composites was achieved at about 900 - 1420 °C. The 7075 alloy was infiltered into the SiC - B_4C preform and the rate of heating was 5°C/min up to 900 °C and after this temperature the heating rate was 10°C/min till the temperature reached 1420 °C. After the complete fabrication of composites, the samples were allowed to cool down at the rate of 10°C/min till the temperature reaches to 900 °C and then the rate of cooling afterwards was 5°C/min till the room temperature was attained.

Purohit et al., (2012) designed a horizontal ball mill for powder mixing and fabricate aluminium composites through powder metallurgy route. The powder of aluminium and SiC was mixed in a ball mill container also made with the combination of aluminium and SiC (Al – 15wt% SiC) so as to avoid contamination from the container walls. Figure 2.4 shows the horizontal ball mill. For the compaction of Al-SiC mixture, a die with 15 mm diameter and 30 mm length was made. The powder mixture in the die was pressed with the help of a mild steel punch using an arbor press. The compacted mixture was then removed from the die for the further processing.

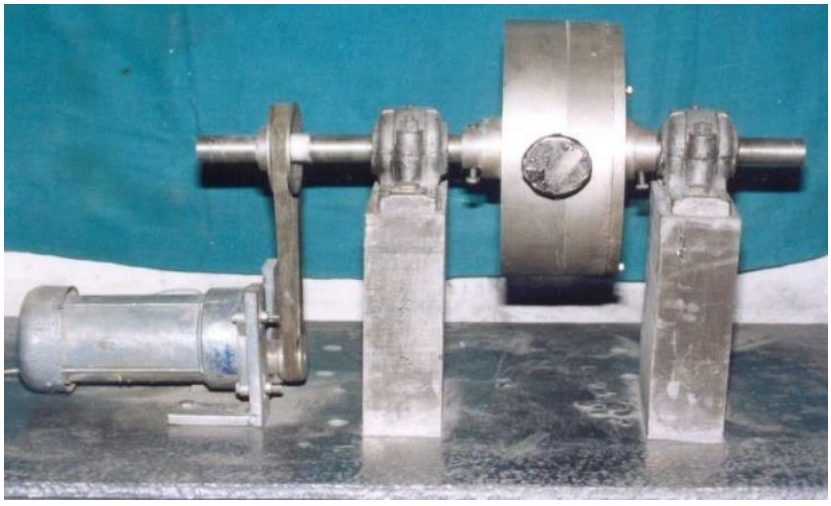

Figure 2.4 – Horizontal ball mill (Purohit et al., 2012)

Monje et al., (2013) fabricated aluminium/diamond composites through gas pressure infiltration process. The aluminium used in the process was 99.9% pure and the diamonds were in the form of particles. Preforms were prepared with the diamond particles and liquid aluminium was infiltered into the preforms by using gas pressure infiltration technique. Before the melting process, vacuum was attained in the preform until the preached to a value of 0.2 mbar. A piece of solid material was also placed over the preform during the fabrication process. In order to achieve the thermal equilibrium, the pressure was raised up to 5 bar using the argon gas in the pressure chamber designed for the infiltration process. After the composite fabrication, the specimens were removed and allowed to cool down at normal room temperature. These types of composites involve a main complication in handling and that is it becomes very difficult to machine these because of the hardness of diamonds and to perform the operations turns to be very hard.

Lee et al., (2014) used low pressure infiltration (LPI) technique to fabricate coal tar pitched carbon fiber reinforced aluminium composites (CF/Al). As suggested by the authors, this technique of fabrication has an added advantage that it is cost efficient because of the requirement of extremely low pressure only. The coal tar carbon fibers (CF) used in the process had a diameter of 11 μm and the density of 2.2 Mg/m^3. The unidirectional CF preforms were prepared by implanting Cu particles to CFs using the technique of spark sintering. Cu particles of bimodal size were prepared by mixing the average particle size of 2.25 and 77.79 μm. The powders of polyethylene glycol and Cu were mixed and scattered over the CF preforms so as to make proper spacing in the CFs for the infiltration of liquid aluminium. The mixture is then placed into the mould under the effect of pressure and voltage. The sintering temperature was maintained at 1123 K for 30 minutes under the vacuum environment of 2.7×10^{-2} Pa. The infiltration of liquid aluminium begins at 1073 K as shown in Figure 2.5 and after that the material cool down in the electrical finance. The temperature, grasp time and the pressure maintained during the fabrication process were 1073 K, 60 s and 0.8 MPa respectively.

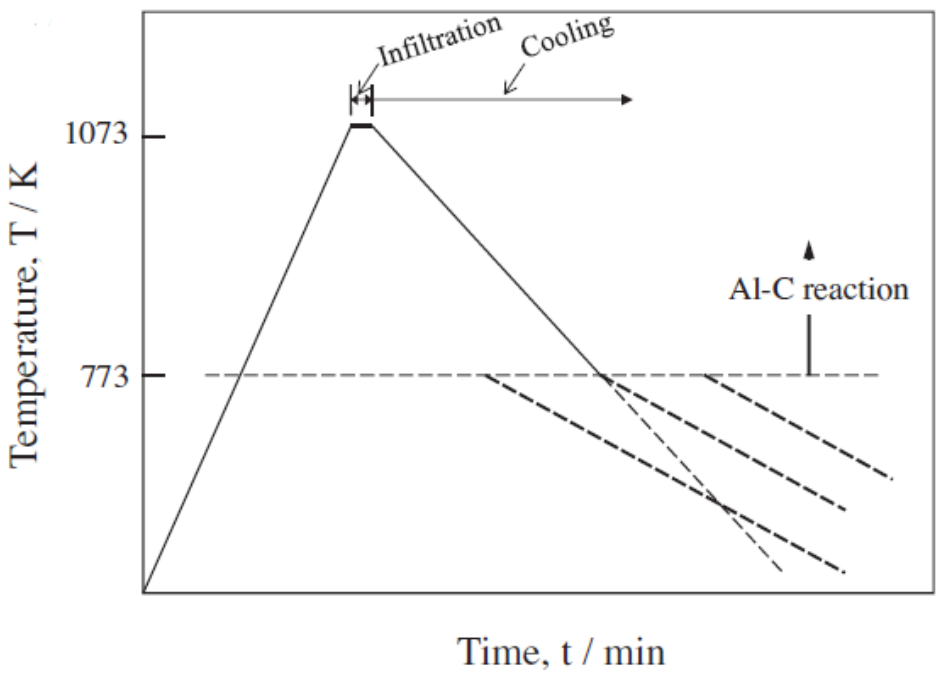

Figure 2.5 - Temperature versus time condition of LPI process for CF/Al composite (Lee et al., 2014)

Wang et al., (2015) used nano sized TiC_2 with 10-30 vol % to fabricate TiC_2/2009 Al composites through combustion synthesis with vacuum hot pressing followed by hot extrusion. The starting material used for the composite fabrication were Ti powder with particle size 48 µm, carbon nanotubes with 20-100 µm in length and 10-20 nm in diameter along with 2009 aluminium powder with average particle size of 75 µm. Al 2009 powder with 70, 80, 85 and 90 vol % were mixed with Ti and carbon nano tubes in a steel ball milling machine at 50 rpm for 50 hours. The mixture was then condensed in cylindrical from with 45 mm diameter and 30 mm in length. The process of compression and hot pressing was conducted in a vacuum container and the temperature during the process was recorded by W5-Re26 thermocouples.

2.1.2 Composite Fabrication through Stir casting

As the literature suggested a number of researchers employed different methods to fabricate composites but one method which attracts and becomes the most preferred fabrication process to large group of researchers in the method of stir casting. Although all

the methods have their own merits and demerits but the method of stir casting had an edge over the others and that is it can produce complex shaped casting and is highly economical **(Ravi et al., 2007; Shorowordi et al., 2003)**. High volume percentage of reinforcement that is up to 30 % can be used to produce the composites with significantly uniform distribution of particles through stir casting **(Pai et al., 1992).** Better chemical bonding between matrix and reinforcement particles can be achieved in stir casting process because of stirring action of particles in the melt **(Kok, 2005).** Owing to all these advantages, stir casting was also employed for composite fabrication in the present work. Convention stir casting method was in the practise from the past number of decades and various investigators had adopted this approach for the production of composites.

Singla et al., (2009) employed the stir casting technique for the fabrication of metal matrix composites (MMC). The schematic view of the experimental set is shown in Figure 2.6. to set up the system, the motor was coupled with a gear box and the stirrer. The mild steel stirrer with 45° angled blades was used for mixing the reinforcement in the metal matrix. The starting material used for mixing method was solid aluminium with 98.5 % purity and SiC particulates with 320 grit size. Experiments were conducted with different weight percentage of SiC (5%, 10%, 15%, 20%, 25% and 30%). In this experimental set up an oil filled furnace and a graphite crucible was used. The apparatus was also equipped with a fan for the supply of sufficient air. The particles of SiC were preheated at 1100 °C for 1 hour in the oven and the aluminium scrap was heated at 450 °C for 3-4 hours before placing into the graphite crucible. The stirrer was placed in such a way that approximately 30 % of the material should be below the stirrer and the rest should be along and above the stirrer. The reinforcement was added to the molten metal and stirred at approximately 600 rpm for nearly 10 minutes and after that the molten mixture was removed from the crucible and poured in a preheated sand mould. A thermocouple was also used in the experimental set which indicated the temperature inside the furnace.

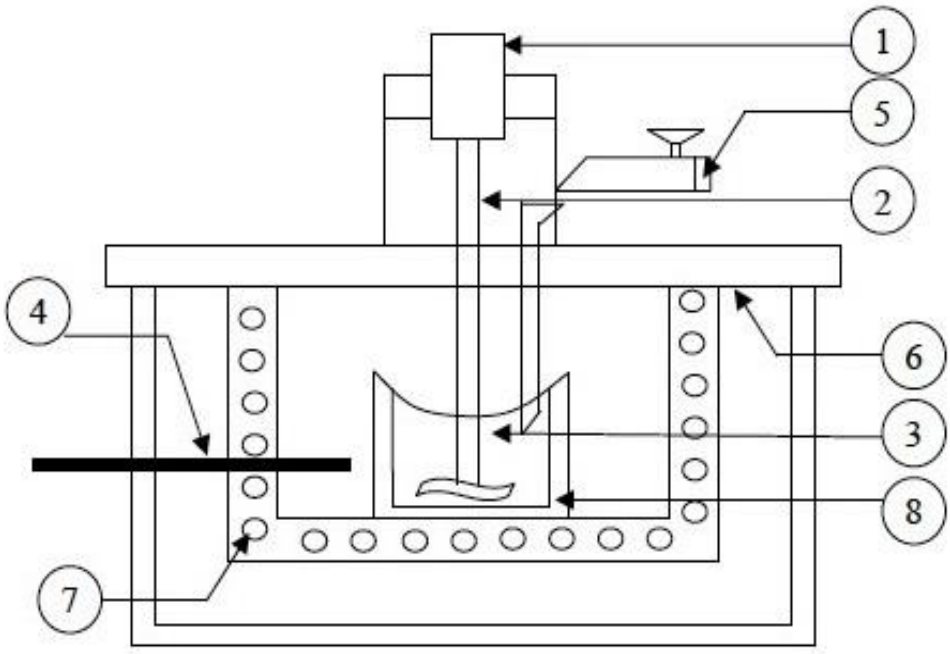

1. Motor
2. Shaft
3. Molten aluminium
4. Thermocouple
5. Particle injection chamber
6. Insulation hard board
7. Furnace
8. Graphite crucible

Figure 2.6 – Schematic view of Sir casting experimental set up (Singla et al., 2009)

Suresha and Sridhara, (2010) produced Al-SiC-Gr hybrid composites, Al-SiC and Al-Gr composites through stir casting route. The size of the SiC and Gr particles was 10-20 µm and 70-80 µm respectively whereas the densities were 3.22 g/cm^3 and 2.1 g/cm^3 respectively. For the hybrid composite equal fraction of SiC and Gr was used. The base material was melted in a graphite crucible at 700 °C placed in an electric furnace. The preheated particles of SiC and Gr were added to the molten mixture and stirred with the help of a graphite stirrer for about 15 minutes. After the complete mixing the homogeneous mixture was poured in a mould and allowed to solidify. All the composites were prepared from the same procedure and the dimensions of the cast composites were 10 mm in diameter and 50 mm in length. The specimens were then machined for further processing.

Akbari et al., (2013) worked on stir casting technique to fabricate A356/nano-Al_2O_3 composites. The authors used Al and Cu powder as reinforcement component which were milled with nano sized Al_2O_3 powder and incorporated in A356 alloy via vortex method to

produce the cylindrical composites. The powder ratio of Al/Al_2O_3 and Al/Cu was maintained as 1 during mixing. The average particle size of Al and Cu powder was 50 µm. The powders were milled continuously for 4 hours in a steel ball milling machine. For the fabrication of composites, 500 g of A356 was weighted and placed in a resistance finance equipped with a graphite stirrer. The powder mixture was wrapped in an aluminium foil and added to the molten A356 alloy to fabricate the composites. The stirrer was rotated at 450 rpm for 4, 8, 12 and 16 minutes at the temperature of 850 °C. The homogeneous mixture was then poured in a cylindrical mould as shown in Figure 2.7.

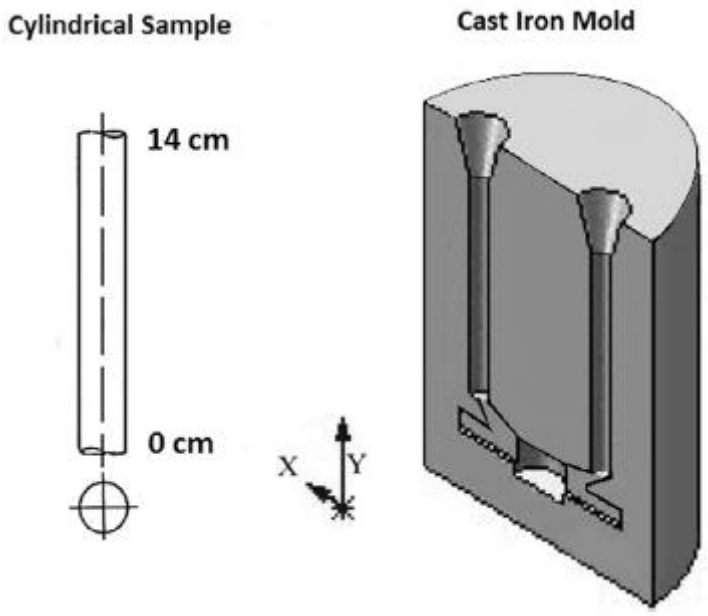

Figure 2.7 – Graphical scheme of the mould and cylindrical casting (Akbari et al., 2013)

The cylindrical mould was 40 mm in diameter and 140 mm in length. The produced castings were then removed from the mould and heat treated to attain the T6 condition.

Umanath et al., (2013) fabricated Al6061/SiC/Al_2O_3 hybrid composites reinforced with SiC and Al_2O_3. The average particles size of the reinforcements was 25 µm. The authors also suggested that the stir casting technique help in minimizing the oxidation level and porosity in the cast metal matrix composites. The process also helps in attaining the optimum wettability between the matrix and the reinforcement content. I Kg of Al6061 was heated and melted in a ceramic crucible at 725 °C. After complete melting and degassing of aluminium alloy with nitrogen gas, the reinforcement was added to the molten matrix. The four blades of the stirrer used for stirring operation was made of alumina coated stainless steel and the

purpose of alumina coating was to prevent the migration of ferrous ions into the molten mix. The stirrer was rotated at 600 rpm for 20 minutes to attain the homogeneous mixing. After the complete mixing, the molten mixture was tilted and poured in a permanent steel mould which was preheated at 250°C. The schematic view of the experimental set up is shown in Figure 2.8.

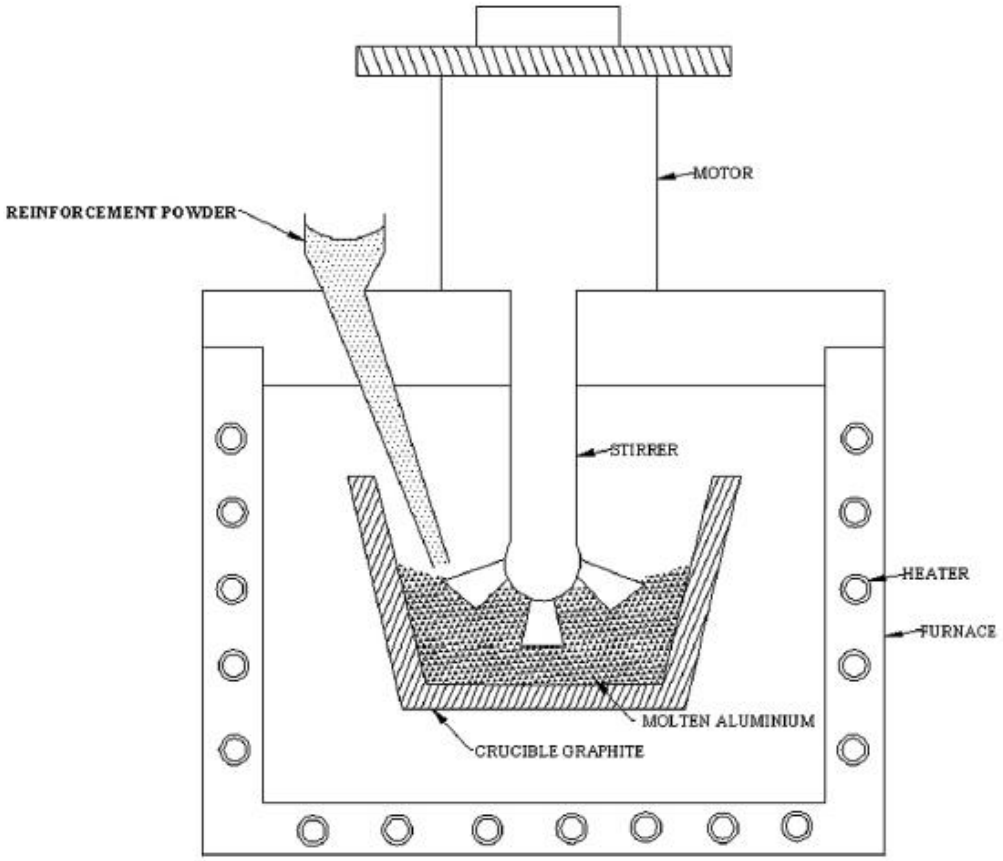

Figure 2.8 – Stir casting set up (Umanath et al., 2013)

Poovazhagan et al., (2013) also worked on Al 6061 alloy along with SiC and B_4C nano particulates to fabricate hybrid metal matrix composites. The vol % of 0.5, 1.0 and 1.5 for SiC and 1.5 fixed for B_4C was used during fabrication process. The experimental set up used for the process is shown in Figure 2.7 (a). The set up consists of a non ferrous furnace, a generator with transducer and argon gas generator. The ultrasonic processing device consists of a transducer with a power of 2 KW and a frequency of 20 KHz. The stainless steel crucible used in the process is shown in Figure 2.7 (b). The ultrasonic probe made of titanium alloy (Ti6Al4V) was dipped into the melt for about 30 mm height. The horn connected with the transducer is shown in Figure 2.7 (c). Al alloy was melted in the crucible at 680 °C and argon gas was supplied so as to avoid the oxidation of aluminium. The nano particles of SiC and

B_4C were added form the top into the molten matrix and stirring was continued to get the homogeneous mixture. The stirrer was then taken out and the horn was inserted into the mixture which was ultrasonically processes for about 60 minutes. The molten mixture was then poured into the preheated permanent steel mould and the cast composites in the steel mould are shown in Figure 2.9 (d). After solidification the composites were removed from the mould allowed to cool down.

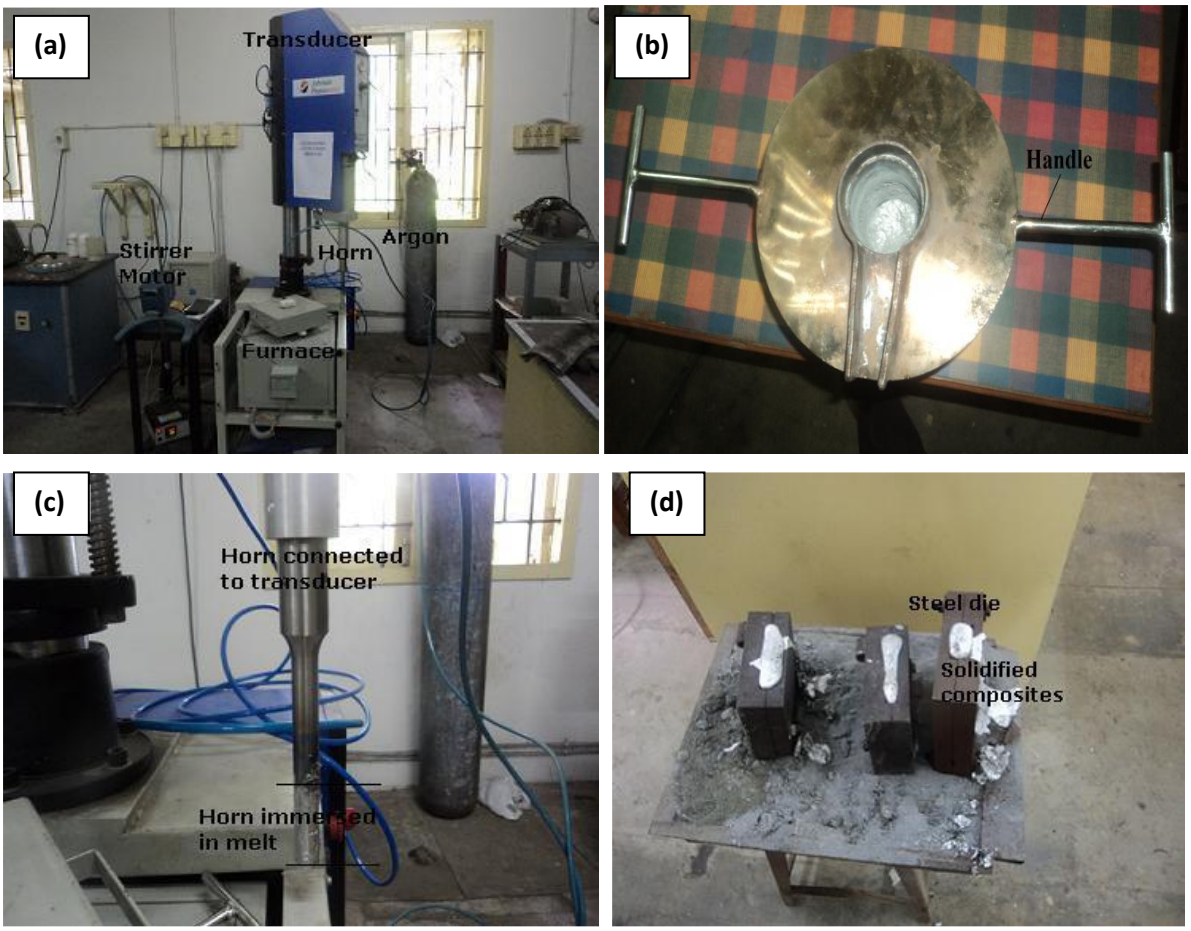

Figure 2.9 (a-d) – (a) Experimental setup, (b) SS crucible, (c) Ultrasonic horn and (d) Solidified composites (Poovazhagan et al., 2013)

Dwivedi et al., (2014) used electromagnetic stir casting for the fabrication of A356/SiC metal matrix composites. The added advantage of SiC particulates was suggested by the authors and that is SiC particles are not attacked by any acids or alkalis up to 800 °C. The average size of SiC particles used for the fabrication of composites was 25 µm. The experimental set up is shown in Figure 2.10. The apparatus consists of a Temperature recorder, thermocouple, three phase power supply, transducer, argon gas cylinder and a muffle furnace. A356 was

heated and melted in the muffle furnace and the temperature was recorded in the temperature recorder with the help of thermocouple wires. After melting of the alloy at 356 °C the liquid was poured in the crucible. SiC wt % was varied from 0 to 15 and added into the crucible above the molten matrix. Power was supplied from three phase motor through the transducer to run the stirrer by the electromagnetic field. The stirring was remained constant at 210 rpm for 7-10 minutes and the after this the mixture was removed from the crucible to obtain the solid cast.

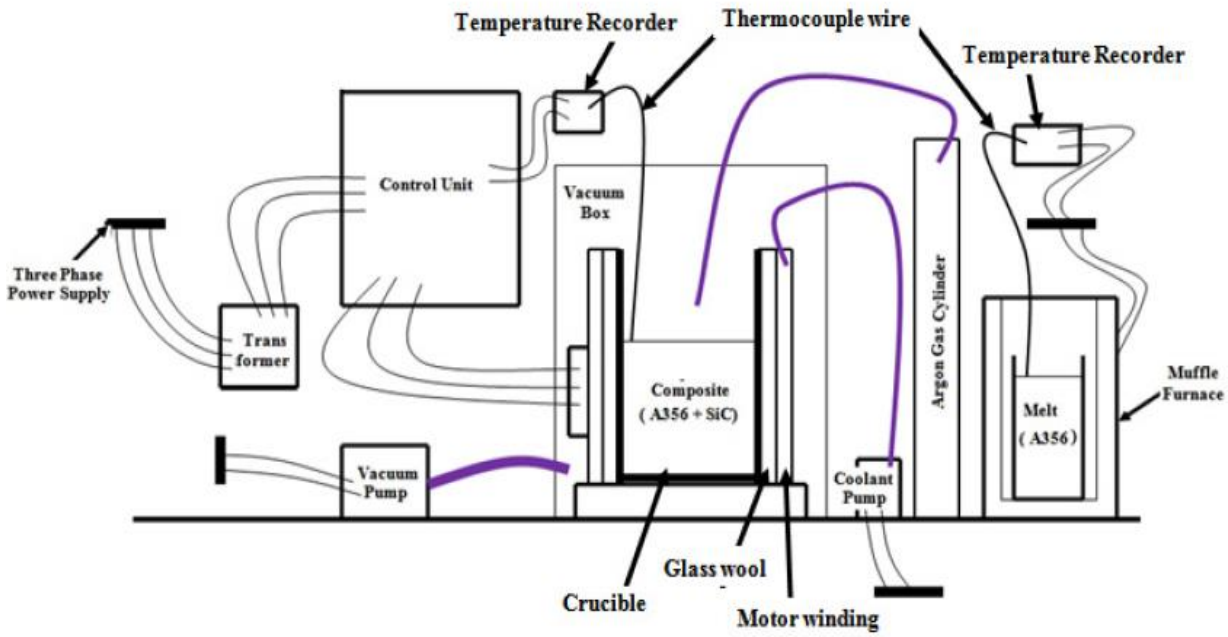

Figure 2.10 - Schematic view of electromagnetic stir casting set-up (Dwivedi et al., 2014)

Madheswaran et al., (2015) employed calcium carbide (CaC_2) and Boron Carbide (B_4C) particulates along with base material AA6063 for the production of aluminium matrix composites. The average particle size of CaC_2 and B_4C was 100 µm and 45 µm respectively. The stir casting apparatus used for the fabrication shown in Figure 2.11 consists of a motor of stirring operation, a stirrer, a crucible and an electric furnace. The apparatus was a simple stir casting apparatus in which AA6063 alloy was superheated in the graphite crucible at the temperature of 800 °C and then the temperature was lowered down below the liquids temperature so as to keep the matrix in the semi-solid state. At this temperature, the preheated powders of CaC_2 and B_4C with different volume fraction (10 % B_4C, 8 % B_4C + 2 % CaC_2, 9 % B_4C + 1 % CaC_2) were added into the matrix. The temperature in the crucible was again raised to accomplish the complete melting of the matrix and the mixture of reinforcement and

liquid matrix was stirred continuously at 350 rpm for 10 minutes. The mixture was then poured in a permanent mould and the castings later on removed from the mould.

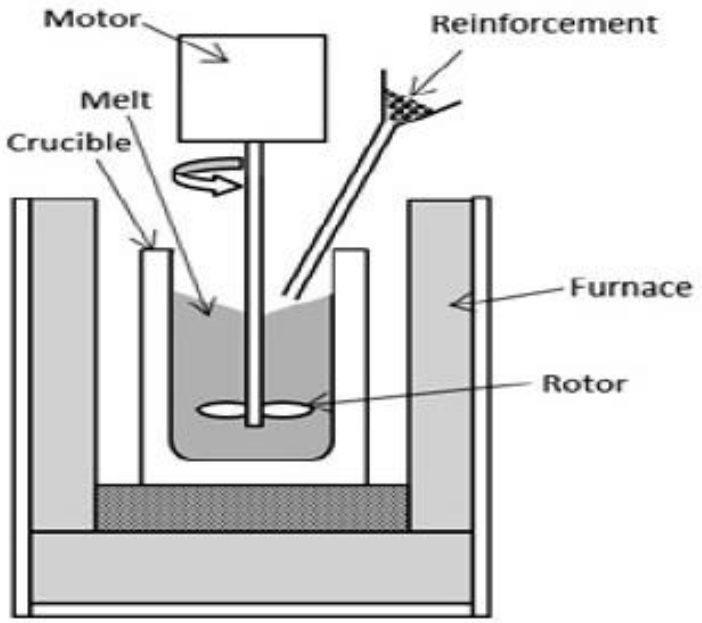

Figure 2.11 – Schematic of the experimental set up (Madheswaran et al., 2015)

Ibrahim et al., (2015) worked on B357 alloy containing Mg, Fe, and Sr. Pure magnesium was added to the B357 alloy to obtain the magnesium levels of 0.4 wt. %, 0.6 wt. % and 0.8 wt. %. The alloy was melted and the homogeneous mixture was poured in pre heated ASTM B-108 permanent mold shown in Figure 2.12. The cast as produced from the mould was in the shape of the tensile specimen which was thereafter processed further for mechanical investigation.

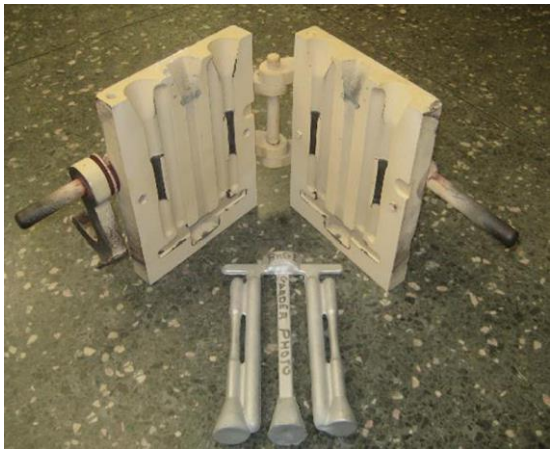

Figure 2.12 - ASTM B-108 permanent mold used for casting (Ibrahim et al., 2015)

Das et al., (2016) fabricated Al–4.5%Cu-5%TiC MMCs through stir casting technique. The authors also suggested that the stir casting technique helps in attaining good bonding between the matrix and the reinforcement along with fast cooling and less porosity in the fabricated product. The schematic stir casting apparatus is shown in Figure 2.13 which consists of a speed control motor used to control the stirrer speed, a furnace, graphite crucible and a graphite stirrer.

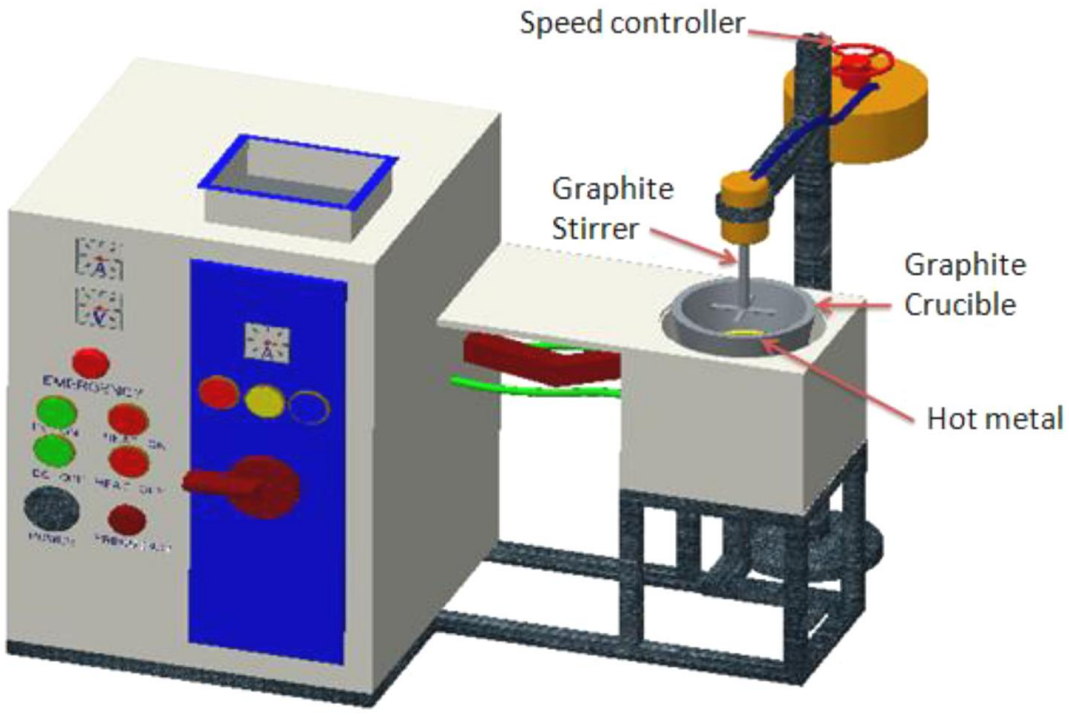

Figure 2.13 - A schematic view of the induction melting furnace (Das et al., 2016)

Titanium and copper with 99.8% purity, aluminium with 99.9% purity and charcoal powder with particle size 100 µm were used as the starting material. Pure aluminium was heated and melted at 685 °C in a graphite crucible in the electrical furnace and afterwards copper was added at the temperature of 800 °C. The mixture of aluminum and copper was stirred at different stirring speeds according to the different set of experiments. Titanium was introduced into the crucible at 1000 °C and stirred continuously for 10 minutes. As the temperature in the crucible reached at 1100 °C, the charcoal powder wrapped in an aluminium foil was introduced in to the crucible and stirred continuously to form Al-Cu–Ti melt. After the complete mixing of Aluminium, titanium and charcoal, the liquid mixture was poured in the rectangular preheated metallic mould with the size of 30mm×30mm×80 mm.

The cast was then allowed to cool and solidify in the mould and then removed for further processing.

Li et al., (2016) followed sophisticated stir casting route for the fabrication of B_4C reinforced aluminium matrix composites. The schematic stir casting apparatus is shown in Figure 2.14.

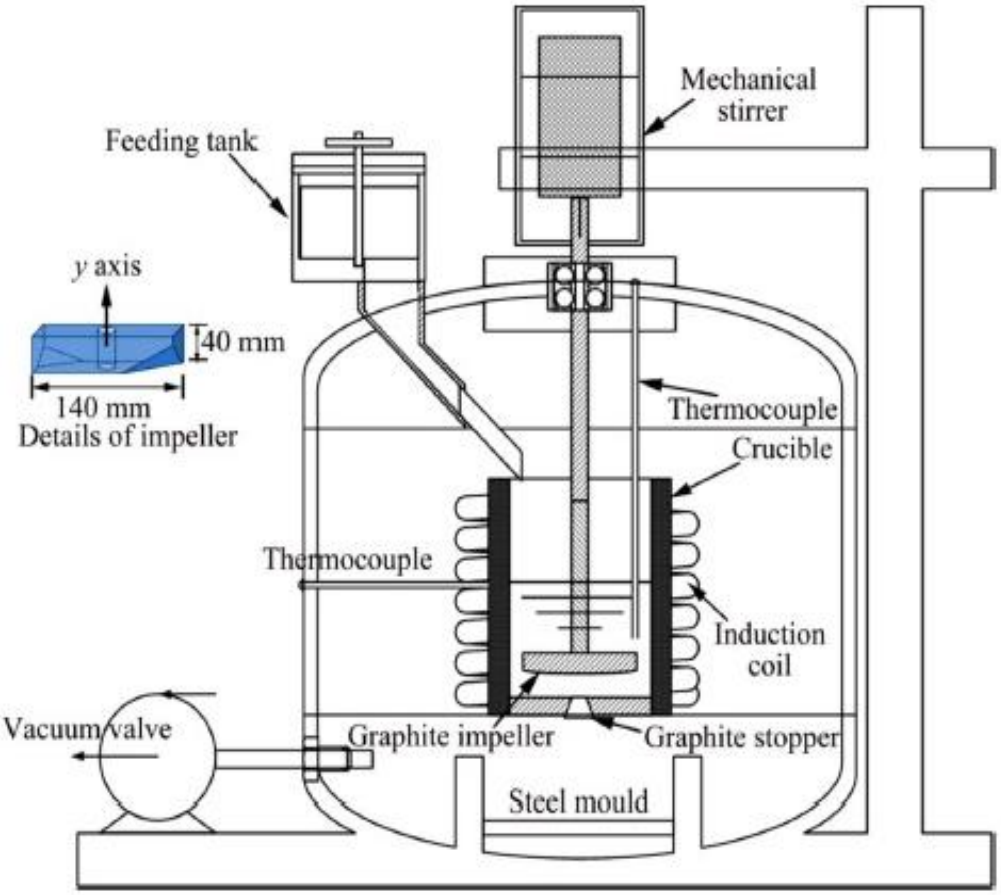

Figure 2.14 – Schematic of Designed equipment (Li et al., 2016)

It consists of a graphite crucible placed at the center of the furnace surrounded by induction heating coils. Thermocouples were used to maintain the heating inside and outside of the crucible. A stopper was provided at the bottom of the crucible to pour the liquid slurry into the steel mould. There was a provision to rotate and adjust the height of the stirrer in the crucible. A feeding tank was used to feed the reinforcement into the crucible during the stirring operation. The function of the vacuum tank is to create the vacuum in the whole system and the argon gas was passed to improve the wettability between the ceramic powder and the aluminium. Initially aluminium was heated and melted in the crucible at about 750 °C and B_4C powder wad preheated for 2 hours at 400 °C. After the melting of the aluminium, the

furnace was opened to remove the slag. After this, the preheated B_4C and Mg (99.9 % pure) were added into the furnace through the feeding tank. The mixture was stirred at 550 rpm and continued for 15 minutes. Finally, the stirred wad stopped and the stopper was pulled out to collect the slurry in the mould.

Kant and Verma, (2017) elaborate the fabrication through stir casting technique taking ceramic particles as reinforcement. As suggested by the authors, the main factors that are primarily to be taken care of during fabrication through stir casting are stirring speed, stirring time, blade angle, pouring temperature, solidification rate, reinforcement particle size and percentage. The stir casting apparatus shown in Figure 2.15 was similar to the one used by previous researchers. The apparatus consists of a mechanical stirrer, muffle furnace, heating element, stirring motor, a shaft, impeller of stirrer and a refractory material.

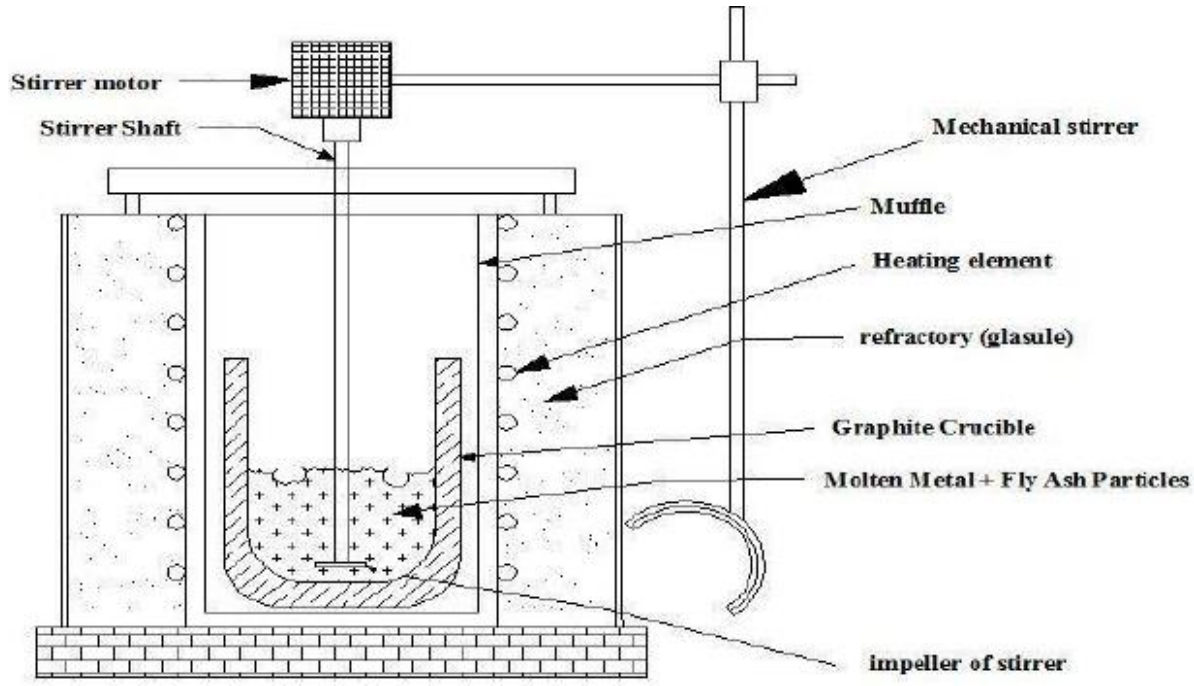

Figure 2.15 - Schematic Stir casting apparatus (Kant and Verma, 2017)

2.2 BASES ON THE MECHANICAL PROPERTIES OF AMC'S

This section of the literature covers the findings on the mechanical characteristics by the investigators over the years. Authors have used different types of ceramic particles with the base material to fabricate the composites and study their mechanical behaviour using distinct methodologies.

Kok, (2005) examined the hardness, tensile strength, density and porosity of the 2024 aluminium alloy metal matrix composites fabricated using Al_2O_3 ceramic particles. The authors used different weight percentage and particle size to evaluate the mechanical and physical characteristics. The density of the composite was calculated using Archimedian method hardness of the composites was determined using the Rockwell hardness tester with a 2.5 mm steel ball indenter and applying a load of 187.5 Kg. The tensile strength was evaluated at Hounsfield testing machine. The density of the composites increases with the increase in particle size and weight percentage of reinforcement whereas it was found that the porosity increases with the decreasing particle size and increases with the weight percentage of reinforcement. Figure 2.16 shows the variation of density and porosity with the particle size and reinforcement content. The authors also reported an increase in hardness and tensile strength with the decreasing particle size and increasing reinforcement content. Figure 2.17 shows the variation for hardness and tensile strength.

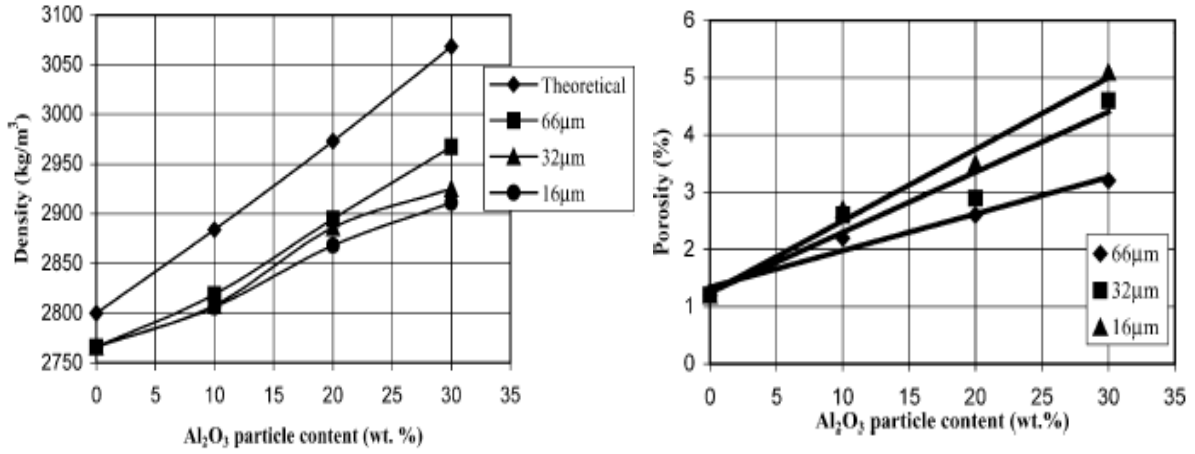

Figure 2.16 - The variation of density and porosity with Al_2O_3 particle content and size (Kok, 2005)

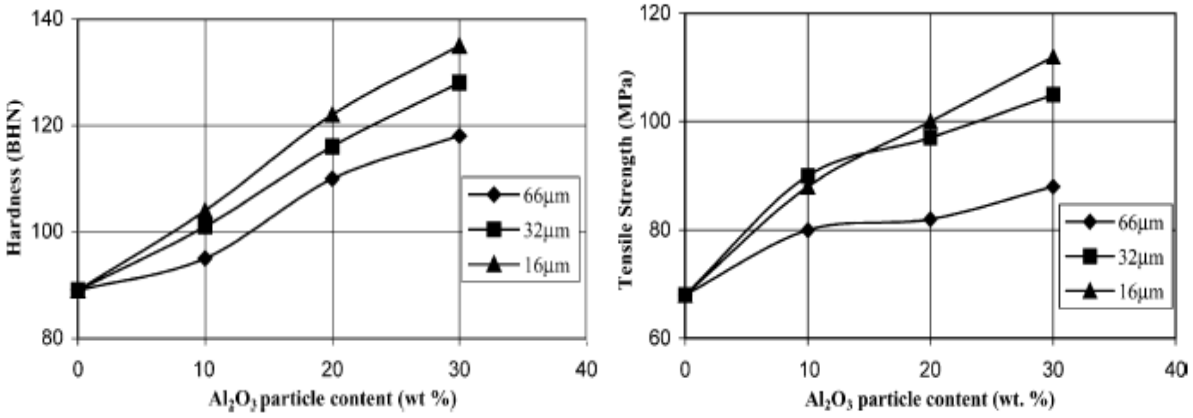

Figure 2.17 - The variation of hardness and tensile strength with Al_2O_3 particle content and size (Kok, 2005)

Ahlatci et al., (2006) fabricated aluminium hybrid composites by pressure infiltration technique. The composites were fabricated using Al-Mg alloy and the particulates of SiC and Al_2O_3 with average diameters of 23 and 60 µm respectively. The authors found an increase in hardness and decrease in porosity with the addition of Mg in the matrix. The addition of Mg also increases the compression strength of the hybrid composites. Figure 2.18 shows the variation in hardness and compressive strength as found by the investigators.

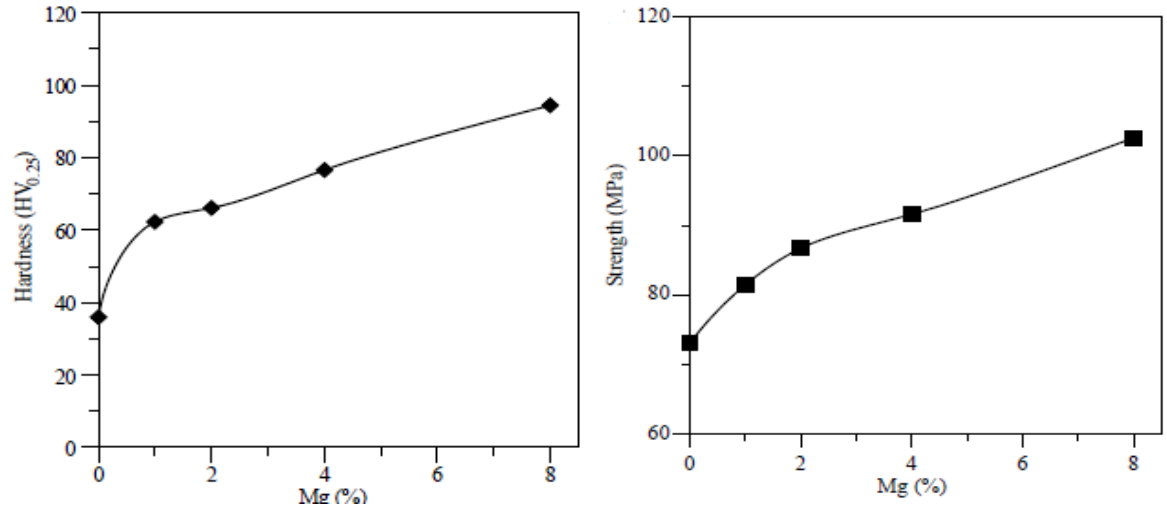

Figure 2.18 - The variation of the matrix hardness and compressive strength with Mg content (Ahlatci et al., 2006)

Aigbodion and Hassan, (2007) studied the effect of Silicon carbide (SiC) reinforcement on microstructure and properties of Al-Si-Fe/SiC particulate composite. Density was evaluated

using the mass and volume of the tensile specimen. Porosity was calculated using the Equation 2.1 where,

$$\frac{W-D}{W-S} \times 100 \qquad \ldots\ldots\ldots\ldots\ldots\ldots [2.1]$$

W represents the weight of the water soaked specimen, *D* is the weight of the specimen that was baked at 110 °C for 3 hours in a baking oven, and *S* represents the specimen weight that was boiled for 30 minutes. The hardness of the composites was determined using the Rockwell hardness tester with a 1.56 mm steel ball indenter and applying a minor load of 10 Kg and a major load of 100 Kg respectively. For the evaluation of Impact strength and the tensile strength, the charpy impact testing machine and the universal tensile testing machine was employed respectively. The authors reported increase in tensile strength, hardness, and porosity with slight decrease in impact energy and density with increase in wt % of reinforcement in metal matrix. The Variation of Density, Porosity, Hardness and tensile strength with increase in weight percentage of SiC is shown in Figure 2.19

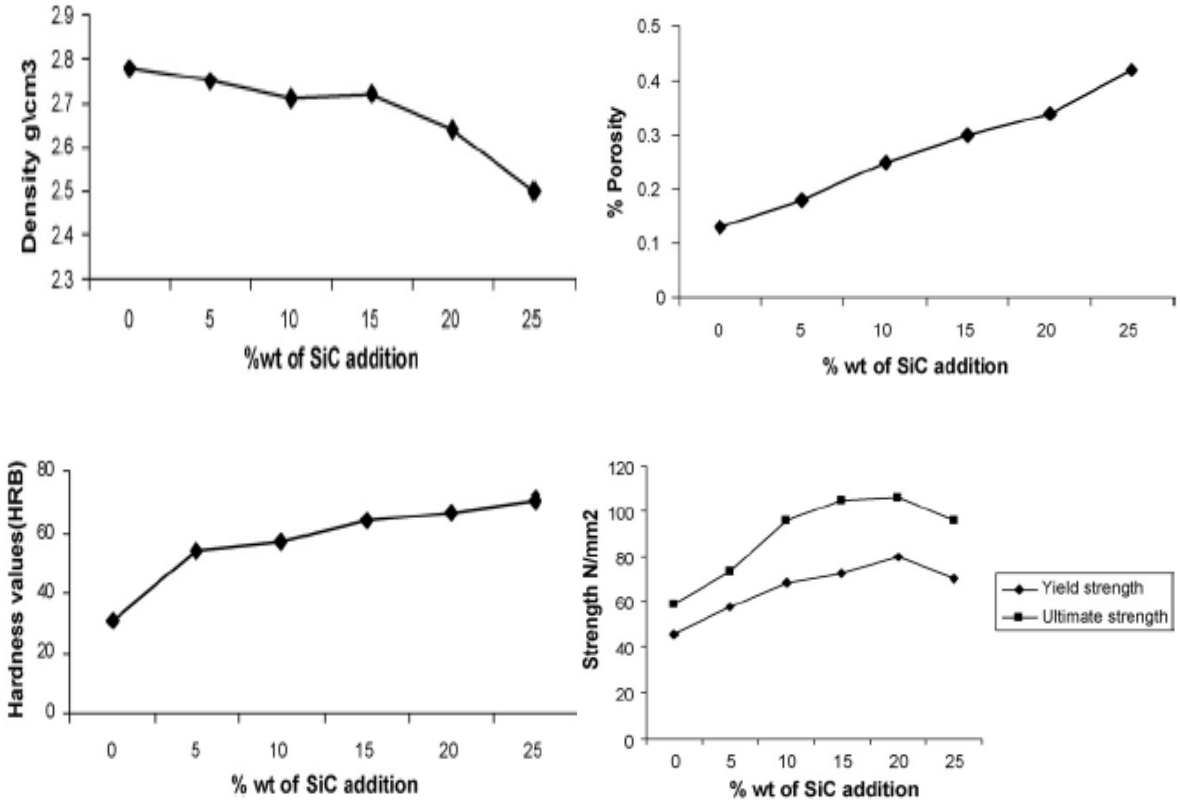

Figure 2.19 - Variation of Density, Porosity, Hardness and tensile strength with SiC addition (Aigbodion and Hassan, 2007)

Ozben et al., (2008) investigated the mechanical and machinability properties of SiC reinforced aluminium matrix composites. The SiC was added in weight percentage of 5, 10 and 15 to form the composites. The equipment that was used to investigate the mechanical properties were Precisa 125 A/SCC model equipment for density, Rockwell hardness tester for hardness and Monsanto Tensometer Type "W" equipment for evaluating the tensile strength. The authors found that with the increase in reinforcement, the density and hardness of the composites increases however, the toughness or the impact strength decreases with the increase in reinforcement content. The tensile strength of the composites found to be increased up to the addition of 10 weight % of reinforcement. Beyond this weight %, the authors reported some decrease in tensile strength which was due to the broken particles in the structure and the inadequate bonding between the matrix and reinforcement. The variation of impact strength, hardness and tensile strength with the addition of SiC particles in the matrix is shown in Figure 2.20.

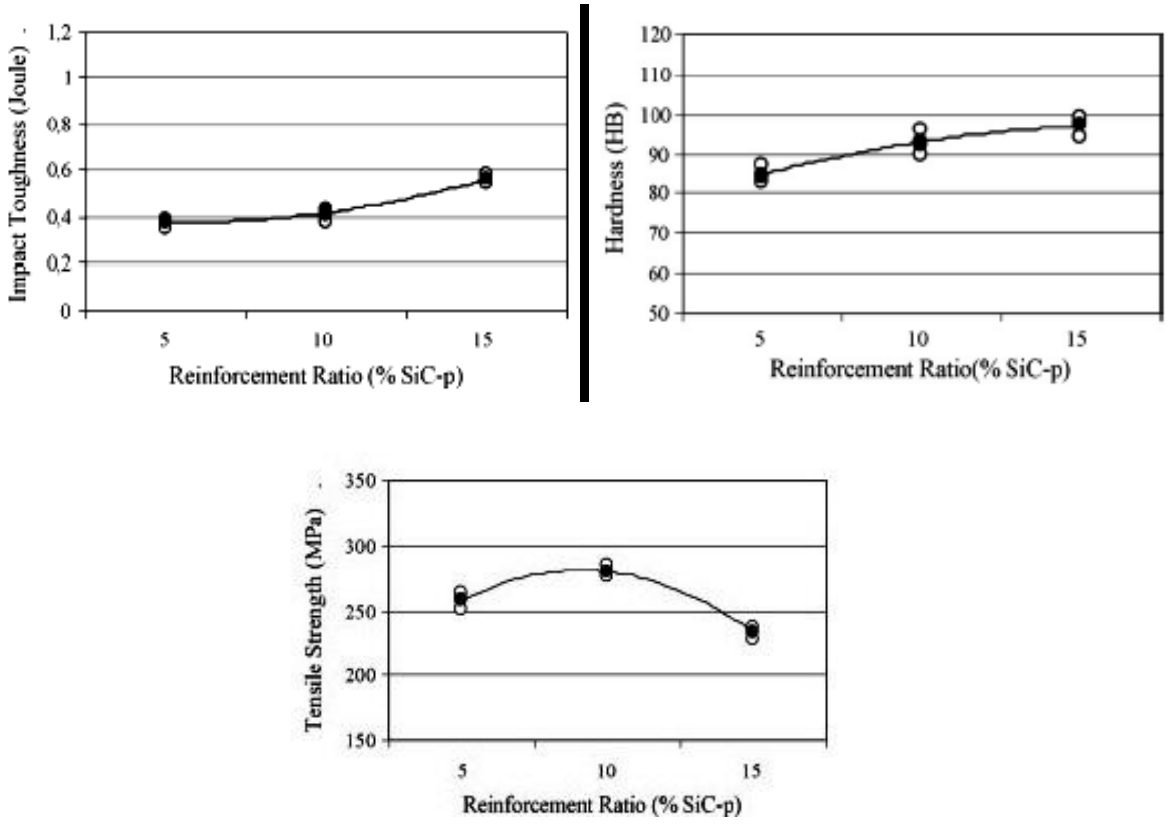

Figure 2.20 – Variation in Impact strength, hardness and Tensile Strength with SiC addition (Ozben et al., 2008)

Kumar et al., (2010) fabricated Al6082/SiC and Al7075/Al_2O_3 composites to conduct the mechanical and tribological characteristics. The tests were conducted as per ASTM standards

and all the specimens were prepared accordingly. Shimadzu Japan Vickers testing machine was used for hardness evaluation and a universal testing machine with 40 ton capacity was employed to conduct the tensile strength analysis. The authors have evaluated the mass and volume of the specimens to evaluate the density of the composites. The results revealed that the density increases with the addition of filler material in the matrix for both the Al6082/SiC and Al7075/Al_2O_3 composites. However, Al7075/Al_2O_3 composites exhibit higher densities as compared to Al6082/SiC. The hardness was evaluated using a diamond indenter and the result shows that the reinforcement addition enhances the hardness for both the composites. Again the Al7075/Al_2O_3 composites exhibit higher hardness as compared to Al6082/SiC. The trend was same for the tensile strength as well; the tensile strength also gets higher as compared to the base material and Al7075/Al_2O_3 composites display superior hardness than that of Al6082/SiC. The graph of density, hardness and tensile behaviour of both the composites against the addition of reinforcement particles is shown in Figure 2.21.

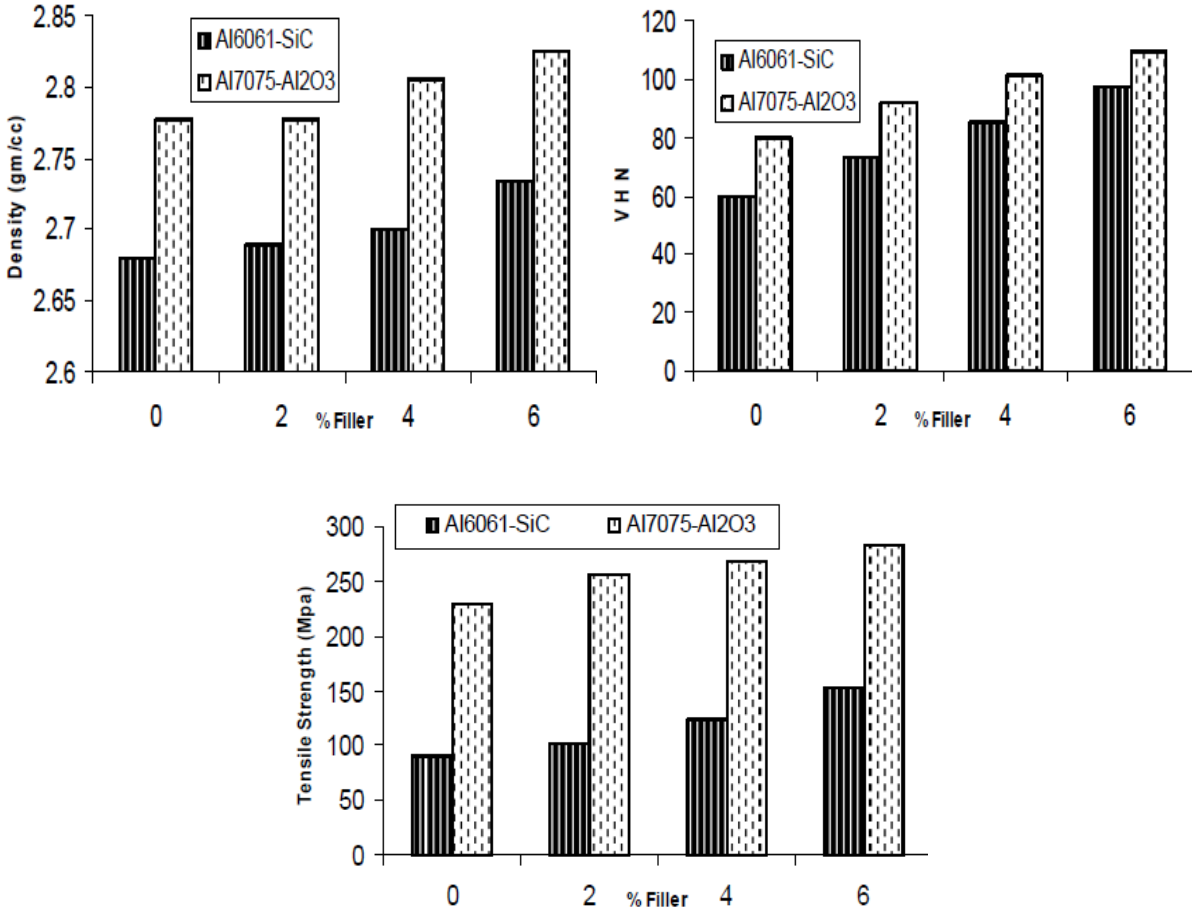

Figure 2.21 – Graph of Density, Hardness and Tensile Strength with increasing %'age particulate content (Kumar et al., 2010)

Wang et al., (2011) investigated the combined effect of particle size and the distribution on the mechanical behaviour of SiC reinforced Al-Cu composites. The authors of this work found that smaller the ration of matrix to reinforcement size (matrix/reinforcement size) better will be the distribution of particles within the matrix. The Al-Cu and the SiC reinforcement with particle size of 4.7 µm and77 µm were mixed in a V-shaped rotor with a speed of 35 rpm for 2h, 7h, 16h and 40hrs. The tests were conducted to evaluate the yield strength, ultimate tensile strength and elongation in the SiC reinforced composites. The Figure 2.22 shows the variation of Yield strength, ultimate tensile strength and elongation of the composites containing 20 vol. % SiC particles with different mixing time. The authors reported that the yield strength and the ultimate tensile strength for the composites fabricated with SiC having particle size 4.7 µm was superior as compared to the composites fabricated with particle size of 77 µm. However the result for elongation was opposite to that of yield strength and the ultimate tensile strength.

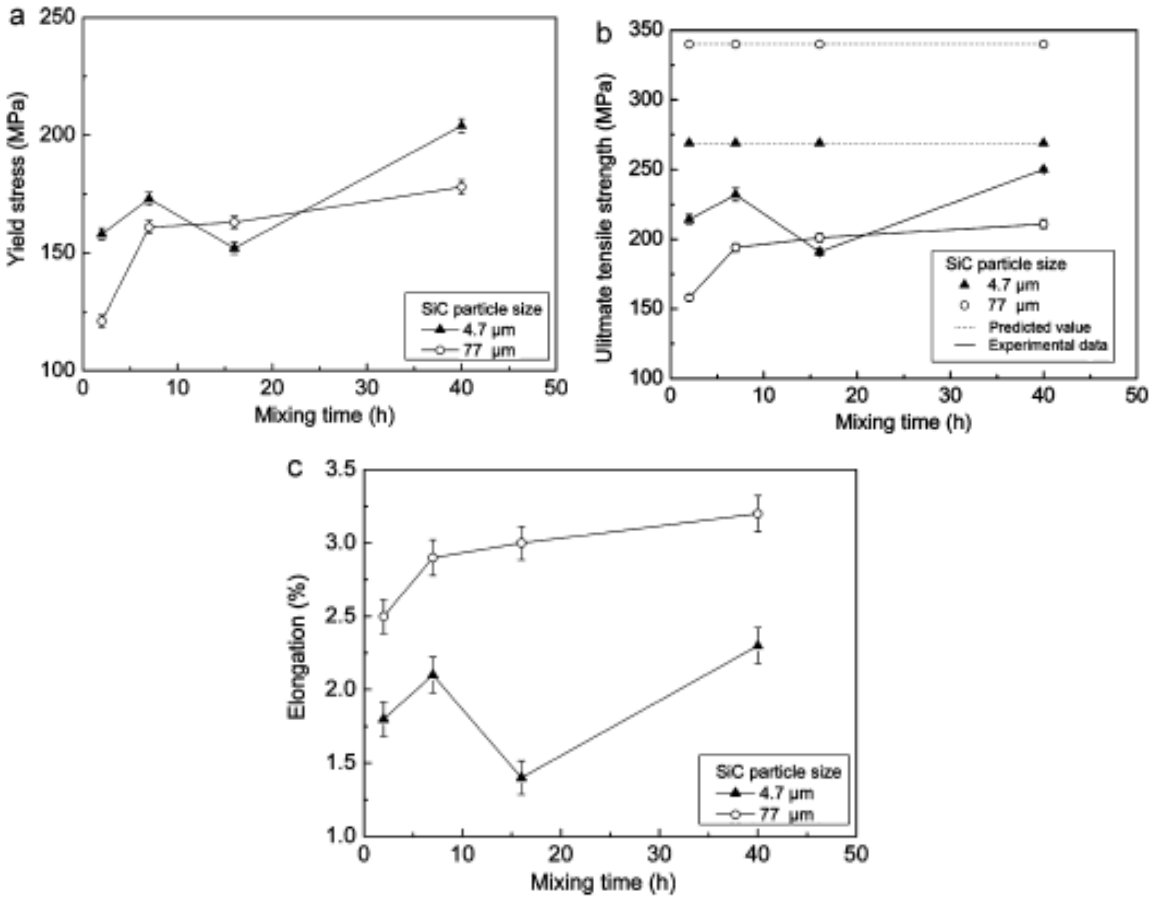

Figure 2.22 - (a) Yield strength, (b) ultimate tensile strength and (c) elongation of the composites containing 20 vol. % SiC particles with different mixing time (Wang et al., 2011)

Mazahery and Shabani, (2012) used different volume fractions of B_4C to fabricate A356/B_4C composites and studied the mechanical behaviour which includes the study of porosity, tensile behaviour and hardness. The porosity was evaluated using the difference between the observed and the expected density in the cast samples. The hardness was calculated using the Brinell hardness testing machine with a indenter ball diameter of 2.5 mm at a load of 31.25 Kg. The hardness was calculated at 5 different places on the sample and the average value was taken. Universal tensile testing machine was used to carry out the ultimate tensile strength. The variation of porosity, hardness and tensile strength with increase in B_4C content is shown in Figure 2.23.

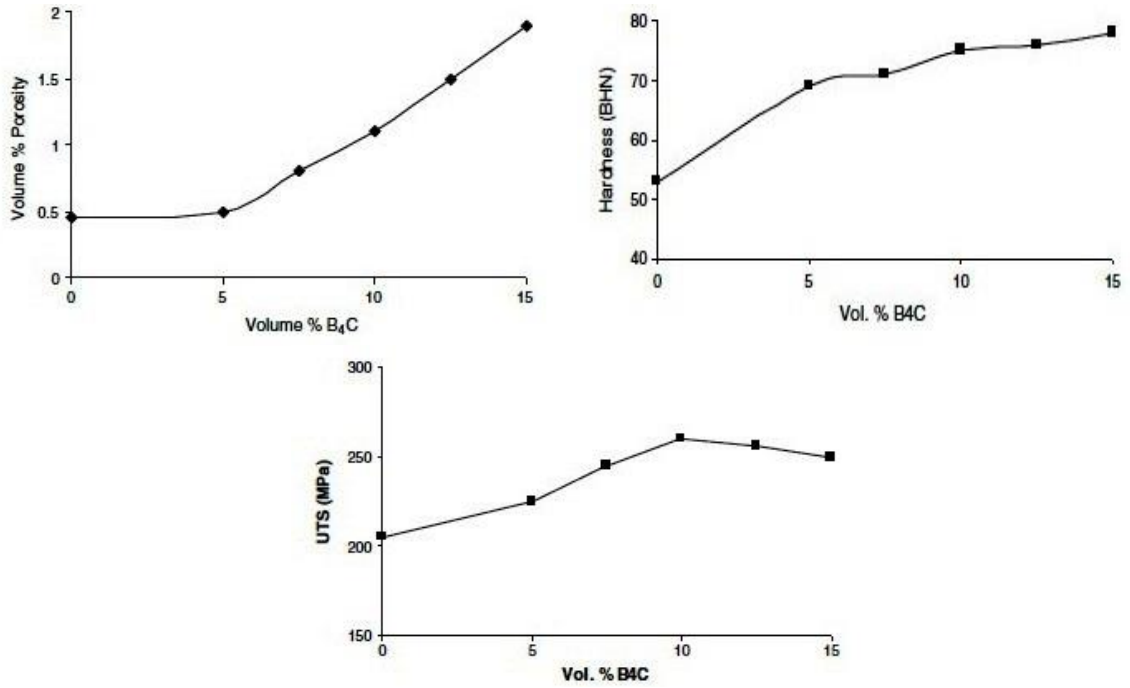

Figure 2.23 - Variations of porosity, hardness and tensile strength value with addition of B_4C Content (Mazahery and Shabani, 2012)

The results revealed that increasing the reinforcement content enhances the porosity levels in the composites and this is because of the increasing gas layers around the particles and the high number of gaps between the adjacent particles. The authors also reported an increase in the hardness with the increased volume % of B_4C Content and this was because the B_4C particles act as the obstacle in the dislocation of the particles. As the B_4C content increases in the matrix, the dislocation of particles was even more restricted and this eventually increases the hardness in the composite. Increase in tensile strength was observed up to 10% volume of B_4C but further addition of reinforcement results in reduction of tensile strength.

Gopalakrishnan and Murgan, (2012) fabricated TiC reinforced aluminium matrix composites taking AA6061 as the base material. The tensile specimens were prepared using ASTM E8 standards and tensile strength was evaluated on universal tensile testing machine. Figure 2.24 shows the results of Tensile strength and percentage elongation as reported by the authors.

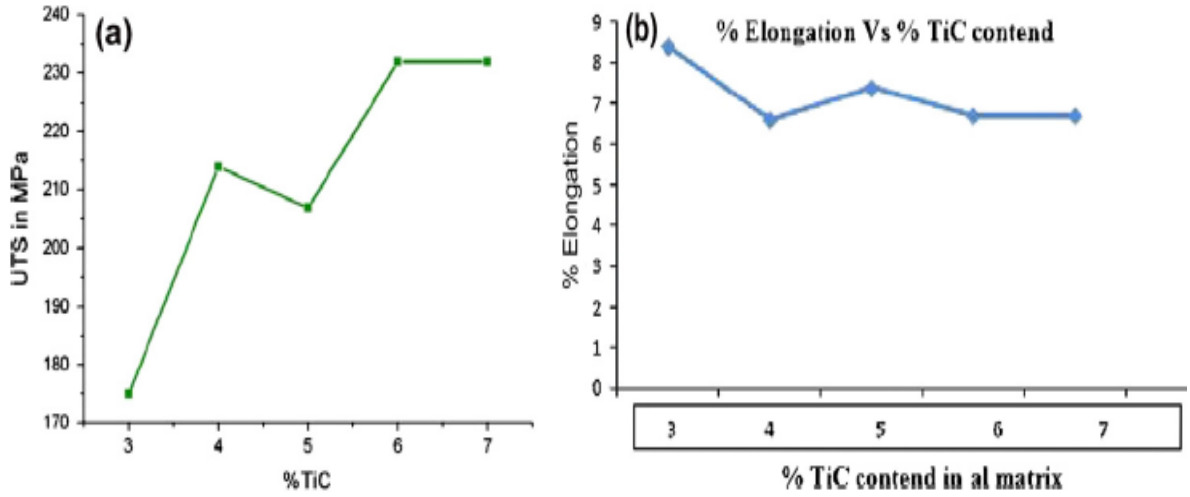

Figure 2.24 - Effect of TiC addition on the (a) Tensile strength and (b) percentage Elongation (Gopalakrishnan and Murgan, 2012)

The results obtained by the authors revealed that the addition of TiC increases the ultimate tensile strength of the AA6061/TiC composites. The addition of ceramic particles restricts the plastic deformation under loading which helps in improving the strength of the composites. The percentage elongation for TiC reinforced composites decreases with the addition of TiC as the addition of particles makes the material brittle which ultimately reduces the percentage elongation.

Aruri et al., (2013) used 6061-T6 aluminum alloy as base material and fabricated hybrid composites [(SiC + Gr) and (SiC + Al_2O_3)] to evaluate the wear and mechanical properties of the composites. Hardness tests were conducted on Vickers hardness tester with a load of 15 g for15s. Tensile tests were carried out on computer controlled universal testing machine with a cross head speed of 0.5 mm/min. As the hybrid composites were fabricated through friction stir processing (FSP) so the authors have used the speed of the rotational tool as one of the process parameters. In this work, the tool rotational speed of 900, 1120 and 1400 was used. The authors found that as the rotational speed increases the hardness in the composites decreases and the reason was the high heat generation at higher rotational speed which makes

the material softer and thereby reducing the micro hardness. The results of tensile properties as reported by the authors are given in Table 2.1.

Table 2.1 – Tensile Properties of the composites (Aruri et al., 2013)

Surface composite	UTS(MPa)	YS (MPa)	%EL
Al–SiC/Gr at			
900 rpm	219	185	9.1
1120 rpm	178	137	6.4
1400 rpm	157	115	7.2
Al–SiC/Al_2O_3 at			
900 rpm	192	152	7.8
1120 rpm	149	112	5.9
1400 rpm	124	102	4.8
As-received alloy	295	271	12
An Average of three values.			

The results revealed that ultimate tensile strength was optimum with the lowest rotational speed and as the speed increases the tensile strength gradually decreases for both the hybrids composites. Similar trend was observed in case of yield strength and the percentage elongation in Al–SiC/Gr and Al–SiC/Al_2O_3 hybrid composites. As reported by the authors, the increase in the heat input due to the increasing rotational speed was the reason for reduction in the tensile and yield strength.

Ghazi, (2013) developed SiC reinforced aluminium matrix composites using three different volume fractions 7, 14 and 21 of SiC. The tests were conducted to evaluate the mechanical behaviour of the cast composites which includes tensile tests, hardness tests, Yield and impact tests. The specimens were prepared using ASTM standards. Tensile specimen were machined using ASTM E8-95 standards; Hardness specimens were machined using ASTM E18-79 standards using indenter diameter of 1.56 mm, minor load 10 Kg and major load of

100 Kg. and to carry out the charpy impact tests the specimens were machined using ASTM E32-02A standard.

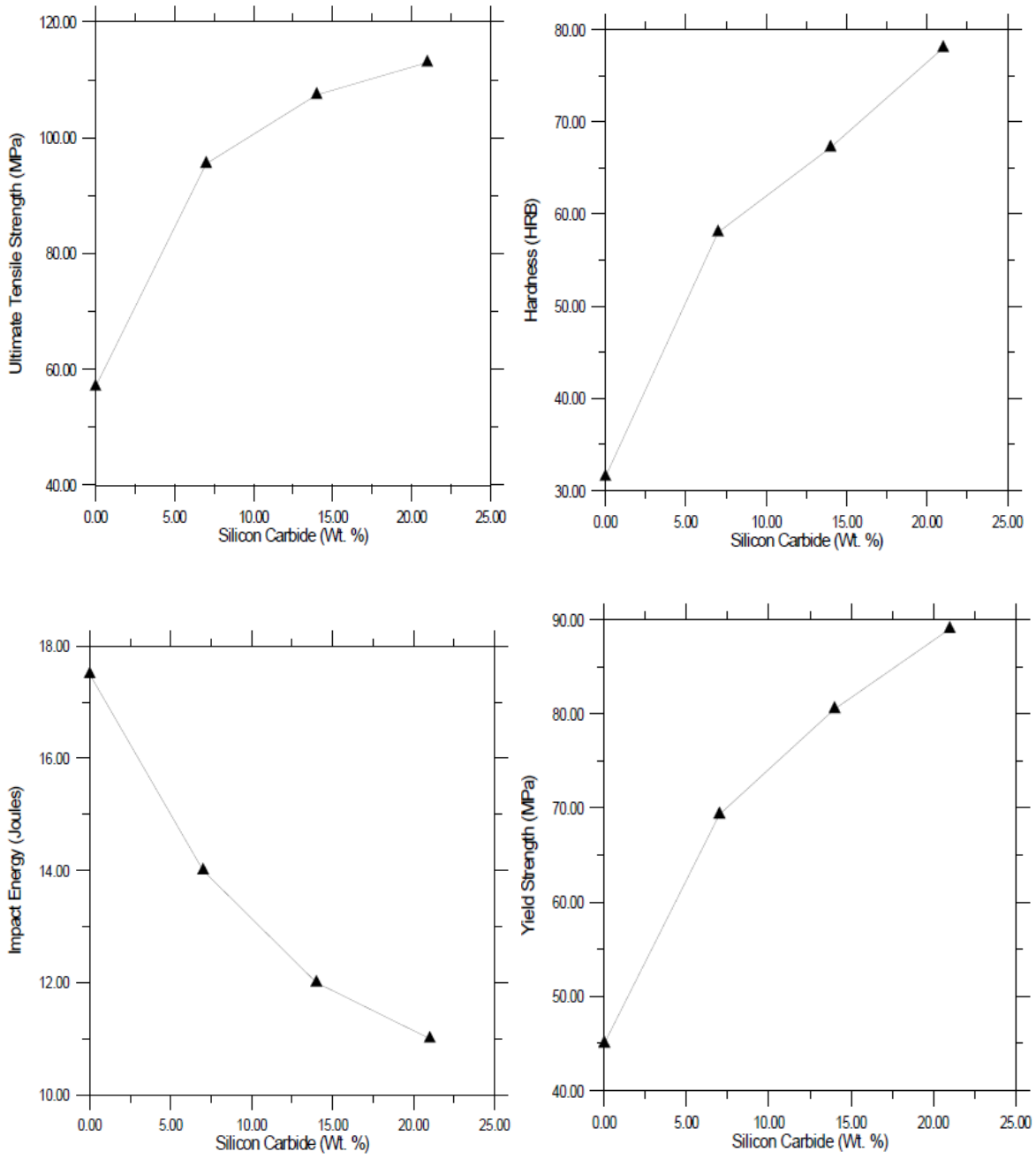

Figure 2.25 – Variation of Tensile strength, Hardness, Impact strength and Yeild strength with SiC addition (Ghazi, 2013)

Figure 2.25 shows the results for Tensile strength, Hardness, Impact strength and Yield strength with SiC addition in the composites. The authors reported that the addition of SiC improves the tensile strength, hardness and yield strength of the composites. The results of

Impact strength were however contrary to the others as it was found that the addition of reinforcement reduces the impact strength in the composites.

Madheswaran et al., (2015) developed aluminium matrix composites reinforced with boron carbide (B_4C). The effect to calcium carbide was also taken into account and for that three samples were prepared as follows: Specimen I (90 % LM25 Al + 10% B_4C), specimen II (90 % LM25 Al + 9 % B_4C + 1% CaC_2), and specimen III (90 % LM25 Al + 8 % B_4C + 2 % CaC_2). The tests were conducted to evaluate the impact strength, tensile strength, shear strength and hardness. The results obtained for impact strength, tensile strength, hardness and shear strength are shown in Figure 2.26.

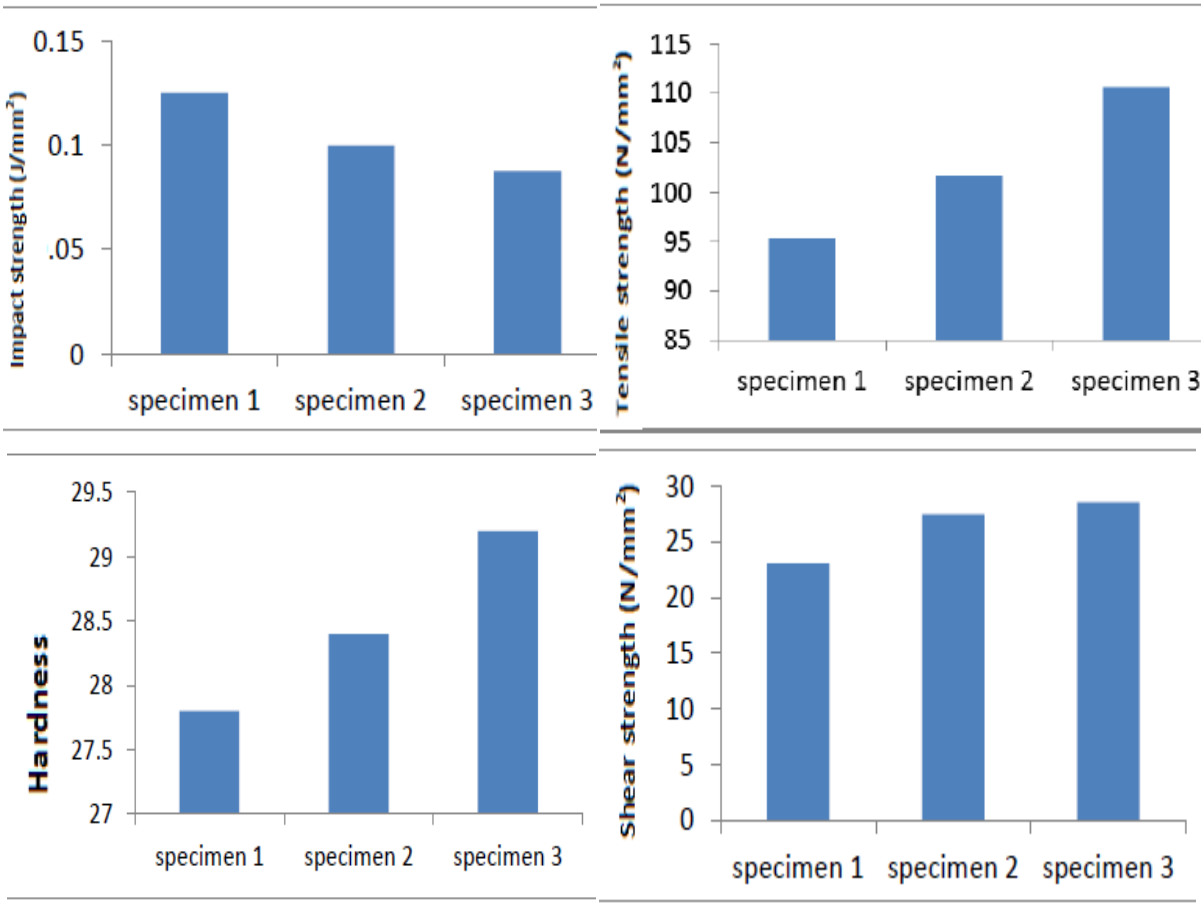

Figure 2.26 – Impact, Tensile, hardness and Shear strength results (Madheswaran et al., 2015)

The impact test samples were prepared according to ASTM E23 standard to conduct the experiments on Izod impact tester. The tensile specimens were prepared according to ASTM D638 standard and universal testing machine was used for the experiments. Hardness tests were carried out on Brinell hardness tester with a 10 mm diameter steel ball under the load of

3000 Kg for 10-15 seconds. The shear tests were carries out to determine the shear modulus and shear stress in the composite. It gives an idea that how the material actually behaves under the influence of shear stresses.

The results obtained by the author's confirm that the impact strength was highest for the specimen who shows the reduction in B_4C content and addition of CaC_2 had reduced the impact strength of composite material. The tensile strength and the hardness were the most for the specimen 3 which shows that the reduction in B_4C content and adding the same amount of CaC_2 in the composite enhances both the hardness and tensile strength. A similar trend was observed in case of shear strength where it was found that the specimen 3 has the maximum shear strength.

Shirvanimoghaddam et al., (2016) investigated the mechanical and physical properties of B_4C reinforced aluminium matrix composites. The authors have produced the Al/B_4C composites through stir casting at 800 °C and at 1000 °C so as to find out the effect of temperature change on the mechanical and physical behaviour of the cast composites. The tests were evaluated to investigate the hardness, ultimate tensile strength and density. Hardness tests were carried out on the Brinell hardness tester and Instron tensile test system 1195 was used to obtain maximum tensile strength.

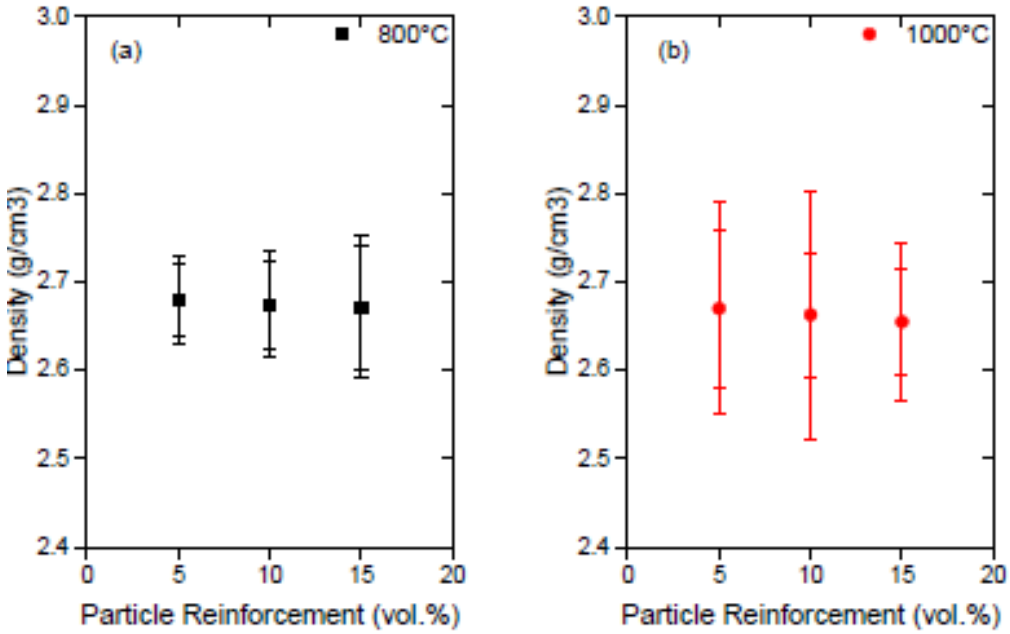

Figure 2.27 - Density of composites casted at (a):800°C and (b):1000°C (Shirvanimoghaddam et al., 2016)

Figure 2.27 shows the variation in density at 800 °C and at 1000 °C. The result shows that the density in the composites decreases with increase of B_4C in the matrix. However, the reduction in density was marginal only. This was due to the low density of B_4C (2.504g/cm3) than the density of Aluminium A356.1 (2.685g/cm3).

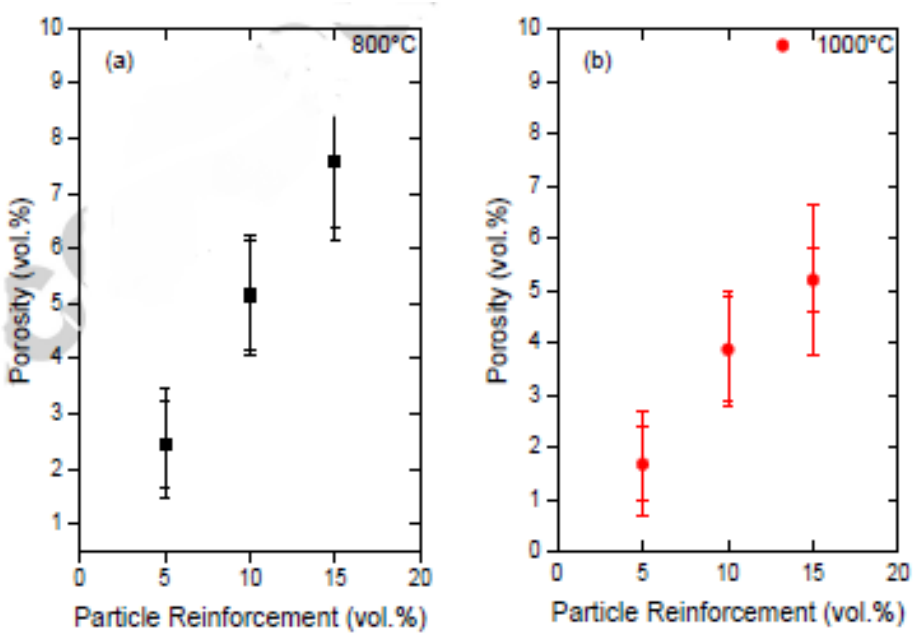

Figure 2.28 - Porosity of composites casted at (a):800°C and (b):1000°C (Shirvanimoghaddam et al., 2016)

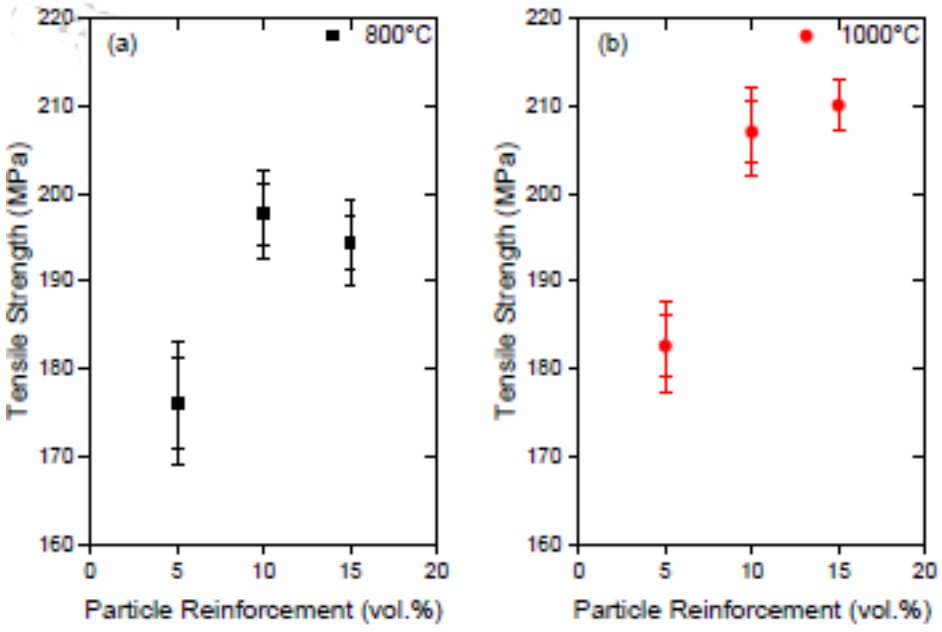

Figure 2.29 – Tensile strength of composites casted at (a):800°C and (b):1000°C (Shirvanimoghaddam et al., 2016)

The porosity in the composites gets increased at 800 °C and at 1000 °C as shown in Figure 2.28. It was observed that the increase in porosity was more at 800°C than that at 1000 °C. The tensile tests results are shown in Figure 2.29. The authors reported that the ultimate tensile strength (UTS) increases with increase in reinforcement content. For the composites produced at 800 °C, the UTS increases with the addition of 5% and 10% addition of B_4C but it has been reported that UTS tends to decrease with 15% addition of B_4C. The reason for this reduction was the rejection of B_4C particles to the slag at 800 °C and the formation of agglomerations. The tensile strength in the cast composites produced at 1000 °C was found to the even superior and no reduction was observed up to 15 % addition of B_4C. Hardness values for the cast composites produced at 800°C and 1000 °C are shown in Figure 2.30. The hardness values of composites cast at 1000 °C were reported to be higher than that produced at 800°C for each volume fraction of B_4C.

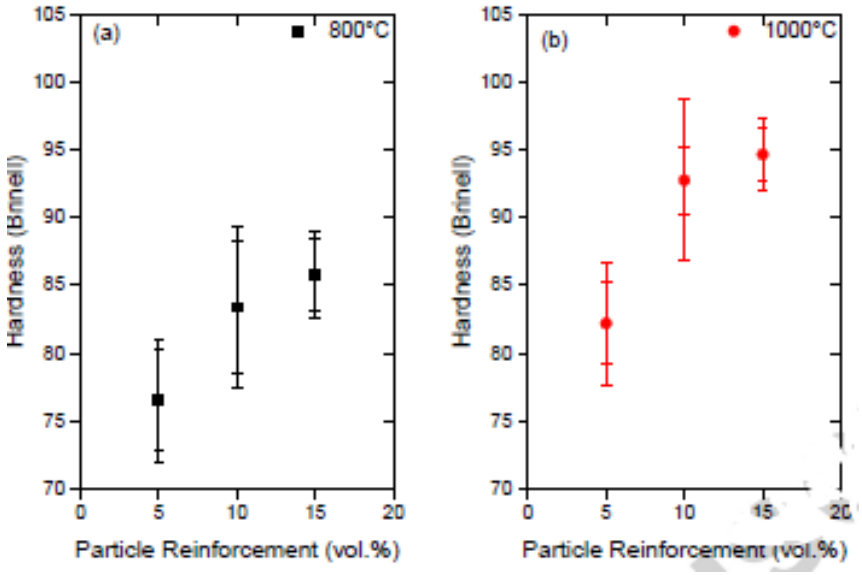

Figure 2.30 – Hardness of composites casted at (a):800°C and (b):1000°C (Shirvanimoghaddam et al., 2016)

From the literature it has been found that various researchers utilized SiC, Gr, CaC_2, $ZrSiO_4$, TiC, B_4C, and Al_2O_3 alone or in combination with different aluminum alloys in order to Evaluate the mechanical properties the composites, but till date no research has been carried out on AA6082 in order to manufacture the hybrid composites by using a mixture of (SiC & B_4C) as reinforcement and further no comparison have been drawn on SiC and B_4C reinforced composites using the base material AA6082.

2.3 BASED ON THE WEAR BEHAVIOUR OF AMC'S

This section of the literature covers the findings on the wear behaviour of aluminium matrix composites by the investigators over the years. Authors have used different types of ceramic particles with the base material to fabricate the composites and study their wear behaviour using distinct methodologies.

Sahin, (2003) studied the wear behaviour of SiC reinforced aluminium composites using statistical analysis. The abrasive wear behaviour was investigated on pin on disc apparatus shown in Figure 2.31 using against SiC and Al_2O_3 emery papers. The variables used were applied load, sliding distance and particle size as variables. The authors found that the wear rate in the composites increases with increasing the applied load, sliding distance and particle size for SiC paper while the wear rate decreases with the increasing sliding distance in case of Al_2O_3 paper. Among the variables, the particle size was found to be most effective followed by applied load and sliding distance.

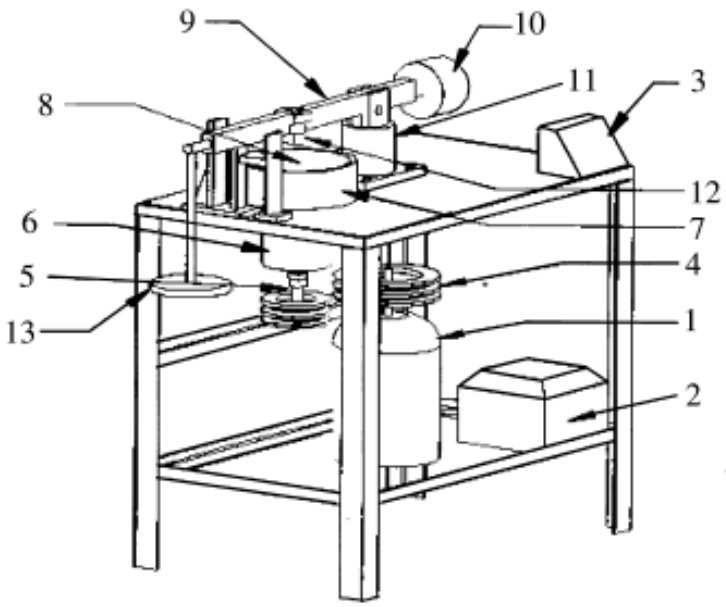

Parts of the wear machine

1- Motor	2-Electrical control panel	3-Contol panel	
4-Wheel and belt	5-Fixed shaft	6-Supporting shaft	7-Covering part
of the rotational disc	8-Hardened steel disc	9-Arm loading	10-End pin
11-Bearing	12-Table	13-Application of loads	

Figure 2.31 – Pin on disc apparatus (Sahin, 2003)

Basavarajappa and Chandramohan, (2005) investigated the wear behaviour of Al-SiC-Gr hybrid composites and Al-SiC composites. The tests were conducted on pin on disc apparatus and the tests were conducted on various load, speed and distance. Sliding speed of 1.53 m/s, 3 m/s, 4.6 m/s and 6.1 m/s were taken along with the sliding distance of 5000 meters and normal load of 10N, 20N, 30N and 40N. Figure 2.32 shows the variation of wear rate with sliding distance, sliding speed and load. The result shows the increase in sliding speed increases the wear rate in the composites. The wear in unreinforced alloy was more followed by Al-SiC and Al-SiC-Gr composites. The authors also reported that the increase in sliding speed decreases the wear rate in the alloy and the composites but beyond a certain speed the wear rate increases in both the alloy and the composites. The load of effect shows an increasing wear rate in the unreinforced alloy, Al-SiC and Al-SiC-Gr composites.

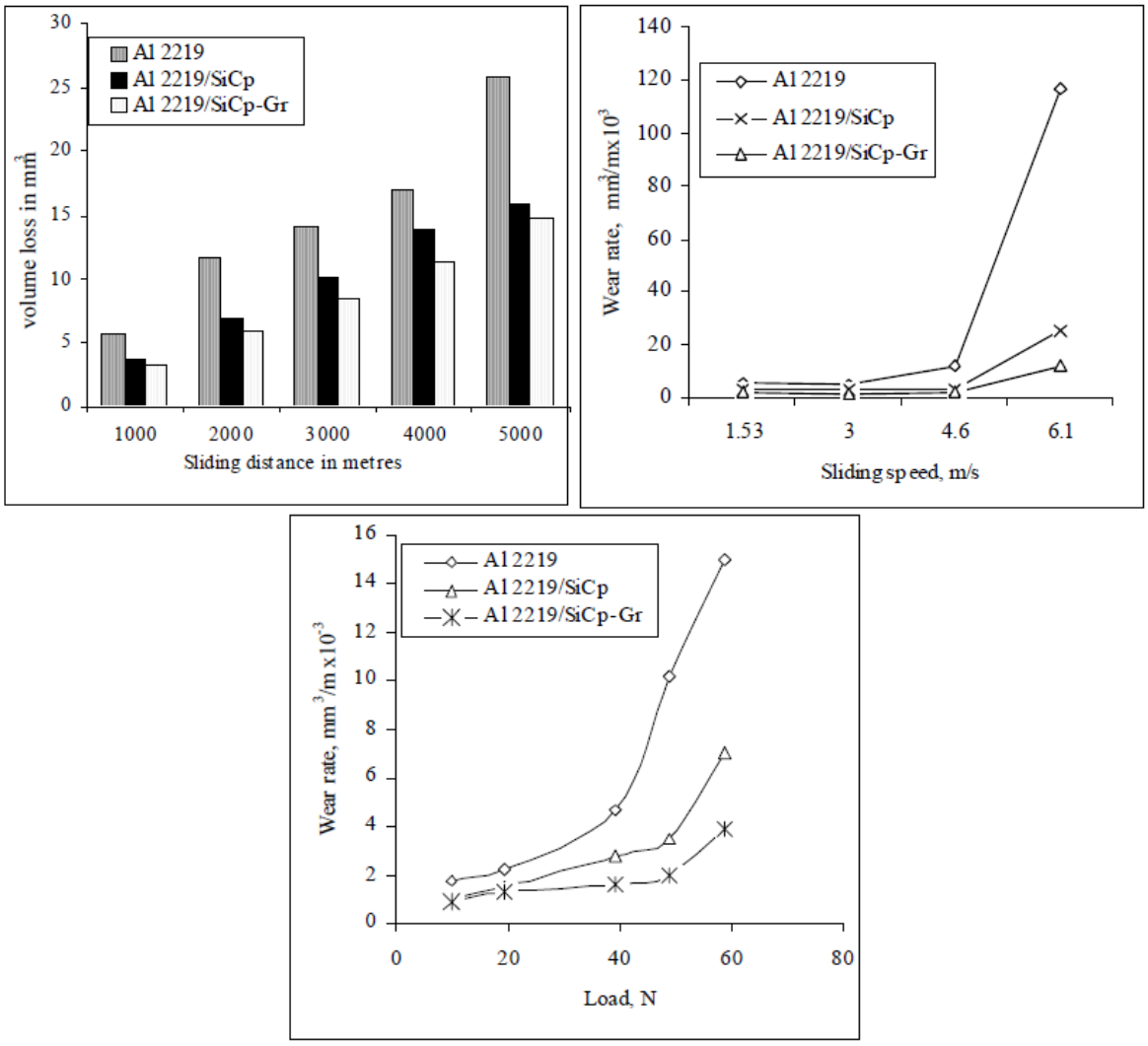

Figure 2.32 - Variation of wear rate with sliding distance, sliding speed and load (Basavarajappa and Chandramohan, 2005)

Sahin and Ozdin, (2008) investigated the abrasive wear behaviour of SiC reinforced aluminium composites. Pin on disc apparatus was used for the investigation where the samples were rubbed against the SiC abrasive of different grit sizes. The parameters used for the study were applied load, sliding distance and particle size and factorial design was employed for the process optimization. With the help of established equations, the authors concluded that the wear rate increases with the increase in applied load, particle size and decreases with the increase in sliding distance. The interaction between applied and particle size was also found to be an effective parameter for wear rate in case of both the alloy and the composites.

Gopalakrishnan and Murgan, (2012) worked on titanium carbide aluminium matrix composites (Al–TiCp) to study the wear characteristics. The tests were conducted on pin on disc apparatus equipped with a En-32 steel disc having hardness of 65 HRC. The results show that the wear rate increases marginally with the addition of TiC in the composites. The effect of sliding velocity was also having the similar effect on the wear rate. It was observed that wear rate increases with the increase of sliding velocity and the reason was the plastic deformation of the material at the surfaces. The gradual increase in load also tends to increase the wear rate in the composites.

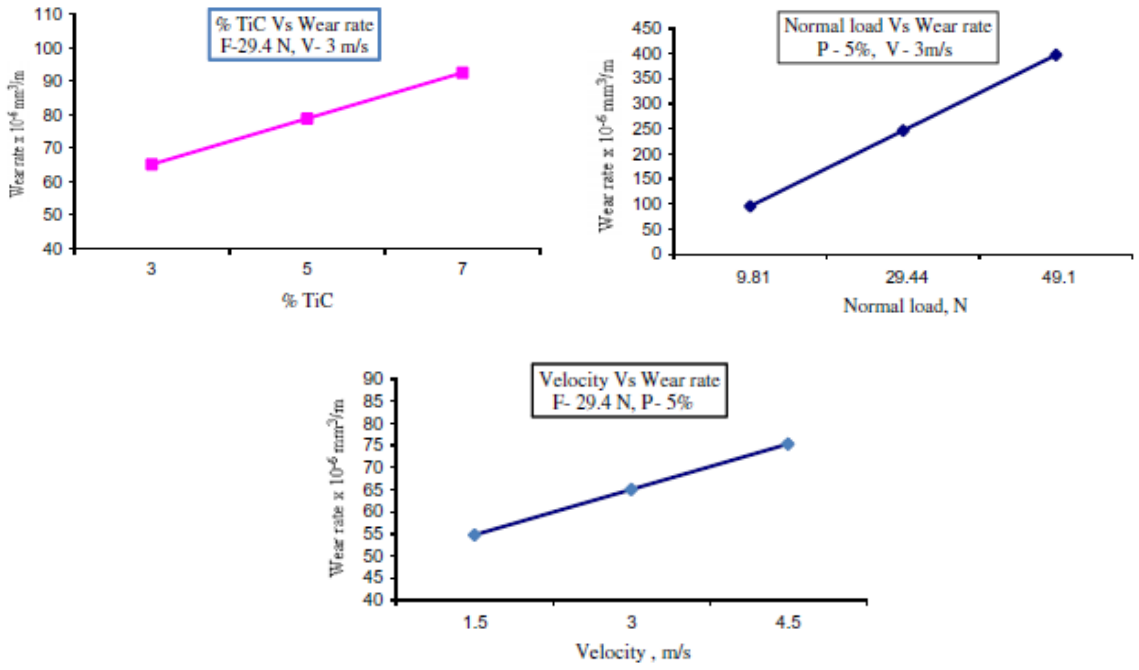

Figure 2.33 - Effect of % TiC, Normal Load and sliding velocity on the wear rate (Gopalakrishnan and Murgan, 2012)

The authors suggested that this increase was mainly due to the addition of normal load which results in higher coefficient of friction and thereby increased the wear rate. The variation of addition of TiC, sliding velocity and normal load with wear rate of the Al–TiCp is shown in Figure 2.33. The interaction between % TiC and normal load was found to be a significant one it was reported that the wear rate increases with the increase in % TiC and normal load. Figure 2.34 shows the interaction effect of normal force and % TiC on the specific wear rate.

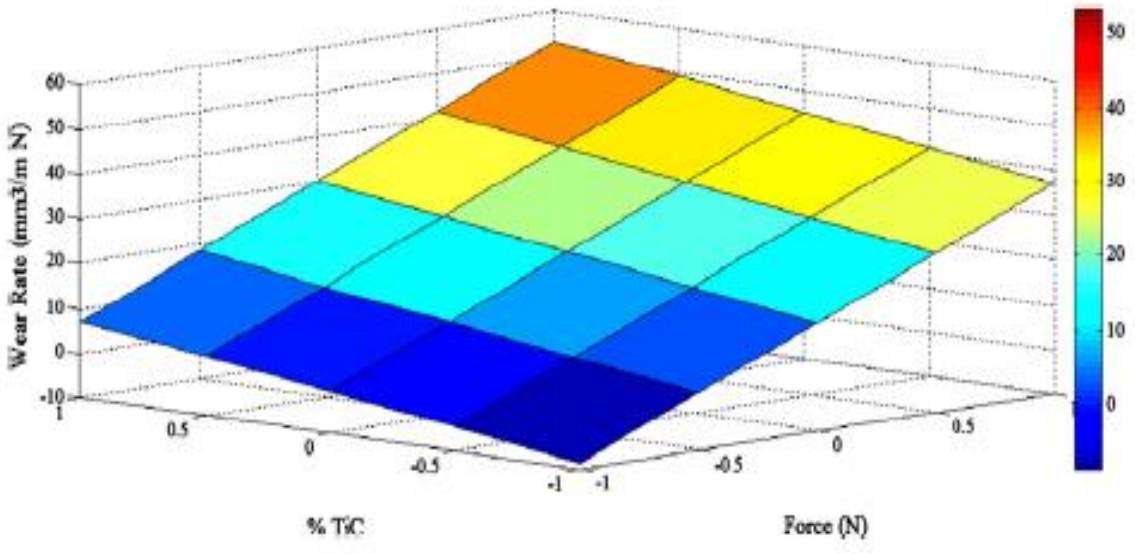

Figure 2.34 - Interaction effect of normal force and % TiC on the specific wear rate (Gopalakrishnan and Murgan, 2012)

Attar et al., (2015) has made an attempt to study the wear properties of Al7025-B_4C reinforced aluminum metal matrix composites against the varying load and sliding speed. Load was varied from 2 to 4 kg and the disc speed varies from 200 to 400 rpm. The sliding distance take for the experiments was 2000 m. The authors have calculated the volumetric wear loss using the Equation 2.2 and the wear rate using Equation 2.3.

$$\text{Volumetric wear Loss} = \frac{\text{Initial weight} - \text{Final weight}}{\text{Density of the material}} \quad \ldots\ldots\ldots\ldots [2.2]$$

$$\text{Wear rate} = \frac{\text{Volumetric Loss}}{\text{Sliding Distance} \times \text{Load}} \quad \ldots\ldots\ldots\ldots\ldots [2.3]$$

The graphs of Volumetric wear loss Vs Load and Wear rate Vs load is shown in Figure 2.35. The authors reported that the volumetric wear loss and wear rate increases with the increase

in load. The graphs of Volumetric wear loss Vs speed and Wear rate Vs speed is shown in Figure 2.36 and the results were similar as well. The disc speed was varied from 200 rpm to 400 rpm and it was found that volumetric wear loss and wear rate increases with the increase in disc speed.

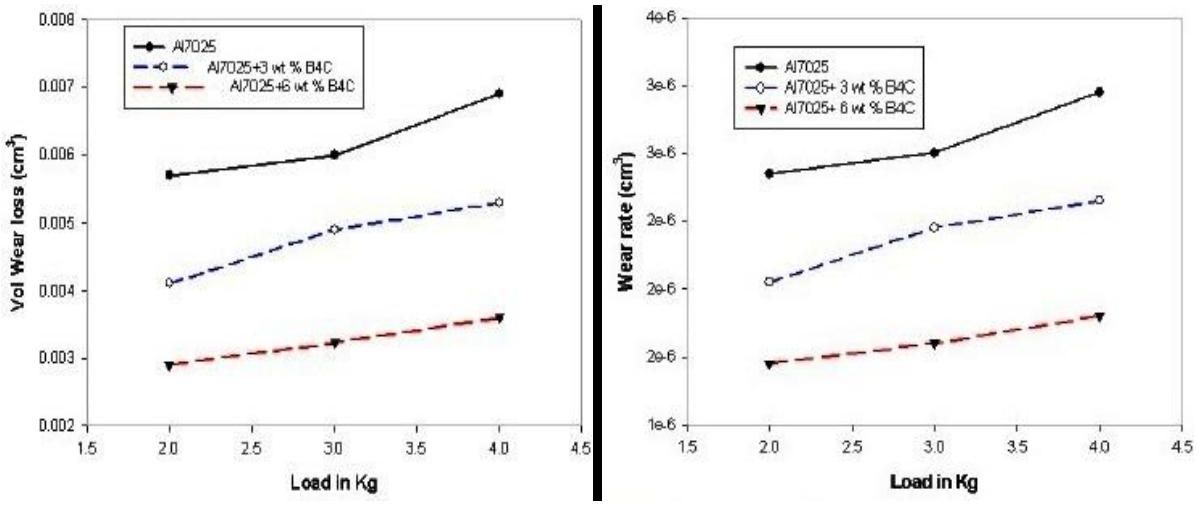

Figure 2.35 - Volumetric wear loss Vs Load and Wear rate Vs load (Attar et al., 2015)

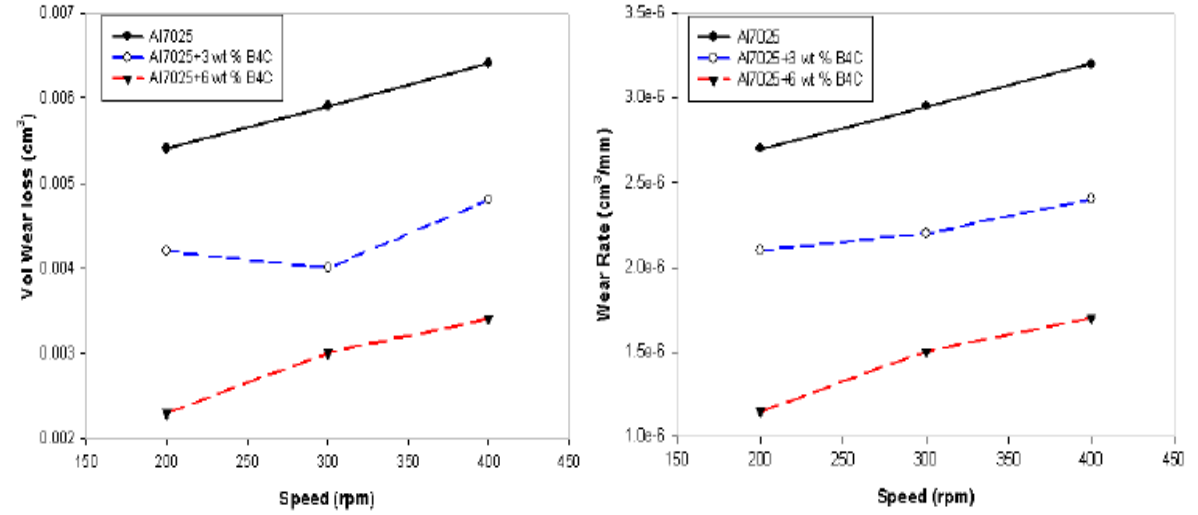

Figure 2.36 - Volumetric wear loss Vs Speed and Wear rate Vs Speed (Attar et al., 2015)

Thirumalai et al., (2015) fabricated and investigated the wear behaviour of B_4C and Gr reinforced aluminium hybrid composites. Four different weight % of B_4C (3, 6, 9 and 12) and fixed amount of Gr (3% wt) were used to fabricate the hybrid composite samples. The samples were tested for wear resistance against various sliding speed (1m/s to 2m/s) and loads (10 to 30 N). The variation in wear loss with different levels of reinforcement and normal load at different sliding speeds is shown in Figure 2.37. The authors observed that

with the increasing load, the wear loss increases and it was highest at the maximum load. The increase in reinforcement content decreases the wear loss at constant sliding speed and distance.

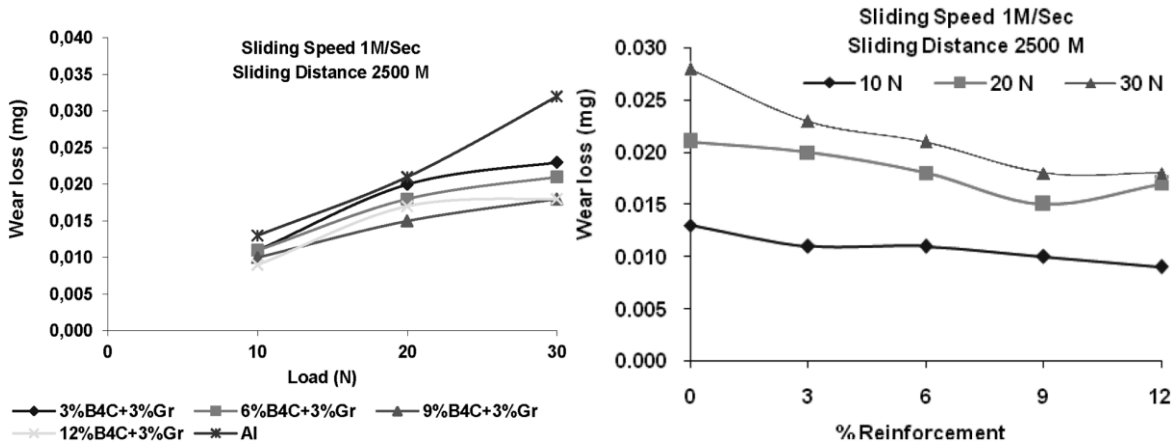

Figure 2.37 - Variation in wear rate with different levels of reinforcement and normal load at different sliding speeds (Thirumalai et al., 2015)

Sharma et al., (2015) fabricated aluminium hybrid composites reinforced with silicon nitride (Si_3N_4) and graphite (Gr) and evaluated the dry sliding wear behaviour using percentage reinforcement, sliding distance, load and sliding speed as process parameters. The experiments were performed at room temperature. The authors used response surface methodology for process optimization. The reinforcement range was varied from 0 to 12%, load values were taken between 15 N to 75 N, Sliding speed was varied from 0.4 m/s to 2 m/s and the sliding distance was varied from 400 m to 1200 m. The effect of the process parameters on the wear of the composites is shown in Figure 2.38 (a-d). The results show that the increase in reinforcement decreases the wear in the composites and this was because of the increase in hardness with the addition of ceramic particles. The increase in load increases the wear in composites which was attributed to the higher pressure applied in the material due to higher load. The higher pressure also increases the contact area between the material and the counter surface which results in increased wear. However, the increase in sliding speed decreases the wear which was due to the lower contact time between the mating surfaces at higher speeds. The wear in composites was observed to be increased with the increase in sliding distance which was due to the increase in interaction time at higher sliding distance between the counter surface and the composite specimen.

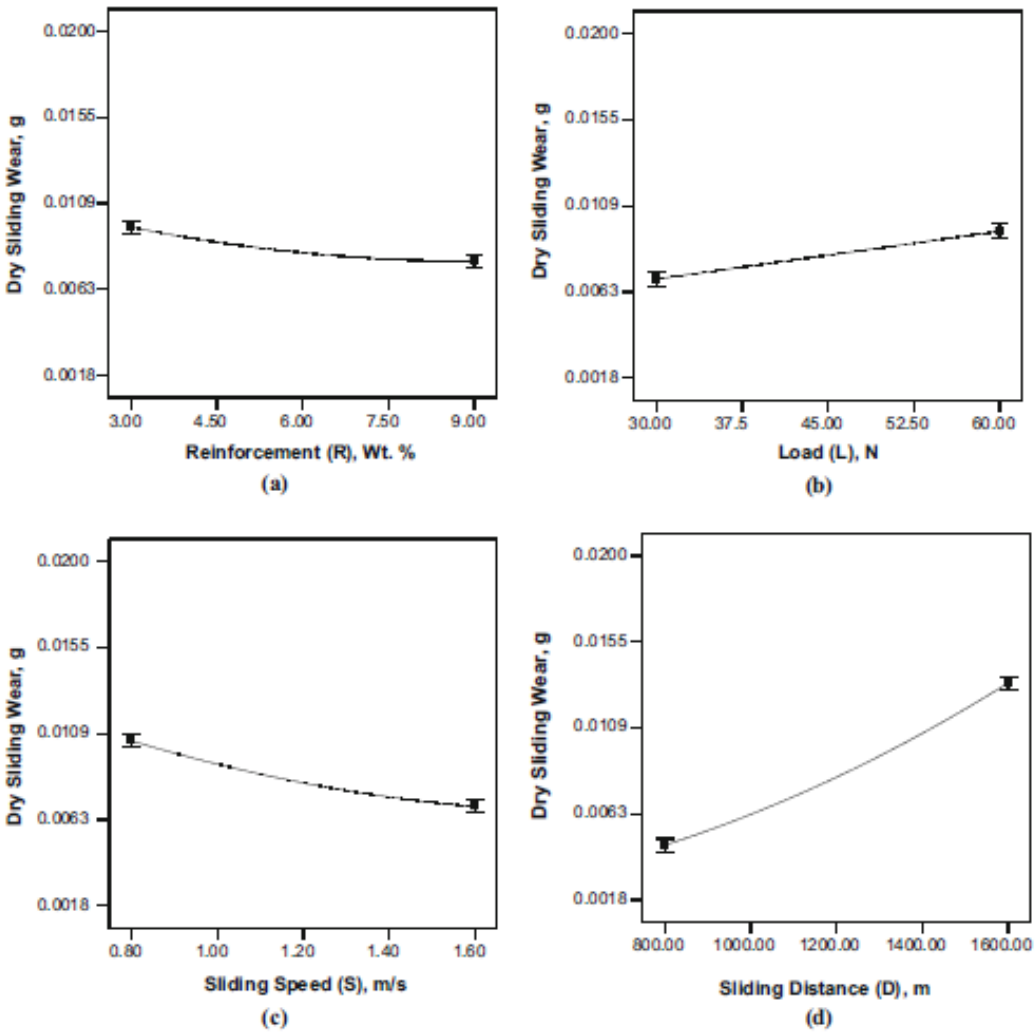

Figure 2.38 (a-d) - Effect of individual factors on dry sliding wear (a) reinforcement wt percentage (b) load (c) sliding speed and (d) sliding distance (Sharma et al., 2015)

The authors also reported that the interaction between sliding speed and load; sliding distance and load; and sliding distance and sliding speed were also significant in the wear of the composites. The 3-D interaction plots between sliding speed and load; sliding distance and load; and sliding distance and sliding speed are shown in Figure 2.39 (a-c). At lower values of load, the interaction showed that with the wear increases with decrease in sliding speed whereas the interaction between load and sliding distance shows that the wear increases with the increase in load and sliding distance. Similarly the interaction between sliding distance and sliding speed shows that the wear decreases with escalation in sliding speed at a smaller value of sliding distance. The wear also found to be decreased with higher values of sliding distance. The authors found that the interaction between sliding distance and load was more predominant effect on wear as compared to the other interactions.

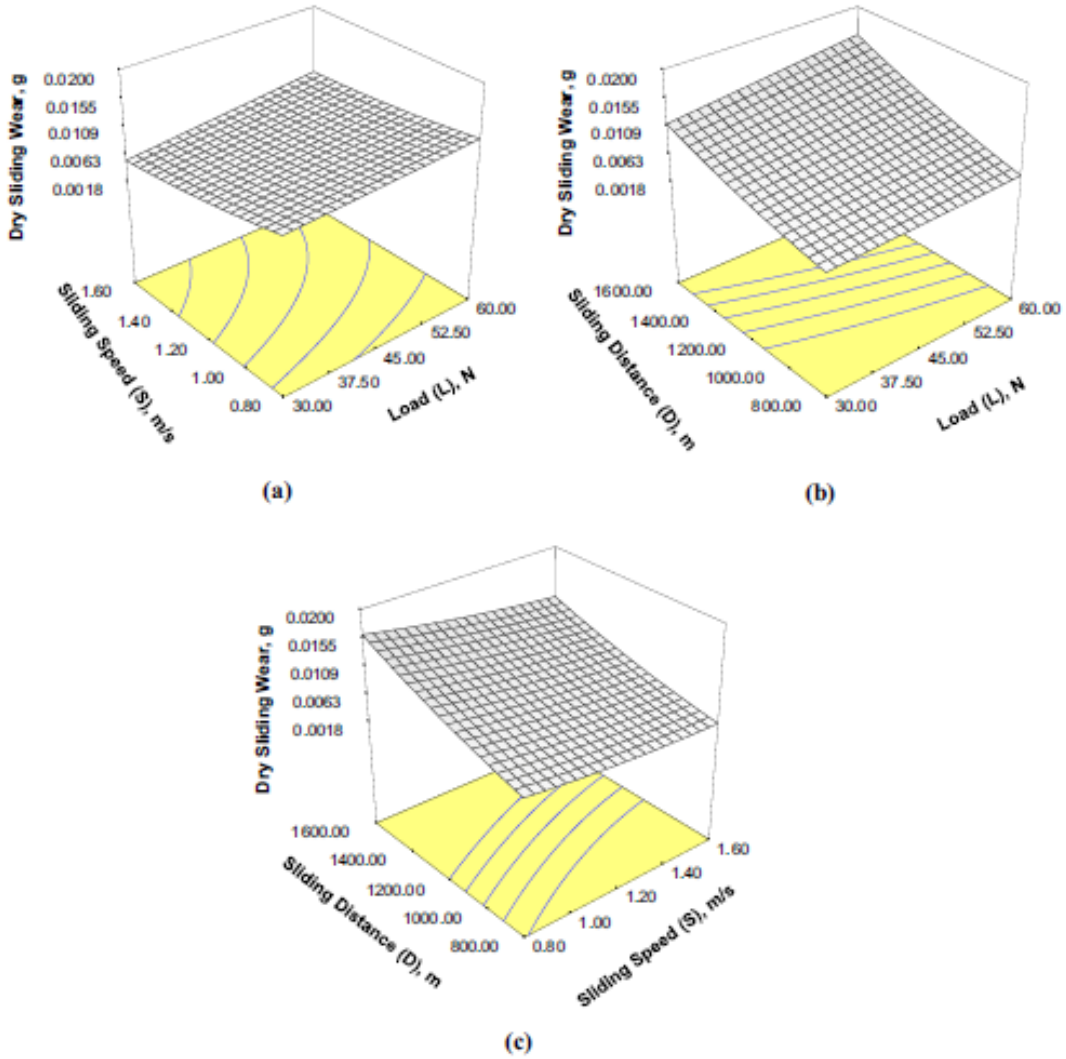

Figure 2.39 (a-c) - Effect of interaction on dry sliding wear (a) load-sliding speed, (b) load-sliding distance, and (c) sliding speed-sliding distance (Sharma et al., 2015)

Sharma et al., (2016) also investigated the wear behaviour of aluminium matrix composites using 6061 alloy along with (Si_3N_4) and graphite (Gr) as reinforcement. The experiments were performed on pin on disc apparatus. The experiments shows that the increase in reinforcement decreases the wear and the lower values of sliding distance and load are favourable for lesser wear in the composites. ANOVA was used to find out the wear and the influence of each process parameter. Different levels of process parameters were taken into consideration. The authors reported that the sliding distance was the most influencing factor in the wear of composites followed by the load, sliding speed and the percentage reinforcement.

2.3 RESEARCH GAPS

The literature review has presented a number of gaps in the previous investigations which are as follows:

A lot of work has been done on the fabrication of composites using different type of materials but very limited attempts have been made to prevent oxidation during fabrication and to increase the wettability of ceramic particles. In the present work, an attempt has been made to add Magnesium (Mg) in the form of wire in a certain amount along with the presence of Argon gas. The use of Mg and Argon together along with other process parameters gives superior casting results.

Compared to the reinforcements like (Gr, Al_2O_3, TiC) which are most commonly used in research, the work on B_4C and (B_4C+SiC) as reinforcement is very less. A very limited work has been reported on the physical and mechanical properties of (B_4C+SiC) reinforced hybrid composites. The comparative analysis of hybrid composites with Al-SiC and Al-B_4C reinforced composites using same alloy has also not been reported.

The literature also suggests that the parametric study using five or more levels of each process parameter on the dry sliding wear behaviour of aluminium composites is very limited.

No work has been reported on the wear behaviour of (B_4C+SiC) reinforced aluminium hybrid composites using the technique of response surface methodology for process optimization. The authors also have drawn the wear behaviour analysis of Al-SiC and Al-B_4C reinforced composites in parallel using the similar methodology.

CHAPTER – 3

MATERIALS AND METHODS

This chapter describes about the details of the starting materials and methods adopted for the fabrication and characterization of the composites under the present work. The chapter includes the discussion on the experimental set-up, the process parameters used for the production of composites, the machining of specimens from the produced composites and the apparatus employed for the mechanical behaviour analysis.

3.1 MATERIALS

Commercially available AA6082-T6 was selected as the base material in the present work and its chemical composition and mechanical properties are shown in Table 3.1 and Table 3.2 respectively.

Table 3.1 - Chemical composition of AA6082–T6 in wt %

Element	Mg	Si	Mn	Fe	Cu	Cr	Zn	Ti	Vn	Al
Content (Wt %)	0.69	0.91	0.56	0.23	0.06	0.035	0.098	0.019	0.01	97.4

Table 3.2 - Mechanical Properties of AA6082-T6

Tensile Strength (MPa)	Proof stress (0.2% MPa)	Density (g/cm^3)	Vickers Hardness (HV)	% Elongation (Min %)
320	310	2.67	100	9

AA6082 is the alloy from 6xxx series with excellent corrosion and wear resistance property and this is mainly because of the high amount of silicon in it **(Sharma et al., 2015).** The presence of significant amounts of magnesium in AA6082 controls the grain structure and makes it a strong and hard alloy **(Kumar and Dhiman, 2013).** AA6082 has high strength and shows excellent mechanical properties due to which it finds application in transport and structural application where high stress resistance is essential **(Mocko et al., 2012)**. Figure 3.1 shows the base alloy AA6082-T6 used in the present work.

Figure 3.1 – Base alloy AA6082-T6

AMCs can be produced using numerous types of ceramic particulates such as SiC, Al_2O_3, TiC, B_4C, Gr, TiO_2, etc. with the merits and demerits of each in the metal matrix. In the present work, the particles of SiC and B_4C are selected for the fabrication of composites. SiC particulates form excellent bonding with molten matrix and shows adequate thermal conductivity and machinability along with the low cost which makes it one of the most preferred reinforcements for composites **(Mocko et al., 2012; Baradeswaran et al., 2014).** The purpose of adding B_4C is to further enhance the mechanical properties of aluminum composites. B_4C shows many mechanical properties to be an effective reinforcement material such as high stiffness and hardness combined with low density. The small density difference between B_4C and aluminum means that particle sedimentation rates are low, minimizing the settling problem during solidification of molten matrix **(Kennedy, 2002)**. Better tribological characteristics can be obtained using B_4C because of high stiffness and hardness along with low density, even lower than most of the aluminum alloys **(Kennedy, 2002)** but B_4C is not readily adopted as reinforcement for the fabrication of AMCs because of its high cost as compared to SiC and many other particulates **(Kennedy, 2002)**. As abundantly reported in literature, several aspects regarding AMCs reinforced with SiC and B_4C have been studied. SiC has been extensively used as reinforcement for AMCs, finding application in pistons, cylinder heads, bearings and many other automotive components **(Natarajan et al., 2006).**

Due to its hardness, B_4C provides higher strength to aluminum-based composites and finds industrial applications in the nuclear field, automotive and army weapons **(Nazik et al., 2016)**. The details of SiC and B_4C particulates used in the present work are given in Table 3.3. Figure 3.2 and Figure 3.3 shows the reinforcement particles of SiC and B_4C respectively.

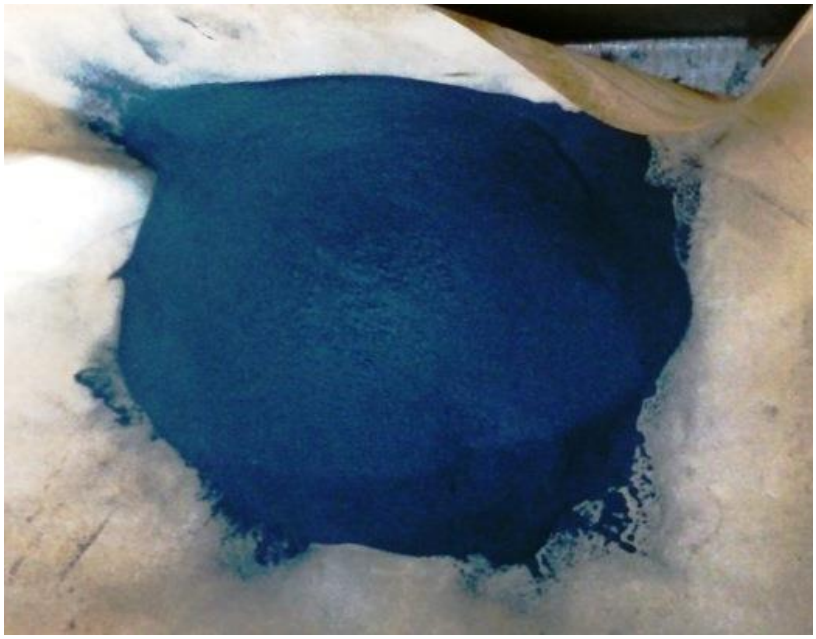

Figure 3.2 – SiC Particulates

Figure 3.3 – B_4C Particulates

Table 3.3 - Details of SiC and B_4C Particulate

Reinforcement	Average Particle Size (μm)	Density (g/cm^3)	Melting Point ºC	Hardness (HV)
SiC	35	3.20	2700	285
B_4C	35	2.52	2450	305

3.2 FABRICATION OF COMPOSITES

There are number of methods available for the fabrication of composites such as liquid state fabrication of composites, infiltration technique, squeeze casting infiltration and stir casting etc. The most commonly used method for composite fabrication is the conventional stir casting method as it can be used to produce complex shapes and is also economical compared to other methods **(Ravi et al., 2007; Shorowordi et al., 2003).** In Stir casting, a dispersed phase is mixed with a molten matrix metal in a crucible usually made of graphite and the mixture is stirred for 10-15 minutes to produce a homogeneous mixture which after solidification forms a composite. Stir Casting is the simplest and the most cost effective method of liquid state fabrication.

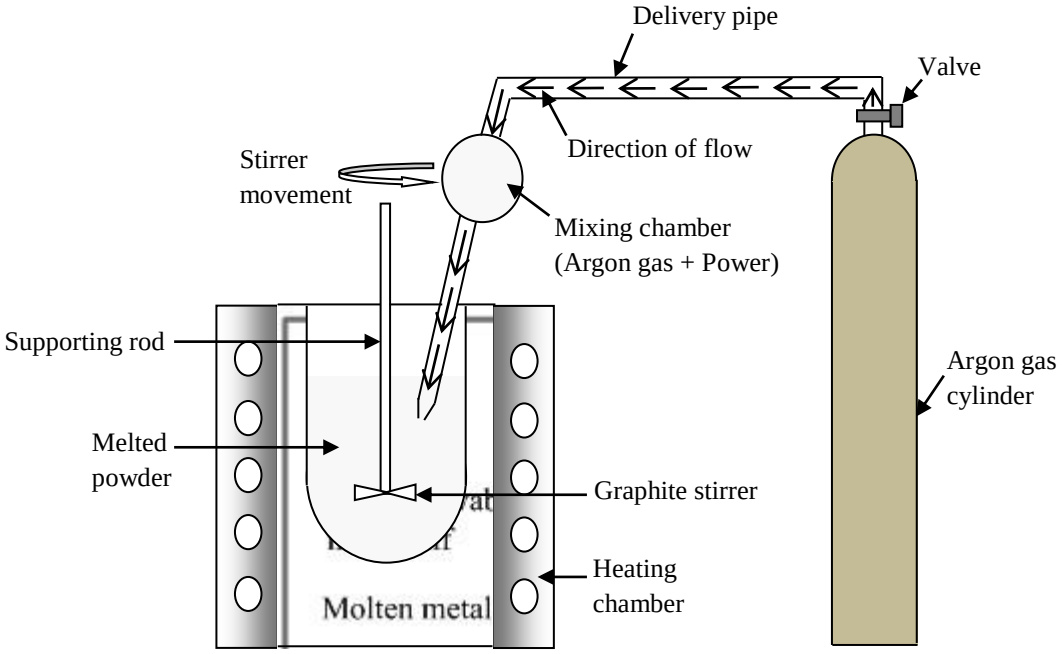

Figure 3.4 – Schematic of the Experimental set up

Another advantage with stir casting technique is that up-to 30% of volume fraction can be employed to produce composite by this method **(Pai et al., 1992).** Better chemical bonding between matrix and reinforcement particles can be achieved in stir casting process because of stirring action of particles in the melt **(Kok, 2005).** Owing to all these advantages, stir casting technique is used in the present work to fabricate aluminium metal matrix composites.

The schematic of experimental set up used in this work is shown in Figure 3.4. 1000 grams of aluminium in the form of small sheets was melted to 800ºC in a graphite crucible in an electric furnace under argon atmosphere for the fabrication of each sample. The addition of Argon gas prevents the formation of oxidising layer over the composites to be formed through the process. This modification in the stir casting is done with the help of 99% pure argon gas. Magnesium (2 wt %) in the form of thin wire as shown in Figure 3.5 was added to the molten metal to enhance the wettability of reinforcements with the matrix alloy. Magnesium considers being a good wettability agent particularly for SiC particulates **(Hashim et al., 2001).** The particulates of SiC and B_4C were preheated in a baking oven shown in Figure 3.6 to a temperature of 200ºC for 3-4 hours to get their surface oxidised.

Figure 3.5 – Magnesium used in Composite fabrication

The preheating in baking oven is also helpful in drying of the moisture content from the particulates **(Sharma et al., 2016)**. The preheated mixture was then added to the molten metal in the crucible at a constant feed rate and continuously stirred at approximately 400 rpm with a vortex shaped graphite stirrer for 12-15 minutes to form a homogeneous casting. Table 3.4 shows the parameters with its values used in stir casting process. After 12-15 minutes of continuous stirring, the molten mixture was poured in a sand mould with dimensions of 300 mm in length, 80 mm width and 40 mm depth (Figure 3.7). The material was then allowed to cool down and solidify before being separated from the sand mould.

Table 3.4 – Process Parameters used in Stir casting

Parameter	Value	Unit
Spindle speed	400	Rpm
Stirring time	12-15	Minutes
Stirring temperature	800	°C
Preheated temperature of B_4C	200 °C	°C
Preheating time	120-180	Minutes

Figure 3.6 – Baking Oven

In the present work, AA6082-T6/SiC, AA6082-T6/B_4C and hybrid composites AA6082-T6/(SiC + B_4C) were prepared using the same method as discussed above. The weight percentage of 5, 10, 15 and 20% of SiC and B_4C particulates was used respectively for the fabrication of Al-SiC and Al-B_4C composites. For the hybrid composites, mixture of SiC and B_4C (SiC + B_4C) with weight percentage 5, 10, 15 and 20% was used again taking equal fraction of SiC and B_4C in each of the hybrid composite sample. The Details of the hybrid composites AA6082-T6/(SiC + B_4C), AA6082-T6/SiC and AA6082-T6/B_4C are given in Table 3.5, Table 3.6 and Table 3.7 respectively. Figure 3.8 shows all the composite samples fabricated in the present study.

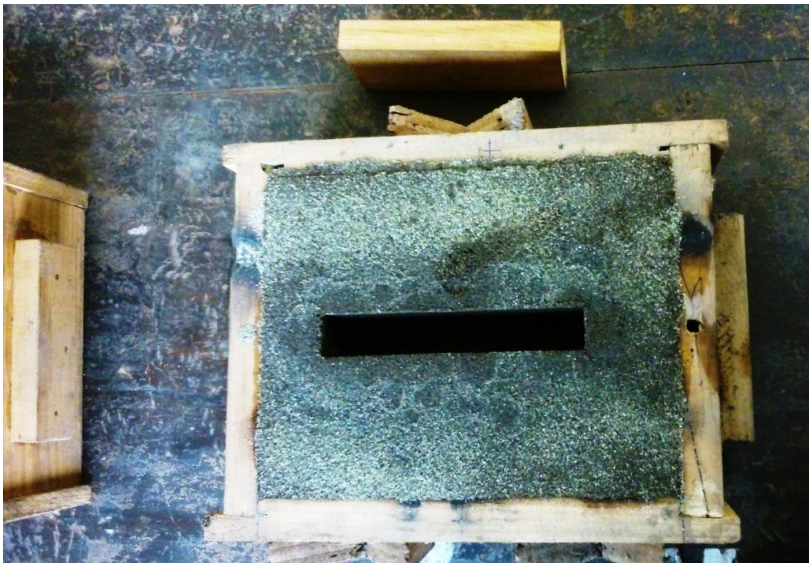

Figure 3.7 – Sand Mould

Figure 3.8 – Composite samples fabricated through stir casting

Table 3.5- Details of Al-SiC-B_4C hybrid composites

Sr No	Base Alloy	Wt % of SiC	Wt % of B_4C	Combined Wt% of (SiC + B_4C)
1	AA6082-T6	2.5	2.5	5
2	AA6082-T6	5	5	10
3	AA6082-T6	7.5	7.5	15
4	AA6082-T6	10	10	20

Table 3.6 - Details of Al-SiC composites

Sr No	Base Alloy	Wt % of SiC
1	AA6082-T6	5
2	AA6082-T6	10
3	AA6082-T6	15
4	AA6082-T6	20

Table 3.7 - Details of Al-B_4C composites

Sr No	Base Alloy	Wt % of B_4C
1	AA6082-T6	5
2	AA6082-T6	10
3	AA6082-T6	15
4	AA6082-T6	20

3.3 SAMPLE PREPARATION AND TEST METHODS

After the fabrication of Al-SiC-B_4C, Al-SiC and Al-B_4C composites, the samples were machined to conduct various experimental tests and to study the mechanical behaviour of the composites**.**

3.3.1 Hardness

Micro hardness of Al-SiC-B_4C, Al-SiC and Al-B_4C composites were tested on Vickers hardness tester from Fuel Instruments & Engineers Pvt. Ltd, Maharashtra with a maximum capacity of 50 Kgf. The apparatus is shown in Figure 3.9.

Figure 3.9 - Micro-hardness Tester

Each sample was tested 3 times on different locations and the average value has been taken. Small cuboids samples as shown in Figure 3.10 were used to examine the micro-hardness. The specimens were indented with a diamond indenter in the form of pyramid having a square base and the angle between the square bases is 136°. The load of 1 kg was applied for 15 s during each run of experiments.

Figure 3.10 – Samples for Micro-hardness Test

3.3.2 Tensile Strength

Flat plate specimens were used to examine the tensile strength of the specimens. Figure 3.11 shows the schematic of the specimen with thickness 6 mm and the other dimensions are as follows: L_O = 60 mm, L_C = 80 mm, b = 10mm, and R = 10 mm.

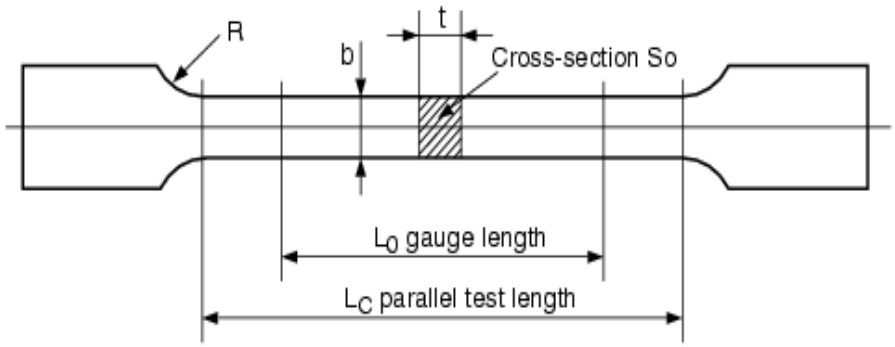

Figure 3.11 - Schematic of Flat Tensile Test Specimen

Tensile behaviour of the composites were examined and tested as per ASTM-E8 standard. The tests were performed on universal testing machine from Fuel Instruments & Engineers Pvt. Ltd, Maharashtra. The pictorial view of the Universal testing machine is shown in Figure 3.12.

Figure 3.12 – Ultimate Tensile testing machine

The length of the specimen was adjusted by one of the crosshead while the other crosshead was used to apply the tensile force on the specimen. It is necessary that the alignment between the specimen and the crosshead should be correct as any error in the alignment may cause the bending stresses or even break the material outside the gauge length. The constant crosshead speed was maintained during each run of experiment and the results were used to calculate the tensile strength. Figure 3.13 shows the samples for tensile testing (only few).

3.3.3 Percentage Elongation

Percentage elongation was evaluated by recording the elongation in the initial gauge length of the specimen. The extensometer was used to measure the elongation. Equation 3.1 shows the formula to calculate the elongation which was also used in the present work.

$$\text{Percentage Elongation} = \frac{\text{elongation at rupture}}{\text{initial gauge length}} \times 100 \qquad [3.1]$$

Figure 3.13 – Flat Tensile specimen

3.3.4 Impact Strength

The Charpy impact tests were carried out on impact testing machine with specimen of 56 mm x 10 mm x 10 mm in dimensions having notch depth of 2 mm and notch tip radius of 0.25 mm at an angle of 45º. The schematic diagram of the samples used for this study is shown in Figure 3.14. The Samples employed for Impact testing (Only few) and the charpy impact testing machine is shown in Figure 3.15 and Figure 3.16 respectively. For each of the composite, three samples were prepared for testing and the average value has been taken.

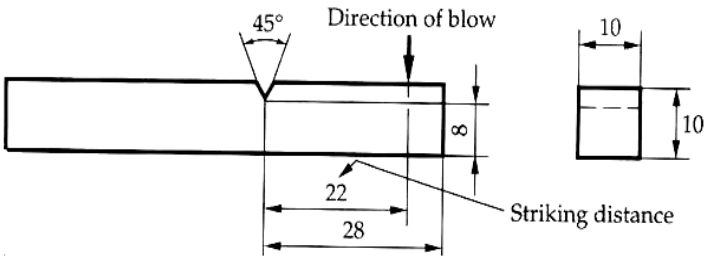

Figure 3.14 - Schematic of samples for Impact strength

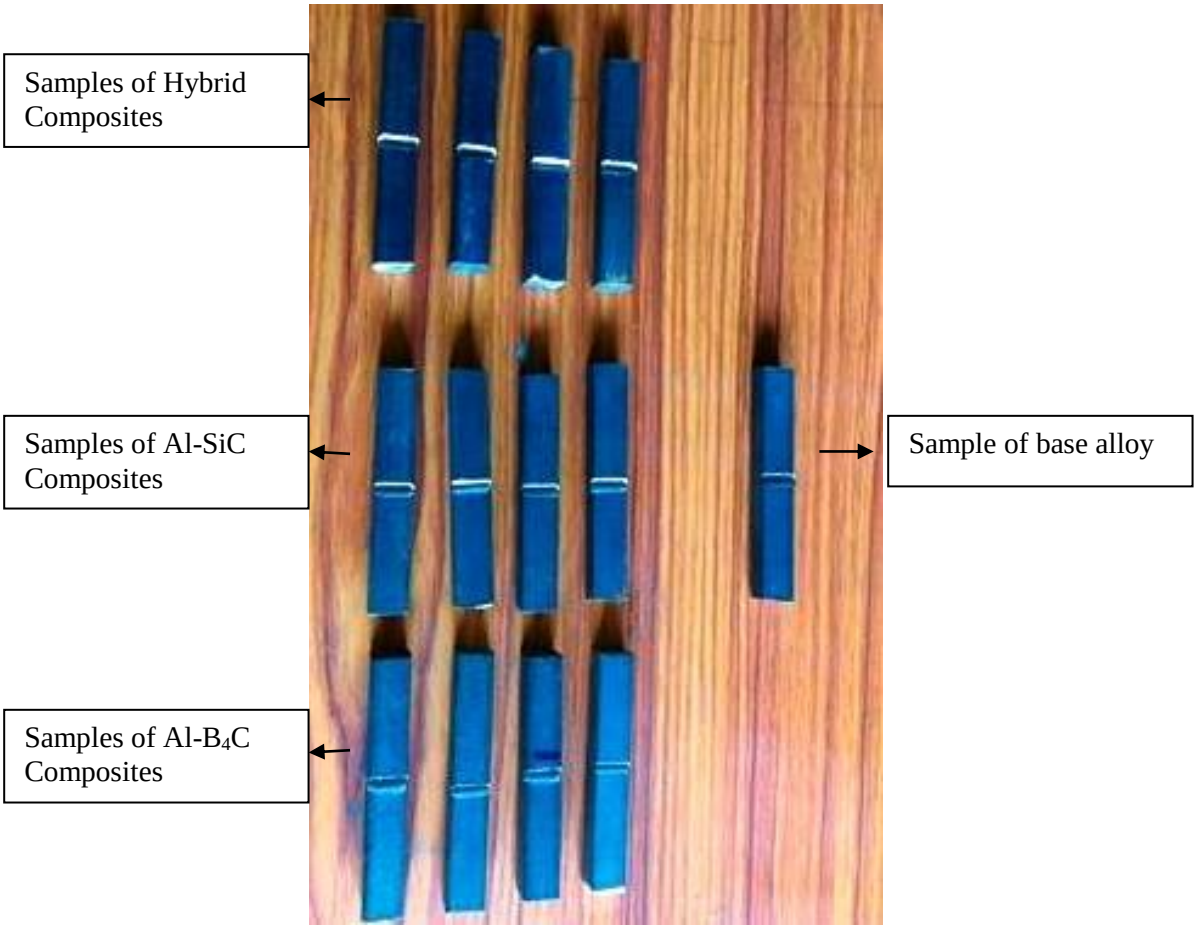

Figure 3.15 - Samples for Impact Testing

Figure 3.16 – Impact Testing Machine

3.3.5 Density

The density of a specimen was determined by knowing the mass and volume of the specimen used. By measuring the mass and volume, the density can be calculated using Equation 3.2

$$\text{Density } (\text{g/cm}^3) = \frac{\text{Mass}}{\text{Volume}}. \qquad \text{..... [3.2]}$$

3.3.6 Porosity

Porosity can easily be measured by weighing method in which the weight of specimen is measured. Equation 3.3 was used to calculate the porosity.

$$\text{Porosity } = 1 - \frac{d}{d_a} \qquad \text{... ... ... [3.3]}$$

where d = mass of sample/ volume of sample

d_a = density of the alloy

With this method even the closed porosity will be taken into account.

3.3.6 Wear Test

Dry sliding wear test of fabricated composites and un-reinforced alloy were conducted at room temperature of 30-35^{o}C and relative humidity of 25-35 %, using a pin-on-disc apparatus. EN31 steel disc was used as a counter surface with hardness of 860 HV and surface roughness of 0.1 Ra (micrometers). The pictorial view of the apparatus employed for the research work is shown in Figure 3.17. The apparatus consists of a lever mechanism for applying the normal load, a steel disc which was used as the counter surface and holder to position the wear pin against the rotating steel disc. Cylindrical Samples with 6 mm diameter and 35 mm height were machined to carry out wear analysis. The pin was held stationary against the rotating steel disc and with the help of a lever mechanism normal load was applied. The cylindrical pins were cleaned with acetone and weights have been recorded before and after the testing to an accuracy of 0.0001 g.

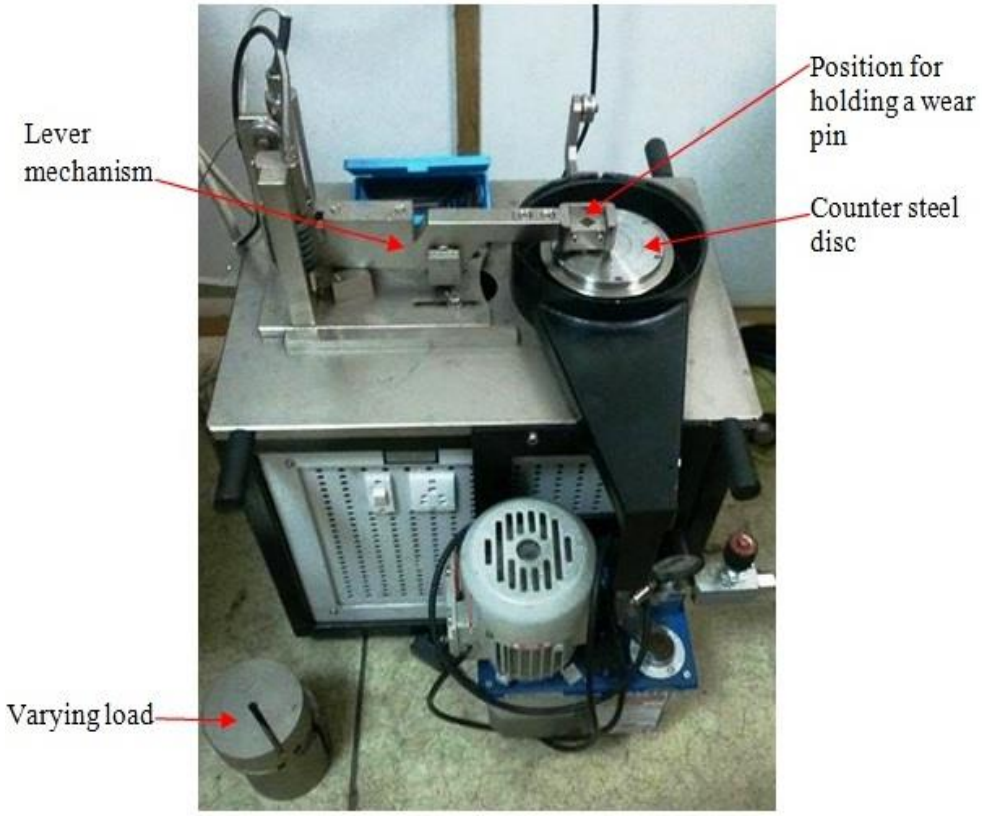

Figure 3.17 – Pin on disc apparatus

Figure 3.18 – Wear pins used for wear tests

Table 3.8 - Factors and the levels of four process parameters

Factors	Levels				
Reinforcement,(wt%)	0	5	10	15	20
Sliding speed (m/s)	0.6	1.2	1.8	2.4	3.0
Load (N)	14.71	29.42	44.13	58.84	73.55
Sliding distance (m)	400	800	1200	1600	2000

Weight percentage (wt %) of reinforcement, sliding speed, load and sliding distance are the four process parameters adopted to analyse the wear behaviour. Optimization of process parameters was done using Response Surface methodology (RSM). The wear pin samples (only few) and the levels of four factors are shown in Figure 3.18 and Table 3.8 respectively.

CHAPTER – 4

RESPONSE SURFACE METHODOLOGY

4.1 INTRODUCTION

To carry out the experiments in an effectual approach, it becomes essential to plan the experiments through a scientific approach. The statistical designs are usually employed for the planning of experiments as these helps in achieving the convincing conclusions. This is the one ideal approach for experimental planning that involves the data subjected to experimental error. For any experimental problem, the design of experiments is one of the most important aspects along with statistical study. The main benefits associated with the design of experiments are:

1) Numbers of trials is significantly reduced in comparison to full factorial experiments.
2) The most significant variables which drive the performance of the product can be identified.
3) Optimum set of variables can be framed.
4) Qualitative as well as quantitative estimation of parameters can be made
5) It is easy to find out the experimental error.
6) Effect of parameters on the performance of the product can be analysed.

4.2 RESPONSE SURFACE METHODOLOGY

Researchers in the past used the technique of Response surface methodology (RSM) and studied the effect of different factors and the interactions among them on the analysis of the wear behaviour of materials **(Kumar and Dhiman, 2013; Baradeswaran et al., 2014).** In the present analysis, the authors have used RSM for the planning of experiments and modelling of process parameters.

As an important subject in the statistical design of experiments, the Response Surface Methodology (RSM) is a collection of mathematical and statistical techniques useful for the modelling and analysis of problems in which a response of interest is influenced by several variables and the objective is to optimize this response. In many experimental conditions, it is possible to represent the independent factors in quantitative form as given in Equation 4.1.

Then these factors can be thought of as having a functional relationship with response as follows:

$$y = f(x_1, x_2) + e \qquad [4.1]$$

This represents the relation between response Y and $x_1, x_2, \ldots, x_k$ of k quantitative factors. The function f is called response surface or response function. The residual 'e' measures the experimental errors. For a given set of independent variables, a characteristic surface is responded. When the mathematical form of f is not known, it can be approximated satisfactorily within the experimental region by a polynomial. Higher the degree of polynomial better is the correlation but at the same time costs of experimentation become higher.

4.2.1 Central Composite Design

In statistics, a central composite design is an experimental design, useful in response surface methodology for building a second order (quadratic) model for the response variable without needing to use a complete three-level factorial experiment. After the designed experiment is performed, linear regression is used, sometimes iteratively, to obtain results. Coded variables are often used when constructing this design.

Central Composite Design (CCD) as it is an effectual tool for building quadratic model consisting of a number of factors **(Kuehl, 2000).** Another advantage with CCD plan is that it can be employed to study factors when numbers of levels are high and that too with lesser number of tests **(Montgomery, 2007).**

A central composite design is the most commonly used response surface designed experiment. Central composite designs are a factorial or fractional factorial design with center points, augmented with a group of axial points (also called star points) that let you estimate curvature. You can use a central composite design to:

- Efficiently estimate first- and second-order terms.
- Model a response variable with curvature by adding center and axial points to a previously-done factorial design.

Central composite designs are especially useful in sequential experiments because we can often build on previous factorial experiments by adding axial and center points. When possible, central composite design has the desired properties of

- Orthogonal blocks and
- Rotatability.

Orthogonal blocks

Often, central composite designs are done in more than one block. Central composite designs can create orthogonal blocks, letting model terms and block effects be estimated independently and minimizing the variation in the regression coefficients.

Rotatability

Rotatable designs provide constant prediction variance at all points that are equidistant from the design center.

4.2.2 Analysis of Variance

The purpose of product or process development is to improve the performance characteristics of the product/process relative to customer needs and expectations. The purpose of experimentation should be to reduce and control variations of a product or process, subsequently decisions must be made concerning which parameters affect the performance of a product or process. ANOVA is the statistical method used to interpret experimental data and make the necessary decisions. Table 4.1 shows the ANOVA for Central Composite Second Order Rotatable Design. For the analysis of variance, the total sum of squares may be divided into four parts:

- The contribution due to the first order terms
- The contribution due to the second order terms
- A Lack of fit component which measures the deviations of the response from the fitted surface
- Experimental error which is obtained from the centre points

Table 4.1 - ANOVA for Central Composite Second Order Rotatable Design

S. No.	Source	Sum of Squares	Degree of freedom
1	First order terms	$\sum_{q=1}^{k} b_i \left(\sum_{q=1}^{N} x_{iq} Y_q \right)$	K
2	Second order terms	$b_o \left(\sum_{q=1}^{N} y_q \right) + \sum_{i=1}^{k} b_{ii} \left(\sum_{q=1}^{N} x_{iq}^2 Yq \right) + \sum_{i<j}^{k} b_{ij} \left(\sum_{q=1}^{N} x_{iq} x_{jq} y_q \right) - \frac{\left(\sum_{q=1}^{N} y_q \right)^2}{N}$	$\frac{k(k-1)}{2}$
3	Lack of fit	Found by subtraction	$N - n_o - \frac{k(k+3)}{2}$
4	Experimental error	$\sum_{s=1}^{n_0} (y_s - \bar{y}_0)^2$	n_o-1
5	Total	$\left(\sum_{q=1}^{N} y_q \right)^2 - \left[\frac{\left(\sum_{q=1}^{N} y_q \right)^2}{N} \right]$	N-1

The F ratio is given by: $$F(1, n_0) = \frac{b_i^2 / c_{ii}}{S_e^2} \quad [4.2]$$

Where b_i =Regression Coefficient

c_{ii} = Element of error matrix $(X'X)^{-1}$

Se = Standard deviation of experimental error calculated from replicating observation at zero level as:

$$S_e^2 = \frac{1}{n_o - 1} \sum_{s=1}^{n_o} (y_s - \bar{y}_o)^2 ; \quad [4.3]$$

Where, $y_0 = \frac{1}{n_0} \sum_{s=1}^{n_0} y_s$ $Y_s = s^{th}$ response value at the centre

This calculated value of F can be compared with theoretical value of F at 95% confidence level. If for a coefficient the computed value of F is greater than the theoretical value, then the effect of that term is significant.

CHAPTER – 5

MICROSTRUCTURE STUDY

Microstructure of a solid can be defined as the structure of a solid specially alloys or ceramics which can be viewed or examined on the microscopic scale under a microscope after providing etching and polishing to the surface. Microstructure of a material can have a great role in the hardness, strength and tribological behaviour of a material **(Sharma et al., 2015)**. These properties in turn govern the application of these materials in the industrial practice. The composition of the material and the type of fillers plays an important role in defining the characteristics of a material.

In the present work aluminum matrix composites were fabricated using base material AA6082-T6 as already discussed in chapter 3. SiC and B_4C particulates were used as reinforcement to obtain hybrid and non-hybrid composites through the conventional stir casting process. AA6082-T6/SiC composites with 5, 10, 15 and 20 wt % of SiC; AA6082-T6/B_4C composites with 5, 10, 15 and 20 wt % of B_4C and AA6082-T6/(SiC+B_4C) hybrid composites with 5, 10, 15 and 20 wt % of (SiC+B_4C) taking equal fraction of SiC and B_4C were made and the microstructure study was carried out. X-Ray diffraction (XRD) patterns were studied for the presence of reinforcement within the matrix along with some other compounds. The microstructure of the fabricated composites was examined with the help of Scanning electron microscope (SEM) and the micrographs revealed that the dispersion of reinforced particles was reasonably uniform at all weight percentages. This section is divided into two sub-sections as follows:

- X-Ray diffraction (XRD) Analysis
- Scanning electron microscope (SEM) Analysis

5.1 X-RAY DIFFRACTION (XRD ANALYSIS)

X-ray diffraction (XRD) patterns were recorded using PANalytical X'pert PRO x-ray diffractometer which is shown in Figure 5.1. The cylindrical samples for XRD analysis were machined from the fabricated composites. The cross-section of the samples was taken as 5 mm diameter × 2 mm height and is shown in Figure 5.2.

Figure 5.1: PANalytical X'pert PRO x-ray Diffractometer

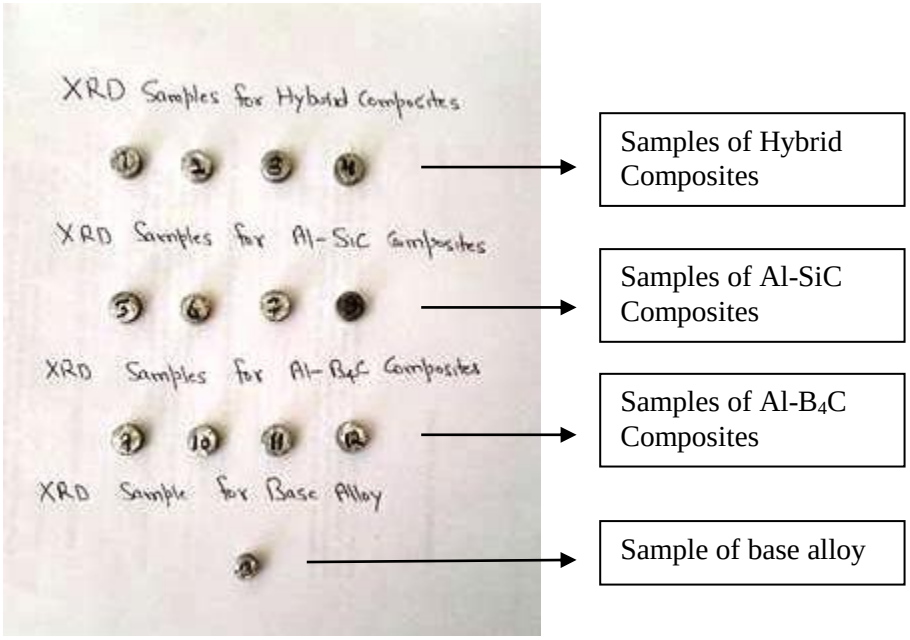

Figure 5.2: Samples employed for XRD analysis

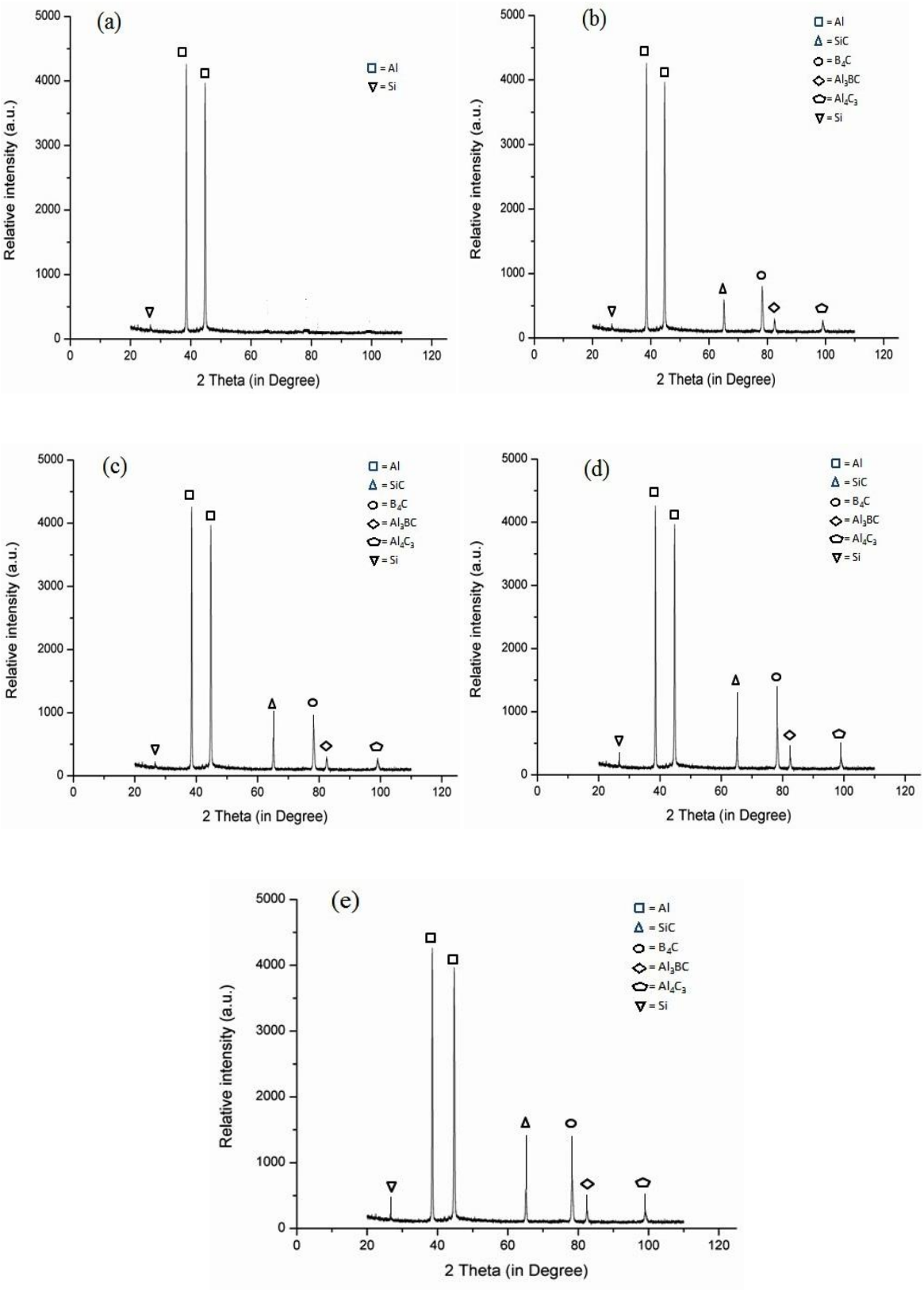

Figure 5.3 (a-e) - XRD pattern for 0% (a), 5% (b), 10 % (c), 15% (d) and 20% (e) of (SiC + B_4C) reinforced hybrid composite

The samples were grinded with emery paper of different grades (400, 600, and 1,000) and etched with Keller's reagent containing 2 ml HF, 3 ml HCl, 20 ml HNO_3, and 175 ml H_2O. The diffractometer is equipped with graphite curved single crystal monochromator to select CuK radiation ($\lambda = 1.54\dot{A}$) at the goniometer receiving slit station. Angle of 20º to 110º for diffraction angle (2θ) was maintained during XRD analysis.

X-Ray diffraction (XRD) pattern of the matrix alloy and hybrid composites is shown in Figure 5.3 (a-e). The results obtained from XRD analysis reveals that the strong peaks belongs to the parent material i.e. aluminum. The smaller peaks also reveal the presence of SiC and B_4C in the hybrid composites.

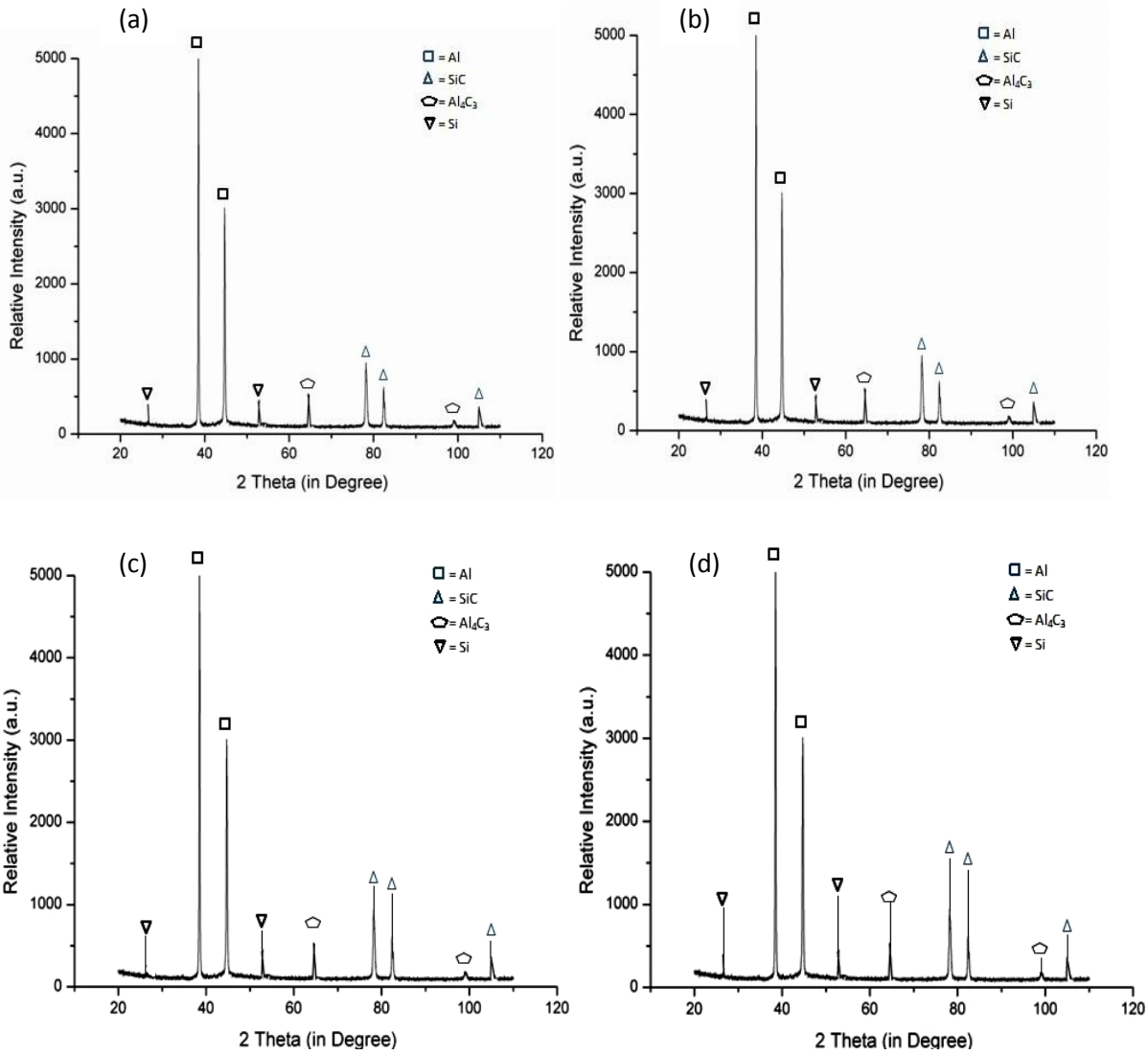

Figure 5.4 - XRD patterns for (a) 5%, (b) 10%, (c) 15% and (d) 20% of Al-SiC composites.

Figure 5.3 (a-e) also reveals the presence of Al_3BC, Al_4C_3 and Si in the prepared samples. However, the peaks for Al_3BC and Al_4C_3 were observed to be very small in all the hybrid composites. The formation of Al_3BC and Al_4C_3 was due to the direct reaction of aluminium with carbon and aluminium with boron carbide in an electric furnace **(Viala et al., 1997; Besterci, 2006).**

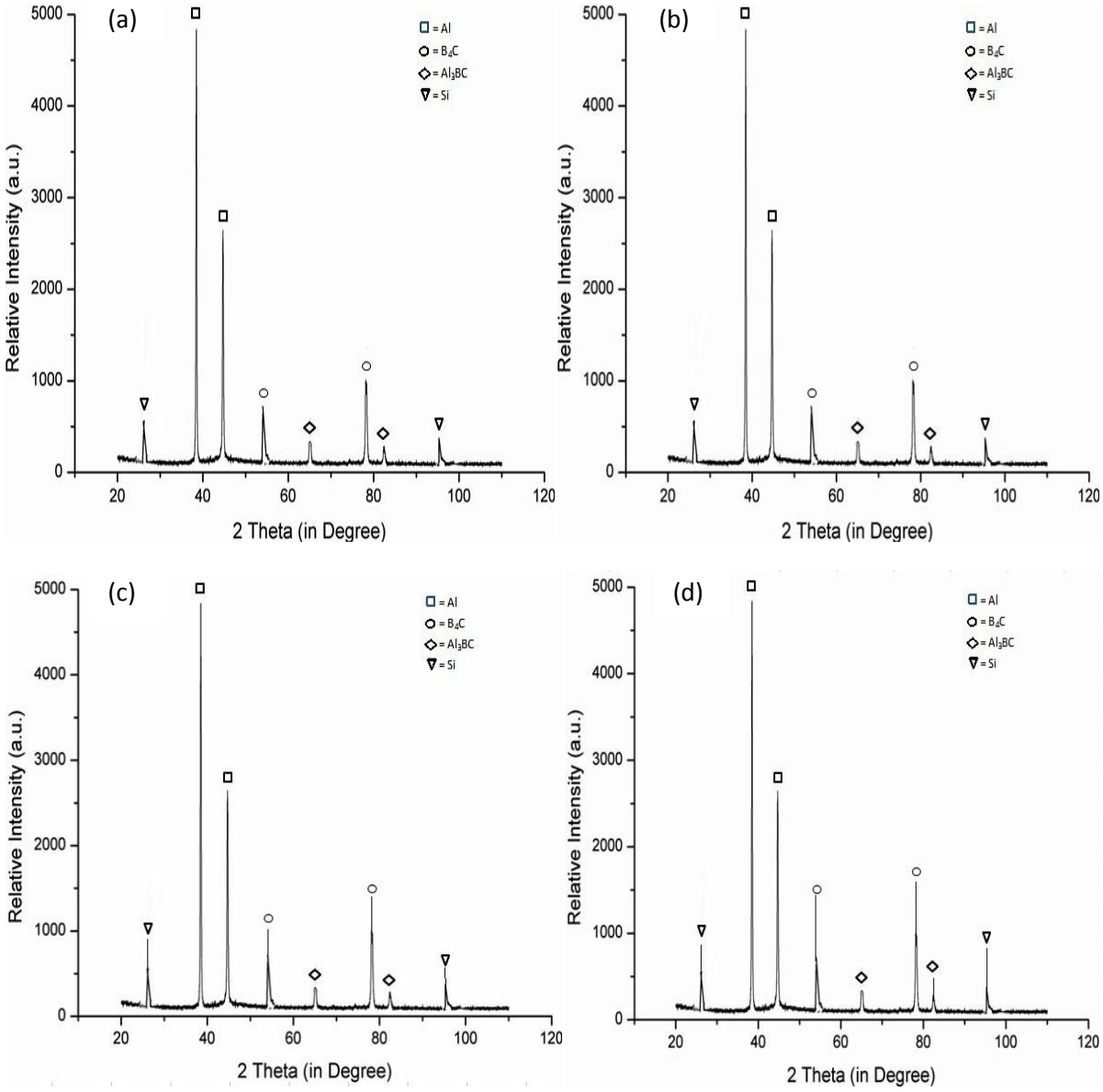

Figure 5.5 (a-d): XRD patterns for (a) 5%, (b) 10%, (c) 15% and (d) 20% of Al-B_4C Composites.

XRD patterns for AA6082-T6/SiC composites with 5, 10, 15 and 20 wt% of SiC are shown in Figure 5.4 (a-d). The patterns reveal the presence of SiC particulates in the composites along

with Al, Al_4C_3 and Si. It can be seen that as the wt% of SiC increases, there was a gradual increase in the peaks corresponds to SiC. Figure 5.5 (a-d) shows the patterns for B_4C reinforced composites. In Al-B_4C composites, the presence of B_4C and Al_3BC was observed along with Al and Si. However, the peaks for Al_3BC and Al_4C_3 were small in the respective composites.

In a study conducted by **Vazquez et al., (2016)**, it was reported that the phase Al_4C_3 can be obtained in most of the composites reinforced with carbides including SiC, TiC and B_4C. Production of Al_4C_3 has adverse effect on the aluminum composites because it readily reacts with water or the moisture present in the atmosphere and form aluminum hydroxide ($Al(OH)_3$), which degrades the quality of the composites. No technique can completely restrict the formation of Al_4C_3 in composites reinforced with carbides; however, its formation can be reduced by coating the reinforcements with SiO_2 **(Ortega-Celaya et al., 2007)**, optimizing the process parameters **(Arslan et al., 2003)** or modifying the chemical composition of the aluminum matrix **(Ortega-Celaya et al., 2007)**. **(Viala et al., 1997)** also observed the presence of Al_4C_3 and Al_3BC in the microstructure of aluminium composites.

5.2 SCANNING ELECTRON MICROSCOPE (SEM) ANALYSIS

SEM analysis is a microscope analysis which helps to take the images of a surface by scanning it with the focused beam of electrons. The electrons in the beam interrelate with the atoms present in the material surface and produces signals which further helps to evaluate the surface topography. In the present thesis, Scanning electron microscope (JOEL, JSM-6510LV) was used for micro structural analysis (Shown in Figure 5.6)

SEM samples are usually solid that can get easily adjusted in the specimen holder. Samples are rigidly mounted on a holder called as specimen stub using a conductive adhesive. The cylindrical samples with 6 mm diameter and 30 mm height were prepared to examine the microstructure of the cast composites. The samples for microstructure evaluation are shown in Figure 5.7. The SEM micrograph of the base metal AA6082-T6 and hybrid composites are reported in Figure 5.8 (a-e). The microstructure observation shows the dendritic growth of primary α-Al grains with inter-dendritic region of aluminium silicon eutectic. The formation of α-Al is mainly due to thermal mismatch of reinforced particles and the molten matrix.

Figure 5.6: Scanning electron microscope (JOEL, JSM-6510LV)

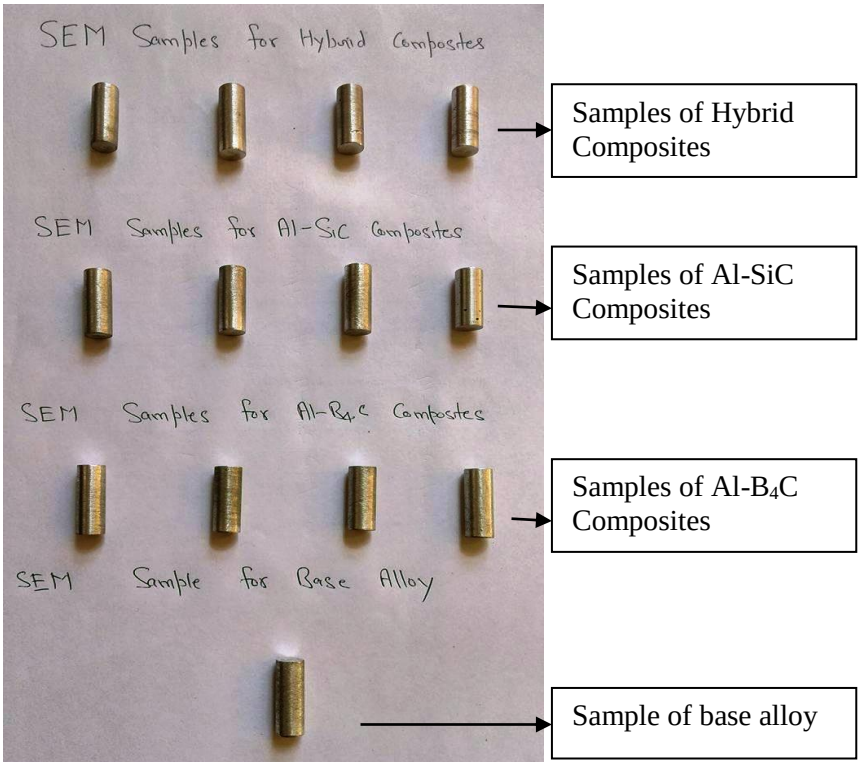

Figure 5.7: Samples employed for SEM analysis

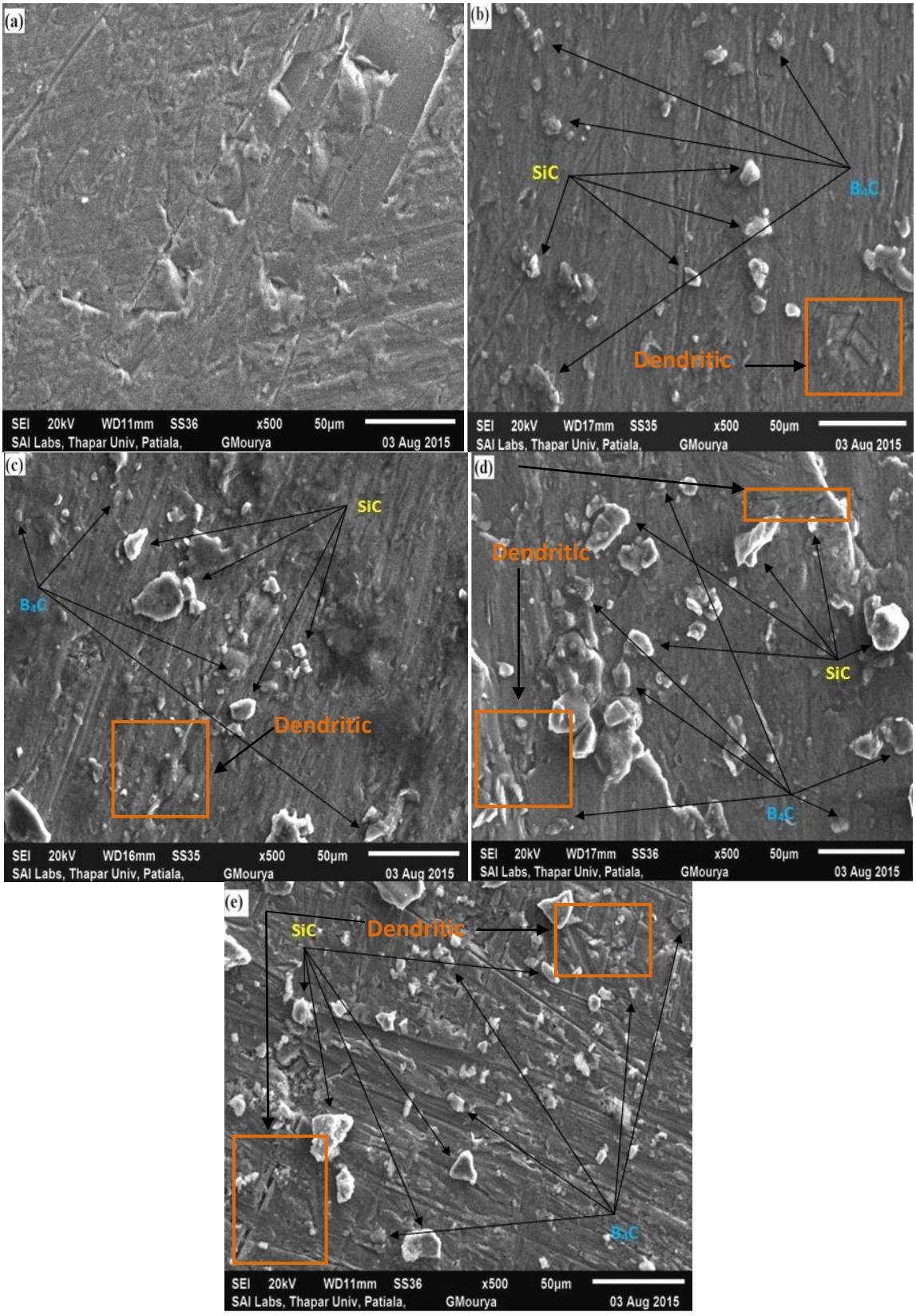

Figure 5.8 (a-e): SEM micrographs for 0% (a), 5% (b), 10 % (c), 15% (d) and 20% (e) of (SiC + B_4C) reinforced hybrid composite

Thermal conductivity of ceramic particles are lower as compared to aluminum melt and because of this the temperature of particles are high than molten matrix. As a result, hotter particles take more time for cooling during solidification and in the process, heat up the liquid alloy in their vicinity. Due to this thermal mismatch, nucleation of α-Al appears in the liquid alloy. Formation of dendritic region was mainly due to the cooling of fabricated hybrid composites while solidification. Relatively good dispersion of reinforced particles is shown in Figure 5.8 (b-e). The clusters of particles were also observed at some places where distributions of reinforced particles were not so good.

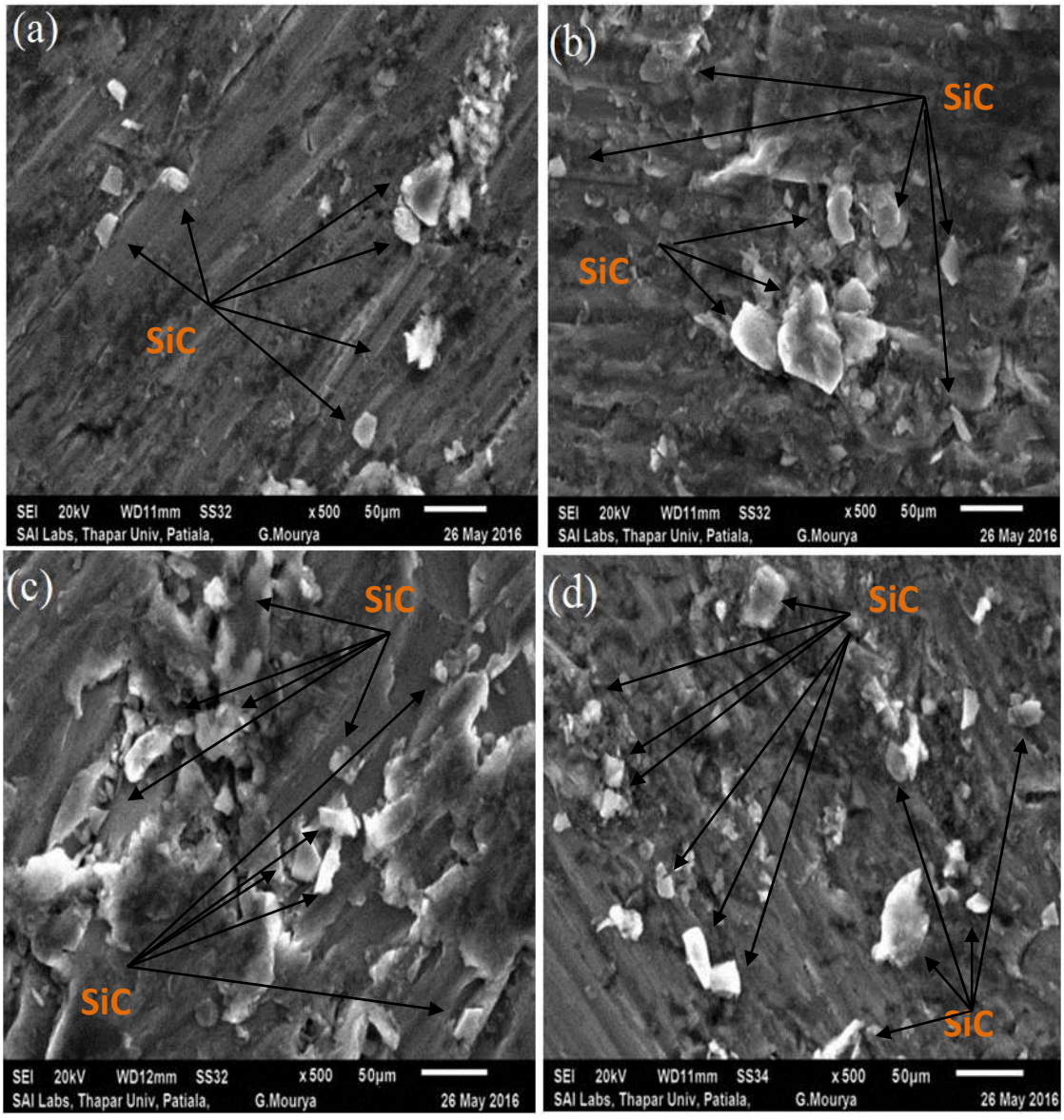

Figure 5.9 (a-d): SEM micrographs for (a) 5%, (b)10 %, (c) 15% and (d) 20% of Al-SiC Composites.

The interfacial bonding between particles and matrix was observed to be relatively good, as there is lack of voids in the interface. **(Zhou and Xu, 1997)** in their work reported that the reinforcement particulate can act as a barrier to the dendritic growth. The degree of agglomeration of clusters also increases with increase in wt % of reinforcement. However, the agglomeration can contribute towards strengthening of composite if well bonded in the matrix **(Maz et al., 1997)**

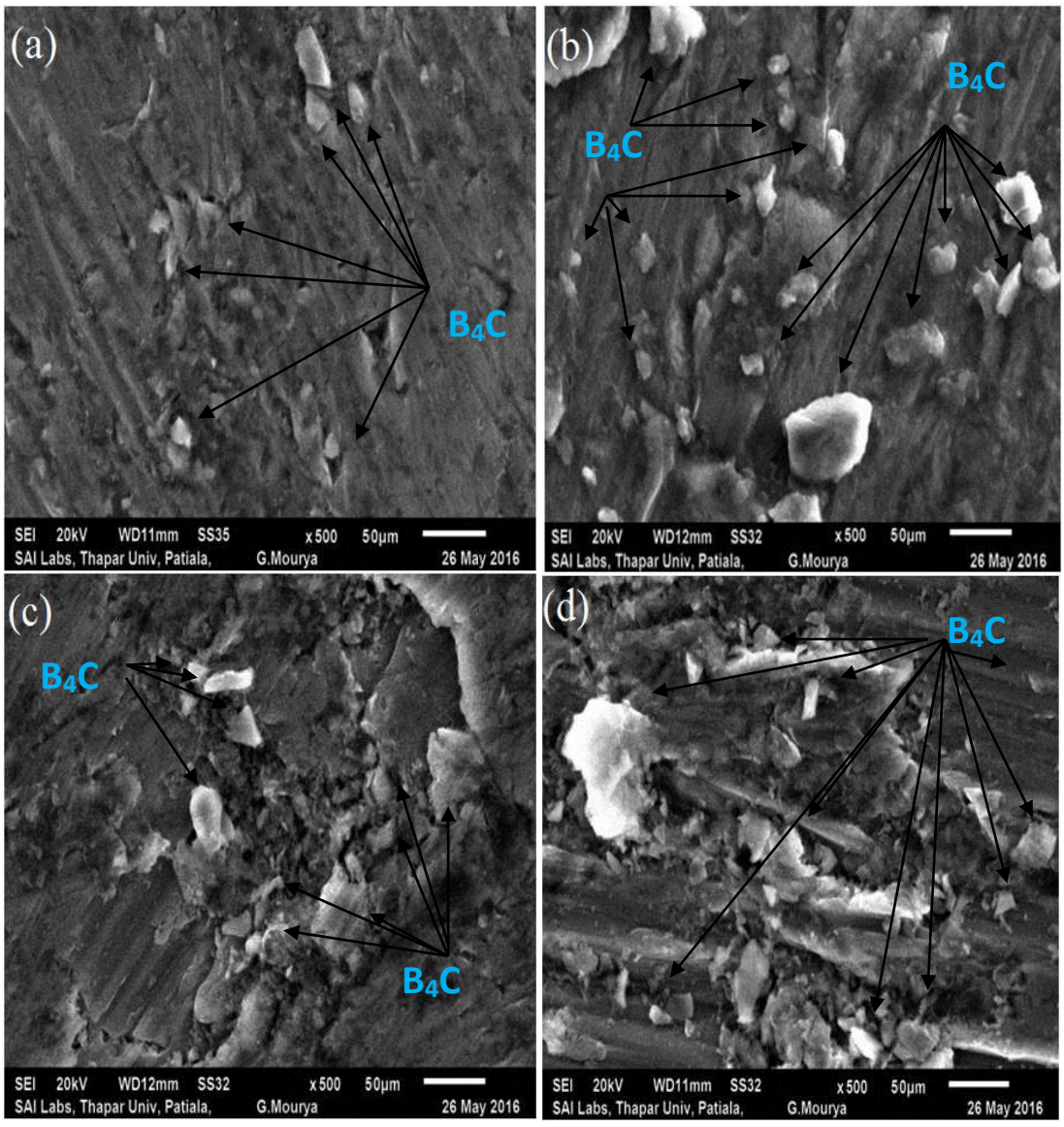

Figure 5.10 - SEM micrographs for (a) 5%, (b)10 %, (c) 15% and (d) 20% Al-B_4C composites.

Fig. 5.9 (a-d) and Fig. 5.10 (a-d) shows the images for SiC and B_4C reinforced composites with 5, 10, 15 and 20 wt% of the respective reinforcement in order. SEM micrographs show good dispersion of SiC and B_4C in the respective composites. However, with the increase in the reinforcement content from 5 to 20 wt. %, particles clusters were observed, for both AA6082-T6/SiC and AA6082-T6/B_4C composites. In AA6082-T6/SiC composites, SiC particles seemed more prone to agglomeration, possibly due to the high density of SiC (3.20 g/cm^3) when compared with aluminum (2.67 g/cm^3). Nevertheless, reinforcements agglomeration can contribute towards strengthening of a composite, if they are well boded in the matrix **(Maz et al., 1997)**. The produced AA6082-T6/SiC and AA6082-T6/B_4C composites revealed lack of voids at the interface, indicating a good interfacial bonding between particles and matrix.

CHAPTER – 6

MECHANICAL CHARACTERIZATION

In this chapter, the mechanical behaviour of the AMC's fabricated with different weight percentage of SiC and B_4C has been discussed. Tests were conducted to study the mechanical properties such as Hardness, Tensile strength, Percentage elongation and Impact strength along with the physical properties like density and porosity. The experimental results are discussed subsequently in the following sections.

6.1 HARDNESS EVALUATION

Hardness is considered as one of the most important property of any given material and is characterized by the strong intermolecular bonding. In the present work, the micro hardness of hybrid composites (Al6082-T6/SiC/B_4C) and the composites with single reinforced particles (Al6082-T6/SiC and Al6082-T6/B_4C) were examined on Vickers hardness tester with the test method IS 1501-2002 at a load of 1 kg for the duration of 15 s on all the samples. Small cuboids-shaped specimens were obtained and the specimens were given metallographic finish using emery paper of grit size 150, 400, 600, and 1,000. The specimens were indented with a diamond indenter in the form of pyramid having a square base and the angle between the square bases is 136°. Three tests were conducted on each of the specimen at different positions and the average value has been taken

The hardness values of the base metal AA6082-T6 and samples of hybrid composites are reported in Table 6.1. The tests reveal that hardness values of hybrid composites are higher in comparison to unreinforced counterpart and increases with increase in wt% of reinforcement. Addition of hard reinforcement particles in the matrix enhances the hardness and resists the plastic deformation of the material **(Raviteja et al., 2014)**. Figure 6.1 shows the increasing trend of hardness up to 15 wt% fraction. Beyond 15 wt %, the hardness tends to decrease slightly as the particulate mixture forms clusters within the matrix which in turn lowers the density of SiC and B_4C particles, thereby, lowering the hardness **(Singla et al., 2009)**. Reinforced composite with 15 wt % of (SiC + B_4C) mixture yields optimum hardness among hybrid composites with 11.9 % increase as compared to the un-reinforced alloy.

Table 6.1: Micro hardness of base alloy and hybrid composites

Nomenclature of sample	HV 1	HV 2	HV 3	HV Average	% Improvement (Compared to base alloy)
Alloy (AA6082-T6)	100	102	101	101	NA
Alloy + 5% (SiC + B_4C)	104	103	105	104	2.3
Alloy + 10% (SiC + B_4C)	107	108	111	109	7.9
Alloy + 15% (SiC + B_4C)	112	113	115	113	11.9
Alloy + 20% (SiC + B_4C)	111	110	111	111	9.9

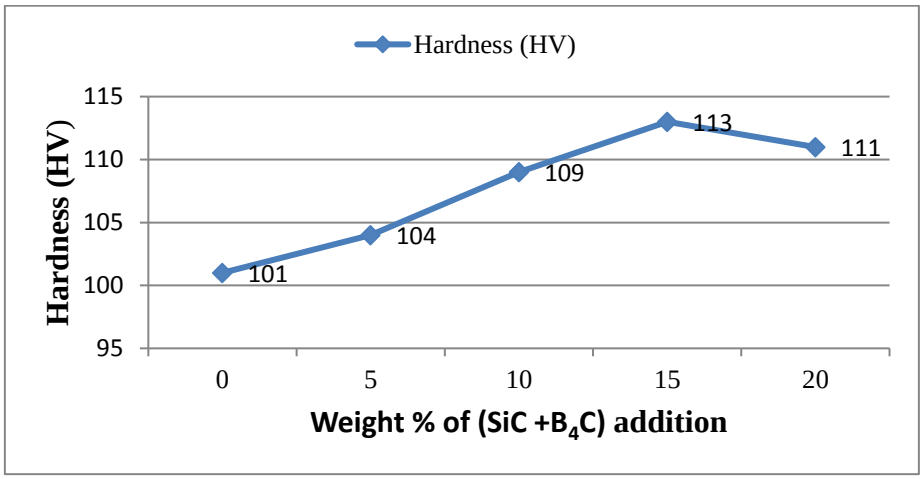

Figure 6.1 - Hardness distributions for un-reinforced alloy and hybrid composites

On a similar note, the micro hardness of Al-B_4C and Al-SiC composites were carried out and the results are shown in Table 6.2 and Table 6.3 respectively.

Table 6.2: Micro hardness of Al-B_4C composites

Nomenclature of sample	HV 1	HV 2	HV 3	HV Average	% Improvement (Compared to base alloy)
Alloy + 5% B_4C	104	103	105	104	3
Alloy + 10% B_4C	112	113	112	112	10.9
Alloy + 15% B_4C	118	117	116	117	15.8
Alloy + 20% B_4C	115	115	115	115	13.86

Table 6.3: Micro hardness of Al-SiC composites

Nomenclature of sample	HV 1	HV 2	HV 3	HV Average	% Improvement (Compared to base alloy)
Alloy + 5% SiC	102	104	103	103	2
Alloy + 10% SiC	107	108	117	107	6
Alloy + 15% SiC	111	111	111	111	10
Alloy + 20% SiC	114	112	114	113	11.9

Figure 6.2 shows the variation of Micro-hardness for Al-SiC and Al-B_4C composites with increase in reinforcement within the metal matrix.

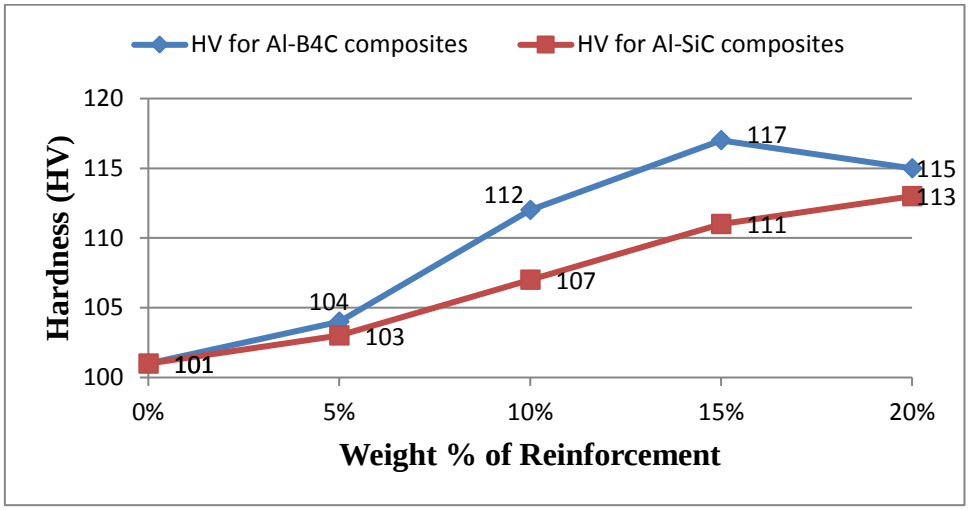

Figure 6.2 - Hardness distributions for Al-SiC and Al-B_4C composites

Figure 6.2 show that AA6082-T6/B_4C composites attain higher hardness values as compared to AA6082-T6/SiC. Results shows that the gradual increase in the reinforcement content tends to increase the hardness of the composites. This outcome is mainly attributed to the higher hardness of SiC (285 HV) and B_4C (305 HV) particles used in this work, which contributes towards resisting plastic deformation, thus leading to higher hardness. The measured micro-hardness of the un-reinforced alloy was calculated as 101 HV. SiC additions led to a gradual increase in hardness, with the highest value (113 HV) being attained with 20 wt. % SiC. B_4C additions led to higher hardness than that displayed by the Al-SiC composites

with optimum hardness valve of 117 HV, obtained when adding 15 wt. % B_4C to the aluminium matrix. Compared to the conventional alloy, the optimum percentage improvement in hardness for B_4C reinforced composites was 15.8 % attained at the addition of 15 wt % of B_4C particulates while in case of Al/SiC composites the percentage improvement was observed to be 11.9 % attained at the addition of 20 wt % SiC particulates. A slight decrease in AA6082-T6/B_4C composites hardness was observed with 20 wt% addition of B_4C. This decrease in hardness could be related with the formation of B_4C clusters within the metal matrix, which can lead to hardness lowering. **(Poovazhagan et al., 2013)** also observed fluctuations in the hardness of the composites due to the reinforced particles agglomeration. Another reason for having the superior hardness in the Al-B_4C composites as compared to other fabricated composites is brittle phase of B_4C particles compared to SiC particles.

6.2 TENSILE STRENGTH AND PERCENTAGE ELONGATION

Tensile behaviour of the Al/SiC/B_4C, Al-SiC and Al-B_4C composites was examined and tested as per ASTM-E8 standard. The tests were performed on universal testing machine at room temperature of 25 ± 3°C with relative humidity 40–60%. This type of machine has two crossheads; one is adjusted for the length of the specimen and the other is driven to apply tension to the test specimen. The tensile behaviour of hybrid composites indicates the increase in ultimate tensile strength (UTS) with increase in wt% of (SiC + B_4C) mixture which was attributed to the presence and relatively good dispersion of reinforcement mixture.

Table 6.4: Tensile tests results with percentage elongation for hybrid composites

Nomenclature of sample	UTS (MPa)	% Improvement	% Elongation
Al alloy	318	--------	8.38
Alloy + 5% (SiC + B_4C)	333	4.7	7.90
Alloy + 10% (SiC + B_4C)	357	12.26	7.30
Alloy + 15% (SiC + B_4C)	385	21.06	6.96
Alloy + 20% (SiC + B_4C)	371	16.6	6.8

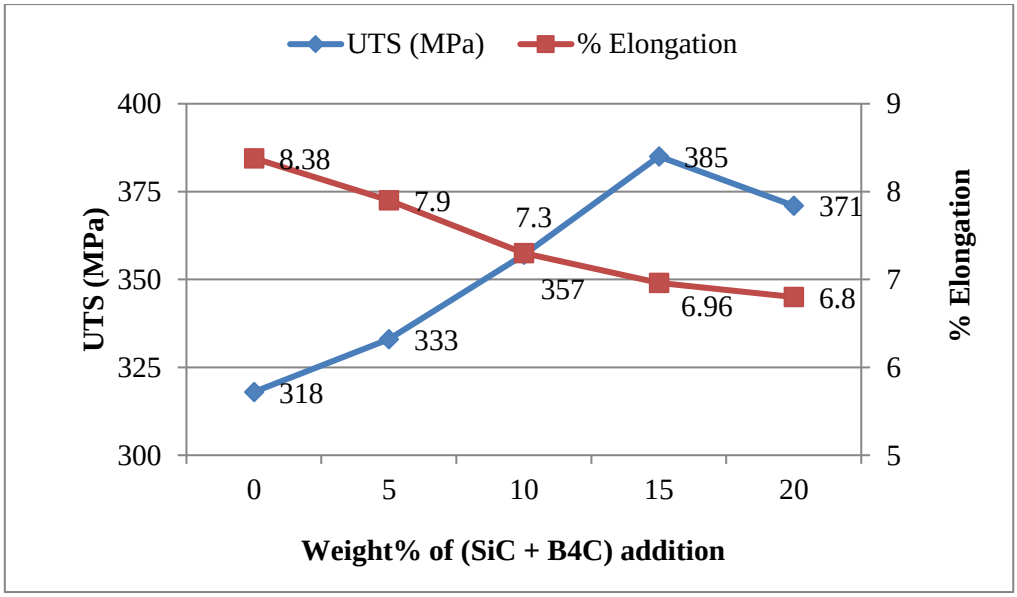

Figure 6.3 - Variation of UTS and percentage elongation for hybrid composites

Tensile results along with percentage elongation for Al/SiC/B_4C hybrid composites are reported in Table 6.4. The graphical representation of variation in UTS and percentage elongation with increasing wt% of reinforcement in aluminum matrix content is shown in Figure 6.3.

The tests reveal that UTS rose from 318 MPa at 0% addition of reinforcement mixture to 385 MPa at 15% addition of (SiC + B_4C) particles enhancing the UTS of hybrid composites by 21%. It was observed that the hybrid composite with 15 wt% of reinforcement gives superior UTS as compared to the counterpart with 20 wt% reinforcement. The possible reason of decline in UTS could be the high level of agglomeration of reinforcement particles at 20 wt% and increased porosity within the microstructures **(Poovazhagan et al., 2013)**. The clusters of particles which are the result of particle agglomeration make the material a weaker structure and the existence of porosity in the solidified hybrid composites reduces the ultimate tensile strength at 20 % addition of particles **(Singh and Goyal, 2016)**. Compared to un-reinforced aluminum alloy 6082-T6, the percentage elongation of the hybrid composites was observed to lower down as the wt% of reinforcement increases. The degradation in percentage elongation could be due to the resistance in flow ability of aluminum matrix with the addition of reinforcement particles and reduced nature of ductility of aluminum alloy matrix content.

On a similar note, the tensile strength and percentage elongation of Al-B_4C and Al-SiC composites were carried out and the results are shown in Table 6.5 and Table 6.6 respectively.

Table 6.5: Tensile tests results with percentage elongation for Al-B_4C composites

Nomenclature of sample	UTS (MPa)	% Improvement	% Elongation
Al alloy	318	--------	8.38
Alloy + 5% B_4C	341	7.2	8.01
Alloy + 10% B_4C	379	19.1	7.7
Alloy + 15% B_4C	417	31.1	7.4
Alloy + 20% B_4C	401	26.1	7.3

Table 6.6: Tensile tests results with percentage elongation for Al-SiC composites

Nomenclature of sample	UTS (MPa)	% Improvement	% Elongation
Al alloy	318	--------	8.38
Alloy + 5% SiC	331	4.1	7.8
Alloy + 10% SiC	350	10	7.2
Alloy + 15% SiC	373	17.3	6.9
Alloy + 20% SiC	379	19.1	6.8

The tests reveal that UTS rose from 318 MPa at 0% addition of reinforcement mixture to 417 MPa at 15% addition of B_4C particles, enhancing the UTS by 31% in comparison to base material. However, at the addition of 20% weight of B_4C slight decrease in UTS was also reported which may be due to the agglomeration of reinforcement particles. **(Poovazhagan et al., 2013).** The clusters of particles which are the result of particle agglomeration make the material a weaker structure and existence of porosity in the solidified composites reduces the ultimate tensile strength at 20 % addition of particles **(Singh and Goyal, 2016)**. The graphical representation of UTS and percentage elongation of Al-B_4C and Al-SiC composites is shown in Figure 6.4 and Figure 6.5 respectively.

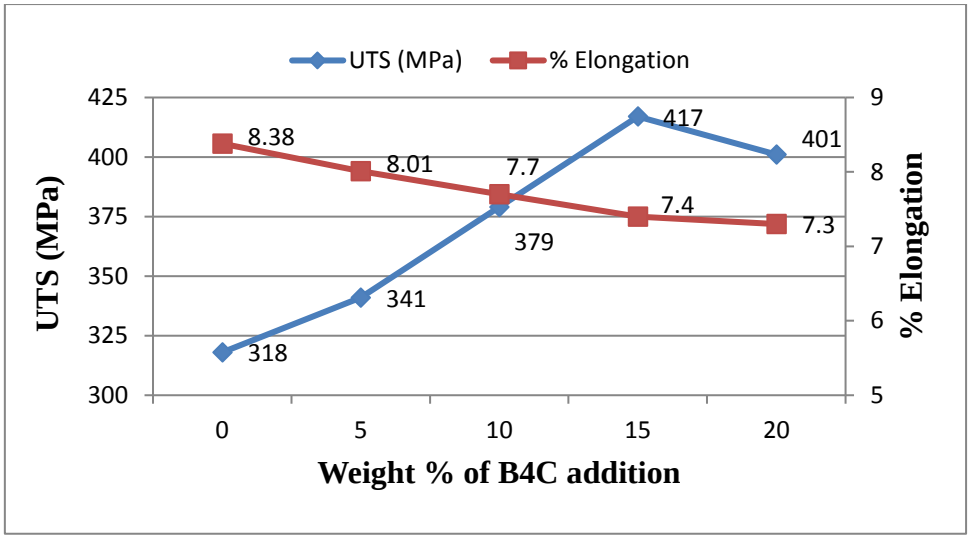

Figure 6.4 - Variation of UTS and percentage elongation for Al-B_4C composites

Al-SiC composited also showed increase in UTS but the results were not as significant as that of Al-B_4C composites. The optimum value of UTS was reported to be 379 MPa at the addition of 20% weight of SiC particulates with an increase of 19.1 % in UTS as compared to base material. The percentage elongation of the Al-B_4C and Al-SiC composites was observed to lower down as the wt% of reinforcement increases.

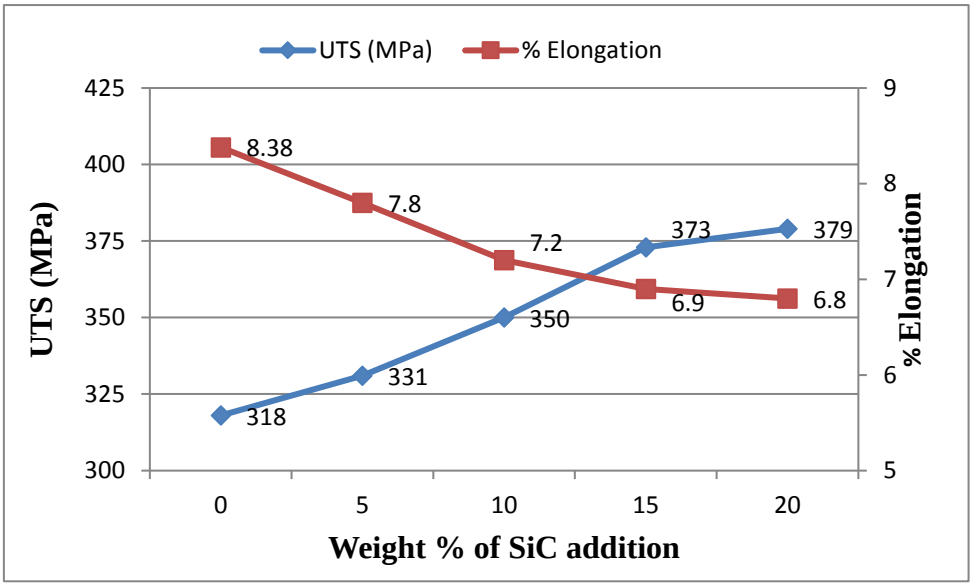

Figure 6.5 - Variation of UTS and percentage elongation for Al-SiC composites

The degradation in percentage elongation could be due to the same reason as in case of hybrid composites which was the resistance in flow ability of aluminum matrix with the addition of reinforcement particles and reduced nature of ductility of aluminum alloy matrix content. The results shows that the percentage elongation in B_4C reinforced composites is less as compared to the hybrid and SiC reinforced composites and the reason could be the low density of B_4C particles as compared to SiC particles.

6.3 IMPACT STRENGTH EVALUATION

Impact strength or toughness is another important property of a material and to evaluate this, two types of tests are generally being carried out namely charpy and Izod tests. In the present work, charpy tests have been employed to evaluate the impact strength of the AMC's. Specimen of 56 × 10 × 10 mm dimensions were machined having notch depth of 2 mm and notch tip radius of 0.25 mm. From each of the composite, three samples were prepared and tested, and the average value has been taken. During the fall from its raised position the pendulum's potential energy decreases, changing into kinetic energy. The kinetic energy is at its greatest just before impact. This is the impact energy. The energy absorbed by the test specimen during failure is worked out from the height of the pendulum after impact. The impact test results of the un-reinforced alloy and the hybrid composites are tabulated in Table 6.7. Figure 6.6 indicates, as the wt% of particulates increases in the metal matrix, the impact strength of the composites decreases as compared to the un-reinforced alloy. Even though the impact strength of hybrid composites tends to lower down, the reduction amount was very marginal.

Table 6.7 - Results of Impact Tests for hybrid composites

Nomenclature of sample	Trail 1 (Nm)	Trial 2 (Nm)	Trial 3 (Nm)	Average Impact strength (Nm)
Al alloy	9.4	9.7	9.4	9.50
Alloy + 5% (SiC + B_4C)	9.3	9.3	9.1	9.23
Alloy + 10% (SiC + B_4C)	8.6	8.7	8.7	8.66
Alloy + 15% (SiC + B_4C)	8.3	8.3	8.1	8.23
Alloy + 20% (SiC + B_4C)	7.9	7.9	7.8	7.80

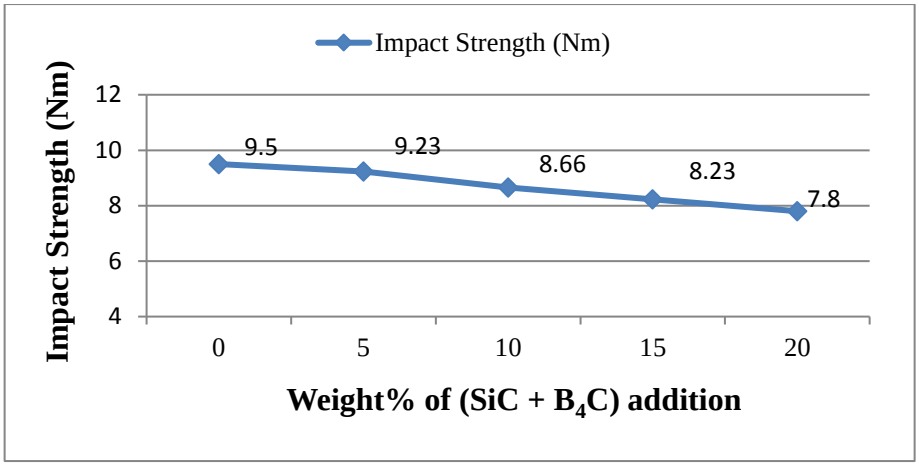

Figure 6.6: Impact strength variations for hybrid composites

The result shows that the impact strength for the hybrid composite with 20% wt of (SiC + B_4C) reduces to 7.8 Nm as compared to the 9.5 Nm impact strength of the base material. Addition of hard particles as reinforcement causes slight transition of material from ductile to brittle which could be one reason for this reduction **(Jansen and Technimet, 2008).** Failure of reinforcement particles by cracking and decohesion because of the presence of intrinsic defects in the composite microstructure also contributes to reduction in impact strength in composites. The failure rate generally increases with increase in wt% of reinforcement which ultimately results in decrease of impact strength.

The impact strength results for Al-B_4C and Al-SiC composites are shown in Table 6.8 and Table 6.9 respectively. The results revealed that as the weight percentage of B_4C and SiC increases, the impact strength of the material decreases. The reason for this reduction could be the addition of hard particles in the metal matrix.

Table 6.8 - Results of Impact Tests for Al-B_4C composites

Nomenclature of sample	Trail 1 (Nm)	Trial 2 (Nm)	Trial 3 (Nm)	Average Impact strength (Nm)
Al alloy	9.4	9.7	9.4	9.50
Alloy + 5% B_4C	9.3	9.3	9.4	9.33
Alloy + 10% B_4C	8.8	8.10	8.9	8.9
Alloy + 15% B_4C	8.3	8.3	8.6	8.4
Alloy + 20% B_4C	8.0	8.1	8.1	8.0

Table 6.9 - Results of Impact Tests for Al-SiC composites

Nomenclature of sample	Trail 1 (Nm)	Trial 2 (Nm)	Trial 3 (Nm)	Average Impact strength (Nm)
Al alloy	9.4	9.7	9.4	9.50
Alloy + 5% SiC	9.0	9.1	9.1	9.06
Alloy + 10% SiC	8.4	8.3	8.3	8.35
Alloy + 15% SiC	7.8	7.6	7.9	7.75
Alloy + 20% SiC	7.7	7.6	7.7	7.6

Impact strength of base material AA6082-T6 without the addition of reinforcement was 9.5 Nm and as the reinforcement was added from 5% weight to 20% weight in a step of 5, the impact strength reduced from 9.5 Nm to 8.0 Nm in Al-B_4C composite and 9.5 Nm to 7.6 Nm in Al-SiC composite respectively. Reduction in Impact strength was again due to the translation of ductile to brittle nature of the material with increase in weight percentage of reinforcement.

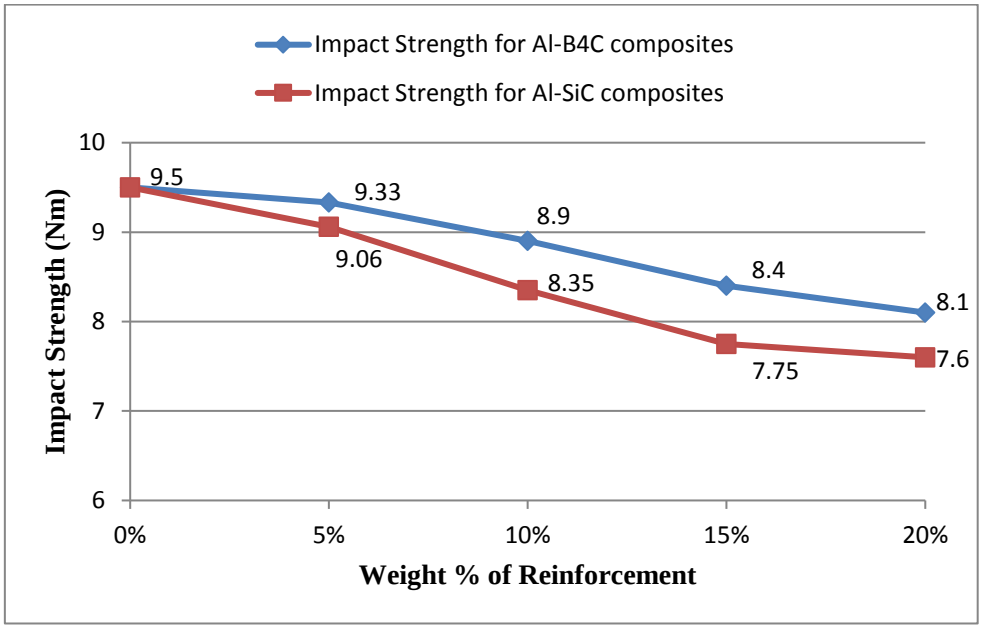

Figure 6.7: Impact strength variations for Al-B_4C and Al-SiC composites

6.4 DENSITY

The density, or more precisely, the volumetric mass density, of a substance is its mass per unit volume. The symbol most often used for density is ρ. For a pure substance the density has the same numerical value as its mass concentration and different materials usually have different densities. The density of a specimen was determined by knowing the mass and volume of the specimen used. By measuring the mass and volume, the density can be calculated using Equation 6.1

$$Density\ (g/cm^3) = \frac{Mass}{Volume}. \qquad \text{..... (6.1)}$$

The results reveal that addition of reinforcement particulates in the metal matrix has not much effect on the density of the hybrid composite, since the decrease in density was observed from 2.67 g/cm^3 at 0% (SiC+B_4C) addition to 2.53 g/cm^3 at 20% (SiC+B_4C) addition. The decrease in density was reported to be 5.2% in case of hybrid composites. Figure 6.8 shows the variation in density with addition of (SiC + B_4C) mixture for the hybrid composites.

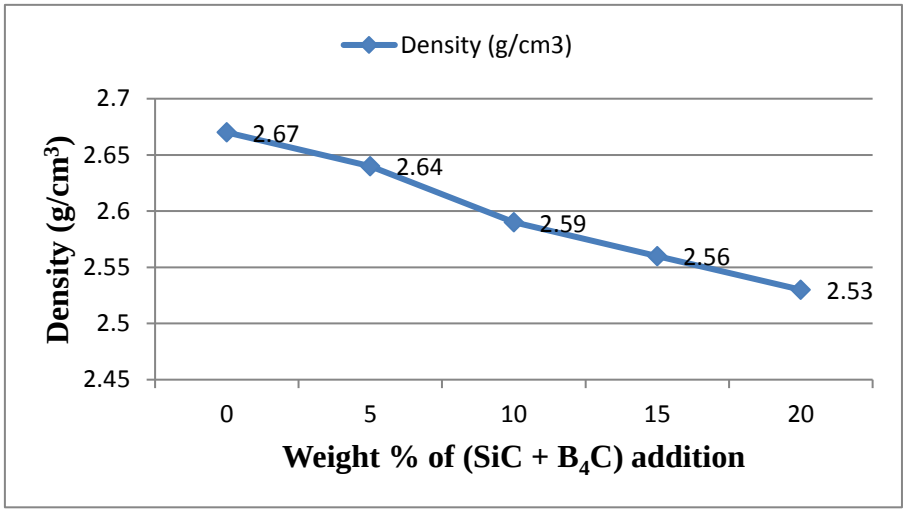

Figure 6.8: Density variations for hybrid composites

Similar trend was observed in the Al-B_4C and Al-SiC composites. The density tends to decrease slightly with the addition of SiC and B_4C in the molten metal. The decrease was observed from 2.67 g/cm^3 at 0% B_4C addition to 2.48 g/cm^3 at 20% B_4C in Al-B_4C composite while decrease in Al-SiC composites was from 2.67 g/cm^3 at 0% SiC addition to 2.56 g/cm^3 at 20% SiC addition. The decrease in density was reported to be 7.1% in Al-B_4C composites

and 4.1% in Al-SiC composites. Hence the addition of reinforcement has not change the density of the composite to a great extent.

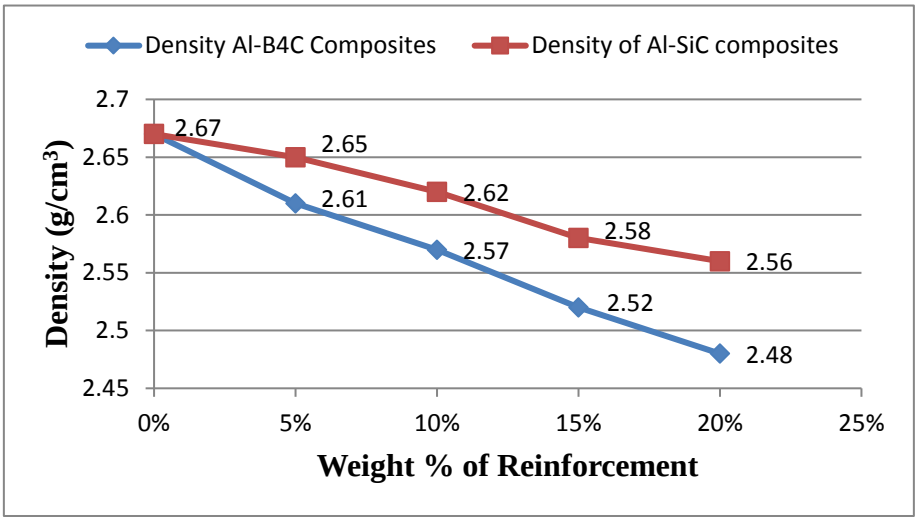

Figure 6.9: Density variations for Al-B_4C and Al-SiC composites

The variation in density for Al-B_4C and Al-SiC composites is shown in Figure 6.9. As the results shows, the density in B_4C reinforced composites is lowest followed by the hybrid composites and SiC reinforced composites. The probable reason for this is the low density of B_4C particles which is even less than the base alloy and this plays a significant part in the outcome of these results**.**

6.5 POROSITY

Every material contains some gap in it. This opening can be infinitely small or may be as big as a cave. But whatever be the space a solid contains, it is called as a void. The other part of the material is called solid and the total space inside a material is called porosity.

There are three other ways to classify porosity. Primary porosity is the amount of empty space caused by the creation of the rock itself. Secondary porosity is the amount of space created after the rock was formed, such as a crack in the rock. Finally, effective porosity is the amount of empty space that is connected, allowing a fluid, such as water, to move through the empty spaces.

In the present work, the porosity of AMC's was determined using the mass of the sample, volume of the sample and the density of the base alloy. The porosity of the specimen can be determined by using the simple relation as in Equation 6.2

$$Porosity = 1 - \frac{d}{d_a} \quad \text{..... (6.2)}$$

Where d = mass of sample/ volume of sample

d_a is the density of the base alloy.

With such a simple method, even the closed porosity will be taken into account.

Figure 6.10 shows the variation in porosity for the hybrid composites with increase in reinforcement (SiC + B_4C).

The results show that the porosity values of the reinforced hybrid composites slightly increases with addition of reinforcement. The value increases from 0.35% at 0% (SiC+B_4C) addition to 2.14% at 20% (SiC+B_4C) addition. Similar trend for porosity was reported by (**Aigbodion and Hassan., 2006)**. Variation in Porosity for Al-B_4C and Al-SiC composites with increase in reinforcement percentage is shown in Figure 6.11. Porosity in Al-B_4C and Al-SiC composites tends to increase slightly with the addition of B_4C and SiC in the molten metal.

The increase was observed from 0.35 at 0% B_4C addition to 2.23 at 20% B_4C in Al-B_4C composite while increase in Al-SiC composites was from 0.35 to 1.77 at 20% SiC addition. Hence not much change in the porosity was reported. As the results shows, the porosity in B_4C reinforced composites is higher followed by the hybrid composites and SiC reinforced composites.

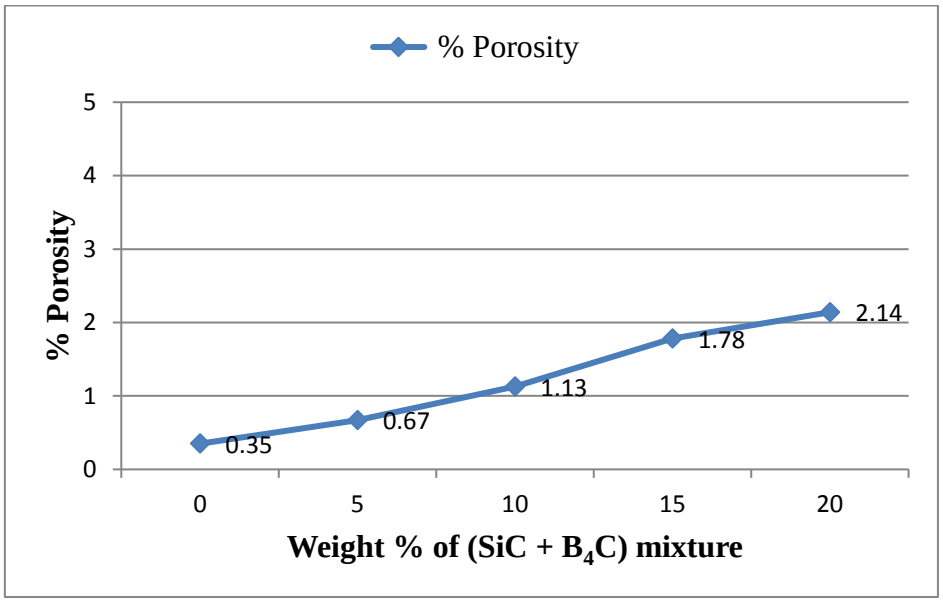

Figure 6.10: Porosity variations for hybrid composites

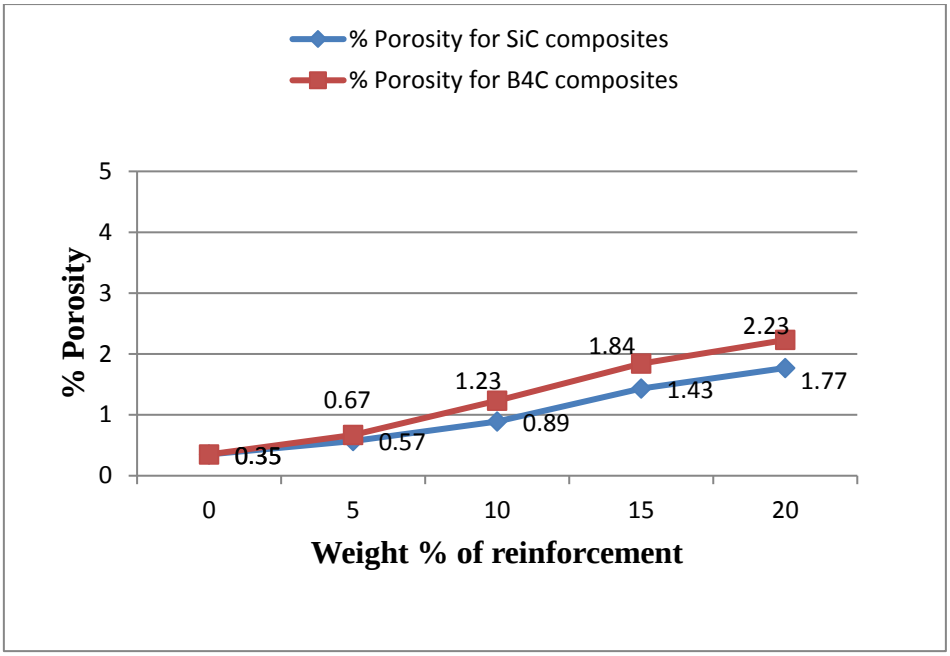

Figure 6.11: Porosity variations for Al-B_4C and Al-SiC composites

The low density of B_4C particles makes them to afloat in the middle and upper layer of molten mixture better in comparison to SiC particulates which have relatively higher density and probably due to this; the crack and formation of little voids are higher in the vicinity of B_4C particles. Moreover, the high density of SiC improves the chances of agglomeration of reinforcement particles which also contributes in the lesser formation of voids in the composite.

CHAPTER – 7

WEAR BEHAVIOUR ANALYSIS

Over the years, Aluminum based composites have arrived as an excellent substitute for conventional aluminum alloys because of their superior mechanical and tribological properties. The additions of hard particles in aluminum matrix composites (AMCs) combines the high hardness and wear resistance of particulates with low density and ductility of matrix resulting in good dimensional stability of the material **(Sannino and Rack, 1995).**

The operating conditions where contact between the sliding surfaces occurs, such as cams, gears, clutches and other applications, the phenomena of material removal is obvious and the wear behaviour analysis may become critical. AMCs have also been used in several sectors like automobile and defence as they present several advantages like high specific strength, excellent workability and high thermal conductivity. On the other hand, the hardness and wear resistance of aluminium restricted AMCs use in certain engineering applications where wear performance is crucial **(Meyveci et al., 2010).** Works found in literature (As discussed in Chapter 2) show that the parametric study of AA6082-T6/SiC/B_4C, AA6082-T6/SiC and AA6082-T6/B_4C composites tribological behaviour is limited. In this sense, AMCs were fabricated by conventional stir casting technique using AA6082-T6 matrix and SiC and B_4C reinforcing particulates in order to analyse the composites wear behaviour. This study intends to evaluate the influence of four parameters (reinforcement content, sliding speed, sliding distance and load) on these composites wear performance. Additionally this work intends to assess how the effects of these process parameters differ on SiC and B_4C reinforced composites. Response surface methodology (RSM) was used for the planning of experiments and modelling of the four parameters, taking five levels of each parameter to study their influence on composites wear behaviour. Confirmation tests validated the predictive models that were developed.

7.1 PIN ON DISC APPARATUS

Dry sliding wear tests were conducted using pin-on-disc apparatus at room temperature of 30-35 °C. Figure 7.1 shows the schematic diagram of the pin-on-disc apparatus used in this research work. (Figure 3.16 in chapter 3 shows the pictorial view of the apparatus). EN31

steel disc was used as a counter surface with hardness of 860 HV and surface roughness of 0.1 µm. The pin was held stationary against the rotating steel disc and with the help of a lever mechanism normal load was applied. The samples for wear tests were machined from fabricated composites with 6 mm diameter and 35 mm in length. The cylindrical pins were cleaned with acetone and weights have been recorded before and after the testing to an accuracy of 0.0001 g.

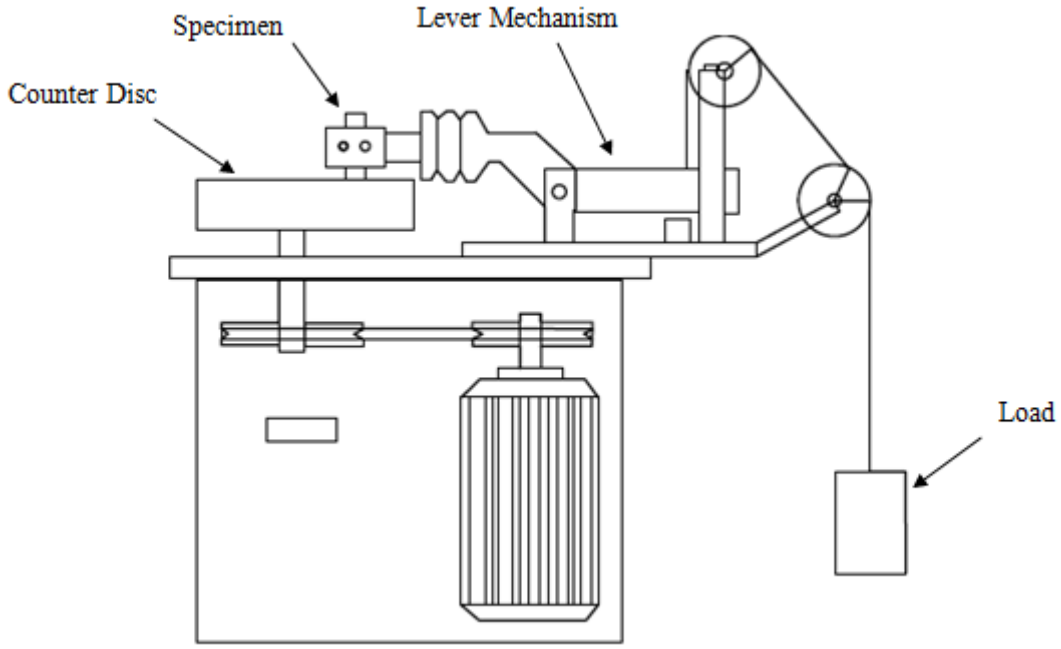

Figure 7.1 – Schematic of Pin on disc apparatus

7.2 SELECTION OF VARIABLES

In the present study of dry sliding wear behaviour of different composites, RSM has been used for the planning of experiments and modelling of different process parameters. Addition of reinforcement has great influence on the hardness of composites as the increase in reinforcement content tends to increase the hardness in AMC's **(Arslan et al., 2009; Poovazhagan et al., 2013).** In view of this, percentage reinforcement was chosen as one of the factor in the present study along with the sliding speed, load and sliding distance. Five levels have been selected for each parameter as given in Table 7.1 and the experiments were

constructed using Central Composite Design (CCD), as it is an effectual tool for building quadratic model consisting of a number of factors **(Kuehl, 2000).** Another advantage with CCD plan is that it can be employed to study the factors when numbers of levels are high and that too with lesser number of tests **(Montgomery, 2007).**

Table 7.1 - Factors and the levels used in CCD experimental plan

Factors	Designation	Levels				
		-2	-1	0	1	2
Reinforcement,(wt%)	R	0	5	10	15	20
Sliding speed (m/s)	S	0.6	1.2	1.8	2.4	3.0
Load (N)	L	14.71	29.42	44.13	58.84	73.55
Sliding distance (m)	D	400	800	1200	1600	2000

7.3 WEAR TESTS FOR HYBRID COMPOSITES

The experimental results for wear were analysed using Design Expert 7.0.0 software, a tool that is widely used in many engineering applications **(Suresha and Sridhara, 2010).** The experimental plan for the present study is shown in Table 7.2 with the coded and actual values of four factors, along with the results obtained in terms of weight loss.

7.3.1 Analysis of Variance (ANOVA) for Wear

ANOVA results using CCD design for Al-SiC-B_4C hybrid composites are given in Table 7.3. The results were evaluated with a confidence level of 95% or P-value 0.05 suggesting that any factor or their interactions with value less than 0.05 was significant as indicated by the right most column in ANOVA Table. Only the significant factors and their interactions were admitted for the wear analysis while the non-significant factors (having P-value > 0.05) were omitted. Lack of fit with p-value > 0.05 comes out to be a non-significant factor in the present model. All the factors selected for wear analysis, i.e. % reinforcement (R), sliding speed (S), load (L) and sliding distance (D) have p-values less than 0.05 and were significant.

Table 7.2 - Details of test combinations in coded and actual values of factors and corresponding experimental results

Run No.	R	S	L	D	% Reinforcement, R	Speed, S	Load, L	Sliding distance, D	Wear, Al-SiC-B_4C (g)
1	-1	-1	-1	-1	5	1.2	29.42	800	0.0076
2	1	-1	-1	-1	15	1.2	29.42	800	0.0062
3	-1	1	-1	-1	5	2.4	29.42	800	0.0038
4	1	1	-1	-1	15	2.4	29.42	800	0.0031
5	-1	-1	1	-1	5	1.2	58.84	800	0.0103
6	1	-1	1	-1	15	1.2	58.84	800	0.0077
7	-1	1	1	-1	5	2.4	58.84	800	0.0074
8	1	1	1	-1	15	2.4	58.84	800	0.0041
9	-1	-1	-1	1	5	1.2	29.42	1600	0.0178
10	1	-1	-1	1	15	1.2	29.42	1600	0.0132
11	-1	1	-1	1	5	2.4	29.42	1600	0.0101
12	1	1	-1	1	15	2.4	29.42	1600	0.0079
13	-1	-1	1	1	5	1.2	58.84	1600	0.0201
14	1	-1	1	1	15	1.2	58.84	1600	0.0178
15	-1	1	1	1	5	2.4	58.84	1600	0.0171
16	1	1	1	1	15	2.4	58.84	1600	0.0129
17	-2	0	0	0	0	1.8	44.13	1200	0.0116
18	2	0	0	0	20	1.8	44.13	1200	0.0094
19	0	-2	0	0	10	0.6	44.13	1200	0.0148
20	0	2	0	0	10	3.0	44.13	1200	0.0077
21	0	0	-2	0	10	1.8	14.71	1200	0.0059
22	0	0	2	0	10	1.8	73.55	1200	0.0111
23	0	0	0	-2	10	1.8	44.13	400	0.0019
24	0	0	0	2	10	1.8	44.13	2000	0.0188
25	0	0	0	0	10	1.8	44.13	1200	0.0093
26	0	0	0	0	10	1.8	44.13	1200	0.0089
27	0	0	0	0	10	1.8	44.13	1200	0.0081
28	0	0	0	0	10	1.8	44.13	1200	0.0091
29	0	0	0	0	10	1.8	44.13	1200	0.0077
30	0	0	0	0	10	1.8	44.13	1200	0.0087

The interaction between load and sliding distance represented by LD was the only significant interaction in the wear model. The quadratic terms of all the four factors were also significant with p-value less than 0.05. ANOVA calculates F value which is the ratio between

the regression mean square and the mean square error. It is also called as the variance ratio which is defined as the ratio of variance due to factors effect and variance due to error term. F value also signifies the effect of factors used in the investigation of wear behaviour. An increase in F value increases the significance of factors involved in the present analysis as shown in ANOVA Table.

Table 7.3 - Analysis of Variance for wear of Hybrid composites

Source	Sum of Squares	DOF	Mean Square	F Value	p-value Prob > F	percentage	
Model	6.36×10^{-4}	8	7.94×10^{-5}	82.19	< 0.0001		significant
Reinforcement, R	2.75×10^{-5}	1	2.75×10^{-5}	28.48	< 0.0001	4.20	significant
Sliding speed, S	9.80×10^{-5}	1	9.80×10^{-5}	101.41	< 0.0001	14.95	significant
Load, L	6.05×10^{-5}	1	6.05×10^{-5}	62.58	< 0.0001	9.22	significant
Sliding distance, D	4.21×10^{-4}	1	4.21×10^{-4}	435.45	< 0.0001	64.17	significant
Interaction, LD	6.38×10^{-6}	1	6.38×10^{-6}	6.6	0.0179	0.97	significant
$(\text{Reinforcement})^2$	7.38×10^{-6}	1	7.38×10^{-6}	7.64	0.0116	1.13	significant
$(\text{Sliding speed})^2$	1.38×10^{-5}	1	1.38×10^{-5}	14.23	0.0011	2.10	significant
$(\text{Sliding distance})^2$	6.34×10^{-6}	1	6.34×10^{-6}	6.56	0.0182	0.97	significant
Residual	2.03×10^{-5}	21	9.67×10^{-7}			3.10	significant
Lack of Fit	1.84×10^{-5}	16	1.15×10^{-6}	3.04	0.1121	2.81	Not significant
Pure Error	1.89×10^{-6}	5	3.79×10^{-7}			0.29	
Cor Total	6.56×10^{-4}	29					

Std. Dev.	0.000983087	R-Squared	0.9691
Mean	0.010003333	Adj R-Squared	0.9573
C.V. %	9.827592615	Pred R-Squared	0.9279
PRESS	4.72734E-05	Adeq Precision	32.933

The percentage contribution of each factor was calculated using Equation 7.1 and it was found that sliding distance has the maximum contribution with (64.17%) followed by sliding speed (14.95%), load (9.22%) and % reinforcement (4.20%). The percentage contribution of other significant terms was also calculated and is shown in Table 7.3

$$\text{Percentage (\%) contribution} = \frac{\text{Sum of Squares of a factor}}{\text{Total number of squares}} \times 100 \qquad [7.1]$$

The value of R^2 shows that the wear model has a variabilty of 96.9% as described by significant and non-significant terms. Adjusted R^2 is influenced by significant terms only and that is why $R^2 \geq$ Adjusted R^2 always and the difference between the two should be less than 0.2 for a satisfactory model which is also true for the present analysis. Adequate precision which gives the signal to noise ratio is another measure to evaluate the model. A ratio of greater than 4 is desirable and in the present work it is 32.93 which indicates that the model is adequate. The final Equation in terms of coded factors which was used to analyse variables effect on wear behaviour is given below.

Equation in Terms of Coded Factors:

$$Wear = + 8.651E\text{-}003 - 1.071E\text{-}003 * R - 2.021E\text{-}003 * S + 1.588E\text{-}003 * L + 4.188E\text{-}003 * D + 6.313E\text{-}004 * L * D + 5.134E\text{-}004 * R^2 + 7.009E\text{-}004 * S^2 + 4.759E\text{-}004 * D^2 \qquad [7.2]$$

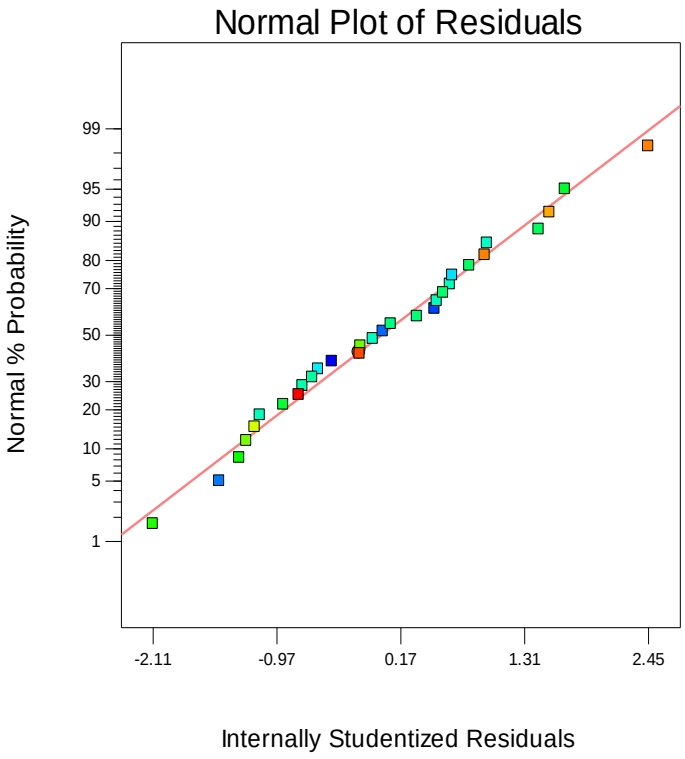

Figure 7.2 - Normal Plot of residuals for hybrid composites

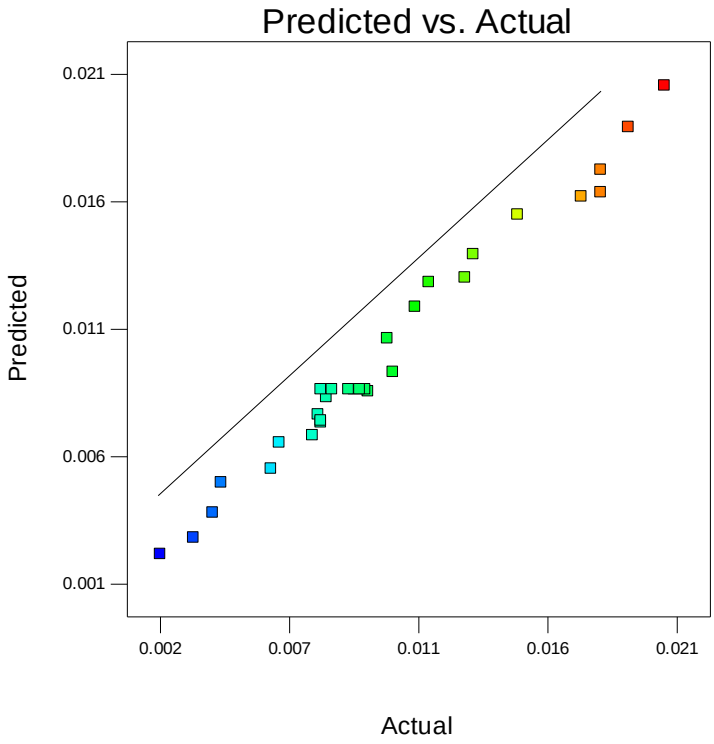

Figure 7.3 – Predicted vs Actual Plot for hybrid composites

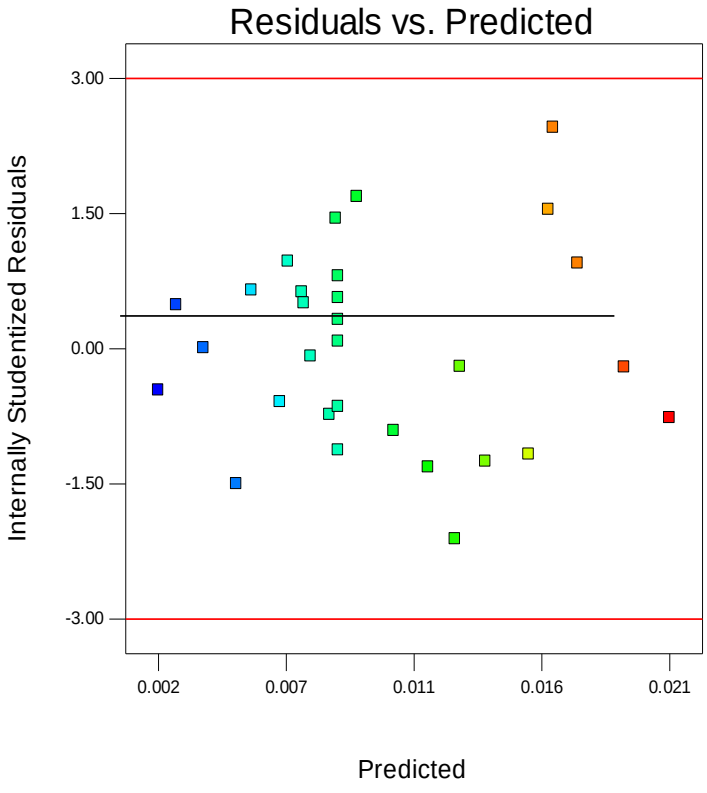

Figure 7.4 – Residual vs Predicted Plot for hybrid composites

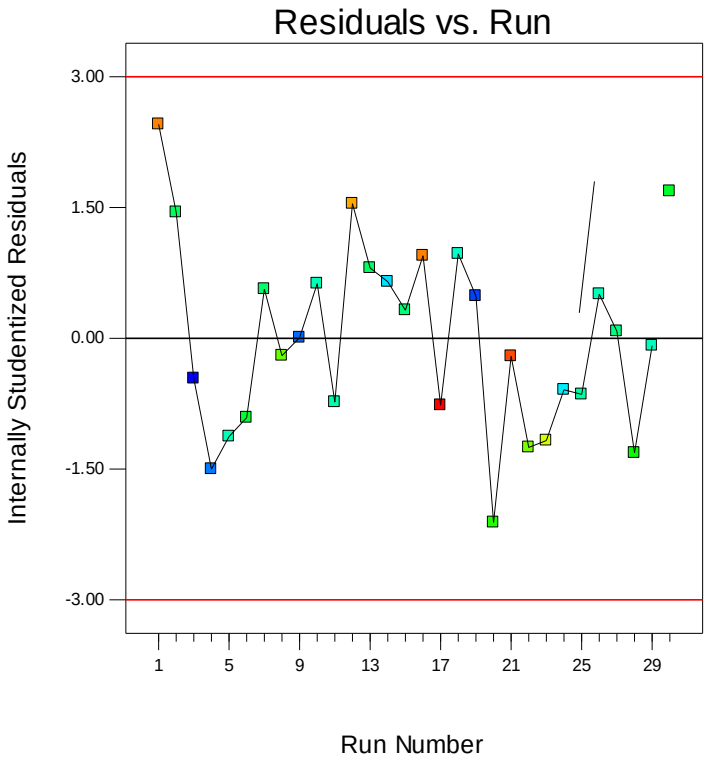

Figure 7.5 – Residual vs Run Plot for hybrid composites

Figure 7.2 shows a normal plot of residuals which indicates that all the residuals gets collected along the inclined line and there was no significant deflection from normal probability. Figure 7.3 shows the graph of predicted vs actual in which all the residuals gets collected in the vicinity of the inclined line which shows a strong corelation between the model's prediction and its actual values. Figure 7.4 represents the graph of residuals vs predicted where the prediction made by the model was on the x-axis and the accuracy of that prediction was on the y-axis. The distance from line zero shows how bad the prediction is for that value. Positive values of residuals on the y-axis means that the prediction was too low whereas negative values means that the prediction was too high. A scattered graph of residual vs predicted considers to be an ideal graph **(Umanath, 2013).** The plot of residuals versus run in Figure 7.5 indicates the sequence of positive and negative runs, which again signifies that residuals were distributed properly.

7.3.2 Variables effect on wear behaviour of hybrid composites

The four factors or process parameters, the interaction LD and quadratic terms (R^2, S^2 and D^2) have a significant effect on the wear of Al-SiC-B_4C hybrid composites as indicated

in Equation [2]. In the present work, Equation [7.2] was considered to analyse the contribution of Individual factors as all the factors were at the same level in this equation. The first constant + 8.651×10^{-3} indicates the average wear of the hybrid composites **(Sharma et al., 2015)**. Further the negative value – 1.071×10^{-4} associated with % reinforcement indicates a decreases in wear with the increase in reinforcement in the hybrid composites. Figure 7.6 shows the decreasing trend of dry sliding wear with increase in % reinforcement. This is attributed to the increase in hardness of the composite with the increasing percentage reinforcement **(Das et al., 2007).** The particle mixture of SiC and B_4C provides resistance to destructive action of abrasion by wear debris and thereby helps in reduction of wear.

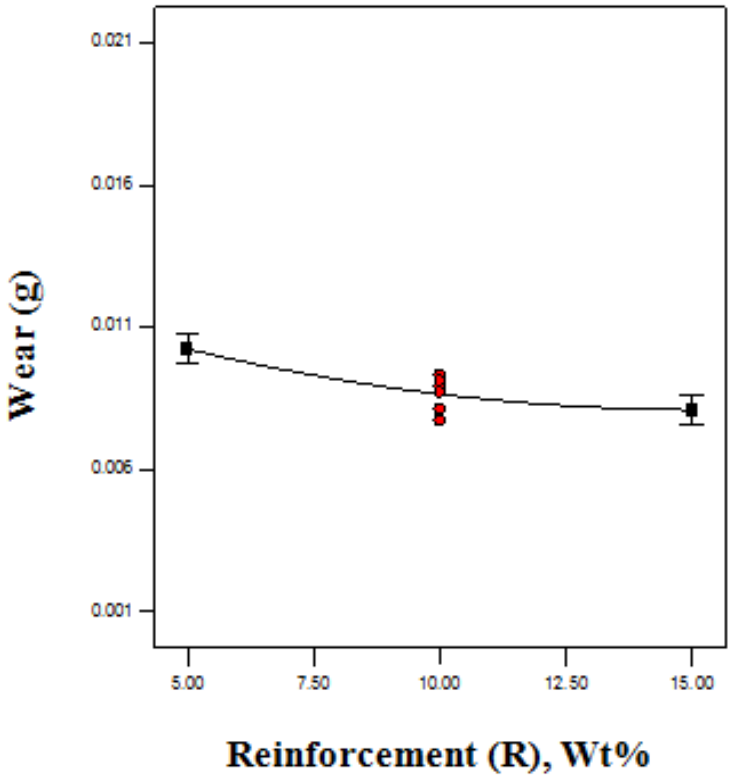

Figure 7.6 – Effect of reinforcement addition on wear

The coefficient - 2.021×10^{-3} with sliding speed is also negative, which signifies a decrease in wear with increased sliding speed as shown in Figure 7.7. The possible reason for the decrease in wear due to the increase in sliding speed was the change in shear rate at higher speeds which affects the mechanical behaviour of the mating surfaces **(Chowdhury, 2011).**

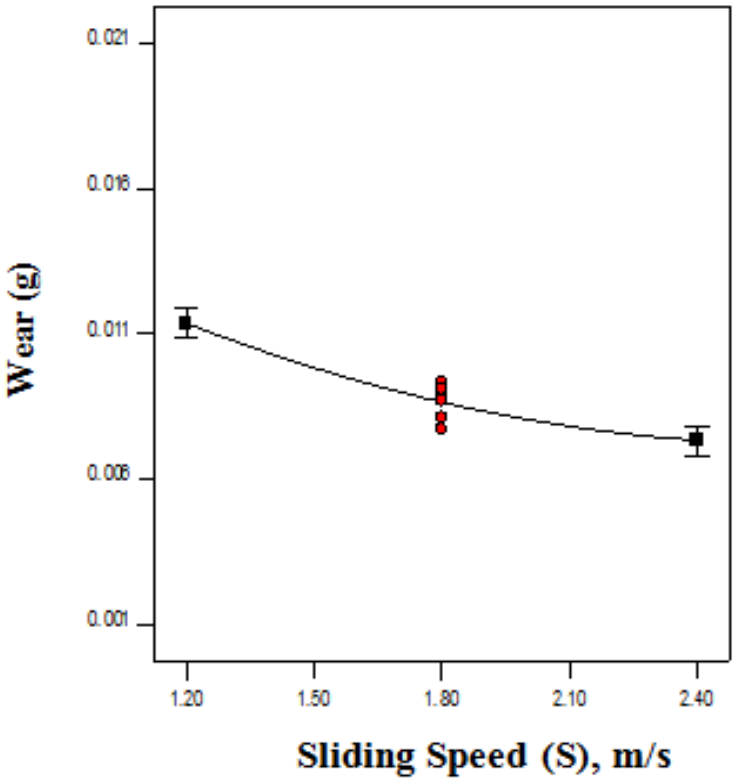

Figure 7.7 – Effect of increase in sliding speed on wear

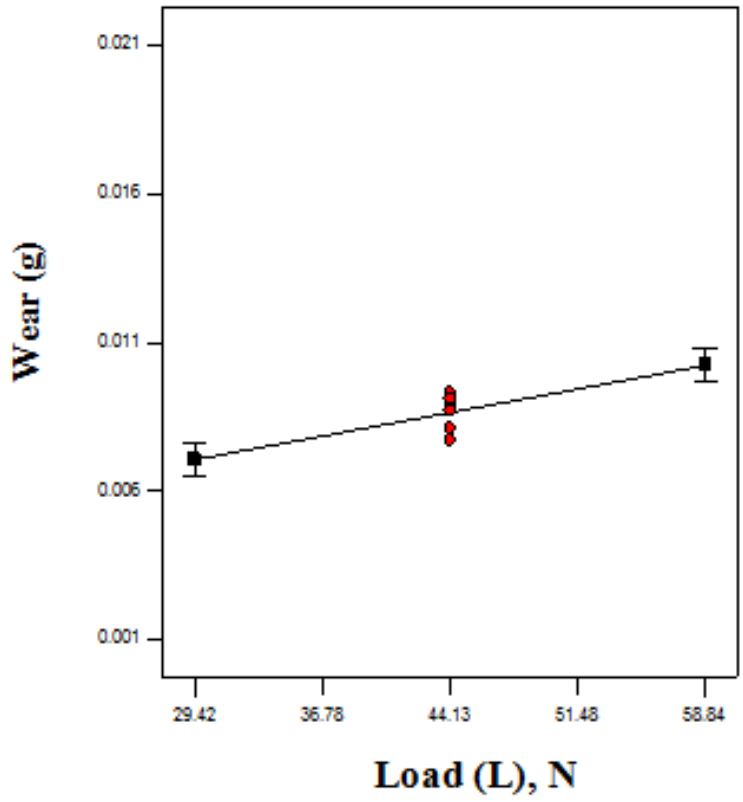

Figure 7.8 – Effect of increase in Load on wear

The material strength was large at increasing shear strain rates, which results in lower contact area and consequently in lesser wear **(Bhushan and Jahsman, 1978).** At higher sliding speeds, the time of contact between the sliding surfaces decreases which, in turn, decreases the wear **(Bhushan and Jahsman, 1978).**

The positive values of coefficients 1.588×10^{-3} and 4.188×10^{-3} affiliated with load and sliding distance reveals the increase in wear with increasing load and sliding distance. Here, the larger coefficient value of sliding distance signifies that wear rate was highly influenced by sliding distance as compared to the other process parameters. Figure 7.8 and 7.9 shows the variation in wear against load and sliding distance respectively, which again acknowledge the rise in wear with the load and the sliding distance.

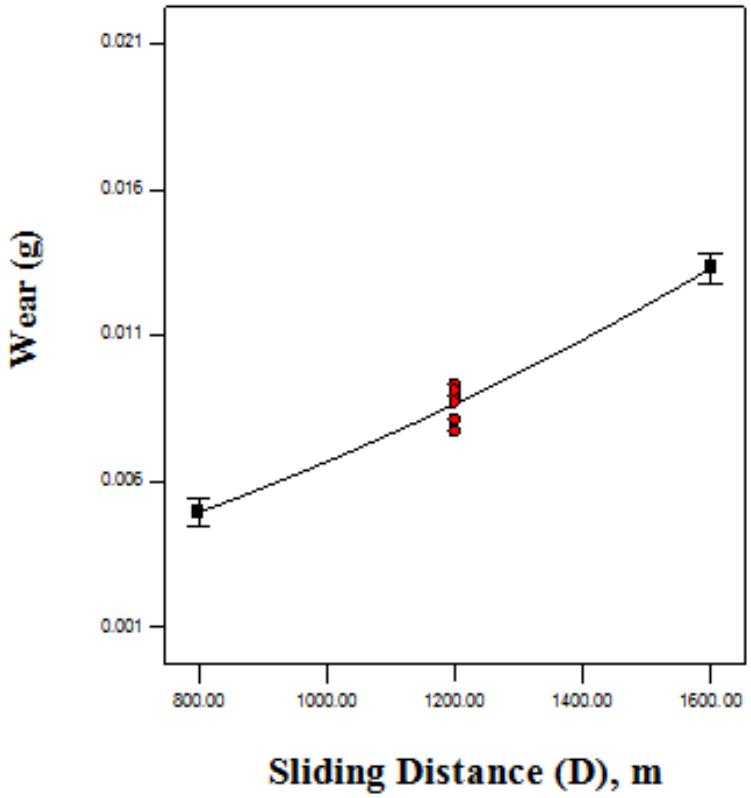

Figure 7.9 – Effect of increase in Sliding Distance on wear

Load determines the deformation and the pressure applied on the contacting surface. Increase in the load increases the contact stresses in the area where the wear pin comes in contact with the counter surface and this causes greater surface damage in the wear pin which eventually results in higher wear. In the present study, results predict the sliding distance to be the most dominant parameter as the material removal incremented abruptly at higher values of sliding

distance as shown in Figure 7.9 and the reason for this could be the longer period of interaction of wear pins with the counter surface.

Figure 7.10 gives 3-D interaction plot between load and sliding distance (LD) against the wear. It was evident from the interaction that the sliding distance has an enormous effect on the wear and with its increase, the wear of the hybrid composites increases significantly both at lower and higher values of sliding distance. This could be due to the increases in sliding distance which eventually increases the interaction time between the pins and the counter surface and results in increase of contact area and hence wear **(Sharma et al., 2015)**.

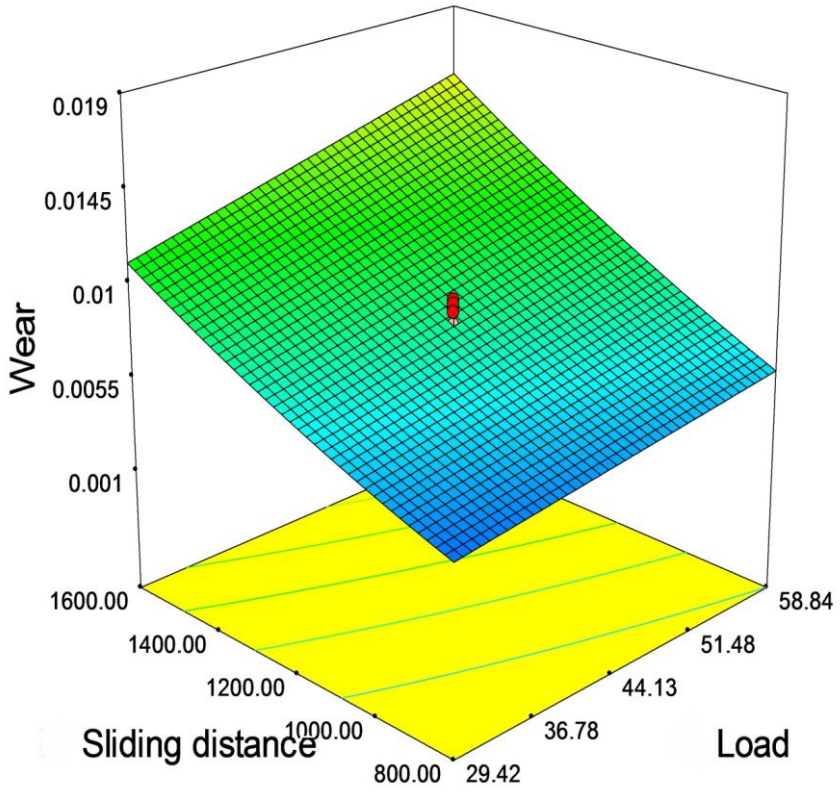

Figure 7.10 - 3-D interaction plot between load and sliding distance (LD) against the wear

Wear increases at lower and higher values (29.42 N and 58.84 N) of load with an escalation in the sliding distance as the incremental load gradually increases the contact pressure between the rubbings surfaces, resulting in removal of material at higher rate. The 3-D interaction suggests optimum or minimum wear at lower values of load and sliding distance

and shows that the combined effect of load and distance enhances the wear of Al-SiC-B_4C composites.

7.3.3 Confirmation Tests

After conducting the dry sliding wear analysis of Al-SiC-B_4C hybrid composites, it was important to carry out the confirmation tests in order to evaluate the validity of the present model. Confirmation tests were performed at optimum combinations of process parameters for wear, which gives the minimum amount of material removed from the hybrid composites. The three optimum combinations of the four process parameters, as given by the model, were selected for the tests. Table 7.4 shows the set of test parameters. The optimum or minimum wear of 0.029 g was achieved at reinforcement 14.82%, sliding speed 2.4 m/s; load 29.42 N and sliding distance 800 m as suggested by the RSM model.

Table 7.4 - Optimum Parameters used in Confirmation Tests

Test No	Reinforcement, (wt %)	Sliding speed (m/s)	Load (N)	Sliding Distance (m)
1	14.82	2.4	29.42	800
2	14.95	2.4	29.51	800.28
3	14.98	2.38	29.42	800.10

Table 7.5 - Experimental and Modelled results with Error

Test No	Experimental Results	Modelled Results	% Error
1	0.002198	0.002129	3.14
2	0.002256	0.002114	6.30
3	0.002216	0.002123	4.20

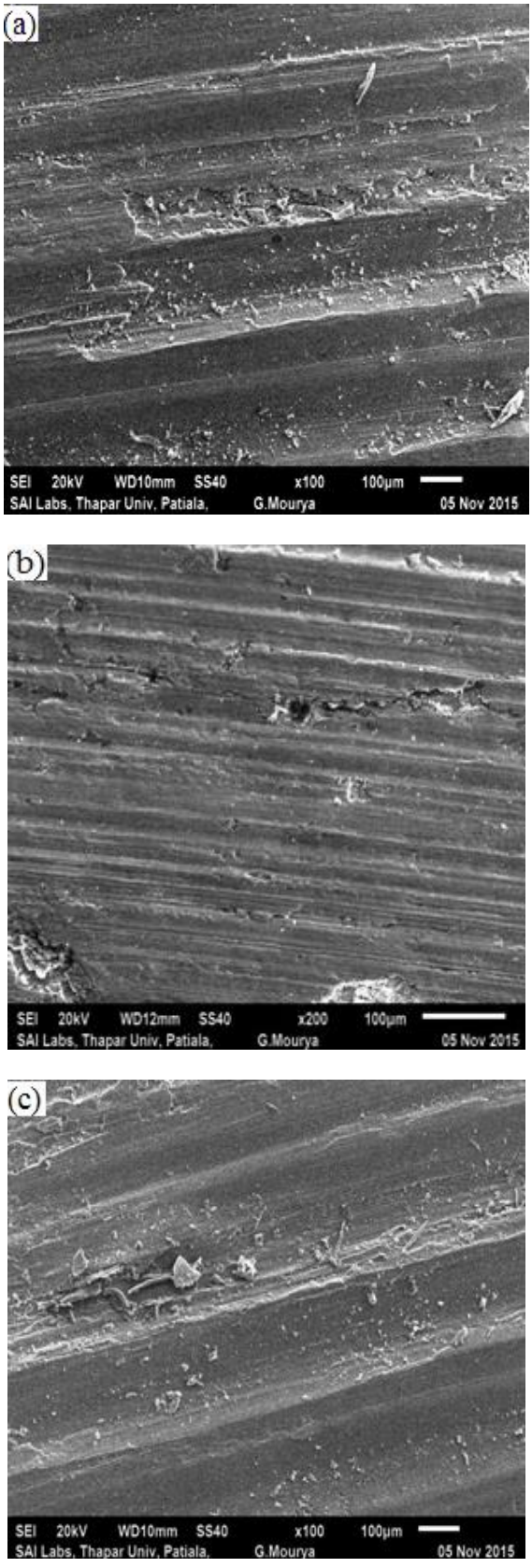

Figure 7.11 (a-c) - SEM micrographs showing worn surfaces of hybrid composites used for confirmation tests (a) Test 1 (b) Test 2 and (c) Test 3

The SEM micrographs of the worn surfaces of the composites used for the confirmation tests are shown in Figure 7.11 (a-c). Wide parallel lines represent the wear track formed by the reinforcement particles with little plastic deformation. The micrographs show distinct grooves on the worn surfaces which eventually gets crushed off to become debris.

The results predicted by the present model and obtained from the experimental tests are listed in Table 7.5. It was found that the errors vary from 3% to 7%, which were small enough to conclude that the present model and the wear analysis were appropriate.

7.4 WEAR TESTS FOR Al-SiC AND Al-B_4C COMPOSITES

The experimental results for Al-SiC and Al-B_4C composites wear were also analysed using Design Expert 7.0.0 software. The experimental plan for Al-SiC and Al-B_4C composites as given by the CCD design is shown in Table 7.6 with coded and actual values of four factors, along with the results obtained in terms of weight loss.

7.4.1 ANOVA for Wear of Al-SiC and Al-B_4C composites

ANOVA was again used to investigate the effect of process parameters on wear rate and to check the competency of the present model. ANOVA results using Central Composite Design (CCD) for Al/SiC and Al/B_4C composites are given in Table 7.7 and Table 7.8 respectively. The results were evaluated with a confidence level of 95% or p-value 0.05 suggesting any factor or their interaction with p-value less than 0.05 is significant as indicated by the right most columns in ANOVA Tables. Any factor or interaction which is non-significant (p-value > 0.05) was excluded from the analysis. The ANOVA results for both the composites shows the four process parameters i.e.% reinforcement (R), Sliding speed (S), Load (L) and Sliding Distance (D) as significant since p value for all the factors comes out to be less than 0.05. The quadratic terms of reinforcement, sliding speed, sliding distance and the interaction between Load and sliding distance (L*D) were also found as significant in the present work. The only difference between the models obtained for the two composites was the presence of the quadratic term of Load as significant factor in ANOVA analysis of Al/SiC composites, which was not found to be significant in Al/B_4C composites. In both the SiC and B_4C reinforced composites, the value of R-Squared was greater than adjusted R-Squared which is adequate for a good model.

Table 7.6 - Details of test combinations in coded and actual values of factors and corresponding experimental results.

Run No.	R	S	L	D	% Reinforcement, R	Speed, S	Load, L	Sliding distance, D	Wear Al-SiC (g)	Wear Al-B4C (g)
1	-1	-1	-1	-1	5	1.2	29.42	800	0.0084	0.0073
2	1	-1	-1	-1	15	1.2	29.42	800	0.0066	0.0061
3	-1	1	-1	-1	5	2.4	29.42	800	0.0041	0.0039
4	1	1	-1	-1	15	2.4	29.42	800	0.0033	0.0031
5	-1	-1	1	-1	5	1.2	58.84	800	0.0111	0.0099
6	1	-1	1	-1	15	1.2	58.84	800	0.0087	0.0071
7	-1	1	1	-1	5	2.4	58.84	800	0.0082	0.0072
8	1	1	1	-1	15	2.4	58.84	800	0.0047	0.0036
9	-1	-1	-1	1	5	1.2	29.42	1600	0.0189	0.0152
10	1	-1	-1	1	15	1.2	29.42	1600	0.0148	0.0126
11	-1	1	-1	1	5	2.4	29.42	1600	0.0113	0.0103
12	1	1	-1	1	15	2.4	29.42	1600	0.0085	0.0075
13	-1	-1	1	1	5	1.2	58.84	1600	0.0231	0.0195
14	1	-1	1	1	15	1.2	58.84	1600	0.0181	0.0179
15	-1	1	1	1	5	2.4	58.84	1600	0.0197	0.0173
16	1	1	1	1	15	2.4	58.84	1600	0.0139	0.0121
17	-2	0	0	0	0	1.8	44.13	1200	0.0119	0.0107
18	2	0	0	0	20	1.8	44.13	1200	0.0106	0.0089
19	0	-2	0	0	10	0.6	44.13	1200	0.0163	0.0141
20	0	2	0	0	10	3	44.13	1200	0.0081	0.0069
21	0	0	-2	0	10	1.8	14.71	1200	0.0066	0.0061
22	0	0	2	0	10	1.8	73.55	1200	0.0147	0.0109
23	0	0	0	-2	10	1.8	44.13	400	0.0021	0.0017
24	0	0	0	2	10	1.8	44.13	2000	0.0193	0.0174
25	0	0	0	0	10	1.8	44.13	1200	0.0088	0.0084
26	0	0	0	0	10	1.8	44.13	1200	0.0087	0.0084
27	0	0	0	0	10	1.8	44.13	1200	0.0084	0.0072
28	0	0	0	0	10	1.8	44.13	1200	0.0102	0.0087
29	0	0	0	0	10	1.8	44.13	1200	0.0089	0.0075
30	0	0	0	0	10	1.8	44.13	1200	0.0077	0.0077

This is because R-Squared explains the variability of the model due to significant and non-significant factors whereas adjusted R-Squared includes significant terms only. These models adequacy can also be assured by analysing their adequate precision, which must be

greater than 4 for a good model. In the present work, adequate precision values of 27.705 and 32.878 for SiC and B_4C reinforced composites were obtained, respectively.

Table 7.7 - ANOVA for wear of Al /SiC composites

Source	Sum of Squares	DOF	Mean Square	F Value	p-value Prob > F	
Model	0.000769488	9	8.55×10^{-5}	54.62154	< 0.0001	significant
R	0.00003456	1	3.46×10^{-5}	22.07895	0.0001	significant
S	0.000114407	1	0.000114	73.08968	< 0.0001	significant
L	9.5×10^{-5}	1	9.52×10^{-5}	60.8204	< 0.0001	significant
D	4.82×10^{-4}	1	0.000482	308.1896	< 0.0001	significant
LD	7.56×10^{-6}	1	7.56×10^{-6}	4.831368	0.0399	significant
R^2	1.19×10^{-5}	1	1.2×10^{-5}	7.64265	0.012	significant
S^2	2.21×10^{-5}	1	2.21×10^{-5}	14.12798	0.0012	significant
L^2	7.14×10^{-6}	1	7.15×10^{-6}	4.565177	0.0452	significant
D^2	7.50×10^{-6}	1	7.5×10^{-6}	4.791515	0.0406	significant
Residual	3.13×10^{-5}	20	1.57×10^{-6}			significant
Lack of Fit	2.79×10^{-5}	15	1.86×10^{-6}	2.783225	0.1317	Not significant
Pure Error	3.348×10^{-6}	5	6.7×10^{-7}			
Cor Total	8.0×10^{-4}	29				
Std. Dev.	1.25×10^{-3}			R-Squared	0.9609	
Mean	0.011			Adj R-Squared	0.9433	
C.V. %	10.02			Pred R-Squared	0.8954	
PRESS	8.374×10^{-5}			Adeq Precision	27.705	

The percentage contribution of each process parameter was calculated by dividing the sum of squares of each factor with total sum of squares and is given in Table 7. It was found that for Al/SiC composites, the contribution of sliding distance was maximum (60.24 %) followed by sliding speed (14.28 %), Load (11.88 %) and Reinforcement (4.31 %).

Table 7.8 - ANOVA for wear of Al/ B_4C composites

Source	Sum of Squares	DOF	Mean Square	F Value	p-value Prob > F	
Model	0.000582672	8	7.28×10^{-5}	80.3035	< 0.0001	significant
R	0.000024401	1	2.44×10^{-5}	26.90418	< 0.0001	significant
S	0.000084375	1	8.44×10^{-5}	93.02809	< 0.0001	significant
L	6.080×10^{-5}	1	6.08×10^{-5}	67.03719	< 0.0001	significant
D	0.000380807	1	0.000381	419.8603	< 0.0001	significant
L*D	1.19×10^{-5}	1	1.19×10^{-5}	13.12316	0.0016	significant
R^2	0.000007	1	0.000007	7.717886	0.0113	significant
S^2	1.27×10^{-5}	1	1.28×10^{-5}	14.06585	0.0012	significant
D^2	5.39×10^{-6}	1	5.36×10^{-6}	5.909006	0.0241	significant
Residual	1.90×10^{-5}	21	9.07×10^{-7}			significant
Lack of Fit	1.72×10^{-5}	16	1.08×10^{-6}	3.015785	0.1135	Not significant
Pure Error	1.78×10^{-6}	5	3.58×10^{-7}			
Cor Total	0.000601719	29				

Std. Dev.	9.52×10^{-4}	R-Squared	0.9683
Mean	9.50×10^{-3}	Adj R-Squared	0.9563
C.V. %	11.52	Pred R-Squared	0.9213
PRESS	4.73×10^{-5}	Adeq Precision	32.878

Table 7.9 – Percentage contribution of main parameters, interaction and

Factor	Reinforcement (R)	Sliding Speed (S)	Load (L)	Sliding Distance (D)	L*D	R^2	S^2	L^2	D^2	Others	Error
Al/SiC	4.31	14.28	11.88	60.24	0.94	1.49	2.76	0.89	0.93	3.9	0.41
Al/B_4C	4.05	14.02	10.1	63.28	1.97	1.16	2.12	NA	0.89	3.16	0.29

quadratic effects affecting wear of Al/SiC and Al/B_4C composites

Similar trend was observed in Al/B_4C with slightly different values for contributions of sliding distance (63.28%), Sliding speed (14.02 %), Load (10.10 %) and Reinforcement (4.05%). The contribution of interaction and quadratic terms was also calculated and shown in the Table 7.9.

Eq. [7.3] and Eq. [7.4] represent the final equations in terms of coded factors which will be used further to explain the effect of the selected variables on wear (weight loss).

Equation for Al/SiC in Terms of Coded Factors:

$$Wear = +8.783E\text{-}003 - 1.200E\text{-}003 * R - 2.183E\text{-}003 * S + 1.992E\text{-}003 * L + 4.483E\text{-}003 * D + 6.875E\text{-}004 * L * D + 6.604E\text{-}004 * R^2 + 8.979E\text{-}004 * S^2 + 5.104E\text{-}004 * L^2 + 5.229E\text{-}04 * D^2 \quad [7.3]$$

Equation for Al/ B_4C in Terms of Coded Factors:

$$Wear = + 8.217E\text{-}003 - 1.008E\text{-}003 * R - 1.875E\text{-}003 * S + 1.592E\text{-}003 * L + 3.983E\text{-}003 * D + 8.625E\text{-}004 * L * D + 5.000E\text{-}004 * R^2 + 6.750E\text{-}004 * S^2 + 4.375E\text{-}004 * D^2 \quad [7.4]$$

Figure 7.12 (a) and (b) show the normal plot of residual for Al/SiC and Al/B_4C composites and it can be seen that all the residuals were aligned along the inclined line which certifies the normal distribution of ANOVA. Almost similar trend was followed in Predicted vs Actual plots as shown in Figure 7.13 (a) and (b). The graph of residuals versus predicted for the two composites are shown in Figure 7.14 (a) and (b), where no significant pattern was followed by residuals, which is again a sign of a good model **(Umanath et al., 2013).**

7.3.2 Variables effect on wear behaviour of Al/SiC and Al/B_4C Composites

The effect of variables or process parameters on dry sliding wear behaviour of Al/SiC and Al/B_4C composites are given in Eq [7.3] and Eq [7.4] in terms of coded values. The coefficients -0.00*12* and-*0.001008* associated with reinforcement content have negative values in both the equations which suggests that the reinforment addition to the metal matrix

decreases the wear in these composites. This is related with the composites micro-hardness, as the addition of reinforcement enhances hardness, which lowers the material removal rate.

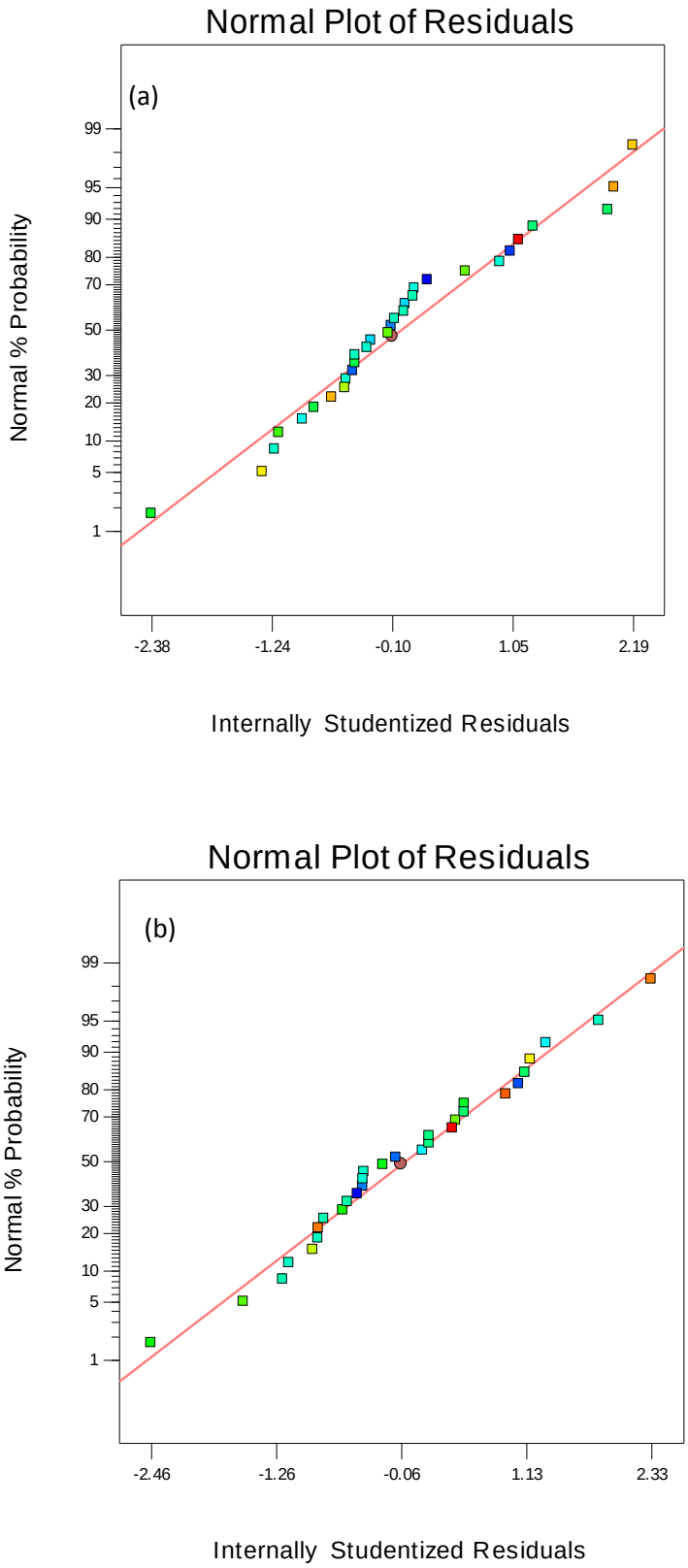

Figure 7.12 (a-b) - Normal plot of residuals for (a)Al//SiC and (b) Al//B_4C models

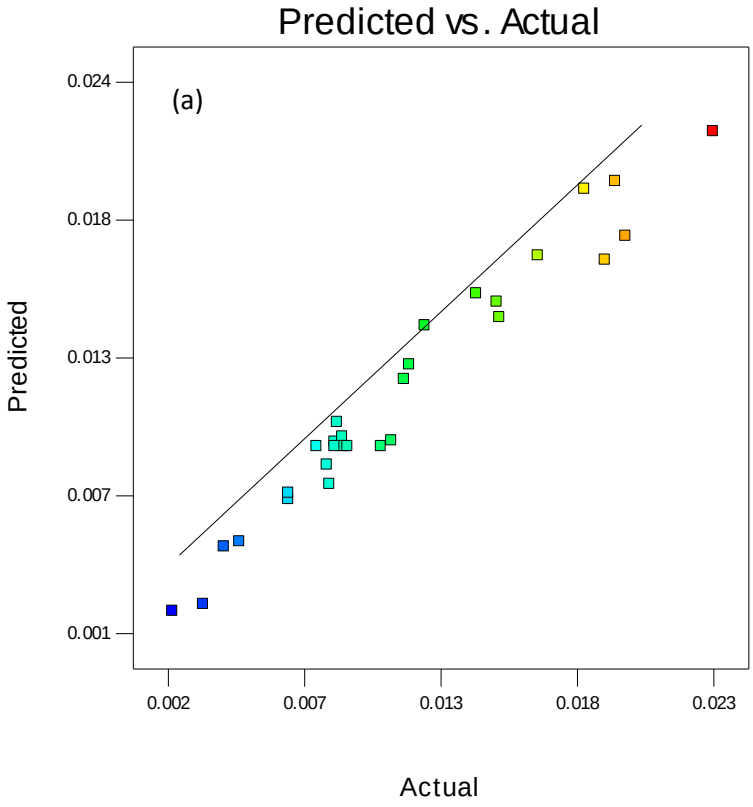

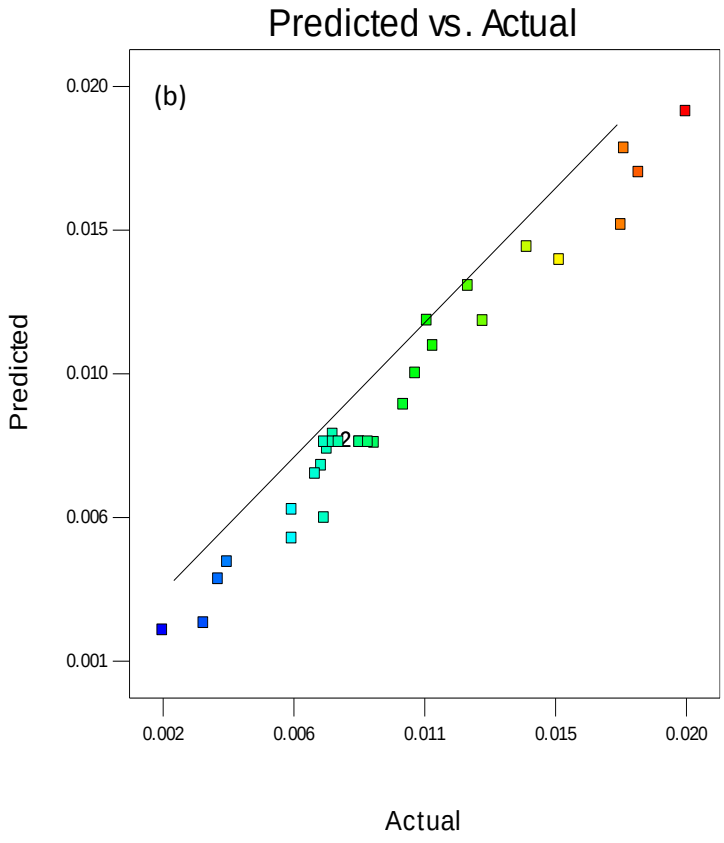

Figure 7.13 (a-b) - Predicted vs Actual plots for (a) Al//SiC and (b) Al//B_4C models

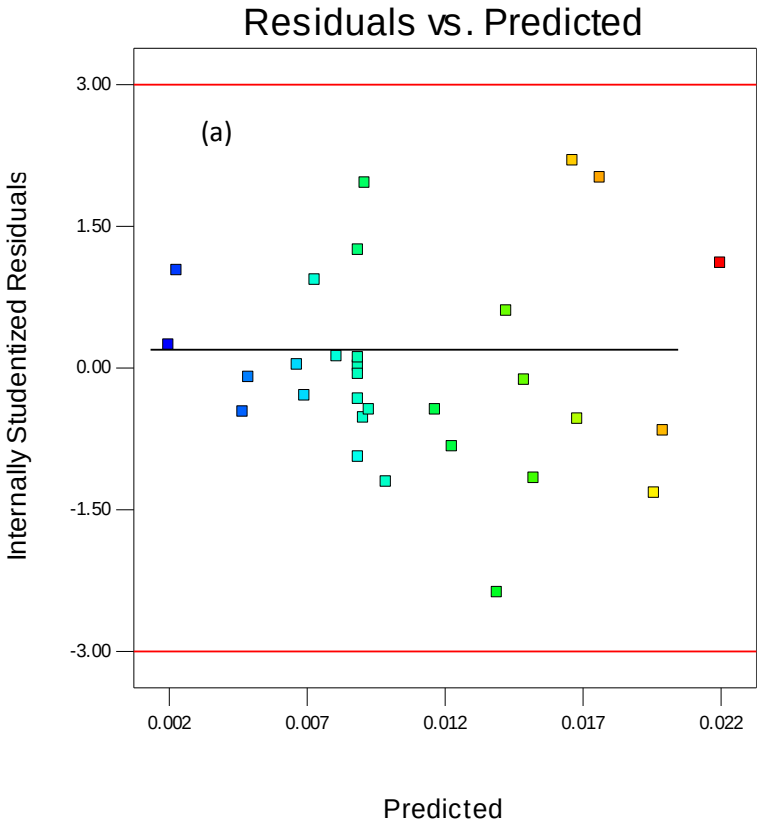

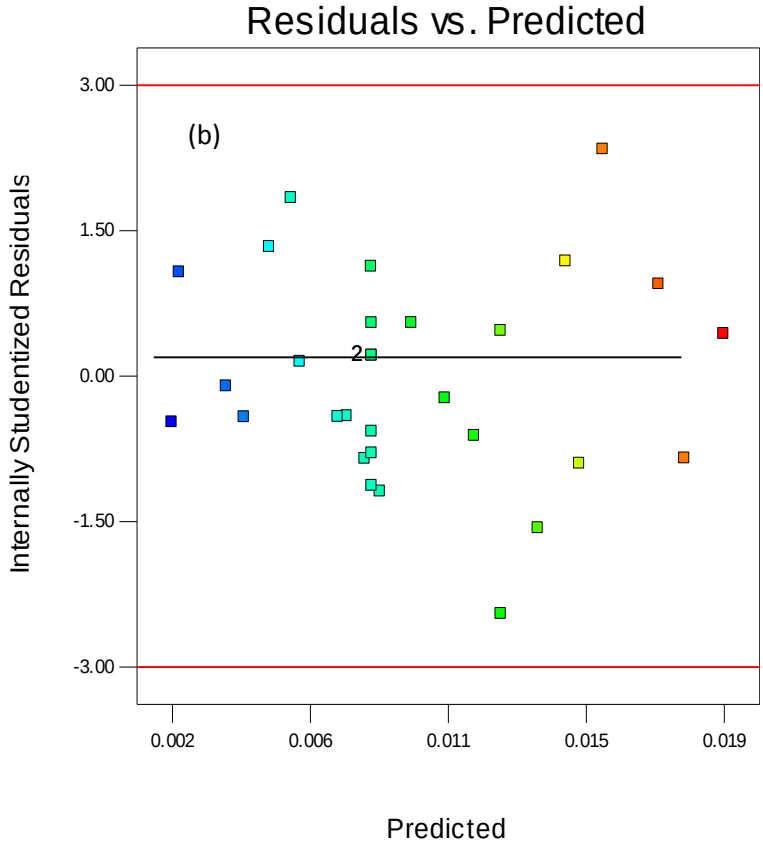

Figure 7.14 (a-b) - Residual vs Predicted plots for (a) Al//SiC and (b) Al//B_4C models

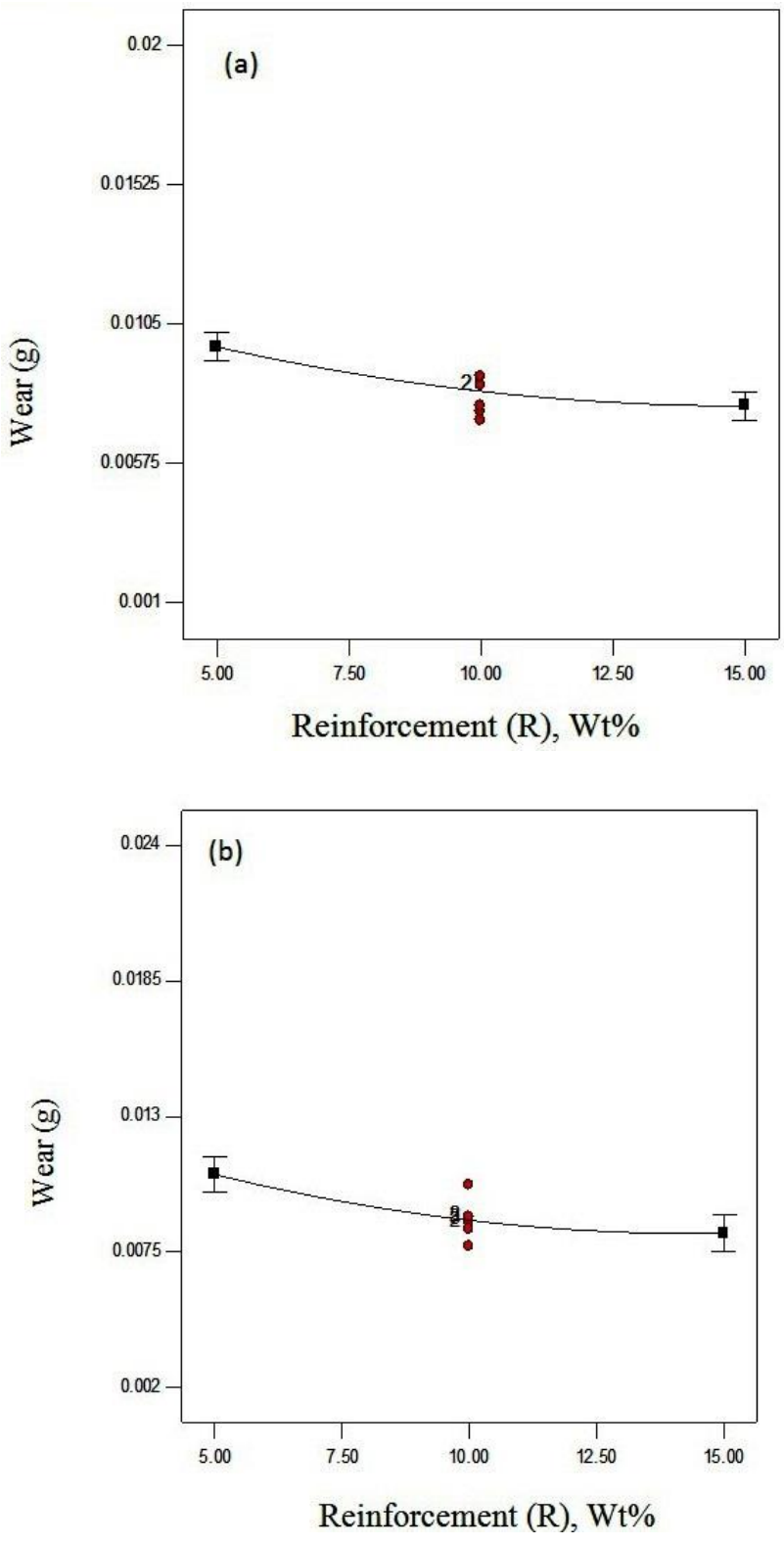

Figure 7.15 (a-b) - Variation in wear (weight loss) with addition of reinforcement in (a) Al/SiC and (b) Al/B_4C composites.

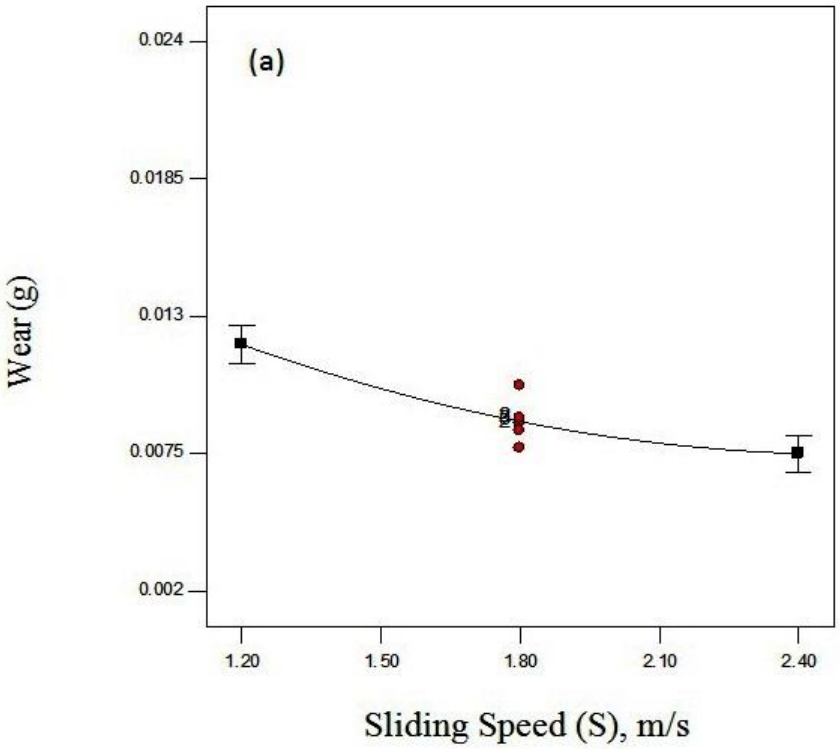

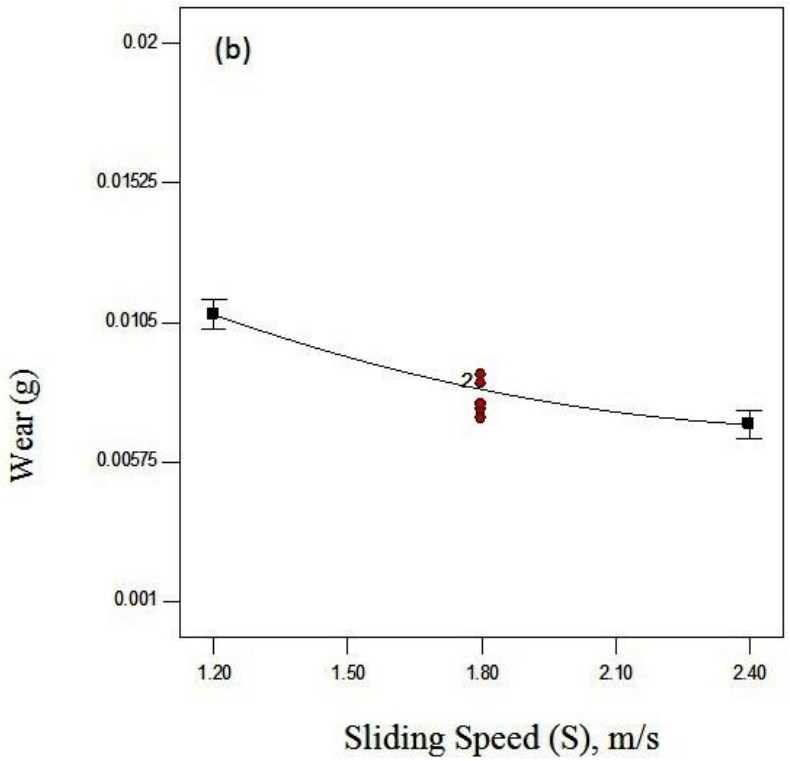

Figure 7.16 (a-b) - Variation in wear (weight loss) with increasing sliding speed in (a) Al/SiC and (b) Al/B_4C composites.

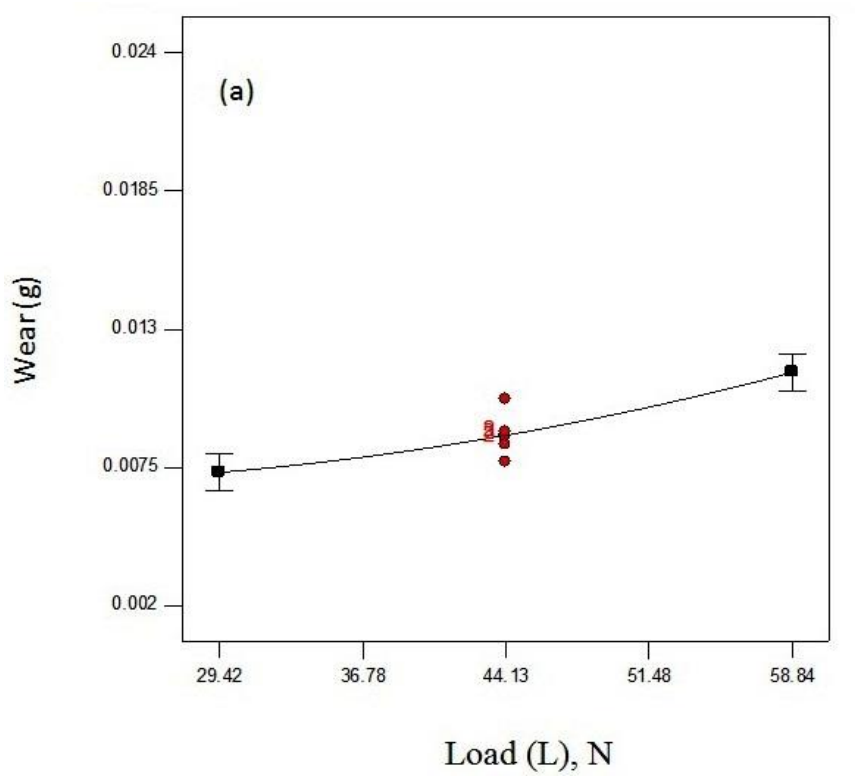

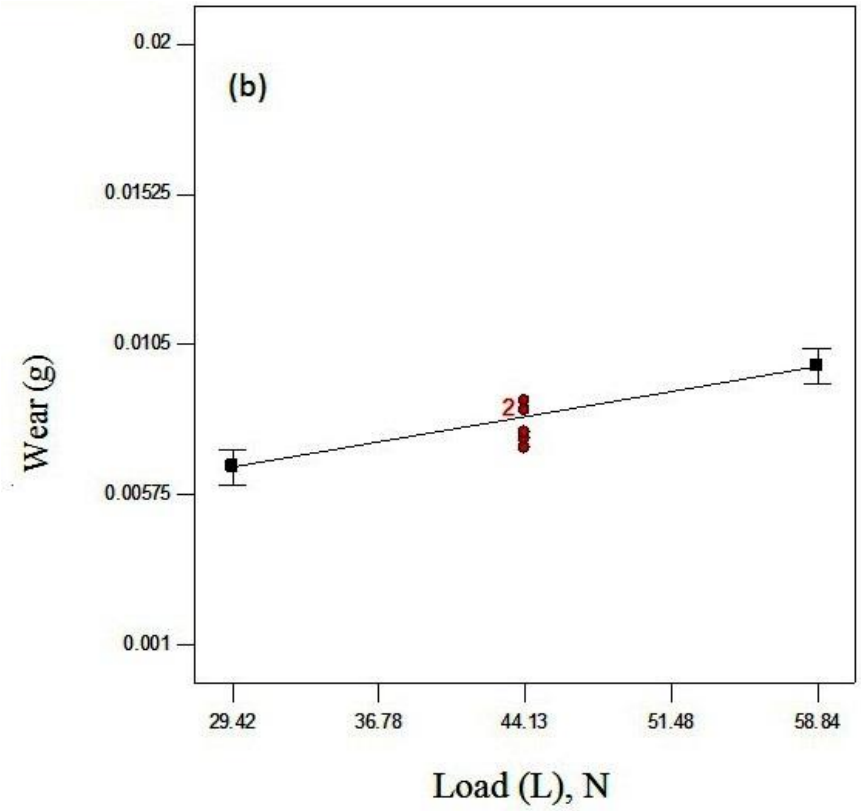

Figure 7.17 (a-b) - Variation in wear (weight loss) with increasing load a) Al/SiC and (b) Al/B_4C composites.

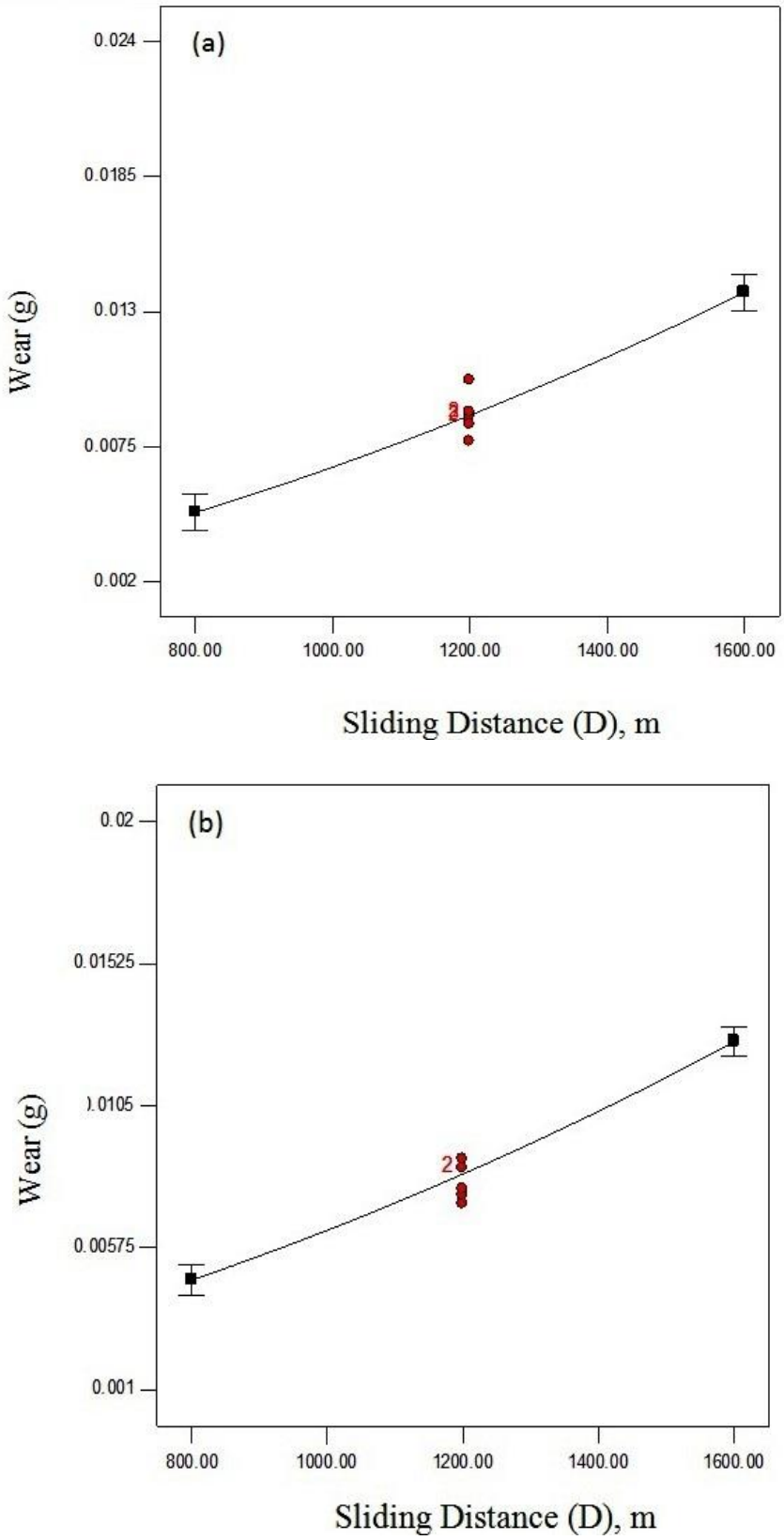

Figure 7.18 (a-b) - Variation in wear (weight loss) with increasing sliding distance in a) Al/SiC and (b) Al/B_4C composites.

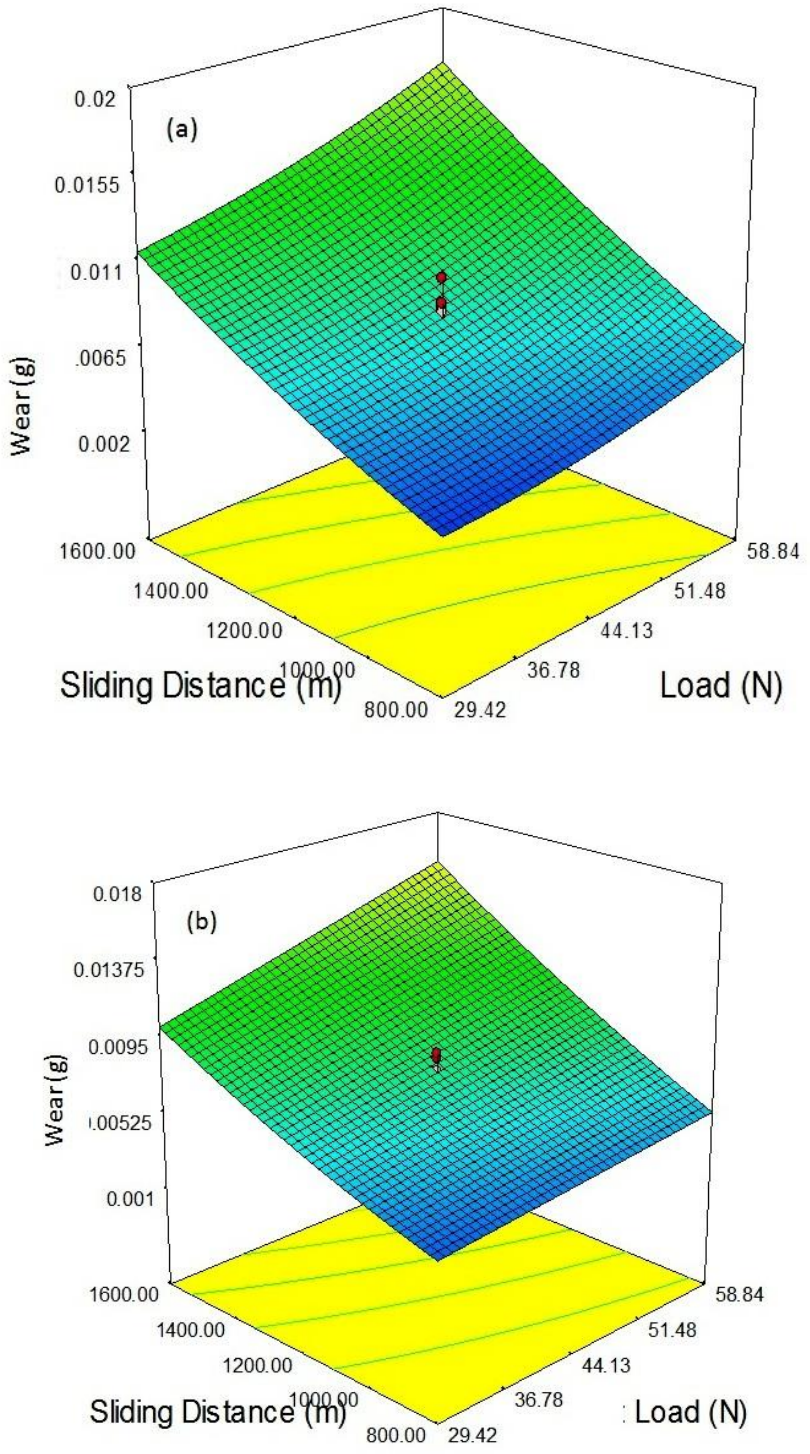

Figure 7.19 (a-b) - 3D interaction plot between load (L) and sliding distance (D) against wear in (a) Al/SiC and (b) Al/B_4C composites.

Figure 7.15 (a) and (b) shows the variation of wear with addition of reinforcement in both the composites. Similar trend was observed with sliding speed, as the negative coefficients -0.00*2183* and *-0.001875* represents decrease in wear with increasing sliding speed as also shown in Figure 7.16 (a) and (b). The possible reason for this wear reduction was the change in shear rate (due to changing speed), which disturbs the mechanical behaviour of the two surfaces in contact while sliding. The strength of a material is higher at greater shear strain rates, thus resulting in lower contact area and consequeltly lesser wear. Moreover, the positive coefficients 0.00*1992* and 0.00*1592* in Eq [1] and Eq [2], associated with load, indicate that a gradual load increase, increases the wear in these composites which was also revealed by the Figure 7.17 (a) and (b). By increasing load, higher pressure is applied at the mating surfaces, which causes greater deformation and results in higher material removal. Regarding the sliding distance, the positive coefficient values 0.00*4483* and 0.00*3983* for SiC and B_4C reinforced composites respectively, were relativey high which suggests that sliding speed has amore detrimental effect on wear. The increment in sliding distance increases the contact time between the pin and the counter surface which in turn enhances wear. The variation in wear in both the composite materials due to increase in sliding distance is shown in Figure 7.18 (a) and (b).

ANOVA results suggests that in Al/SiC and Al/B_4C composites, the interaction between Load and sliding distance (L*D) was the only significant interaction. Figure 7.19 (a) and (b) shows the 3-D interaction between load and sliding distance for the SiC and B_4C reinforced composites. The maximum weight loss value attained in SiC reinforced composites is slightly higher than the maximum value obtained in B_4C reinforced composites. This can suggest that wear in Al/SiC composites is higher than in Al/B_4C composites. The optimum wear suggested by the RSM model for SiC and B_4C reinforced composites was 0.031 g and 0.026 g respectively. In both the 3-D interactions it was evident that sliding distance was the predominant factor in increasing the wear, mainly due to the increase in interaction time between the pin and counter surface. Wear increases at lower and higher applied loads (29.42 N and 58.84 N) with escalation in the sliding distance. As the incremental load leads to higher pressure on the contacting surfaces, a high removal of material occurs. Figure 7.19 shows that the minimum wear was attained at lower values of load and sliding distance for both the composites and the combined effect of load and sliding distance enhances wear in these composites.

7.4.3 Confirmation Tests

The final step in the wear behaviour analysis of Al/SiC and Al/B_4C composites was to validate the developed models and for this purpose, confirmation tests were carried out by selecting different set of process parameters suggested by RSM as shown in Table 7.10. Three confirmation tests were performed on both SiC and B_4C reinforced composites and the weight loss comparison was done between the obtained experimental results and the predicted results by using the developed quadratic models (Table 7.11)

Table 7.10 – Set of process parameters for confirmation tests

Composite	Test No	Reinforcement, (wt %)	Sliding speed (m/s)	Load (N)	Sliding Distance (m)
Al/SiC	1	7.12	1.6	30	800
	2	10.5	2.3	50	800
	3	12	2.4	30	1000
Al/B_4C	1	5.5	2.4	60	800
	2	10	2.4	30	800
	3	15	2.25	30	1000

Table 7.11 - Experimental and modelled results with error

		Wear (g)		
Composite	Test No	Experimental Results	Modelled Results	% Error
Al/SiC	1	0.00561	0.00544	3.03
	2	0.00444	0.00417	6.08
	3	0.00424	0.00395	6.84
Al/B_4C	1	0.00573	0.00557	2.79
	2	0.00308	0.00286	7.14
	3	0.00458	0.00432	5.67

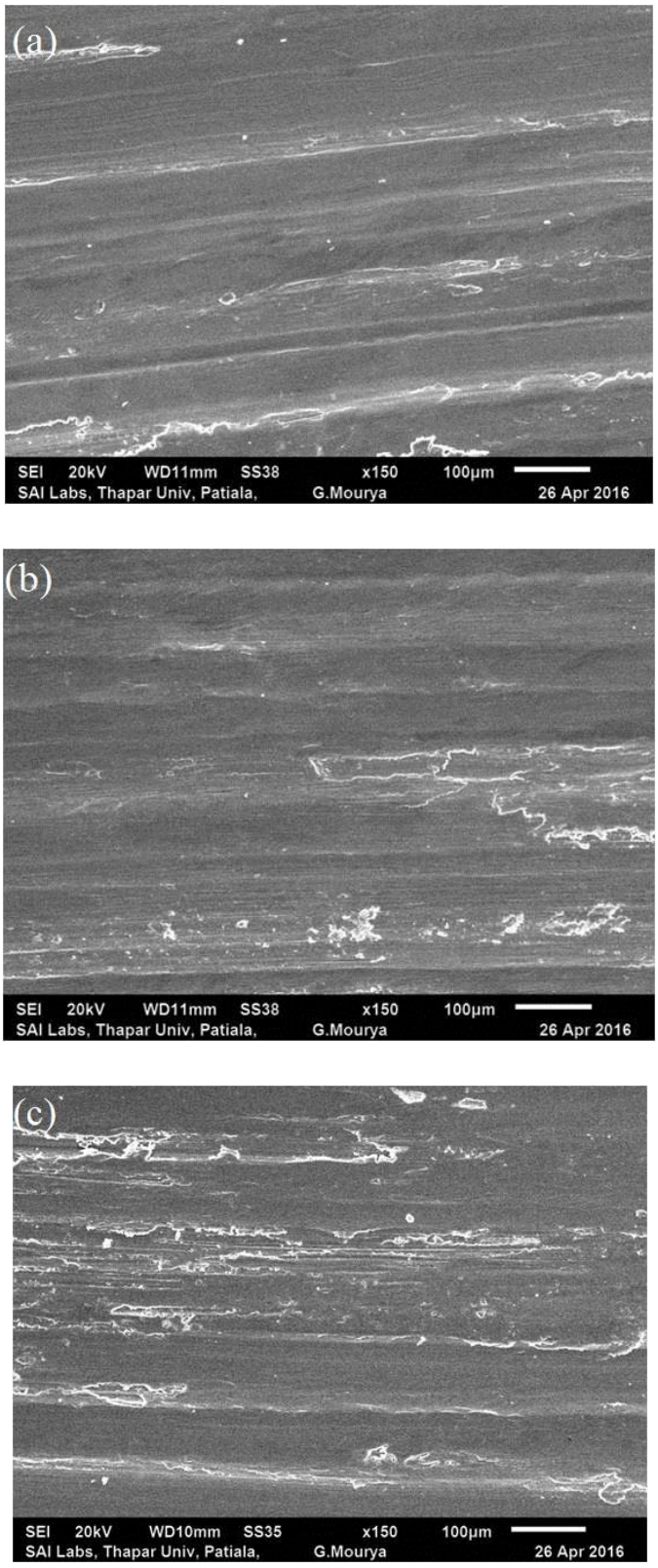

Figure 7.20- Wear Track of Al/SiC composites used for confirmation tests (a) Test 1, (b) Test 2 and (c) Test 3.

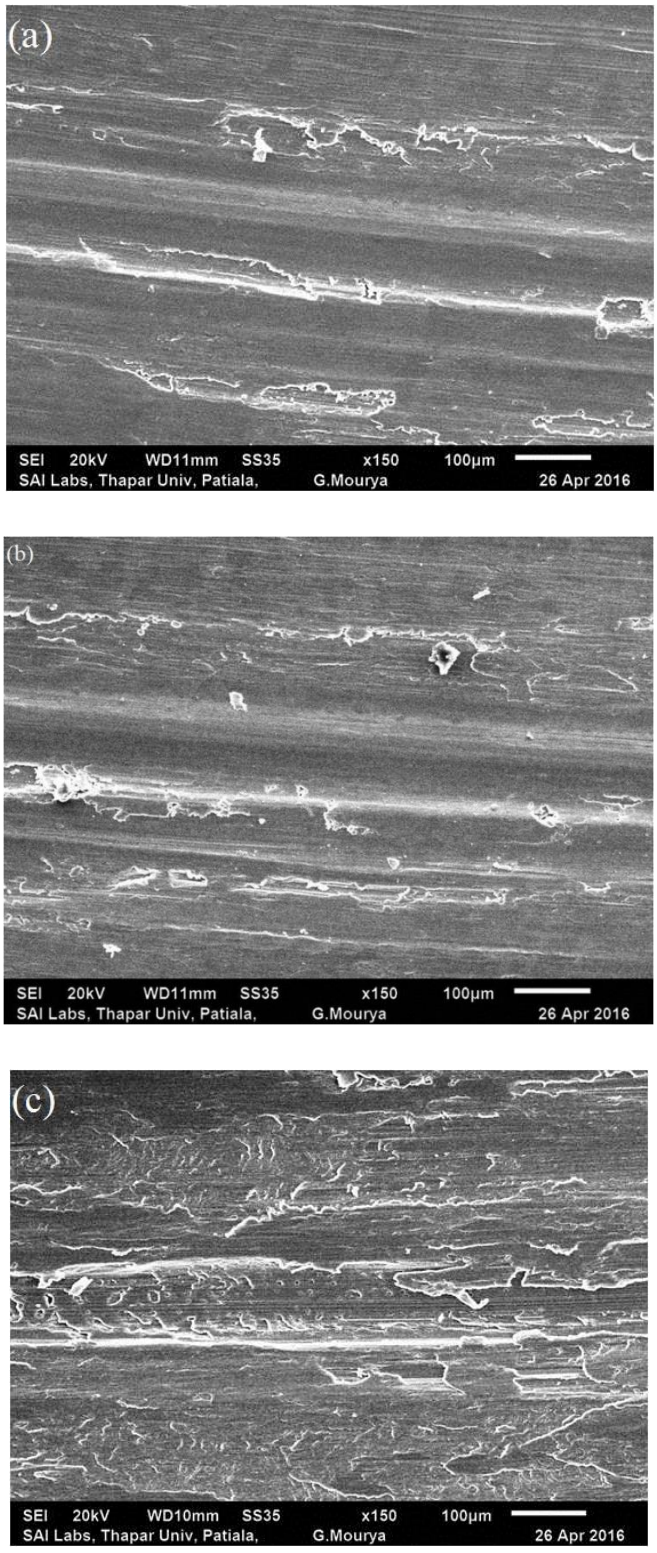

Figure 7.21 - Wear Track of Al/B_4C composites used for confirmation tests (a) Test 1, (b) Test 2 and (c) Test 3.

SEM micrographs of the worn surfaces of SiC and B_4C reinforced composites that were tested for confirmation are shown in Figure 7.20 (a-c) and Figure 7.21 (a-c) respectively.The micrographs ofthe worn surfaces of the pins have one feature in common and that was the formation of parallel lines representing wear tracks in the sliding direction which eventually gets crushed off to become debris. As shown in Table 7.11, the differences between experimental and predicted results were found to be below 7.5% in both Al/SiC and Al/B_4C composites, which were small enough to conclude that the present models and the dry sliding wear behaviour analysis here performed were accurate and can be used as predictive tools for wear applications.

CHAPTER 8

CONCLUSIONS AND FUTURE SCOPE OF RESEARCH

8.1 CONCLUSIONS

In the previous chapters aluminum matrix composites were fabricated using base material AA6082-T6 and employing the conventional stir casting process in the presence of argon atmosphere. SiC and B_4C particulates were used as reinforcement to obtain hybrid and non-hybrid composites through the conventional stir casting process. AA6082-T6/SiC composites with 5, 10, 15 and 20 wt % of SiC; AA6082-T6/B_4C composites with 5, 10, 15 and 20 wt % of B_4C and AA6082-T6/(SiC+B_4C) hybrid composites with 5, 10, 15 and 20 wt % of (SiC+B_4C) taking equal fraction of SiC and B_4C were made and the microstructure study was carried out using X-Ray diffraction (XRD) patterns and Scanning electron microscope (SEM). Specimens were machined to examine the mechanical properties such as micro-hardness, impact strength, ultimate tensile strength, percentage elongation, density, and porosity on the fabricated composites at room temperature. The wear behaviour of the composites is investigated using a pin-on-disc apparatus at room temperature, and the optimization of process parameters was done using response surface methodology (RSM). The weight percentage of reinforcement, sliding speed, load and sliding distance were selected as process parameters with five levels of each for the dry sliding wear behaviour analysis. Experiments were constructed using Central Composite Design (CCD) as it is an efficient tool for building quadratic models consisting of a number of factors. Further, the experimental results obtained are verified by conducting confirmation tests. The predictive models were validated and certified that the developed wear predictive models are accurate and can be used as predictive tools for wear apllications. The conclusions that can be drawn from the present research work are as follows:

1. AA6082-T6/SiC composites with 5, 10, 15 and 20 wt % of SiC; AA6082-T6/B_4C composites with 5, 10, 15 and 20 wt % of B_4C and AA6082-T6/(SiC+B_4C) hybrid composites with 5, 10, 15 and 20 wt % of (SiC+B_4C) taking equal fraction of SiC and B_4C were made successfully using the stir casting method in the presence of argon atmosphere. Table 8.1, Table 8.2 and Table 8.3 represents the composites produced in the present work.

Table 8.1 Al-SiC-B_4C hybrid composites

Sr No	Base Alloy	Wt % of SiC	Wt % of B_4C	Combined Wt% of (SiC + B_4C)
1	AA6082-T6	2.5	2.5	5
2	AA6082-T6	5	5	10
3	AA6082-T6	7.5	7.5	15
4	AA6082-T6	10	10	20

Table 8.2 - Al-SiC composites

Sr No	Base Alloy	Wt % of SiC
1	AA6082-T6	5
2	AA6082-T6	10
3	AA6082-T6	15
4	AA6082-T6	20

Table 8.3 - Al-B_4C composites

Sr No	Base Alloy	Wt % of B_4C
1	AA6082-T6	5
2	AA6082-T6	10
3	AA6082-T6	15
4	AA6082-T6	20

2. XRD patterns reveals the presence of Al, SiC, Al_4C_3 and Si in SiC reinforced composites and the peaks of B_4C and Al_3BC was observed along with Al and Si in B_4C reinforced composites which show the presence of ceramic particles in the metal matrix. However, the peaks for Al_4C_3 and Al_3BC were small in the respective composites. The patterns for AA6082-T6/(SiC+B_4C) hybrid composites shows the peaks of Al, SiC, B_4C, Al_3BC, Al_4C_3 and Si which confirms the occurrence of both the reinforcements along with some other compounds.

3. SEM images shows relatively uniform dispersion of particles in AA6082-T6/SiC, AA6082-T6/B_4C and AA6082-T6/(SiC+B_4C) composites. The growth of α-Al grains with inter-dendritic region of aluminium silicon eutectic was revealed from all the micrographs. With the increase in reinforcement content, the agglomeration of particles also increases at some places and this phenomenon is common for all the composites. These images show a relatively good dispersion of SiC and B_4C particles in the composites. However, when increasing the reinforcement content from 5 to 20 wt. %, particles clusters were observed in all composites. In AA6082-T6/SiC composites, SiC particles seemed more prone to agglomeration, possibly due to the high density of SiC (3.20 g/cm^3) when compared with aluminum (2.67 g/cm^3).

4. The micro hardness results for the fabricated composites are given in Table 8.4, Table 8.5 and Table 8.6 respectively.

Table 8.4: Micro hardness of base alloy and Al-SiC-B_4C hybrid composites

Nomenclature of sample	HV 1	HV 2	HV 3	HV Average	% Improvement (Compared to base alloy)
Alloy (AA6082-T6)	100	102	101	101	NA
Alloy + 5% (SiC + B_4C)	104	103	105	104	2.3
Alloy + 10% (SiC + B_4C)	107	108	111	109	7.9
Alloy + 15% (SiC + B_4C)	112	113	115	113	11.9
Alloy + 20% (SiC + B_4C)	111	110	111	111	9.9

Table 8.5: Micro hardness of Al-B_4C composites

Nomenclature of sample	HV 1	HV 2	HV 3	HV Average	% Improvement (Compared to base alloy)
Alloy + 5% B_4C	104	103	105	104	3
Alloy + 10% B_4C	112	113	112	112	10.9
Alloy + 15% B_4C	118	117	116	117	15.8
Alloy + 20% B_4C	115	115	115	115	13.86

Table 8.6: Micro hardness of Al-SiC composites

Nomenclature of sample	HV 1	HV 2	HV 3	HV Average	% Improvement (Compared to base alloy)
Alloy + 5% SiC	102	104	103	103	2
Alloy + 10% SiC	107	108	117	107	6
Alloy + 15% SiC	111	111	111	111	10
Alloy + 20% SiC	114	112	114	113	11.9

Micro-hardness of hybrid composites increased from 101 HV for un-reinforced alloy to 113 HV for hybrid composite with 15 wt% of reinforcement; 9.9 % improvement in hardness was recorded. Beyond 15 wt% of reinforcement slight decrease in hardness was also reported.

Al/B_4C composites show higher hardness than that displayed by the Al/SiC and Al/SiC/B_4C composites. The optimum hardness valve attained with Al/B_4C was 117 HV adding 15 wt. % B_4C to the aluminium matrix while for Al/SiC composites the maximum hardness comes out to be 113 HV at 20 wt. % SiC. Reduction in Hardness of Al/B_4C at 20 wt % of B_4C was also reported.

Compared to the conventional alloy, the optimum percentage improvement in hardness for B_4C reinforced composites was 15.8 % attained at the addition of 15 wt % of B_4C particulates while in case of Al/SiC composites the percentage improvement was observed to be 11.9 % attained at the addition of 20 wt % SiC particulates.

5. The results of tensile strength and percentage elongation are given in Table 8.7, Table 8.8 and Table 8.9 respectively.

   Addition of reinforcement results in significant improvement in ultimate tensile strength of hybrid Al/SiC/B_4C composites. The tests reveal that UTS rose from 318 MPa at 0% addition of reinforcement mixture to 385 MPa at 15% addition of (SiC + B_4C) particles enhancing the UTS by 21%. It was observed that the hybrid composite with 15 wt% of reinforcement gives superior UTS as compared to the counterpart with 20 wt% reinforcement. The possible reason for this reduction could be the high

level of agglomeration of reinforcement particles at 20 wt% and increased porosity within the microstructures.

Table 8.7: Tensile tests results with percentage elongation for Al-SiC-B_4C hybrid composites

Nomenclature of sample	UTS (MPa)	% Improvement	% Elongation
Al alloy	318	--------	8.38
Alloy + 5% (SiC + B_4C)	333	4.7	7.90
Alloy + 10% (SiC + B_4C)	357	12.26	7.30
Alloy + 15% (SiC + B_4C)	385	21.06	6.96
Alloy + 20% (SiC + B_4C)	371	16.6	6.8

Table 8.8: Tensile tests results with percentage elongation for Al-B_4C composites

Nomenclature of sample	UTS (MPa)	% Improvement	% Elongation
Al alloy	318	--------	8.38
Alloy + 5% B_4C	341	7.2	8.01
Alloy + 10% B_4C	379	19.1	7.7
Alloy + 15% B_4C	417	31.1	7.4
Alloy + 20% B_4C	401	26.1	7.3

Table 8.9: Tensile tests results with percentage elongation for Al-SiC composites

Nomenclature of sample	UTS (MPa)	% Improvement	% Elongation
Al alloy	318	--------	8.38
Alloy + 5% SiC	331	4.1	7.8
Alloy + 10% SiC	350	10	7.2
Alloy + 15% SiC	373	17.3	6.9
Alloy + 20% SiC	379	19.1	6.8

Al/B_4C composites show superior tensile strength followed by Al/SiC/B_4C hybrid composites and Al/SiC composites. The tests reveal that UTS of Al/B_4C composites rose from 318 MPa at 0% addition of reinforcement mixture to 417 MPa at 15% addition of B_4C particles, enhancing the UTS by 31% in comparison to base material. However, at the addition of 20% weight of B_4C, slight decrease in UTS was also reported. For Al/SiC composites, the optimum value of UTS was reported to be 379 MPa at the addition of 20% weight of SiC particulates with an increase of 19.1 % in UTS as compared to base material. The clusters of particles which are the result of particle agglomeration make the material a weaker structure and the existence of porosity in the solidified composites reduces the ultimate tensile strength at 20 % addition of particles.

Percentage elongation was found to be lowered down in all the composites with the addition of the reinforcement content. The degradation in percentage elongation was due to the resistance in flow ability of aluminum matrix with the addition of reinforcement particles and the reduced nature of ductility of aluminum alloy matrix content. The results showed that the percentage elongation in B_4C reinforced composites was comparatively less as compared to the hybrid and SiC reinforced composites and the reason could be the low density of B_4C particles as compared to the SiC particles.

6. The results of impact strength are given in Table 8.10, Table 8.11 and Table 8.12 respectively.

   Impact strength of base material AA6082-T6 without the addition of reinforcement was 9.5 Nm. The impact strength of the hybrid composites comes down gradually with increase in reinforcement with a marginal rate. The result showed that the impact strength for the hybrid composite with 20% wt of (SiC + B_4C) reduces to 7.8 Nm as compared to the 9.5 Nm impact strength of the base material.

   As the reinforcement was added from 5% weight to 20% weight in a step of 5, the impact strength reduced from 9.5 Nm to 8.0 Nm in Al-B_4C composite and 9.5 Nm to 7.6 Nm in Al-SiC composite respectively. Reduction in Impact strength was due to the translation of ductile to brittle nature of the material with increase in weight percentage of reinforcement. The most significant reduction in impact strength was

reported in Al-SiC composites followed by Al-SiC-B_4C hybrid composites Al-B_4C composites.

Table 8.10 - Results of Impact Tests for Al-SiC-B_4C hybrid composites

Nomenclature of sample	Trail 1 (Nm)	Trial 2 (Nm)	Trial 3 (Nm)	Average Impact strength (Nm)
Al alloy	9.4	9.7	9.4	9.50
Alloy + 5% (SiC + B_4C)	9.3	9.3	9.1	9.23
Alloy + 10% (SiC + B_4C)	8.6	8.7	8.7	8.66
Alloy + 15% (SiC + B_4C)	8.3	8.3	8.1	8.23
Alloy + 20% (SiC + B_4C)	7.9	7.9	7.8	7.80

Table 8.11 - Results of Impact Tests for Al-SiC composites

Nomenclature of sample	Trail 1 (Nm)	Trial 2 (Nm)	Trial 3 (Nm)	Average Impact strength (Nm)
Al alloy	9.4	9.7	9.4	9.50
Alloy + 5% SiC	9.0	9.1	9.1	9.06
Alloy + 10% SiC	8.4	8.3	8.3	8.35
Alloy + 15% SiC	7.8	7.6	7.9	7.75
Alloy + 20% SiC	7.7	7.6	7.7	7.6

Table 8.12 - Results of Impact Tests for Al-B_4C composites

Nomenclature of sample	Trail 1 (Nm)	Trial 2 (Nm)	Trial 3 (Nm)	Average Impact strength (Nm)
Al alloy	9.4	9.7	9.4	9.50
Alloy + 5% B_4C	9.3	9.3	9.4	9.33
Alloy + 10% B_4C	8.8	8.10	8.9	8.9
Alloy + 15% B_4C	8.3	8.3	8.6	8.4
Alloy + 20% B_4C	8.0	8.1	8.1	8.0

7. The results reveal that addition of reinforcement particulates in the metal matrix has not much effect on the density of hybrid composite, since the decrease in density was observed from 2.67 g/cm^3 at 0% (SiC+B_4C) addition to 2.53 g/cm^3 at 20% (SiC+B_4C) addition. The decrease in density was reported to be 5.2% in case of hybrid composites. Decrease in density was observed from 2.67 g/cm^3 at 0% B_4C addition to 2.48 g/cm^3 at 20% B_4C in Al-B_4C composite while decrease in Al-SiC composites was from 2.67 g/cm^3 at 0% SiC addition to 2.56 g/cm^3 at 20% SiC addition. The percentage decrease in density was reported to be 7.1% in Al-B_4C composites and 4.1% in Al-SiC composites.

8. The results show that the porosity values of the reinforced hybrid composites slightly increases with addition of reinforcement. The value increases from 0.35% at 0% (SiC+B_4C) addition to 2.14% at 20% (SiC+B_4C) addition. Porosity in Al-B_4C and Al-SiC composites tends to increase slightly with the addition of B_4C and SiC in the molten metal. The increase was observed from 0.35 at 0% B_4C addition to 2.23 at 20% B_4C in Al-B_4C composite while increase in Al-SiC composites was from 0.35 to 1.77 at 20% SiC addition. Hence not much change in the porosity was observed.

9. RSM analysis revealed that in all the composites, wear is decreased by increasing the reinforcement content and sliding speed. On the other hand, increases in load and sliding distance were found to lead to higher wear of these composites. Percentage contribution of Process parameters, Interaction and Quadratic terms on wear on the fabricated composites is given in Table 8.13.

Table 8.13 - Percentage contribution of Process parameters, Interaction and Quadratic terms

Factor	Reinforcement (R)	Sliding Speed (S)	Load (L)	Sliding Distance (D)	LD	R^2	S^2	L^2	D^2	Others	Error
Al/SiC	4.31	14.28	11.88	60.24	0.94	1.49	2.76	0.89	0.93	3.9	0.41
Al/B_4C	4.05	14.02	10.1	63.28	1.97	1.16	2.12	NA	0.89	3.16	0.29
Al/SiC/B_4C	4.2	14.95	9.22	64.17	0.97	1.13	2.1	NA	0.97	3.1	0.29

The variables that presented the most significant effect on wear were sliding distance (with a contribution above 60%), followed by sliding speed, load and finally reinforcement content.

10. Confirmation tests showed that the modelled results are very close to the experimental ones for AA6082-T6/SiC, AA6082-T6/B_4C and AA6082-T6/SiC/B_4C composites. The results predicted by the present model and obtained from the confirmation tests are in close agreement (shown in Table 8.14) and the errors are within 3 to 7%, thus validating the developed wear predictive models.

Table 8.14 - Experimental and modeled results with error

		Wear (g)		
Composite	Test No	Experimental Results	Modeled Results	% Error
Al/SiC	1	0.00561	0.00544	3.03
	2	0.00444	0.00417	6.08
	3	0.00424	0.00395	6.84
Al/B_4C	1	0.00573	0.00557	2.79
	2	0.00308	0.00286	7.14
	3	0.00458	0.00432	5.67
Al/SiC/B_4C	1	0.002198	0.002129	3.14
	2	0.002256	0.002114	6.30
	3	0.002216	0.002123	4.20

11. The optimum wear predicted by RSM is shown in Table 8.15. The optimum wear for AA6082-T6/SiC, AA6082-T6/B_4C and AA6082-T6/SiC/B_4C composites was given on the optimum setting of the four process parameters. The optimum wear for B_4C reinforced composites was reported to be 0.026 g followed by hybrid composites with 0.029 g and SiC reinforced composites with 0.031g.

Table 8.15 – Optimum wear predicted by RSM model

Factor	Reinforcement, (wt %)	Sliding speed (m/s)	Load (N)	Sliding Distance (m)	Wear (g)
Al/SiC	14.82	2.4	29.42	800	0.031
Al/B_4C	14.95	2.4	29.51	800.28	0.026
Al/SiC/B_4C	14.98	2.38	29.42	800.1	0.029

8.2 FUTURE SCOPE OF RESEARCH WORK

The present research work leaves a wide scope for future investigators to explore. Some of the recommendations are as follows:

1. In the present work, mechanical properties like hardness, tensile strength and impact strength are discussed. Other responses like compressive strength and young's modulus can also be addressed.
2. Other ceramic/metallic filers, polymers fibers or natural fibers can also be used for the development of composites.
3. Currently sliding wear behaviour of composites is analysed. Fatigue and Corrosive type of wear can also be considered for future investigation.
4. RSM Technique is applied for planning of experiment and optimization of process parameters. Multi-performance quality characteristics optimization with artificial intelligence techniques like genetic algorithm, fuzzy logic and neural network can also be used for optimization.
5. Cost analysis of these composites to assess their economic viability in industrial applications is another area of interest that can be investigated.

REFERENCES

[1] Adiamak, M. (2006) ‘‘Selected properties of aluminium base composites reinforced with intermetallic particles,” *J. Achiev. Matls Manufac. Tech*., Vol. 14(1–2), pp 43–47.

[2] Agarwala, V. and Dixit, D. (1981) “Fabrication of Aluminium base composite by foundry technique,” *Trans. Japan Inst. Met*., Vol. 22, 521-530

[3] Ahlatci, H., Kocer, T., Candan, E. and Cimenoglu, H. (2006) “Wear behaviour of Al/(Al2O3pCSiCp) hybrid composites,” *Tribology International*, Vol. 39, pp 213–220

[4] Ahmed, I. I., Abdulkarim, K. O., Taiwo, Y. Aremu, I. A. and Alabii, G. F. (2014) “Numerical Modelling of Petroleum Underground Storage Tank Dip Gauge,” *Measurement and Control*, Vol. 47, pp 113-117

[5] Aigbodion, V. S. and Hassan, S .B. (2007) “Effects of silicon carbide reinforcement on microstructure and properties of cast Al–Si–Fe/SiC particulate composites,” *Materials Science and Engineering A*, Vol. 447, pp 355–360.

[6] Akbari, M. K., Baharvandi, H. R. and Mirzaee, R. O. (2013) “Nano-sized aluminum oxide reinforced commercial casting A356 alloy matrix: Evaluation of hardness, wear resistance and compressive strength focusing on particle distribution in aluminum matrix,” *Composites: Part B*, Vol. 52, pp 262–268.

[7] Alaneme, K. K and Aluko, A. O. (2012) “Fracture toughness (K_{1C}) and tensile properties of as-cast and age-hardened aluminium (6063) –silicon carbide particulate composites. *Scientia Iranica* Vol 19(4), pp 992–996.

[8] Alaneme, K. K and Bodunrin, M. O. (2013) “Mechanical behaviour of alumina reinforced AA 6063 metal matrix composites developed by two step – stir casting process” *Acta Technica Corvininesis*, Vol. 6(3), pp 105-110.

[9] Alaneme, K. K. and Olubambi, P. A. (2013) “Corrosion and wear behaviour ofrice husk ash-alumina reinforced Al-Mg-Si alloy matrixhybrid composites,” *J Mater Res Technol*, Vol. 2(2), pp 188–94.

[10] Arslan, G. and Kalemtas, A. (2009) “Processing of silicon carbide–boron carbide–aluminium composites,” *Journal of the European Ceramic Society*, Vol. 29, pp 473–80.

[11] Arslan, G., Kara, F. and Turan, S. (2003) “Quantitative X-ray diffraction analysis of reactive infiltrated boron carbide–aluminium composites,” *Journal of the European Ceramic Society*, Vol. 23, pp 1243-1255.

[12] Aruri, D., Adepu, K., Adepu, K. and Bazavada, K. (2013) *“*Wear and mechanical properties of 6061-T6 aluminum alloy surface hybrid composites [(SiC + Gr) and (SiC

+ Al2O3)] fabricated by friction stir processing." *Journal of Materials research and Technology*, Vol. 3;2(4), pp 362–369

[13] Attar, S., Nagaral, M., Reddappa, H. N. and Auradi, V. (2015) "Effect of B_4C Particulates Addition on Wear Properties of Al7025 Alloy Composites," *American Journal of Materials Science*, Vol. 5(3C), pp 53-57.

[14] Baradeswaran, A., Vettivel, S. C, Perumal, A.E., Selvakumar, N and Issac, R. F. (2014) "Experimental investigation on mechanical behaviour, modelling and optimization of wear parameters of B_4C and graphite reinforced aluminium hybrid composites," *Materials and Design*, Vol. 63, pp 620-632.

[15] Basavarajappa, S. and Chandramohan, G. (2005) "Dry Sliding Wear Behaviour of Hybrid Metal Matrix Composites," *Materials Science*, Vol. 11, pp 253-257.

[16] Beckers, J. L., Carton, M., Schubert, F. and P.J. Ennis, (2002) Materials for advanced power engineering: proceedings of the 7th Liege Conference, Julich, Germany.

[17] Besterci, M. (2006) "Preparation, microstructure and properties of Al–Al4C3 system produced by mechanical alloying," *Materials and Design*, Vol. 27, pp 416–421.

[18] Bhushan, B. and Jahsman, W. E. (1978) "Propagation of Weak Waves in Elastic-Plastic and Elastic-viscoplastic Solids With interfaces," *Int. J. Solids and Struc*. Vol. 14, pp 39-51.

[19] Bhushan, B. and Jahsman, W. E. (1978) "Measurement of Dynamic Material Behavior under Nearly Uniaxial Strain Condition," *Int. J. Solids and Struc*. Vol. 14, pp 739-753.

[20] Boopathi, M., Arulshri, K. P. and Iyandurai, N. (2013) "Evaluation of Mechanical properties of Aluminium alloy 2024 reinforced with silicon carbide and fly ash hybrid metal matrix composites," *American Journal of Applied Sciences*, Vol. 10(3), pp 219-229.

[21] Ceschini, L., Minak, G. and Morri, A. (2006) "Tensile and fatigue properties of the AA6061/20 vol.% Al_2O_3p and AA7005/10 vol.% Al_2O_3p composites," *Composites Science and Technology* Vol. 66, pp 333–342

[22] Chawla, V., Manoj, S., Dwivedi, D. D. and Lakhvit, S. (2009) "Development of aluminium based SiC particulate metal matrix composites", *J. Miner. Matls Charac. Eng*., Vol. 8(6), pp 455–467.

[23] Chowdhury, M. A., Khalil, M. K., Nuruzzaman, D. M. And Rahaman, M. L. (2011) "Effect of Sliding speed and Normal load on Friction and Wear Property of Aluminum," *International Journal of Mechanical & Mechatronics Engineering* 2011; Vol. 11, pp 45-49.

[24] Corrochano, J., Cerecedo, C., Valcarcel, V., Lieblich, M. and Guitian, F. (2008) "Whiskers of Al_2O_3 as reinforcement of a powder metallurgical 6061 aluminium matrix composite," *Materials Letters*, Vol. 62, pp 103–105.

[25] Das, B., Roy, S., Rai, R. N., Saha, S. C. and Majumder, P. (2016) "Effect of in-situ processing parameters on microstructure and mechanical properties of TiC particulate reinforced Al-4.5Cu alloy MMC fabricated by Stir- Casting Technique – Optimization using grey based differential evolution algorithm, *Measurement*, doi: http://dx.doi.org/10.1016/j.measurement.2016.07.044

[26] Das, S., Siddhartha, D. and Karabi, D. (2009) "Abrasive wear of zircon sand and alumina reinforced Al–4.5 wt% Cu alloy matrix composites – A comparative study," *Composites Science and Technology,* 2007; Vol. 67, pp 746–751.

[27] Davis, J. (1999) "Corrosion of aluminum and aluminum alloys. USA: ASM International" pp 25–49

[28] Davis, J. R. ASM Specialty Handbook: Aluminum and Aluminum Alloys, (1993).

[29] Dobrzanski, S. K., Kremzer, M., Nowak, A. J. and Nagel, A. (2009) " Aluminium matrix composites fabricated by infiltration method," *Archives of Materials Science and Engineering,* Vol. 36, pp 5-11**.**

[30] Dwivedi, S. P., Sharma, S., Mishra, R. K. (2014) "Microstructure and Mechanical Properties of A356/SiC Composites Fabricated by Electromagnetic Stir Casting," *Procedia Materials Science,* Vol. 6, pp 1524 – 1532.

[31] Eliasson, J. and Sandstrom, R. (1995) "Applications for aluminium matrix composites" *Key Engineering Materials,* Vols. 104-107, pp 3-36.

[32] Engler, O., Liu, Z. and Kuhnke, K. (2013) "Impact of homogenization on particles in the Al–Mg–Mn alloy AA 5454 – Experiment and simulation," *Journal of Alloys and Compounds*, Vol. 560, pp 111–122.

[33] Ervina Efzan, M. N., Siti Syazwani, N. and Emerson, J. (2016) "Properties of Aluminum Matrix Composite (AMCs) for Electronic Packaging," *Materials Science Forum,* Vol. 857, pp 18-21.

[34] Ezuber, H., El-Houd, A. and El-Shawesh, F. (2008) "A study on the corrosion behavior of aluminum alloys in seawater," *Materials and Design*, Vol. 29, pp 801–805.

[35] Florian, H. G., Malte, H. G. Wichmanna., Fiedlera, B., Bauhoferb, W. and Schultea, K. (2005) "Influence of nano-modification on the mechanical and electrical properties of conventional fibre-reinforced composites," *Composites: Part A* Vol. 36, pp 1525–1535.

[36] Ghazi, J. H. (2013) "Production and Properties of Silicon Carbide Particles Reinforced Aluminium Alloy Composites," *International Journal of Mining, Metallurgy & Mechanical Engineering,* Vol. 1, pp 191-194

[37] Girot, F. A., Albingre, L., Quenisset, J. M. and Naslain, R. (1987) "Rheocasting Al Matrix Composites," *The Journal of The Minerals, Metals & Materials Society,* Vol. 39, pp 18–21.

[38] Gopalakrishnan, S. and Murugan, N. (2012) "Production and wear characterisation of AA 6061 matrix titanium carbide particulate reinforced composite by enhanced stir casting method," Composites: Part B, Vol. 43, pp 302–308.

[39] Hashim, J., Looney, L. and Hashmi, M. S. J. (2001) "The enhancement of wettability of SiC particles in cast aluminium matrix composites," *Journal of Materials Processing Technology,* Vol. 119, pp 329-335.

[40] Hollingsworth, E. and Hunsicker, H. (1987) Metals handbook, ASM International pp 583–609

[41] Ibrahim, M. F., Alkahtani, S. A., Abuhasel, K. A. and Samuel, F. H. (2015) "Effect of intermetallics on the microstructure and tensile properties of aluminum based alloys: Role of Sr, Mg and Be addition," *Materials and Design*, Vol. 86, pp 30–40.

[42] James, J., Venkatesan, K., Kuppan, P. and Ramanujam, R. (2014) "Hybrid Aluminium Metal Matrix Composite Reinforced With SiC and TiB_2," *Procedia Engineering,* Vol. 97, pp. 1018 – 1026

[43] Jansen, J. A. and Technimet, S. (2008) "Understanding the consequence of Ductile-to-Brittle transitions in a plastic material failure." *Technical Article. Materials Technology,* pp 736-742.

[44] Jaradeh, M.R. and Carlberg, T. (2011) "Solidification Studies of 3003 Aluminium Alloys with Cu and Zr Additions*," J. Mater. Sci. Technol,* Vol. 27(7), pp 615-627.

[45] Jurczak, W. and Kyziol, L. (2012) "Dynamic properties of 7000 - series aluminum alloys at large strain rates," *Polish Maritime Research,* Vol. 19, pp 38-43.

[46] Kang, Y. C. and Chan, S. L. P. (2004) "Tensile properties of nanometric Al2O3 particulate-reinforced aluminum matrix composites," *Materials Chemistry and Physics*, Vol. 85, pp 438–443.

[47] Kant, S. and Verma, A. S. (2017) "Stir Casting Process in Particulate Aluminium Metal Matrix Composite: A Review," *International Journal of Mechanics and Solids*, Vol. 9, pp. 61-69.

[48] Kato, K. and Adachi, K. (2011) Wear mechanisms - Modern tribology handbook.

[49] Kaufman, J.G. (2005) Aluminium Alloys, Mechanical Engineers Handbook.

[50] Kaufman, J. G. (1997) Properties of Aluminum Alloys: Tensile, Creep, and Fatigue Data at High and Low Temperature.

[51] Kennedy, A. R. (2000) "The microstructure and mechanical properties of Al-Si-B_4C metal matrix composites," *Journal of Materials Science*, Vol. 37, pp 317-323.

[52] Kissell, J. R. (2004) Aluminium and Aluminium Alloys, Handbook of Advanced Materials

[53] Kok, M. (2005). Production and mechanical properties of Al2O3 particle-reinforced 2024 aluminium alloy composites. *J Mater Process Technol* 161: 381–387.

[54] Krishnan, B. P., Surappa, M. K. and Rohatgi, P. K. (1981) "The UPAL process: a direct method of preparing cast aluminium alloy-graphite particle composites," *J. Mater. Sci.,* Vol.16, pp 1209-1216.

[55] Kuehl, R. O. (2000) Design of experiments. USA: Duxbury

[56] Kumar, G. B., Rao , C. S. P. and Selvaraj, N. (2011) "Mechanical and Tribological Behavior of Particulate Reinforced Aluminum Metal Matrix Composites – a review," Journal of Minerals & Materials Characterization & Engineering, Vol. 10, pp 59-91.

[57] Kumar, G. B.., Rao, C. S. P., Selvaraj, N. and Bhagyashekar, M. S. (2010) "Studies on Al6061-SiC and Al7075-Al2O3 Metal Matrix Composites" *Journal of Minerals & Materials Characterization & Engineering*, Vol. 9, pp 43-55.

[58] Kumar, R. and Dhiman, S. (2013) "A study of sliding wear behaviors of Al-7075 alloy and Al-7075 hybrid composite by response surface methodology analysis," *Materials and Design*, Vol. 50, pp 351–359.

[59] Lee, M., Choi, Y., Sugio, K., Matsugi, K. and Sasaki, G. (2014) "Effect of aluminum carbide on thermal conductivity of the unidirectional CF/Al composites fabricated by low pressure infiltration process," *Composites Science and Technology*, Vol. 97, pp 1–5.

[60] Li, Y. and Ramesh, K. T. (1998) "Influence of particle volume fraction, shape, and aspect ratio on the behavior of particle-reinforced metal–matrix composites at high rates of strain," *Acta Materialia*, Vol. 46, pp 5633–5646.

[61] Liu, W.C., Chen, M.B. and Yuan, H. (2011) "Evolution of microstructures in severely deformed AA 3104 aluminum alloy by multiple constrained compression," *Materials Science and Engineering: A,* Vol. 528, pp 5405–5410.

[62] Madheswaran, K., Sugumar, S. and Elamvazhudi, B. (2015) "Mechanical Characterization of Aluminium – Boron Carbide Composites with Influence of Calcium

Carbide Particles," *International Journal of Emerging Technology and Advanced Engineering,* Vol. 5, pp 492-496.

[63] Maz, Y., Tjong, S. C., Li, Y. L. and Liang, Y. (1997) "High temperature creep behavior of nanometric Si3N4 particulate reinforced aluminium composite," *Materials Science & Engineering. A, Structural Materials: Properties, Microstructure and Processing,* Vol. 225, pp 125–34.

[64] Mazahery, a. and Shabani, M. O. (2011) "Mechanical Properties of Squeeze-Cast A356 Composites Reinforced With B4C Particulates," *Journal of Materials Engineering and Performance,* Vol. 21(2), pp 247-252.

[65] Meyveci, A., Karacan, I., Caligulu, U. and Durmus, H. (2010) "Pin-on-disc characterization of 2xxx and 6xxx aluminium alloys aged by precipitation age hardening," *Journal of Alloys and Compounds*, Vol. 491, pp 278-283.

[66] Miracle, D. B. (2005) ''Metal matrix composites-from science to technological significance,'' *Compos. Sci. Technol*., Vol. 65(15–16), pp 2526–2540.

[67] Mocko, W., Rodriguez-Martinez, J. A. and Kowalewski, Z. L. (2012) "Compressive Viscoplastic Response of 6082-T6 and 7075-T6 Aluminium Alloys Under Wide Range of Strain Rate at Room Temperature: Experiments and Modelling," *Strain* Vol. 48, pp 498-509.

[68] Monje, I. E., Louis, E. and Molina, J. M. (2013) "Optimizing thermal conductivity in gas-pressure infiltrated aluminum/diamond composites by precise processing control," *Composites: Part A*, Vol. 48, pp 9–14.

[69] Montgomery, D. C. (2007) Design and analysis of experiments. New Delhi: Wiley India (P) Ltd

[70] Natarajan, N., Vijayarangan, S. and Rajendran, I. (2006) "Wear behaviour of A356/25SiCp aluminium matrix composites sliding against automobile friction material" *Wear*, Vol. 261, pp 812-822.

[71] Nazik, C., Tarakcioglu, N., Ozkaya, S., Erdemir, F. and Canakc, A. (2016) "Determination of Effect of B_4C Content on Density and Tensile Strength of AA7075/ B_4'C Composite Produced via Powder Technology. International Journal of Materials," *Mechanics and Manufacturing*, vol. 4(4), pp 251-261

[72] Ortega-Celaya, F., Pech-Canul, M. I., Lopez-Cuevas, J., Rendon-Angeles, J. C. And Pech-Canul, M. A. (2007) "Microstructure and impact behavior of Al/SiCp composites fabricated by pressure less infiltration with different types of SiCp," *Journal of Materials Processing Technology*, Vol 183, pp 368-373.

[73] Ozben, T., Kilickap, E. and Cakir, O. (2008) "Investigation of mechanical and machinability properties of SiC particle reinforced Al-MMC." *Journal of materials processing Technology*, Vol. 198, pp 220–225.

[74] Patnaik, A., Satapathy, A., Mahapatra, S. S. and Dash, R. R. (2009) "Tribo performance of polyester hybrid composites: Damage assessment and parameter optimization using Taguchi design," *Materials and Design* Vol. 30, pp 57–67.

[75] Pai, B. C., Ramani, G., Pillai, R. M. and Satyanarayana, K. G. (1995) "Role of magnesium in cast aluminium alloy matrix composites," *Journal of Materials Science*, Vol. 30, pp 1903-1911.

[76] Poovazhagan, L., Kalaichelvan, K., Rajadurai, A. and Senthilvelan. V. (2013) "Characterization of Hybrid Silicon Carbide and Boron Carbide Nanoparticles-Reinforced Aluminum Alloy Composites," *Procedia Engineering*, Vol. 64, pp 681–689.

[77] Prasad, V. and Asthana, R. (2004) "Aluminum Metal-Matrix Composites for Automotive Applications: Tribological Considerations," *Tribology Letters*, Vol. 17, pp 445–453.

[78] Pukanszky, B. and Voros, G. (1993) "Mechanism of interfacial interactions in particulate filled composite," *Composite Interfaces*, Vol. 1(5), pp 411-427.

[79] Qu, S., Geng, L. and Han, J. (2007) "SiC/Al composites fabricated by modified squeeze casting technique," *J. Mater. Sci. Technol*., Vol. 23(5), pp. 641–644.

[80] Ramnath, B. V., Elanchezhian, C., Annamalai, R. M., Aravind, S., Ananda Atreya, T., Vignesh, V. and Subramanian, C. (2014) "Aluminium Metal Matrix Composites - A Review," *Rev. Adv. Mater. Sci.* Vol. 38, pp. 55-60.

[81] Rana, R. S., Purohit R. and Das, S. (2012) "Reviews on the Influences of Alloying elements on the Microstructure and Mechanical Properties of Aluminum Alloys and Aluminum Alloy Composites," *International Journal of Scientific and Research Publications*, Vol. 2, pp 1-7.

[82] Ranganath, S. (1997) "A Review on Particulate-reinforced titanium matrix composites," *Journal of Materials Science*, Vol. 32(1), pp 1-16.

[83] Rajesh Purohit, R., Rana, R. S. and Verma, C. S. (2012) "Fabrication of Al-Sicp Composites Through Powder Metallurgy Process and Testing of Properties," *International Journal of Engineering Research and Applications*, Vol. 2, pp 420-437.

[84] Ravi, K. R., Sreekumar, V. M., Pillai, R. M., Chandan, M., Amaranathan, K. R and Arul, K. R. (2007) "Optimization of mixing parameters through a water model for metal matrix composites synthesis," *Materials & Design,* Vol. 28, pp 871–881.

[85] Raviteja, T., Radhika, N. and Raghu, R. (2014) "Fabrication and Mechanical Properties of stir cast Al-Si12Cu/B_4C Composites," *International Journal of Research in Engineering and Technology,* Vol. 3, pp 343-346.

[86] Reboul, M. C. and Baroux, B. (2011) "Metallurgical aspects of corrosion resistance of aluminium alloys," *Materials and Corrosion*, Vol. 62, pp 215-233.

[87] Sahin, M. and Misiril, C. (2012) "Mechanical and Metallurgical Properties of Friction Welded Aluminium Joints," *Aluminium Alloys - New Trends in Fabrication and Applications,* vol. 30, pp. 277-300, 2012.

[88] Sahin, Y. (2003) "Wear behaviour of aluminium alloy and its composites reinforced by SiC particles using statistical analysis," *Materials and Design,* Vol. 24, pp 95–103

[89] Sahin, Y. and Ozdin, K. (2008) "A model for the abrasive wear behaviour of aluminium based composites," *Materials and Design,* Vol. 29, pp 728–733.

[90] Sahoo, K. L. and Sivaramakrishnan, C. S. (2003) "Some studies on Al–8.3Fe–0.8V–0.9Si alloy for near net shape casting," *Journal of Materials Processing Technology,* Vol. 135, pp 253–257.

[91] Sannino, A. P. and Rack, H. J. (1995) "Dry sliding wear of discontinuously reinforced aluminum composites: review and discussion," *Wear,* Vol. 189, pp 1-19.

[92] Schwartz, M. (2002) Encyclopedia and Handbook of Materials Parts and Finishes.

[93] Sharma, N., Khanna, R., Singh, G. and Kumar, V. (2016) "Fabrication of 6061 Aluminium Alloy Reinforced with Si3n4/N-Gr and Its Wear Performance Optimization Using Integrated RSM-GA," *Particulate Science and Technology,* doi:10.1080/02726351.2016.1196276

[94] Sharma, P., Sharma, S. and Khanduja, D. (2015) "Parametric Study of Dry Sliding Wear Behavior of Hybrid Metal Matrix Composite Produced by a Novel Process" *Metallurgical And Materials Transactions A,* Vol. 46(A), pp 3260-3270.

[95] Sharma, P., Sharma, S. and Khanduja, D. (2015) "A study on microstructure of aluminium matrix composites," *Journal of Asian Ceramic Societies,* Vol. 3, pp 240–244

[96] Shirvanimoghaddam, K., Khayyam, H., Abdizadeh, H., Akbari, M. K., Pakseresht, A. H., Ghasali E. and Naebe, M. (2016) "Boron carbide reinforced aluminium matrix composite: Physical, mechanical characterization and mathematical modelling, *Materials Science & Engineering A,* http://dx.doi.org/10.1016/j.msea.2016.01.114

[97] Shorowordi, K. M., Laoui, T., Haseeb, A. S. M. A., Celis, J. P and Froyen, L. (2003) "Microstructure and interface characteristics of B4C, SiC, and Al2O3 reinforced Al matrix composites: a comparative study," *Journal of Materials Processing Technology,* Vol. 142, pp 738–743.

[98] Singla, M., Dwivedi, D. D., Singh, L. and Chawla, V. (2009) "Development of Aluminium Based Silicon Carbide Particulate Metal Matrix Composite," *Journal of Minerals & Materials Characterization & Engineering*, Vol. 8, pp 455-467.

[99] Suresha, S. and Sridhara, B. K. (2010) "Wear characteristics of hybrid aluminium matrix composites reinforced with graphite and silicon carbide particulates," *Composites Science and Technology,* Vol. 70, pp 1652–1659.

[100] Takei, T., Hatta, H. and Taya, M. (1991) "Thermal Expansion Behavior of Particulate-filled Composites Single Reinforcing Phase," *Materials Science and Engineering*, Vol. A131, pp 133-143.

[101] Tang, F., Meeks, H., Spowart, J. E., Gnaeupel-Herold, T., Prask, H. and Anderson, I. E. (2004) "Consolidation Effects on Tensile Properties of an Elemental Al Matrix Composite," *Mater. Sci. Eng. A*, Vol. 386(1–2), pp 194–204.

[102] Thirumalai, T., Subramanian, R., Dharmalingam, S., Radika, N. and Gowrisankar, A. (2015) "Wear Behaviour of B_4C Reinforced Hybrid Aluminum-Matrix Composites," *Materials and technology*, Vol. 49, pp 9–13.

[103] Thirumalai, T., Subramanian, R., Kumaran, S., Dharmalingam, S. and Ramakrishnan, S. S. (2014) "Production and characterization of hybrid aluminum matrix composites reinforced with boron carbide (B_4C) and graphite," *Journal of scientific and Industrial Research,* Vol. 73, pp 667-670.

[104] Toros, S., Ozturk, F. and Kacar, I. (2008) "Review of warm forming of aluminum–magnesium alloys," *Journal of materials processing technology,* Vol. 207, pp 1-12.

[105] Umanath, K., Palanikumar, K. and Selvamani, S. T. (2013) "Analysis of dry sliding wear behaviour of Al6061/SiC/Al2O3 hybrid metal matrix composites," *Composites: Part B,* Vol. 53, pp 159–168.

[106] Valdez, S., Campillo, B., Perez, R., Martinez, L. and Garcia, H. (2008) "Synthesis and microstructural characterisation of Al–Mg alloy-SiC particulate composite," *Mater. Lett.*, Vol. 62, pp 2623–2625.

[107] Vazquez, E. T., Pech-Canul, M. I., Guia-Tello, J. C. and Pech-Canul M. A. (2016) "Surface chemistry modification for elimination of hydrophilic Al_4C_3 in B_4C/Al composites," *Materials and Design,* Vol. 89, pp 94-101.

[108] Viala, J. C., Bouix, J., Gonzalez, G. and Esnouf, C. (1997) "Chemical reactivity of aluminium with boron carbide," *Journal of Materials Science,* Vol. 32, pp 4559–4573.

[109] Vinson, J. R., Chou, T. W. and McCoy, J. J. (1977) "Composite Materials and their use in Structure," *Journal of Applied Mechanics*, Vol. 44, pp 1-3.

[110] Wang, Z., Song, M., Sun, C. and He, Y. (2011) "Effects of particle size and distribution on the mechanical properties of SiC reinforced Al–Cu alloy composites" *Materials Science and Engineering A*, Vol.28, pp 1131–1137.

[111] Wang, L., Qiu, F., Liu, J., Wang, H., Wang, J., Zhu, L. and Jiang, Q. (2015) "Microstructure and tensile properties of in situ synthesized nano-sized TiCx/2009Al composites*," Materials and Design*, Vol. 79, pp 68–72.

[112] Yih, P. and Chug, D. D. L. (1995) "Powder metallurgy fabrication of metal matrix composites using coated fillers," The International Journal of Powder Metallurgy, Vol. 31, pp 335- 340.

[113] Yu LI, Y., LI, Q. L., LI, D., Liu, W. and SHU, G. G. (2016) "Fabrication and characterization of stir casting AA6061−31%B_4C composite," *Trans. Nonferrous Met. Soc. China*, Vol. 26, pp 2304−2312

[114] Zhang, L. (2015) "The application of composite fiber materials in sports equipment, 5th International Conference on Education, Management, Information and Medicine," pp 450-453.

[115] Zhong, H., Rometsch, P. and Estrin, Y. (2014) "Effect of alloy composition and heat treatment on mechanical performance of 6xxx aluminum alloys," *Transactions of Nonferrous Metals Society of China*, Vol. 24, pp 2174–2178.

[116] Zhou, W. and Xu, Z. M. (1997) "Casting of SiC reinforced metal matrix composites," *Journal of Materials Processing Technology*, Vol. 63, pp 358–63.

[117] Zuo, K., Wang, X. Liu, W. and Zhao, Y. (2014) "Preparation and characterization of Ce−silane−ZrO2 composite coatings on 1060 aluminum," *Transactions of Nonferrous Metals Society of China*, Vol. 24, pp 1474−1480.

APPENDIX A

Table A: Components of Central Composite Second order Rotational Design

Variables (k)	**Factorial Points(2^k)**	**Star Points (2k)**	**Center Points(n)**	**Total (N)**	**Value of α**
3	8	6	6	20	1.68179
4##	16	8	6	30	2.00000
5	$16^{\#}$	10	6	32	2.00000
6	$32^{\#}$	12	10	54	2.37841
## This is used in Present Work, # Half Replication.					

Brief Bio-data

I, Gurpreet Singh Saini, am pursuing PhD in the field of Material Development and Characterization, from Faculty of Engineering and Technology, YMCA University of Science and Technology, Faridabad, Haryana, India. I did Masters of Engineering in Mechanical Engineering - Design from PEC University of Technology, Chandigarh in the year 2010. I obtained by Bachelor of Technology in Mechanical Engineering from Kurukshetra University, Kurukshetra in 2006. I have two years of Industry experience (Post B.Tech) and seven years of teaching experience (post ME). Presently, I am working as Lecturer in Mechanical Engineering Department in Thapar University, Patiala. I have published 3 SCI research papers till date in different Journals and two of these are from my PhD work My area of research interest is material development, characterization and its processing.

LIST OF PUBLICATIONS OUT OF THESIS

List of Published Papers

Sr. No.	Title of the paper and Journal Details	Publisher	Impact factor	Whether referred or non referred	Whether you paid any money for publication	Remarks
1	Dry sliding wear behaviour of AA6082-T6/SiC/B_4C hybrid metal matrix composites using response surface methodology. ***Proceedings of the Institution of Mechanical Engineers Part L:*** *The Journal of Materials: Design and Applications* DOI: 10.1177/1464420716657114	Sage Publications	0.793 SCI	Referred	-No-	Online First Published
2	Microstructure and Mechanical Behaviour of AA6082-T6/SiC/B_4C based Aluminum Hybrid Composites. ***Particulate Science and Technology: An International Journal DOI:*** 10.1080/02726351.2016.1227410	Taylor & Francis	0.707 SCI	Referred	-No-	Online First Published
3	An Investigation on X-Ray Diffraction Technique Using SiC and B4C Particulate**.** ***International Journal of Engineering Studies***. Volume 6, 2014, pp. 77-86	Research Group Foundation	-No-	Referred	Conference registration fees	Published

4	Fabrication Techniques of Metal Matrix Composites: A comprehensive Study. **International Conference on Manufacturing Excellence** (MANFEX 2016) at Amity University, Noida on 17-18 March, 2016. pp 12-21	International Conference, Amity University, Noida	-No-	Referred	Conference Registration Fee	Published
5	**A Comprehensive Study on Aluminium Alloy Series – A review. International Conference on Recent Advances in Mechanical Engineering** at PIET, Panipat on 17-18 March, 2017. Pp 11-27	International Conference, PIET Panipat	-No-	Referred	Conference Registration Fee	Published

List of Communicated Papers

Sr. No.	Title of the paper and Journal Details	Publisher	Impact factor	Whether referred or non referred	Whether you paid any money for publication	Remarks
1	Parametric study of the wear behaviour of AA6082-T6/SiC and AA6082-T6/B_4C composites using RSM. ***Journal of Mechanical Science and Technology***	Springer	0.761 SCI	Referred	-No-	Under Review
2	Comparative Analysis on Microstructure and Mechanical Behaviour of AA6082-T6/B4C and AA6082-T6/SiC Composites Fabricated through Stir Casting Technique. ***Particulate***	Taylor & Francis	0.707 SCI	Referred	-No-	Under Review

List of Accepted Papers

Sr. No.	Title of the paper and Journal Details	Publisher	Impact factor	Whether referred or non referred	Whether you paid any money for publication	Remarks
1	Fabrication and Microstructure study of Aluminum matrix composites reinforced with SiC and B_4C particulates. **5th International Conference on Nano and Materials Science (ICNMS 2017)** on 19-21 January, San Diego, USA	TTP Publication	No	Referred	Conference registration fees	Accepted